# THE EFFECT OF DPP10 IN SMOKING AND VAPING INDUCED APOPTOSIS AND INFLAMMATION

A thesis submitted in partial fulfilment of the requirements of Birmingham City University for the degree of Doctor of Philosophy

June 2024

School of Life and Health Sciences, Birmingham City University

## DEDICATION

For Ayoola and Michael Afonja

ACKNOWLEDGEMENTS

Several people played significant roles in my success, and I would like to take this opportunity to show my gratitude.

My supervisors, Professor Loukia Tsaprouni and Professor Maxine Lintern, provided invaluable support. Despite such a busy schedule they made sure I knew my work was important to them. I am truly grateful for all their patience, wisdom and guidance. I also owe the entire technical staff of the Department of Health science, Faculty of HELS at BCU a debt of gratitude, from troubleshooting equipment failures to helping me navigate the laboratory and supplies. The technical staff answered my every call, and their kind gestures made all the difference.

Finally, I'd like to thank God, my husband Ayoola Afonja and my son Michael Afonja who was just a baby when I embarked on this journey. Thank you for always being there for me.

LIST OF CONTENTS

LIST OF FIGURES

LIST OF TABLES

ABBREVIATIONS

| | |
|---|---|
| AC | Adenyl Cyclase |
| AD | Alzheimer's Disease |
| ADA | Adenosine Deaminase |
| AEC | Airway Epithelial Cells |
| ALI | Air Liquid Interface |
| AMP | Antimicrobial Peptides |
| AO | Acridine Orange |
| AS | Antisense |
| ASD | Autism Spectrum Disease |
| ASH | Action On Smoking and Health |
| ATC | American Tobacco Company |
| BAT | British American Tobacco |
| BD | Bipolar Disorder |
| CDC | Centre For Disease Control |
| CDK | Cyclin Dependent Kinase |
| CF | Cystic Fibrosis |
| CFTR | Cystic Fibrosis Transmembrane Regulator |
| CNS | Central Nervous System |
| CNV | Copy Number Variation |
| COPD | Chronic Obstructive Pulmonary Disease |
| CORESTA | Cooperation Centre for Scientific Research Relative to Tobacco |
| CREB | Camp Response Element Binding Protein |

| | |
|---|---|
| CSE | Cigarette Smoke Extract |
| DC | Dendritic Cells |
| DHBE | Diseased Human Bronchial Epithelium |
| DISC | Death Inducing Signalling Complex |
| DPP | Dipeptidyl Peptidase |
| DR | Death Receptors |
| EVALI | E-cigarette Or Vaping Product Use–Associated Lung Injury |
| FADD | Fas Associated Death Domain Protein |
| FC | Flow Cytometry |
| FEV1 | Forced Expiratory Volume In One Second |
| HBpEC | Human Bronchial Primary Epithelial Cells |
| hCAP | Human Cathelicidin Antimicrobial Protein |
| HSC | Hematopoietic Stem Cell |
| lncRNA | Long non-coding RNA |
| MMP | Matrix Metalloproteinase |
| MSN | Medium Spiny Neurons |
| MSS | Mainstream Smoke |
| NCD | Non-Communicable Disease |
| NFVE | Nicotine Free Vape Extract |
| NHBE | Normal Human Bronchial Epithelium |
| NHS | Health Service |
| NK | Natural Killer |
| NRT | Nicotine Replacement Therapies |

| | |
|---|---|
| NSCLC | Non-Small Cell Lung Cancer |
| NTC | Non-Template Control |
| OD | Optical Density |
| PC | Phosphatidylcholine |
| PG | Propylene Glycol |
| PI | Propidium Iodide |
| PLTP | Phospholipid Transfer Protein |
| PRR | Pattern Recognition Receptors |
| PUFA | Poly Unsaturated Fatty Acid |
| RIP | Receptor Interacting Protein |
| ROS | Reactive Oxygen Species |
| SCLC | Small Cell Lung Cancer |
| SNP | Single Nucleotide Polymorphism |
| SPN | Spiny Projection Neurons |
| SSS | Side Stream Smoke |
| SZ | Schizophrenia |
| T2DM | Type 2 Diabetes Mellitus |
| TEER | Transepithelial Electrical Resistance |
| TLR | Toll Like Receptors |
| TNF | Tumour Necrosis Factor |
| TPD | Tobacco Product Directive, 2014) |
| TRADD | TNFR1-Associated Death Domain Protein |
| TRAF | TNFR Associated Factor |

| | |
|---|---|
| VE | Vape Extract |
| VG | Vegetable Glycerine |
| WHO | World Health Organization |

ABSTRACT

Background:

Cigarette smoke and electronic cigarette (vape) aerosols both induce oxidative stress and inflammation in airway epithelial cells, contributing to the development of chronic respiratory diseases. Dipeptidyl peptidase-like protein 10 (DPP10), a member of the dipeptidyl peptidase family, has been linked to asthma susceptibility and airway epithelial remodelling, yet its role in epithelial responses to smoke or vape exposure remains poorly understood. This study aimed to investigate the role of DPP10 in modulating inflammation and apoptosis in human airway epithelial cells exposed to cigarette smoke extract (CSE), nicotine-free vape extract (NFVE), and nicotine-containing vape extract (VE).

Methods:

Human alveolar (A549) and bronchial (Beas-2B) epithelial cells were treated with CSE, NFVE, or VE standardized for nicotine concentration. Cell viability was assessed using XTT assays to determine sub-toxic concentrations for subsequent experiments. Cytokine production (IL6, IL8, TNFα) was quantified by ELISA and gene expression by qPCR. DPP10 expression was modulated using siRNA knockdown and plasmid overexpression. Cell cycle distribution was analyzed by flow cytometry, and apoptosis was assessed through Annexin V/PI staining and Bcl-2 activation assays.

Results:

CSE exerted the greatest cytotoxicity, followed by VE and NFVE, with Beas-2B cells showing higher sensitivity than A549. CSE and VE significantly upregulated IL6 and IL8 gene and protein expression in both cell lines, whereas NFVE produced minimal effects. TNFα expression was increased at the transcriptional level but not consistently at the protein level. Exposure to all three extracts induced G1/S phase arrest, consistent with DNA damage–induced checkpoint activation. DPP10 knockdown produced a non-significant trend towards enhanced cytokine expression and late apoptosis, while overexpression showed a similar non-significant trend towards reduced response. Bcl-2 activation (Ser70 phosphorylation) was reduced in DPP10-silenced cells, suggesting a role in cell survival signalling.

Conclusions:

Cigarette smoke and vaping extracts promote epithelial inflammation and apoptosis through nicotine-dependent and -independent mechanisms. While DPP10 modulation produced only subtle effects, trends indicate a potential protective role in maintaining epithelial cell viability under oxidative stress by promoting Bcl-2 activation. These findings highlight DPP10 as a possible molecular modulator of airway epithelial resilience to smoke and vape exposure, warranting further mechanistic investigation.

# 1. INTRODUCTION

## 1.1. CIGARETTE AND ELECTRONIC CIGARETTE USAGE

### 1.1.1. SOCIO-ECONOMIC REALITY OF CIGARETTE USE

Smoking of tobacco-related goods dates as far back as 6000BC. At first, the tobacco plant—a species of nightshade in the genus Nicotiana officially known as Nicotiana tabacum—was exclusive to North America. Nicotine, an extremely addictive chemical found in tobacco, causes the release of dopamine, which in turn causes euphoric effects (Tweed et al., 2012).

In 1492, Columbus dried out the tobacco plant leaves gifted to him by American Indians. Later that year, Tobacco was introduced in Europe, and people cultivated tobacco plants. Nearly eight decades later, European physicians began to identify and report the health benefits of tobacco leaves, characterizing them as a treatment for a variety of ailments, including cancer, and even in dentistry. (Shishani, 2018). In North and South America, the leaves were widely accepted because of their important medical potential (Apperson, 1914)

In the early 17th century, many scholars warned about the risks of smoking, Fang Yizhi, claimed that it produced "scorched lungs." While Sir Francis Bacon recognized that Tobacco had a strong addictive quality which was difficult to break, however, the presence of nicotine in Tobacco had not yet been discovered (Parascandola and Xiao, 2019)

In 1760, a French immigrant named Pierre Lorillard established a "manufactory" in New York City (Edwards, 2004). The company's first offerings were cigars, snuff, pipe tobacco, and plug chewing tobacco. The first and second world wars saw the rise in popularity of cigarettes and by supplying millions of cigarette packets to front-line soldiers and the cigarette corporations made thousands of devoted clients. Even K-rations, high calorie boxed meals designed for mobile military forces contained 4 cigarettes per meal (National Army Museum, n.d.; Oransky, 2004; Mendel et al., 2018).

Following the invention of the cigarette rolling machine in 1881, cigarette smoking became increasingly widespread. In the early 1900s, cigarette advertising was often geared towards women, with branding strategies designed to appeal specifically to this demographic. Tobacco companies introduced products with names such as “Mild as May”, reinforcing this shift in marketing focus. By the 1930s, the proportion of female smokers had risen

substantially, with annual per capita consumption reaching approximately 500 cigarettes, compared with negligible levels in 1920 when consumption among women was too low to be reliably recorded (Tinkler, 2001; Wald and Nicolaides-Bouman, 1991). When James 'Buck' Duke started his own company, the American Tobacco Company (ATC) was established. ATC continues to function as a division of British American Tobacco (BAT), a global company valued at 91.6 billion USD in 2021.

Growing concerns about the proportionate rise of cigarette smoking and lung cancer in the first half of the 20$^{th}$ century caused scientists to postulate that cigarette smoking could be an underlying cause of lung cancer. As people's unease about their health grew, cigarette companies like Camel launched advertising campaigns to highlight the safety of cigarettes by using the pictures of doctors. (Scheffels, 2008). By 1950, many case controlled epidemiological studies and longitudinal cohort studies confirmed that smoking was indeed a primary risk factor in developing lung cancer (Müller, 1940; Schairer and Schöniger, 1944; Doll and Hill, 1954; Hammond and Horn, 1954; Proctor, 2012).

The tissues of the body encounter several substances when smoke is inhaled (Zhang et al., 2011, 2016; Zhao et al., 2014). Tar, a resinous substance, coats the teeth and gums, weakening tooth enamel and accelerating tooth decay in the process. Consequent to ciliary destruction due to smoking, there is an increased risk of the development of long-term respiratory conditions such as bronchiectasis and COPD (Brekman et al., 2014; Simet et al., 2010; Leopold et al., 2009; Bird and Memon, 2025; Ancel et al., 2021). Harmful pathogens enter the body due to destructed cilia in the nose and land in tiny alveoli sacs (Watson et al., 1988). The exchange of carbon dioxide and oxygen between blood and lungs is made possible by these air sacs. Rather than attaching to oxygen, carbon monoxide links to haemoglobin to enter the bloodstream. Breathlessness and oxygen deprivation are the eventual results of this process. During smoking, nicotine reaches the brain within as little as 5 seconds (Rose et al., 2010; Berridge et al., 2010). This rapid delivery of nicotine to the brain triggers the release of neurotransmitters such as dopamine and endorphins, which are associated with reward and reinforcement pathways, thereby contributing to the high addictive potential of smoking (Takahashi et al., 2008; Subramaniyan and Dani, 2015; Wing et al., 2015).

Nicotine and other substances in cigarettes cause blood vessels to constrict, reducing normal blood flow. Over time, this leads to the hardening and narrowing of the arteries, which increases the risk of stroke. In the United States, smoking is responsible for 1 in 5 deaths resulting from a heart attack. (Sadeghi et al., 2021)

To improve flavour and increase the enjoyment of smoking, additional ingredients are added to cigarettes in addition to the tobacco plant's dried leaves, which constitute much of the product. These goods emit smoke, which is a complex mixture of chemicals created when tobacco and additional additives burn. The following hazardous substances are present in tobacco smoke and are also present in other materials that come with significant warnings not to breathe in. (Rodgman et al., 2000).

*Table 1: Common chemical compounds found in cigarette smoke and their toxic effect from inhalation.*

| *Chemicals present in cigarette smoke* | *Toxic effect from inhalation* |
|---|---|
| Acetone | Neurotoxicity (Mitran et al., 1997), renal failure (Piatkowski et al., 2007) |
| Arsenic | Haemolysis (Pakulska and Czerczak, 2006) |
| Ammonia | Pulmonary oedema (Caplin, 1941; Walton, 1973), death (Sobonya, 1977) |
| Benzene | Asphyxiation, central nervous system (CNS) depression (Winek Cl and Collom Wd, 1971; Winek Cl et al., 1967; Avis and Hutton, 1993) |
| Butane | Cardiac arrythmia, lung oedema (Nishi et al., 1985), multiple organ failure (Rieder-Scharinger et al., 2000) |
| Cadmium | Cancer (Joseph, 2009), osteoporosis (Staessen et al., 1999; Nawrot et al., 2010) |
| Carbon monoxide | Hypoxia, ischemia (Gozubuyuk et al., 2017) |
| Formaldehyde | Bronchitis, pneumonia (Fischer, 1905) |
| Lead | CNS depression (Cory-Slechta, 1996) |

Currently, the World Health Organization (WHO) estimates that there are about 1.3 billion people who use tobacco containing products globally (WHO, 2021). In England alone for the year 2021, the economic cost of smoking was estimated to be about £17bn which includes death, reduction in productivity, increased need for health and social care, property damage and injuries from smoking related fires (Howard Reed, 2020; Action on Smoking and Health, 2022).

Recent data on smoking in the UK shows that it is closely linked to both socio-economic and demographic factors. Men were more likely to smoke than women, with 13.7% of men and 10.1% of women identifying as current smokers. People aged 25 to 34 had the highest smoking rates at 14.0%, while those aged 65 and over had the lowest at 8.2%. Socio economic disparities were also evident among smokers. 19.7% of unemployed individuals smoked, compared with 11.4% of those in work and 12.2% of those who were economically inactive. 20.2% of those in routine or manual jobs smoked, compared with just 7.9% of those in managerial or professional roles. Education also played a key role, with 27.4% of people with no qualifications smoking, compared to only 5.8% of those with a degree. Overall, smoking remains most common among disadvantaged and lower-educated groups (ONS, 2024).

Numerous legislative measures have been introduced to reduce cigarette consumption and raise awareness about the health risks of smoking. Under the Tobacco and Related Products Regulations (2016) , every tobacco product unit pack must include combined text and coloured photo warnings. Despite these regulations, tobacco brands continue to compete aggressively in the market. Strategies such as the use of appealing flavours, distinctive packaging designs, and claims of lower nicotine content are commonly used to retain consumer loyalty and encourage continued use.

### 1.1.2. VAPING AS AN ALTERNATIVE TO TRADITIONAL CIGARETTES

The invention of the electronic cigarette dates to the 1920s when Joseph Robinson created the mechanical butane ignition vaporizer, a device used to vaporise medicinal compound for inhalation. In 2003, the Chinese pharmacist Hon Lik created and patented the first modern electronic cigarette. Its original purpose was to provide a different method of delivering nicotine to smokers looking to quit smoking (Crotty Alexander et al., 2015).

While the use of traditional cigarettes among adults have declined over time, the use of electronic cigarettes has been on a steady rise. More than half of current vapers are former smokers who transitioned to vaping as an alternative to cigarettes. Around one-third continue to smoke alongside vaping, while fewer than 10% of current vapers have never smoked cigarettes (Table 2) (Action on Smoking and Health, 2023a, 2024). Vaping among

children, however, is on a sharp rise. In 2023, 20.5% of children aged 11–17 had tried vaping, with nearly a third of them identifying as current vapers. This marks a significant increase from 15.8% in 2022 and 11.3% in 2021, highlighting a growing trend of vaping uptake among young people, in contrast to the adult population, where vaping is more often used as a tool for smoking cessation. Promotional awareness has also grown both online and in shops.

*Table 2: Prevalence of cigarette and e-cigarette use among adults in Great Britain (Action on Smoking and Health, 2023a, 2024)*

| | 2020 | 2021 | 2022 | 2023 |
|---|---|---|---|---|
| Current cigarette smokers | 14.5 | 12.7 | 11.2 | 10.5 |
| Current e-cigarette users | 6.3 | 7.1 | 8.3 | 9.1 |
| Stratification of current e-cigarette users by cigarette smoking habit | | | | |
| - Current Smokers | 37.6 | 29.9 | 34.5 | 36 |
| - Former smokers | 59.6 | 65.2 | 57.5 | 57.2 |
| - Never smokers | 2.8 | 4.9 | 8 | 6.8 |

Despite a common misconception among children that vaping poses similar health risks to smoking, this perception does not appear to deter the use of e-cigarettes Although it is currently illegal to sell vapes to minors in the UK, nearly half of youths surveyed by the Action on Smoking and Health reported purchasing them from retail outlets, while 46% stated they obtained them from others. Disposable e-cigarettes were the most used type among young people, with usage rising sharply from 7.7% in 2021 to 52% in 2022 and reaching 69% in 2023. Meanwhile, the use of rechargeable e-cigarettes with either prefilled cartridges or refillable tanks has steadily declined over the same period (Action on Smoking and Health, 2023b).

Research indicates that smokers who use electronic cigarettes as a smoking cessation aid are more likely to quit than those who use nicotine replacement therapy (NRT) (Brown et al., 2014; Caponnetto et al., 2013). In a randomised clinical trial participants who were assigned to vape versus NRT as a smoking cessation tool in a randomised clinical trial were more likely than those who used NRT to maintain abstinence, as judged by consuming no more than five cigarettes two weeks after the quit date (18% vs 9.9%) (Hajek et al., 2019)

There are now a lot of laws pertaining to e-cigarette use. A regulatory framework under the EU Tobacco Product Directive was established in 2014, permitting the regulation of

e-cigarettes with a nicotine content of up to 20 mg/mL as consumer products. The sale of e-cigarettes with a nicotine content greater than 20 mg/mL necessitates a medical license, and the promotion of e-cigarettes is limited to point-of-sale or local advertisements, such as billboards. (Tobacco Product Directive, 2014). In 2015, the Nicotine inhaling product regulation prohibited the sale of e-cigarettes to persons aged under 18 (UK Statutory Instrument, 2015). Recently, the Tobacco and Vapes bill which seeks to make it an offence to proxy purchase or sell tobacco containing product to people born after the 1st of January 2009 was introduced and is currently at its report stage in the House of Commons (Tobacco and Vapes Bill, 2024)

### 1.1.3. IMPACT OF E-CIGARETTE SMOKING ON HEALTH

There is growing evidence suggesting that e-cigarettes may offer a less harmful alternative to traditional cigarettes, primarily because they circumvent the generation of tar, a complex mixture of carcinogenic compounds produced during tobacco combustion (Lee, 2018; Zhao et al., 2020). E-liquids, the substances vaporized in e-cigarettes, typically contain a base mixture of propylene glycol (PG) and vegetable glycerine (VG), nicotine, and a wide array of flavouring chemicals. PG and VG are commonly used humectants in food and pharmaceutical products and are generally regarded as safe for ingestion by the U.S. Food and Drug Administration (FDA). However, their physicochemical transformations during high-temperature aerosolization result in the formation of numerous degradation products that may be harmful to respiratory and cellular health (Jaegers et al., 2021; Ruth et al., 2023; Ebersole et al., 2020; Chen et al., 2018).

One of the major scientific challenges in evaluating the health effects of e-cigarettes lies in the substantial variability of e-liquid formulations, especially the PG to VG ratio. This ratio not only influences user experience but also determines the physicochemical properties, aerosol composition, nicotine, flavour delivery, and biological effects of the inhaled vapor. PG, a low-viscosity, highly volatile compound, produces smaller aerosol particles, a sharper throat hit, and is a more efficient carrier of both nicotine and flavour compounds, delivering them rapidly and with higher intensity (Spindle et al., 2018; Talih et al., 2020). In contrast, VG, which is more viscous and less volatile, generates larger aerosol particles and denser vapor clouds, but carries less nicotine and weaker flavour intensity due to its molecular structure

and slower evaporation (Baassiri et al., 2017; Son et al., 2020a). These physical differences significantly affect the thermal degradation pathways. Both PG and VG, when heated during vaping, can break down into toxic carbonyl compounds such as formaldehyde, acetaldehyde, and acrolein (Kosmider et al., 2014; Tayyarah and Long, 2014; Bekki et al., 2014; Hutzler et al., 2014; Goniewicz et al., 2014). VG-dominant mixtures tend to produce higher levels of acrolein, especially under conditions of high power or prolonged puff duration whereas PG-rich liquids generally yield more formaldehyde and acetaldehyde, although these levels vary with device temperature and coil condition (Wang et al., 2017).

At the cellular level, these degradation products and aerosols have measurable biological effects. VG-dominant aerosols have been associated with impairing mucociliary clearance, increased oxidative stress and inflammation, elevated expression of MMP-9, a protease linked to airway remodelling and chronic respiratory disease (Kim et al., 2022). On the other hand, PG-dominant aerosols tend to exhibit greater acute cytotoxicity in vitro cell cycle disruption and reduced epithelial cell viability (Komura et al., 2022).

Nicotine concentrations in e-liquids also vary widely, from zero to as high as 20 mg/mL in nicotine salt formulations. High concentrations of nicotine can alter the boiling point of the e-liquid and affect the rate and extent of thermal decomposition (Duell et al., 2018). Nicotine itself can oxidize or degrade to produce nitrosamines and other harmful compounds under high-temperature conditions (Son et al., 2018).

Additionally, flavouring agents introduce another layer of complexity. E-liquids are available in many flavour combinations, many of which contain aldehydes, ketones, esters, and other organic compounds which can be harmful to health when thermally decomposed (Behar et al., 2018; Omaiye et al., 2019). For instance, diacetyl, a buttery flavouring agent detected in flavoured e-cigarettes has been linked to bronchiolitis obliterans (Allen et al., 2016; van Rooy et al., 2007; Kreiss, 2014; Omaiye et al., 2019). Other flavouring chemicals, including cinnamaldehyde, benzaldehyde, and vanillin, present distinct hazards. Cinnamaldehyde has been demonstrated to be cytotoxic, promotes the generation of ROS in cells, and has been shown to impair ciliary motility (Behar et al., 2018, 2016; Clapp et al., 2019, 2017; Wavreil and Heggland, 2019). Other aldehyde-based flavourings can react with PG under heating conditions to form PG acetals (Erythropel et al., 2018; Jabba et al., 2020). Vanillin and

benzaldehyde derived PG acetals have both been demonstrated to exert cytotoxic effects (Jabba et al., 2020) .

In addition to chemical variability, the diversity of e-cigarette device designs significantly influences the composition of the aerosol generated. Key device characteristics such as coil material, resistance, wicking efficiency, and battery power affect the heating rate and maximum temperature reached during operation (Cirillo et al., 2019; Son et al., 2020b), for example, sub-ohm devices that operate at high wattages (e.g., >40W) can cause rapid heating of the e-liquid, increasing the likelihood of producing harmful thermal degradation products such as formaldehyde and acrolein (Chen et al., 2018; Li, 2021). Temperature-control features can also alter the aerosol composition. Devices that allow the user to adjust wattage or voltage may change the thermal profile mid-use, which in turn can affect the volatility of components and the resulting health consequences (Son et al., 2019) . Studies have shown that the same e-liquid can produce markedly different chemical profiles when vaporized in two different devices, even under otherwise controlled laboratory conditions (Uchiyama et al., 2020).

Additionally, device wear and tear such as coil state, residue buildup and vaper behaviour for instance in dry hitting where vaping is continued even when the e liquid in the coil is low can influence the production of heavy metals or catalyse additional reactions, adding another unpredictable layer to the vapor's chemical makeup (Beard et al., 2024; Shi et al., 2022).

While e-cigarettes are widely viewed as a potentially safer alternative to smoking, the scientific assessment of their health impacts is severely complicated by multiple layers of variability. The wide range of e-liquid formulations, the diverse array of flavouring compounds and the heterogeneity of device designs collectively make it challenging to establish standardized research protocols or draw generalizable conclusions about safety.

To accurately assess the long-term risks of e-cigarette use, future research must account for these confounding factors by using well-characterized products, consistent methodologies, and robust chemical analytics. Moreover, regulatory efforts should focus on ingredient disclosure and product standardization to support not only transparent and reproducible research but also safety of users. A widely recognized example illustrating the importance of

such measures is the 2019 outbreak of e-cigarette or vaping product use-associated lung injury (EVALI), a severe respiratory condition characterized by acute onset of symptoms such as dyspnea, chest pain, cough, and hypoxemia, often accompanied by gastrointestinal manifestations including abdominal pain, nausea, and vomiting (Winnicka and Shenoy, 2020). Diagnostic criteria included a history of vaping within the previous 90 days, characteristic radiographic findings, and the exclusion of alternative causes such as infection or other forms of respiratory failure. In the United States, the Centers for Disease Control and Prevention (CDC) reported 2,807 hospitalizations and 68 deaths during the outbreak, with vitamin E acetate in illicit THC-containing cartridges identified as the primary causative agent, although some evidence suggested THC vaping itself as a key factor (CDC, 2020; Werner et al., 2020; Blount et al., 2020). In contrast, the UK has reported very few EVALI cases, with no confirmed incidents linked to nicotine containing e-liquids sold through regulated channels, highlighting the protective impact of stringent ingredient controls and market regulation (Evans et al., 2021). The EVALI outbreak underscores both the potential acute harms of poorly regulated products and the existing knowledge gaps surrounding the health impacts of e-cigarette use (Werner et al., 2020; Marrocco et al., 2022; Layden et al., 2020)

## 1.2. SMOKING, VAPING AND LUNG HEALTH

### 1.2.1. AIRWAY HYPERRESPONSIVENESS: INFLUENCE OF SMOKING AND VAPING

Smoking and vaping each have profound implications for lung health. While the detrimental effects of cigarette smoking have been extensively studied over several decades, evidence is increasingly showing that e-cigarette use also contributes to adverse respiratory outcomes. Both practices compromise respiratory health through overlapping and distinct mechanisms that lead to airway hyperresponsiveness (AHR) and chronic diseases such COPD (Sompa et al., 2025; Sutherland and Martin, 2003; Willemse et al., 2004).

AHR refers to an exaggerated constrictive response of the airways to a wide range of stimuli, including allergens, irritants, cold air, and exercise (O'Byrne and Inman, 2003). Although AHR can occur after acute exposure to inhaled irritants, in healthy individuals this reaction is usually transient. The airway epithelium repairs itself, inflammation subsides, and airway tone returns to normal once the exposure ends (Gorguner and Akgun, 2010; Tuck et al., 2008). With chronic or repeated exposure to cigarette smoke or e-cigarette aerosols,

however, these repair mechanisms become dysregulated, and the airways remain in a state of heightened sensitivity (Takeda et al., 2009) .

At the centre of this process is airway epithelial injury. The epithelium, which serves as the first line of defence, is repeatedly damaged by toxins such as nicotine, aldehydes, and volatile organic compounds present in both cigarette smoke and e-cigarette aerosols (Park et al., 2022; Adam et al., 2025). Ongoing injury disrupts epithelial barrier integrity and impairs mucociliary clearance, which allows deeper penetration of harmful substances and pathogens (Carlier et al., 2021; Chung et al., 2019). This persistent insult promotes chronic inflammation as neutrophils, macrophages, and lymphocytes infiltrate the airway wall and release cytokines, chemokines, and proteases that degrade airway tissue (CDC, 2010). At the same time, reactive oxygen species generated by smoke or aerosol exposure amplify oxidative stress, leading to DNA and protein injury, apoptosis, and activation of inflammatory signalling pathways. Repeated exposure also induces hypertrophy and hyperplasia of airway smooth muscle, making the airways more contractile and reactive to even minor stimuli (Dutta et al., 2024). In addition, airway sensory nerves become sensitized, particularly through cholinergic pathways, resulting in excessive acetylcholine release that promotes smooth muscle contraction, mucus hypersecretion, and chronic cough reflex hypersensitivity. Over time, abnormal repair responses produce structural remodelling of the airway wall, with basement membrane thickening, collagen deposition, and goblet cell hyperplasia, all of which fix the airways in a hyperresponsive state (Aslaner et al., 2022; Higham et al., 2022; Gorguner and Akgun, 2010; Yang et al., 2025) .

The presence of AHR worsens a variety of respiratory conditions by amplifying inflammation, restricting airflow, and accelerating structural remodelling. In asthma, smoking and vaping exacerbate disease activity by enhancing eosinophilic and neutrophilic infiltration, increasing smooth muscle contractility, and reducing responsiveness to corticosteroid therapy. This results in more severe symptoms and more frequent exacerbations, complicating disease management (Taha et al., 2020; Spears et al., 2013; Invernizzi et al., 2009; Kotoulas et al., 2021). In COPD, persistent AHR contributes to progressive airflow limitation by driving chronic inflammation, remodelling of small airways, excessive mucus production, and destruction of alveolar walls leading to emphysema (Perng and Chen, 2017; Zanini et al., 2015; Barnes et al., 2003). Patients with COPD frequently display bronchial

hyperresponsiveness to nonspecific stimuli, which correlates with accelerated disease progression and higher exacerbation risk (Snoeck-Stroband et al., 2006).

Other chronic lung conditions are also affected. Interstitial lung diseases such as respiratory bronchiolitis-associated ILD, idiopathic pulmonary fibrosis, and desquamative interstitial pneumonia have been linked to smoking and vaping (Selman, 2003; Flower et al., 2017). Although these primarily affect the lung parenchyma, AHR contributes to symptoms such as cough and dyspnoea (Sieminska and Kuziemski, 2014). Persistent oxidative stress and inflammation further exacerbate alveolar damage and promote fibrotic remodelling, leading to a progressive loss of lung elasticity and diffusion capacity (Makena et al., 2023; Fois et al., 2018; Hu et al., 2024). Through persistent epithelial damage and inflammation, AHR also helps establish a microenvironment that promotes lung carcinogenesis, characterized by enhanced DNA damage, abnormal cell proliferation, neovascularisation, and impaired antitumour immunity (Beaver et al., 2009; Zhao et al., 2021).

Furthermore, smoking and vaping induced AHR weakens host defence mechanisms, increasing susceptibility to respiratory infections such as bacterial pneumonia, viral bronchitis, and exacerbations of chronic lung disease. This occurs because the inflammatory milieu disrupts macrophage and neutrophil function and compromises mucosal immunity, allowing pathogens to colonize more easily (Jansen et al., 1999; Sompa et al., 2025).

### 1.2.2. CHRONIC OBSTRUCTIVE PULMONARY DISEASE

As defined by the GOLD initiative, COPD is a heterogenous lung condition characterized by persistent respiratory symptoms and airflow limitation due to abnormalities in the airways and/or alveoli, often caused by significant and prolonged exposure to noxious particles or gases. This typically worsens over time and cannot be completely reversed (GOLD, 2025).

COPD encompasses a wide range of conditions that induce inflammation of the airways and have systemic effects and complications (Decramer et al., 2008). In 2019, the Global Burden of Disease Study 2016 projected that 251 million individuals suffer from Chronic Obstructive Pulmonary Disease, and it was the fourth major reason for mortalities in those aged fifty to seventy-four years and the 3rd top reason for mortalities in people of age greater than 75 years (GBD 2015 Chronic Respiratory Disease Collaborators, 2017).

The World Health Organization estimates that 80 million people globally have moderate-to-severe COPD. More than 3 million people died from COPD in 2005; this condition accounts for 5% of adult deaths globally and was predicted to become the third most common cause of death by 2020 (WHO, n.d.). Many people with the disease go untreated for extended periods of time, resulting in more severe symptoms, a lower quality of life, and an earlier death (Ko et al., 2008). Tobacco smoking, either actively or through second-hand smoke is a primary risk factor in the development of COPD (Buist et al., 2008) . Research indicates that after 25 years of smoking, up to 40% of smokers acquire COPD (Løkke et al., 2006) rising to 50% in older smokers (Lundbäck et al., 2003). The incidence of COPD is further influenced by additional variables, such as alpha 1 antitrypsin deficiency, air pollution, and occupational exposure to chemicals, dust, and pollutants.(Jindal et al., 2006)

Even though traditional smoking is considered a main cause of COPD (Forey et al., 2011), the connection between e-cigarettes and the threat of developing COPD is not unfounded. According to earlier research conducted in the US, the use of e-cigarettes was confirmed as an independent risk factor in developing emphysema and chronic bronchitis when compared with non-smokers, with the risk increasing in dual users of both e-cigarettes and conventional cigarettes (Bhatta and Glantz, 2020). Nicotine in e-cigarettes is also linked to airway hyper-responsiveness, lung tissue damage and increased release of pro-inflammatory cytokines IL-6 and IL-8, all of which are classical symptoms observed in COPD (Garcia-Arcos et al., 2016). Compared with cigarette smoking however, these pathophysiological changes are not as severe and longitudinal studies of COPD patients who transitioned to e-cigarettes show a considerable improvement in lung function and a large decrease in exacerbations (Polosa et al., 2020).

### 1.3. THE DPP FAMILY IN LUNG INFLAMMATION: AN OVERVIEW

The dipeptidyl peptidase (DPP) family belong to the S9B serine protease subfamily (clan SC, family SB) and is characterised by a conserved β-propeller domain and α/β-hydrolase fold. Although structurally related, individual members differ in enzymatic activity and physiological function. DPP4 is catalytically active and best known for its capacity to cleave dipeptides from the N-terminus of polypeptides, particularly when proline or alanine is in the penultimate position (Thoma et al., 2003). In contrast, DPP6 and DPP10 lack enzymatic

activity owing to substitutions within their catalytic triads (Yokotani et al., 1993) but remain functionally important as ancillary subunits of voltage-gated potassium channels of the Kv4 family (Lin et al., 2013, 2018). Collectively, these enzymes and pseudoproteases may contribute to lung inflammation both by regulating immune signalling and by influencing airway excitability.

DPP4 (also known as CD26) plays a central role in shaping immune and inflammatory responses in the lungs. It truncates a wide range of chemokines, including CXCL12, CXCL10 and CCL5, thereby altering chemotaxis (Proost et al., 1999), receptor binding and receptor antagonism (Lambeir et al., 2001; Metzemaekers et al., 2016). These modifications can profoundly affect the recruitment and activation of leukocytes during pulmonary inflammation. DPP4 is also widely expressed in lung epithelial and endothelial cells (Abbott et al., 1994; Gorrell et al., 1991; Mattern et al., 1991), as well as in immune cells such as macrophages and T lymphocytes (Lee et al., 2013). On activated T cells, it provides costimulatory signals that enhance Th1 cytokine production, including interferon-γ, tumour necrosis factor-α and interleukin-6 (Tanaka et al., 1994; Ohnuma et al., 2001; Pacheco et al., 2005; Ohnuma et al., 2005; Kei et al., 2004; Ohnuma et al., 2007). Through this dual role of chemokine cleavage and immune cell activation, DPP4 may contribute directly to the propagation of chronic inflammation in diseases such as COPD, asthma and acute lung injury.

Unlike DPP4, DPP6 and DPP10 do not possess catalytic activity but may influence pulmonary physiology indirectly by modulating Kv4 potassium channels. DPP6 has been shown to interact with Kv4.2 channels, regulating gating kinetics, channel assembly and trafficking (Lin et al., 2014; Nadal et al., 2003), processes that affect neuronal excitability and airway nerve signaling (Lin et al., 2013, 2018). In the context of lung inflammation, this is relevant because heightened excitability of airway nerves contributes to cough reflexes and airway hyperresponsiveness, both of which are cardinal features of chronic inflammatory airway disease.

DPP10 shares structural similarity with both DPP4 and DPP6 but is rendered catalytically inactive by the substitution of the catalytic serine with glycine in its nucleophile elbow. Structural studies suggest that substrate access to its active site is also restricted compared to DPP4, reinforcing its lack of proteolytic activity (Bezerra et al., 2015). Despite this, DPP10

functions as a component of the Kv4 channel complex. Co-expression of DPP10 with Kv4.2 enhances channel trafficking to the cell membrane, increases peak current, accelerates activation, and modifies recovery from inactivation (Jerng et al., 2004; Pongs and Schwarz, 2010). These modifications of A-type potassium currents, which are key regulators of excitability in neurons and potentially airway nerves, may contribute to altered airway responsiveness during inflammation. Although DPP10 is expressed most strongly in the brain and adrenal gland, it is also detectable in airway tissue (Allen et al., 2003), highlighting its potential relevance to pulmonary disease.

Taken together, the DPP family integrates two complementary mechanisms relevant to lung inflammation: enzymatic cleavage of chemokines and modulation of immune cell responses by DPP4, and regulation of Kv4 channel activity by DPP6 and DPP10. These combined functions link the family to both immune dysregulation and airway hyperresponsiveness, positioning DPPs as important contributors to the pathogenesis of chronic lung diseases such as COPD and asthma, as well as to smoke- and vape-induced airway injury.

## 1.4. DPP10: EMERGING EVIDENCE IN LUNG INFLAMMATION

After DPP10 was identified as an asthma susceptibility gene (Wu et al., 2010), many studies have sought to determine the exact role of DPP10 in asthma and other chronic lung disease associated with airway hyperresponsiveness. Point mutation on the β-propeller region of DPP10 significantly increases total serum IgE level, bronchoalveolar lavage eosinophil count and airway hyperresponsiveness to methacholine in HDM treated mutant mice when compared with wild type mice, confirming that DPP10 does play a protective role in asthma. In asthmatic patients, DPP10 has been observed to have altered expression. Knockdown of DPP10 can alter cytokine response and mitigate the activation of the glucocorticoid receptor by dexamethasone in bronchial epithelial cells (Zhang et al., 2018)

The DPP family encodes a dipeptidyl peptidase, which can cleave two peptides from N-termini of certain proinflammatory chemokines, however, this enzymatic activity does not occur in DPP10 due to the loss of the active serine residue, so it is unclear how this gene is able to mitigate cytokine response.

Significant association between polymorphic marker DPP10, rs10208402 with IgE, percentage eosinophils, and also a moderate association between DPP10 rs1430090 and FEV1 in Han Chinese ethnicity. Both SNPs located on intron 1a and 2 respectively. Specifically, the haplotype rs1430090-D2S308 showed positive association with asthma severity in German children. This SNP rs1430090 was also indicated to affect DPP10 expression by altering the sequence of CdxA, a known promoter element (Gao et al., 2010)

Dietary poly unsaturated fatty acid (PUFA) are often used to improve the quality of life with patients with disease involving systemic inflammation such as COPD and other chronic diseases of the lungs. In an investigation on association of plasma phospholipid or red blood cell measured nPUFA with spirometric measures of pulmonary function test, a novel DPP10 intronic SNP rs1169332 having an association with FVC was discovered. rs1169332 associated with an 88.6mL reduction in FVC at DHA level of 2% total fatty acid, however, at 4% DHA level, this association shifted to a 16.2mL reduction in FVC, indicating an attenuation by higher DHA levels. (Xu et al., 2019)

Genetic variation within DPP10 has been implicated in a range of airway disease related phenotypes. Reported associations include lung function (FEV1) in asthma and COPD (Poon et al., 2014), as well as immunological traits such as log-transformed total IgE levels and eosinophil percentage, supporting a role in allergic inflammatory pathways (Gao et al., 2010). Furthermore, the SNP rs1019293, located ~4 kb upstream of the D2S308 locus, has shown strong association with asthma in a Caucasian cohort (Allen et al., 2003) and has also been linked to bronchial hyperresponsiveness and asthma (Zhou et al., 2009).

EWAS studies using microarrays demonstrates CpG sites mapped to DPP10 as one of the top differentially methylated sites in foetal lung tissue exposed to nicotine (Chhabra et al., 2014). DPP10 appears to be involved in some way with not just chronic lung disease but also exposures such as nicotine that could contribute to chronic lung disease.

## 1.5. RESEARCH JUSTIFICATION

Despite substantial reductions in smoking prevalence, tobacco use remained responsible for an average of approximately 78,000 deaths per year in the UK between 2009 and 2019 (NHS

Digital, 2020). Importantly, smoking related pathologies, frequently persist following cessation (Oelsner et al., 2020; Serapinas et al., 2011; Wang et al., 2022a), highlighting the long-term biological impact of exposure. Concurrently, the rapid uptake of e-cigarettes as a perceived alternative with reduced harm has introduced new uncertainties, given that the health effects of their solvents, flavourings, and additives are not yet fully characterised. This underscores the need for genetic and molecular level investigations to identify early disease mechanisms, potential prognostic markers and impact.

Given prior evidence identifying DPP10 as an asthma susceptibility locus with putative protective effects, it represents a compelling candidate gene for further investigation. Moreover, multiple genetic and epigenetic studies have linked structural variation and dysregulated DPP10 expression to diverse chronic inflammatory disorders with many aggravated by, or associated with, long-term tobacco exposure, supporting a focused examination of its regulatory mechanisms and disease relevance.

Despite being primarily investigated in the heart and brain as an auxiliary subunit and regulator of the ion-gated potassium channel Kv4.2, DPP10 was identified as an asthma susceptibility gene, prompting interest in its role in chronic lung disorders (Allen et al., 2003). This association has since been supported by multiple studies (Wu et al., 2010; Blakey et al., 2009; Zhou et al., 2009; Gao et al., 2010; Mathias et al., 2010). In a study by Zhang et al., (2018), a point mutation in the β-propeller region of DPP10 led to increased airway resistance and elevated serum IgE levels following house dust mite (HDM) exposure. Furthermore, given its established genetic association with asthma and related airway phenotypes, DPP10 has emerged as a candidate gene of interest in airway inflammatory disease mechanisms.

To investigate DPP10 expression in smokers, the search string “DPP10 AND smok*” was applied to Gene Expression Omnibus (GEO) profiles within the NCBI database. Mean expression levels were then calculated for both smokers and non-smoker control groups. This analysis revealed increased expression of DPP10 and its anti-sense RNAs (DPP10-AS1, DPP10-AS2 and DPP10-AS3) in smokers compared with non-smokers (Table 3). While the functions of DPP10-AS2 and DPP10-AS3 remain uncharacterised, DPP10-AS1 has been shown

to be highly expressed in cancer tissues, where it positively regulates DPP10 expression and modulates its epigenetic regulation (Tian et al., 2021; Liu et al., 2021).

*Table 3: Result from GEO profiles of GWAS conducted on smokers using micro arrays showing expression level of DPP10 compared with non-smokers. In all studies, there is an increase in DPP10 gene expression for smokers compared with non-smokers.*

| GEO | SAMPLE | GENE | GENE ID | EXPRESSION LEVEL | | REFERENCE |
|---|---|---|---|---|---|---|
| | | | | Smokers | Non-smokers | |
| GSE5059 | Large AE | DPP10 AS1 | 236351_at | 216.5 | 477.2 | (Carolan et al., 2006) |
| GSE4498 | Small AE | DPP10 AS2 | 236351_at | 70.4 | 81.3 | (Harvey et al., 2007) |
| GSE5059 | Large AE | DPP10 | 228598_at | 126 | 188 | (Carolan et al., 2006) |
| GSE6264 | Lymphoblast | DPP10 | 136651 | 0.6 | 1 | (Philibert et al., 2007) |
| GSE4498 | small AE | DPP10 | 228598_at | 15.5 | 20.2 | (Harvey et al., 2007) |
| GSE6264 | Lymphoblast | DPP10 AS1 | 192861 | 0.17 | 0.33 | (Philibert et al., 2007) |
| GSE6264 | Lymphoblast | DPP10 | 173951 | 0.11 | 0.14 | (Philibert et al., 2007) |
| GSE2125 | Alveolar Macrophage | DPP10 | 228598_at | 5.3 | 5.2 | (Woodruff et al., 2005) |
| GSE2125 | Alveolar Macrophage | DPP10 AS3 | 1561618_at | 6.6 | 6.5 | (Woodruff et al., 2005) |
| GSE7434 | Placenta | DPP10 AS1 | 236351_at | 0.9 | 1.1 | (Huuskonen et al., 2008) |
| GSE7434 | Placenta | DPP10 | 228598_at | 0.17 | 0.24 | (Huuskonen et al., 2008) |
| GSE7434 | Placenta | DPP10 AS3 | 1561618_at | 0.25 | 0.24 | (Huuskonen et al., 2008) |
| GSE17913 | Oral mucosa | DPP10 AS1 | 236351_at | 10.1 | 10.2 | (Jo et al., 2010) |
| GSE17913 | Oral mucosa | DPP10 AS3 | 1561618_at | 10.1 | 10.3 | (Jo et al., 2010) |
| GSE17913 | Oral mucosa | DPP10 | 228598_at | 7.7 | 7.7 | (Jo et al., 2010) |
| GSE27272 | Maternal + Foetal cells | DPP10 | ILMN_1778425 | 1.75 | 1.74 | (Votavova et al., 2011) |
| GSE27272 | Maternal + Foetal cells | DPP10 | ILMN_1805039 | 1.73 | 1.78 | (Votavova et al., 2011) |
| GSE5372 | Airway Epithelium | DPP10 AS1 | 236351_at | 171 | 337.7 | (Heguy et al., 2007) |
| GSE5372 | Airway Epithelium | DPP10 | 228598_at | 89.5 | 158 | (Heguy et al., 2007) |

Two primary themes are being examined in this study. First off, what effects does vaping have on cell health—that is, on cell viability, apoptosis, cell death, and cell cycle—when using both nicotine and nicotine-free systems? How does it compare to smoking with a comparable nicotine profile, and how does it also impact the expression of pro-inflammatory cytokines,

which are indicators of chronic inflammatory lung disease? The aim is to investigate any negative impact that may arise from use of vehicle only e-cigarettes. The second focus of this research project is to examine the effects of smoking and vaping on DPP10 gene expression. It is hypothesized that this gene, which has been shown in the literature to be protective against airway hyperresponsiveness and differentially expressed in cigarette smoking, is also protective against these effects. The protective effect of DPP10 in smoking and vaping can be determined by using methods such as cell health assays, gene expression assays, protein quantification techniques, gene knockout, over-expression, and protein interactions in response to treatment.

## 2. LITERATURE REVIEW: STRUCTURE, FUNCTION AND DISEASE RELEVANCE OF DPP10

### 2.1. INTRODUCTION

DPP10 belong to a MEROPS subfamily of S9B serine protease (Clan SC, family SB). It is a single pass type II transmembrane protein with a very similar structure to both DPP4 and DPP6. The structure of DPP10 is made up of a cytoplasmic domain (residues 1-34), a transmembrane domain (residues 35-55) and an extracellular domain (residues 58-796). Within the extracellular domain lies a β-propeller (residues 82-517) which is also made up of 8 blades each having 4 anti-parallel β-sheets as observed in DPP4, an α/β-hydrolase situated at position 517-679 and 707-796 and an extended arm which lies between the α/β-hydrolase and β-propeller. The small extended arm comprises of 3 α-helices inserted between 2 β-strands of the α/β-hydrolase domain and occupies position 679-707 Fig 7 (Bezerra et al., 2015).

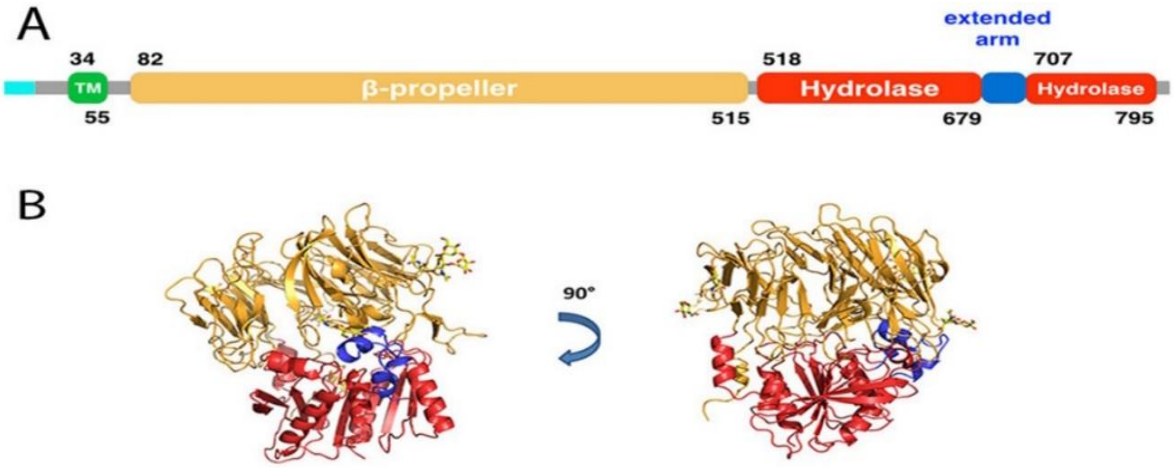


*Figure 1 DPP10 structure: Within the extracellular domain lies a β-propeller (residues 82-517) which is also made up of 8 blades each having 4 anti-parallel β-sheets as observed in DPP4, an α/β-hydrolase situated at position 517-679 and 707-796 and an extended arm. (A) Schematic of DPP10 domain organization: cytoplasmic (cyan), transmembrane (green), β-propeller (yellow), α/β-hydrolase (red), extended arm (blue).(B) Cartoon of DPP10 structure using the same colour scheme; sugars shown as yellow sticks. (Bezerra et al., 2015)*

Analogous to the catalytic triad in DPP4 ($Ser_{640}$ $Asp_{708}$ $His_{740}$) is $Gly_{651}$ $His_{759}$ $Asp_{727}$. Here, the serine residue in the active site is replaced by a Glycine. The corresponding nucleophile elbow of GWSYG or $Gly_{638}Trp_{639}Ser_{640}Tyr_{641}Gly_{642}$ found in DPP4 is indicated by GKGYG or

$Gly_{649}Lys_{650}Gly_{651}Tyr_{652}Gly_{653}$ in DPP10. DPP10 is enzymatically inactive, and mutagenesis studies have shown that neither engineering the $Gly_{651}$ residue to →Ser nor double mutation of $Lys_{650}Gly_{651}$ → Trp-Ser to resemble the nucleophile elbow found in DPP4 restores any form of enzyme activity. The catalytic serine in DPP4 related protein is replaced by glycine in DPP10 causing a lack of peptidase activity.

Two (2) conserved glutamate residues responsible for N-anchor of incoming peptides and the oxy-anion hole make up the active site of DPP4. In DPP10, these analogous sites are also present and so a lack of enzyme activity through mutations within the nucleophile elbow suggests that other unknown factors contribute to the occurrence of enzyme activity even in DPP4. Entry and exit of substrates into a 30-45Å large cavity of active site in DPP4 have been established to occur via either a small bottom opening in the β-propeller domain or a larger side opening between α/β-hydrolase and β-propeller domains (Rasmussen et al., 2003), however this entrance is narrowed by half in DPP10 due to the presence of $Lys_{77}Glu_{763}$ originating from the α/β-hydrolase and $Lys_{126}$ from the β-propeller. In silico triple mutations of these sites showed opening to the active site demonstrating that access to the active site and not just the presence of a catalytic serine in the nucleophile elbow is required for enzyme activity (Chen et al., 2006). Dimer configuration is stabilized by interaction between β-propeller loops (in the β-propeller domain) and C-terminal loops in the α/β-hydrolase domain. This interaction is weaker in DPP10 where only 13 hydrogen bond and zero salt bridges are involved in the monomer interaction compared with DPP4 where 30 hydrogen bonds and 10 inter salt bridges are formed in this monomer interaction. Super imposition of DPP6 and DPP10 β-propeller loops indicate a possibility for hetero-oligomerization. Even though not all the residues within the β-propeller loops are conserved in both DPP6 and DPP10, the disparate amino acids contribute less to the interface. Compared with DPP4, there is less likelihood of it forming hetero-oligomers with DPP6 or DPP10 because of the presence of 2 additional residues in its β-propeller loop Fig.

Residues in the C-terminal loop which is the second major region for dimerization are even more conserved between DPP6 and DPP10 than residues in the β-propeller loop. Superimposed, this region results in a Ca-r.m.s.d. of 0.48 A˚ over 14 atoms. In contrast to DPP4, however, this area is responsible for the highest inconsistency involving dimer

interactions. In DPP4, 23 residues participate directly in the dimer formation, compared to 14 and 11 residues in DPP10 and DPP6 respectively (Bezerra et al., 2015)

DPP10 is expressed strongly in the brain, spinal cord, adrenal gland and pancreas, and less so in the liver, airways and placenta as shown in Figure 2 (Allen et al., 2003)

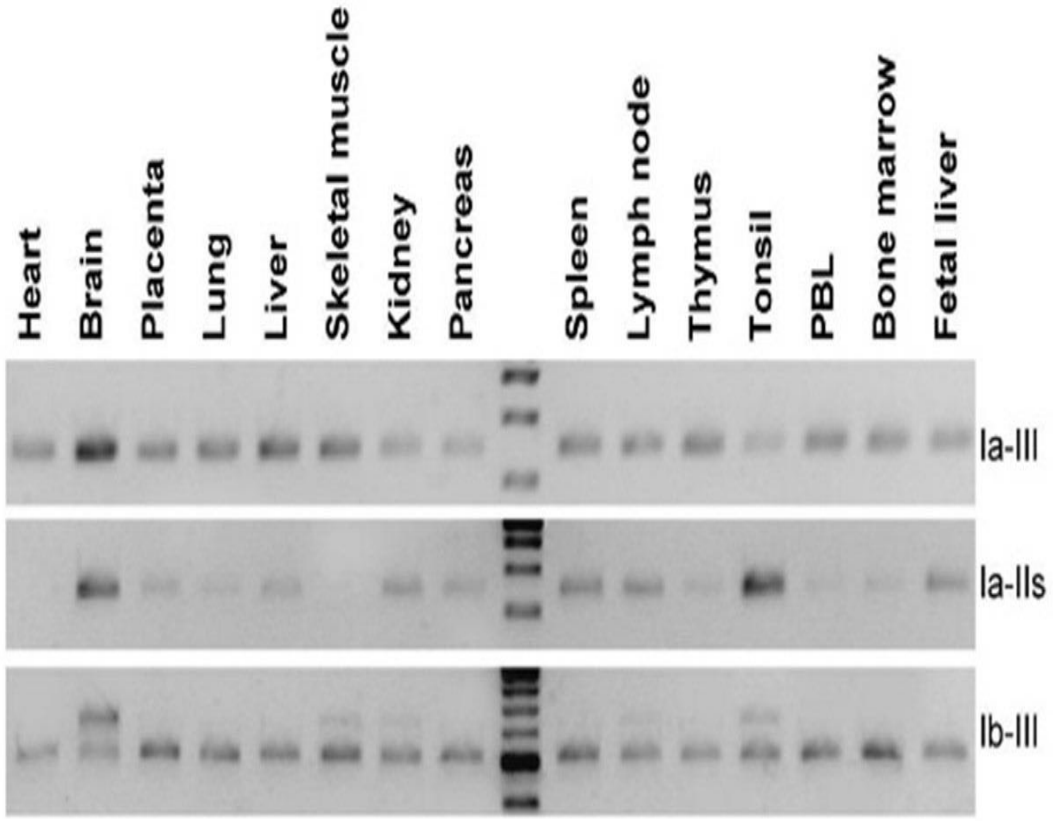


*Figure 2: Expression of DPP10. DPP10 is expressed majorly in the brain, but also in other organs including the heart, liver, lungs, pancreas and spleen (Allen et al., 2003)*

Although DPP10 shows relatively low expression in lung tissue, multiple lines of evidence, including genetic association studies identifying DPP10 as an asthma susceptibility locus and functional experiments demonstrating that DPP10 modulation alters airway responsiveness, inflammation, and cytokine signalling highlight its biological and clinical relevance to pulmonary disease (Zhang et al., 2018). In addition, epigenetic and transcriptomic studies link DPP10 and its antisense transcript) to environmental exposures. CpG sites mapped to DPP10 show differential methylation after in utero nicotine exposure suggesting DPP10 expression

and regulation are responsive to smoking (Chhabra et al., 2014). Furthermore, recent clinical and translational findings report altered DPP10 expression or in airway disease phenotypes reinforcing the case that DPP10 has pathophysiological relevance beyond its low mean expression in in the lungs (Sim et al., 2022).

DPP10 has been identified as a component of the Kv4 channel complex (Maffie and Rudy, 2008; Pongs and Schwarz, 2010; Jerng and Pfaffinger, 2014; Wang et al., 2015). Kv4 channels are a subtype of voltage gate potassium channel (Kv) expressed highly in the brain and heart. They are the key subunits that participate in sending transient outward, voltage-dependent potassium currents (A type) in the heart (Ito) or in the cell soma and dendrites of neurons ($I_{SA}$). A-type currents are rapidly activating and inactivating and have been majorly characterised in the CNS. Transgenic expression of this shal subtype potassium channel indicates that it inactivates rapidly following activation at subthreshold membrane potential and it recovers very quickly, hence the term transient currents (Covarrubias et al., 2008).

Immunofluorescence assay of CHO cells transfected with Kv4.2 demonstrate low level of Kv4.2 located mostly in the endoplasmic reticulum, which increases and is trafficked to the cell membrane in co-transfection with both Kv4.2 and DPP10. The kinetics of Kv4.2 is greatly altered in the presence of DPP10. Co- transfection with DPP10 also increased the peak current by more than 5 times (Erng et al., 2004) and reduced the time to peak by 9.2ms on depolarisation to 48mV. The macroscopic inactivation rate of transient A-type current is also decreased more than 3 folds by DPP10 when depolarised to 18mV. In CHO cells co-transfected with both DPP10 and Kv4.2, the rate of recovery from inactivation at -112v also reduced by 23ms when compared with single transfection with Kv4.2 alone. Further investigation to identify DPP10 domain responsible for Kv4.2 modulation confirm that both α/β-hydrolase and β-propeller play roles in Kv4.2 trafficking and modulation, albeit a small one. The interaction of DPP10 protein with Kv4.2 subunits is through the transmembrane domain and these interactions are important in channel structure modification (Zagha et al., 2005). Although the expression of Kv4.2 is markedly increased in the presence of DPP10, the expression of DPP10 is independent of Kv4.2 as co-expression with the ion channel does not affect DPP10 protein level. (Foeger et al., 2012)

To understand the role of DPP10 in modulation of the Kv channels, it is necessary to understand how the Kv channel's function, and their contribution to disease.

Kv CHANNELS

Kv channels are tetrameric and made of 4 α-subunits arranged symmetrically around a central pore. Each subunit is made up of an N-terminal cytoplasmic domain, a T1 tetramerization domain, 6 transmembrane α-helical domain (S1-S6), a p-loop between S5 and S6, and a C-terminal cytoplasmic domain (Fig 4)

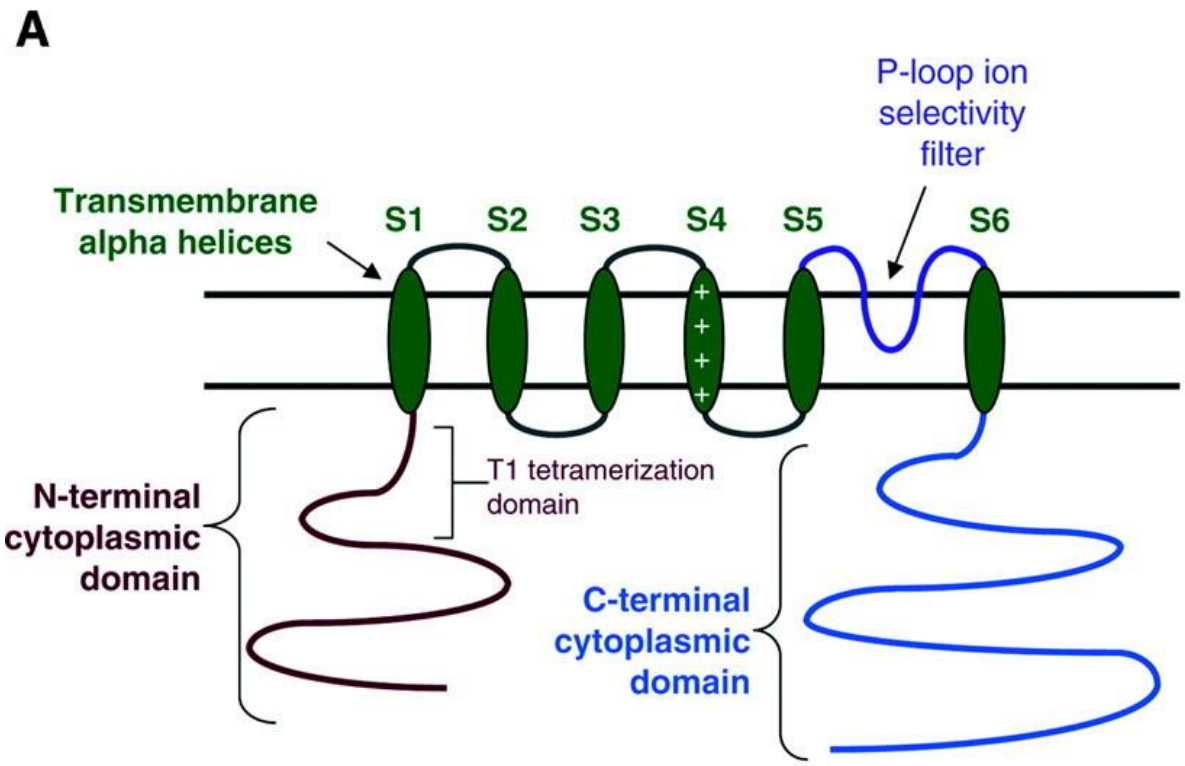


*Figure 3: Kv channel: The Kv channels are made up of an N-terminal cytoplasmic domain, a T1 tetramerization domain, 6 transmembrane α-helical domain and a C-terminal cytoplasmic domain (Birnbaum et al., 2004)*

The Kv channel domains can also be defined based on their function. Four transmembrane α-helices S1 S2 S3 and S4 make up the voltage sensing or regulatory domain. S5, S6 and the P-loop make up the pore forming domain which is structurally responsible for the opening and closing of the ion channel and movement of potassium ions across the cell membrane. In the resting state of the voltage gated channel, the electrical potential difference between the extracellular space and intracellular space is -65mV with the intracellular space having a more

negative electrical potential. During an action potential, this difference in electrical potential continues to reduce as more Na ions flow into the cells after the threshold potential is achieved. Further increase in electrical potential causes deactivation and closure of the Na channel, followed by opening of the Kv channels which are slower to respond to the action potential even though they have the same electrical potential threshold as Na ion channels. As Kv channels open, the efflux of K ions from the cells according to its concentration gradient leads to a more negative electrical potential difference and repolarisation of the ion channel (Grider et al., 2022) Fig 5

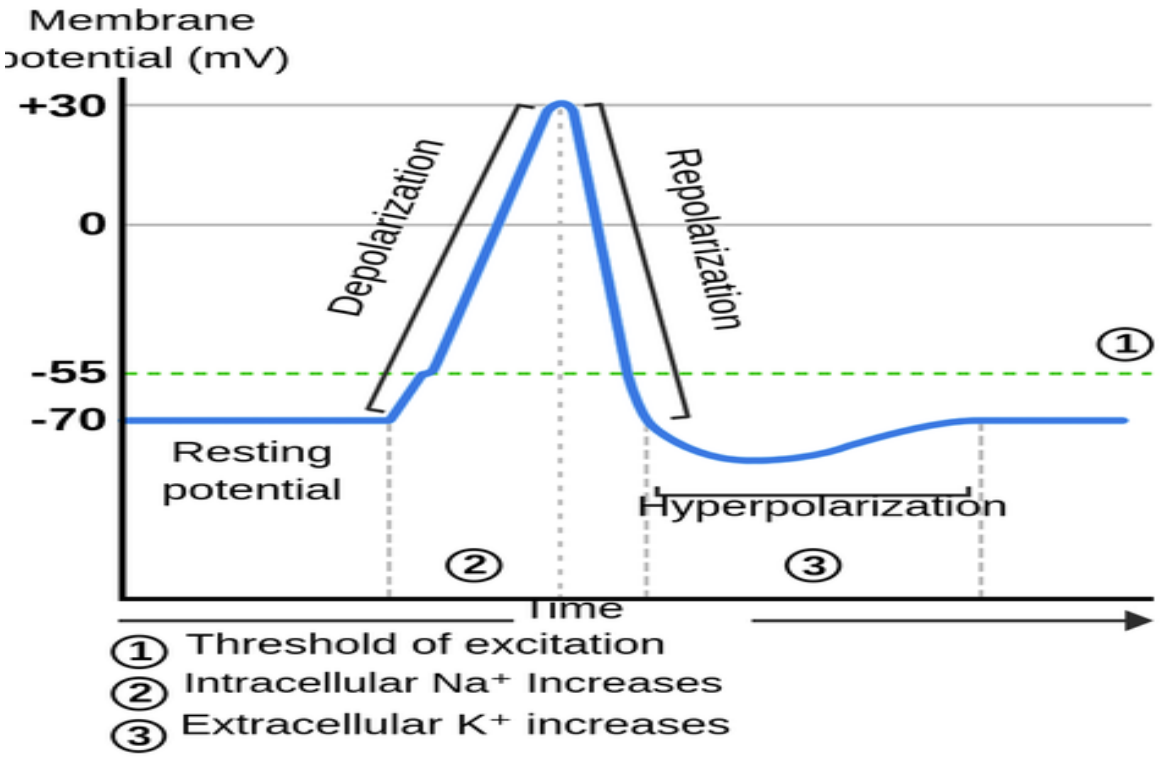


*Figure 4: Depolarisation of Kv channels. After depolarisation, as Kv channels open, the efflux of K ions from the cells according to its concentration gradient leads to a more negative electrical potential difference and repolarisation of the ion channel (Grider et al., 2022)*

The pore forming domain participate in opening and closing of the ion channel in response to activities in S4 within the voltage sensing domain. The presence of 4 positively charged amino acid residues on S4 pulls the S4 domain downwards towards the more negative electrical potential within the cells at its resting state causing the S6 domain to be pulled outwards and maintaining a closed configuration.  As the channels depolarise, the reduction in negative

charge within the cells cause the S4 domain to be pulled upwards and S6 domain pulled apart leading to an opening of the voltage gated potassium channel.

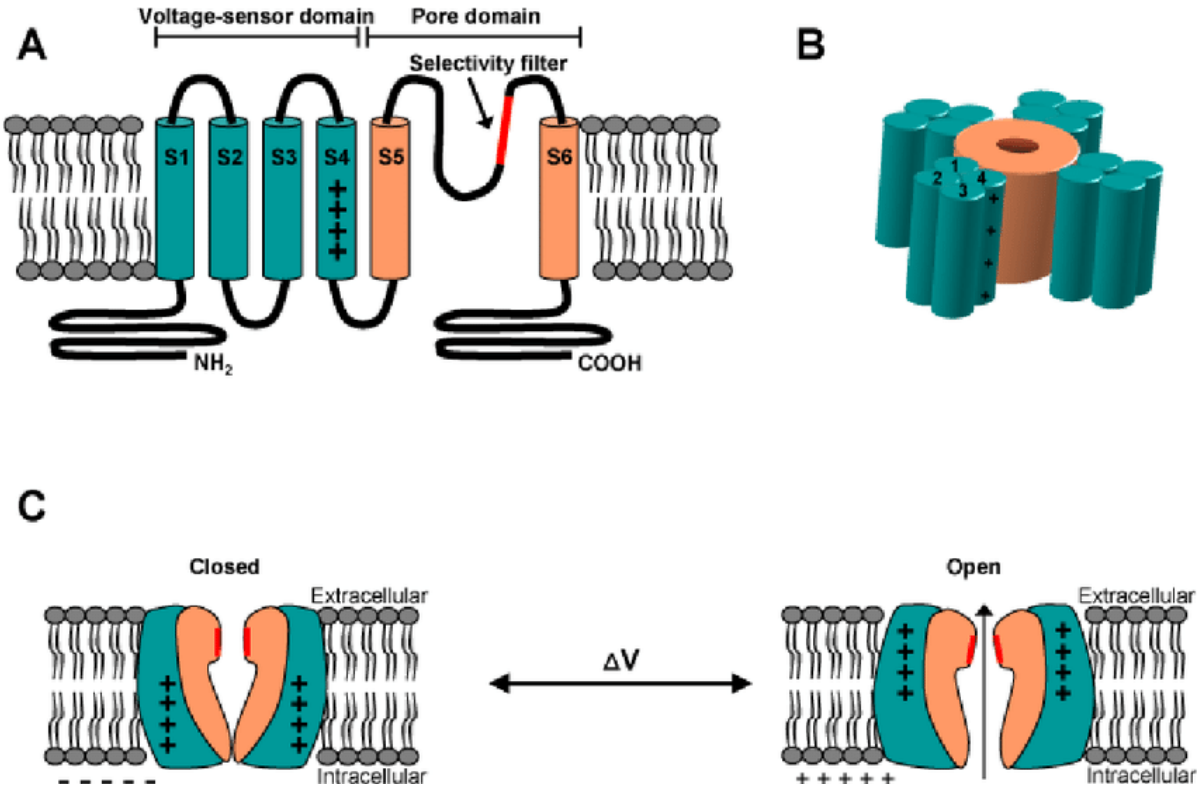


*Figure 5: Kv channel showing its closed and open state (Liin and Elinder, 2008)*

The Kv channels can form either homo-tetramers with α-subunit of the same sub family or form hetero-tetramers with α-subunits of 2 sub-families, each sub-family located diagonally. The tetramerization domain binds the 4 α-subunits of the Kv channels (Birnbaum et al., 2004). Kvs are regulated by ancillary subunits such as DPP6 and DPP10 which are bound to the T1 domain (in ratio 1:1), and use these ancillary subunits to achieve many of their biological functions (Jerng et al., 2004; Pongs and Schwarz, 2010). Ancillary subunits regulate Kv channel gating but can also have a high impact on channel assembly, trafficking to and from cellular surfaces, and on directing Kv channels to different compartments within the cell. The importance of the role of accessory subunits is further emphasized by the number of mutations that are associated in both humans and animals with diseases like hypertension, epilepsy, arrhythmogenesis, periodic paralysis, and hypothyroidism.

## 2.2. DPP10 IN OTHER DISEASES

DPP10 has been implicated in several pathological conditions, highlighting its potential importance beyond airway inflammation.

### CANCER

Altered DPP10 expression has been reported in various cancers. In colorectal cancer, DPP10 expression is often reduced or lost in tumour tissues compared with normal mucosa, and this downregulation correlates with poor prognosis (Park et al., 2013; Fraile et al., 2013). Additionally, the antisense long non-coding RNA *DPP10-AS1* appears to modulate cancer-related pathways by interacting with microRNAs and influencing adenyl cyclase signalling. While *DPP10-AS1* downregulation in colorectal cancer may have tumour-suppressive effects, its overexpression in lung cancer has been associated with increased tumour growth and poorer survival outcomes (Liu et al., 2021; Tian et al., 2021). Together, these findings suggest that DPP10 and its regulatory RNA transcripts may play tissue-specific roles in tumour progression.

### NEUROLOGICAL AND NEUROPSYCHIATRIC DISORDERS

DPP10 is highly expressed in the brain, where it modulates voltage-gated potassium channels and neuronal excitability. Genetic and epigenetic alterations in DPP10 have been linked to neuropsychiatric and neurodevelopmental disorders, including schizophrenia, bipolar disorder, autism spectrum disorder, and attention deficit hyperactivity disorder (Djurovic et al., 2010; Girirajan et al., 2013; Heinrich et al., 2017). DPP10 autoantibodies have also been detected in neurodegenerative diseases such as Alzheimer's disease, suggesting a possible immune-mediated role (Ohkawa et al., 2013; Chen et al., 2014).

### PAIN AND CHRONIC INFLAMMATION

DPP10, as part of the Kv4 channel complex (Kv4.3, DPP10, KCHIP1, KCHIP2), contributes to the regulation of pain sensitivity in sensory neurons. Knockout studies show that loss of DPP10 increases nociceptor hypersensitivity, while restoring complex components rescues function (Kuo et al., 2017). Serum DPP10 levels correlate with 15-HETE, an arachidonic acid metabolite involved in inflammatory signalling and modulated by COX1 inhibition (Wang et al., 2020a). Beyond neuronal regulation, DPP10 has been implicated in inflammatory bowel disease, with studies identifying it as a potential biomarker for ulcerative colitis. Its

expression correlates with immune cell infiltration and shows differential regulation in experimental models of colitis (He et al., 2022; Xu et al., 2019)

Although these studies explore DPP10 in different biological contexts, they collectively demonstrate that DPP10 is functionally versatile, affecting cell survival, signalling, and immune modulation. This supports the rationale for investigating its potential involvement in airway epithelial inflammatory responses to cigarette smoke and vaping exposure.

# 3. METHOD DEVELOPMENT

This chapter details the development and optimization of a novel method for the generation of cigarette smoke extract (CSE) and vape smoke extract (VE) suitable for application in in-vitro cell culture systems. The motivation for this work stems from the need for a consistent, reproducible, and physiologically relevant approach to model cigarette smoke exposure under controlled laboratory conditions. Traditional methods for producing CSE can show high variability in composition and biological activity (Agraval et al., 2022), which can compromise the reliability and comparability of experimental results.

In this chapter, the design, validation, and standardization of a smoke extraction system that enables the efficient capture of cigarette smoke components into a cell culture medium are described. Key parameters such as extraction time and pattern, nicotine content, and storage stability were systematically evaluated to ensure both experimental reproducibility and biological relevance. The resulting optimized protocol provides a robust foundation for the experimental studies presented in the subsequent chapters.

The initial step in this research was to create a technique for extracting vape and cigarette smoke into culture medium. Using a combination of UV absorbance measurement, nicotine content in both cigarettes and nicotine-vape, and the volume of vape liquid extracted between nicotine and nicotine-free vapes, the concentration of extract between cigarette smoke and vape was normalized. The approach was subsequently confirmed using a cell health assay to measure the toxicity level of the extracts and ensure that the potency of extracts was the same across different extraction periods.

The cell health assay also guided the choice of concentration of extracts to use for further analysis. A 25–35% decrease in cell viability show that changes have taken place within the cells, even though the cells have not fully entered apoptosis. Therefore, the concentration of extracts resulting in 65-75% cell viability was examined. After determining the cell lines' viability, baseline research was carried out to investigate the expression of DPP10, and pro inflammatory cytokines by the airway epithelial cells in response to stimulation with CSE and VE. To ascertain whether DPP10 is involved in pro-inflammatory cytokine gene expression and protein production, cytokine expression under DPP10 gene knockdown and over

expression were investigated. A combination of q-PCR, western blot, flow cytometry and ELISA were used in this study.

## 3.1. INTRODUCTION

Two main models are employed in the literature to investigate the effects of vaping and cigarette smoking on respiratory system epithelial cells in vitro. Airway epithelial cells (AEC) are cultured in cell culture flasks using media that has had cigarette smoke extract diluted as part of the submerged culture technique. The air liquid interface (ALI) culture procedure involves cells grown on a permeable cell culture insert being directly exposed to the cigarette or e-cigarette vapour. AECs are defined by 2 distinct layers, the apical which is free and faces the external environment, and a basal layer which is attached to the extra cellular matrix. The peculiarity of ALI culture is that the basal surface of the cells is in contact with liquid culture medium, while the apical surface is exposed to smoke.

A common method employed is to first expand the AEC in culture flasks then seed them onto a porous cell culture insert. These inserts have 2 compartments; the apical compartments where the cells are seeded and the basal compartment. At first, both compartments are supplied with specific culture medium. Once the cells reach confluency, the cells are subjected to a process known as air lifting where only the basal chamber is supplied with culture medium and the apical chamber where the apical layer of the cells are exposed is supplied with the smoke. This conformation imitates conditions found in the human airway and propels differentiation towards a mucociliary phenotype.

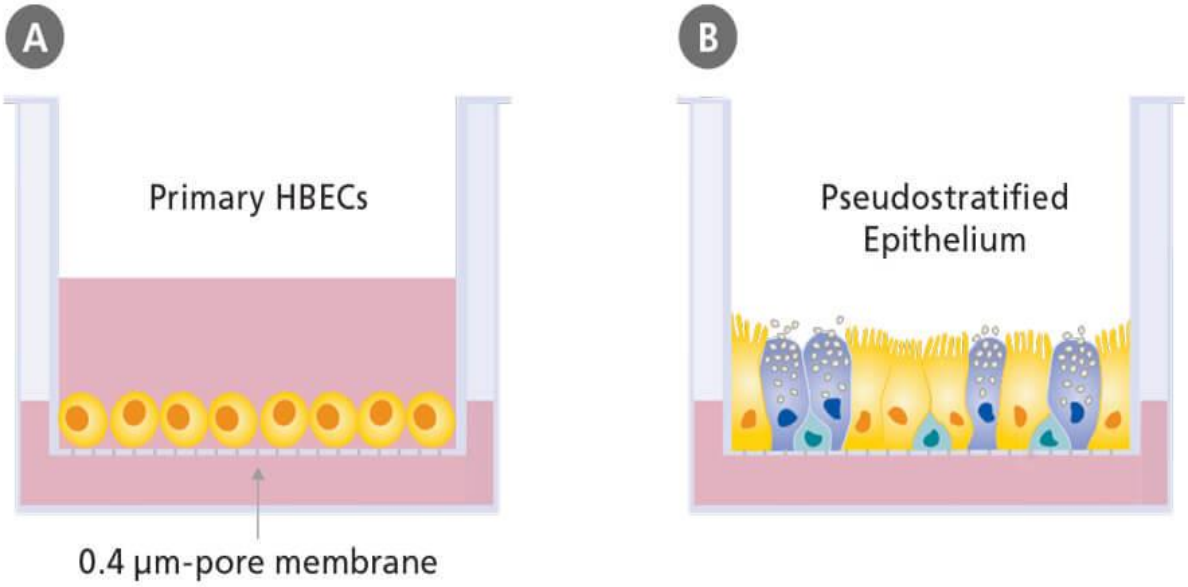


*Figure 6: Differences between submerged and ALI culture. A. Cells are grown in culture flasks in culture medium. B. Cells are grown on special inserts with the basal layer in contact with media and the apical layer is exposed to air. (STEMCELL TECHNOLOGIES, n.d.*

ALI culture of AEC continues to gain increasing recognition as a system that facilitates physiologically relevant respiratory research. AECs cultured at the ALI undergo extensive muco-ciliary differentiation, resulting in an in vitro model that best represents the in vivo environment. Numerous studies have shown significant similarities between cells cultured at ALI and AEC in-vivo. One example is the presence of a pseudostratified morphology and the heterogenous cell population including ciliated and mucus secreting cells found in both systems (Xue et al., 2015; Delgado-Ortega et al., 2014; Grainger et al., 2006), another similarity between these systems are the development of epithelial barrier functions as indicated by the expression of tight junction proteins and the development of high transepithelial electrical resistance (TEER) (O'Boyle et al., 2017; Lee et al., 2005b). TEER measures are widely used as a strong indicator of barrier permeability and integrity prior to evaluation for transport of drugs or chemicals (Srinivasan et al., 2015). Transcriptome analysis of cells cultured in ALI also show a strong correlation to cells in-vivo (Ghosh et al., 2020; Abo et al., 2022) thus adding to its suitability for respiratory in-vitro research.

The submerged culture procedure involves extracting mainstream smoke from the cigarette or vape into culture medium usually using a vacuum pump and a gas washing bottle. This media is then filtered and added to the culture medium used to grow the cells in flasks. The

cells are totally submerged in the liquid medium and have no direct contact with smoke. While the ALI system offers many benefits, it is an often-complicated procedure requiring specialised media and plates. Continuous smoke dispersal into the apical chamber necessitates the use of smoke machines which are often not available in many laboratories. Submerged culture procedure provides very robust and cost-effective method for in-vitro modelling of AEC response to stimuli. Changes in cell physiology such as in gene expression and cytotoxicity can be investigated using submerged culture systems. In addition, many more research have been completed with submerged culture system making it easier to make comparisons with past studies.

Both the submerged and ALI culture systems have distinct advantages and limitations that influence their suitability for in vitro respiratory research. The submerged culture model is straightforward, cost-effective, and very widely used, allowing easy assessment of cytotoxicity, gene expression, and other cellular responses, its simplicity and robust methodology make it particularly suitable for experiments requiring high reproducibility or comparisons with existing literature. However, the model does not replicate direct smoke exposure to the apical surface of airway epithelial cells, and it lacks the structural and functional differentiation observed in vivo. In contrast, the ALI culture system provides a more physiologically relevant model, promoting muco-ciliary differentiation, pseudostratified morphology, and barrier function that closely mimic the human airway. The main drawbacks of ALI culture are its technical complexity, requirement for specialized culture inserts and media, and the need for smoke exposure equipment, which can be expensive, mostly unavailable in many laboratories and time-consuming. Selection of the appropriate model therefore depends on the experimental question, balancing physiological relevance against practical considerations such as cost, complexity, throughput and the ease of comparisons with past studies.

A variety of AECs are employed for in-vitro modelling of smoking and vaping. During smoking and vaping, the epithelial cells that line the trachea, bronchi and alveolar are the initial target of noxious substances from the smoke. AECs protect underlying tissues from this inhaled smoke by forming a structural barrier which prevents the entry of noxious chemicals form smoke and providing muco-ciliary clearance. These cells also play significant roles in both innate and adaptive immunity. The airway epithelium can sense exposure to bacteria and

respond by releasing antimicrobial peptides (AMP) such as β-defensin and the human cathelicidin antimicrobial protein (hCAP18) in addition to its non-conserved c-terminal peptide LL-37 (hCAP18/LL37) into the airway surface fluid. In addition to their direct antimicrobial role, the AMPs contribute to innate immunity by attracting and activating other immune cells such as B-cells, macrophages, neutrophiles and even epithelial cells. They also induce the release of inflammatory mediators such as IL8, IFN, IL6, and LTB4 (Fusco et al., 2017; Semple and Dorin, 2012; Boniotto et al., 2006). AECs can initiate the adaptive immune response by modulating the activation and differentiation of dendritic cells (DC), B-cells and T-cells. AECs express pattern recognition receptors (PRR) such as Toll like receptors (TLR) which when activated by specific patterns on antigens can induce DC maturation and migration in a process culminating in Th2 response and subsequent antibody mediated immune response (Krawczyk et al., 2010; Dearman et al., 2009; Van Tongeren et al., 2008; Gras et al., 2017).

For in-vitro modelling in experiments relating to the airway, primary, cancer and non-cancer immortalised cell lines are often used. The airway epithelium is divided into three (3) sections; the upper oral and nasal cavities, the trachea and bronchi which make up the lower region and the distal alveolar region.  All 3 regions are affected by smoking and vaping.

Human bronchial primary epithelial cells (HBpEC) can be derived from bronchial segments taken from healthy or diseased patients or purchased commercially as normal human bronchial epithelium (NHBE) or diseased human bronchial epithelium (DHBE). Calu-3 a non-small cell lung cancer cell line which displays epithelial morphology, is a cell line derived from a metastatic site in a 25-year-old Caucasian male with lung adenocarcinoma. 16HBE14o- and Beas-2B both immortalised bronchial epithelial cell lines, the former isolated form a 1-year-old male heart-lung patient and transformed with an SV40large antigen while the latter was transformed with an adenovirus-12/SV40 hybrid. These cells display various differences in phenotypes which make them suitable for various research purposes, for instance the expression of cystic fibrosis transmembrane conductance regulator (CFTR) by 16HBE14o- make it suitable for cystic fibrosis research (Cozens et al., 1994; Oliynyk et al., 2010; Haws et al., 1992), while the presence of tight junctions (Tj) in Calu-3 make it best suited for studies investigating transport across the cell membrane (Grainger et al., 2006; Sajjan et al., 2008).

Each airway epithelial cell type used for in vitro modelling offers specific advantages and limitations that influence experimental design and interpretation. Primary bronchial epithelial cells (HBpEC/NHBE/DHBE) closely resemble in vivo airway tissue, providing high physiological relevance and accurate representation of epithelial responses to smoke or vape exposure. However, they are limited by donor variability, slower proliferation, high cost, and finite lifespan, which can restrict the scale and reproducibility of experiments. Immortalized cell lines such as 16HBE14o-, Beas-2B, Calu-3, and A549 are easier to culture, more reproducible, and suitable for high-throughput or long-term studies, making them ideal for cytotoxicity and inflammatory response assessments. On the other hand, these cell lines often exhibit altered phenotypes, reduced differentiation, and may not fully replicate the barrier properties of primary cells useful for ALI models. The choice of cell type therefore balances physiological relevance, experimental practicality, and the specific research questions being addressed.

Both A549, a human alveolar adenocarcinoma cell line, and BEAS-2B, an immortalized bronchial epithelial cell line, are widely used in studies of cytotoxicity and inflammatory responses, including cytokine release profiles in response to small particulate matter, cigarette smoke, and vaping aerosols. Their popularity stems from practical advantages such as ease of culture, rapid proliferation, and minimal requirement for specialized media. Additionally, the extensive use of these cell lines in previous research allows for straightforward comparison with existing literature. DPP10 is also constitutively expressed in airway epithelial cell lines, including BEAS-2B and A549 (Tripathi et al., 2017; Zhang et al., 2018). For these reasons, A549 and BEAS-2B were selected for the present study as representative models of alveolar and bronchial epithelium, providing a balance of physiological relevance and experimental feasibility.

Given the role of DPP10 in airway function and disease, further research is needed to elucidate its expression and potential functional significance in these commonly used airway epithelial cell models. Such studies would provide valuable insights into the molecular mechanisms underlying respiratory responses to environmental exposures.

Smoke types used on the treatment for cells for in-vitro experiment could either be mainstream or side stream smoke. Mainstream smoke (MSS) is smoke inhaled directly from the cigarette or vape while side stream smoke (SSS) is generated form the smouldering end

of the cigarette. With vapes, there are no side stream smokes. SSS pose just as much danger as MSS as the smoke generated here does not pass through a filter. Second hand smoke or passive smoking other terms used to describe MSS has been shown to increase the risk of stroke, COPD, ischemic heart disease, cancer and many other chronic lung diseases. (HSS and Services, 2010, 2006, 2010, 2014; Diver et al., 2018; Korsbæk et al., 2021; Kim et al., 2018). With in-vitro smoking models, MSS and/or SSS can be collected via a vacuum into a medium for submerged cultures or extracted directly to the cell surface of an ALI culture using a smoking machine.

When smoke is extracted from cigarettes and vapes, standardization of the extraction process and a means of measuring concentration to generate data that is comparable across laboratories is essential. One popular method has been to extract a specific number of cigarettes into a defined volume of media and designate this as 100% CSE, dilutions are then made and used from this stock volume. As a further control to mitigate against smoke loss during the extraction process, the extraction is kept at a constant flow rate when using the syringe and stop-cock apparatus (Wang et al., 2019) or at a constant pressure with the use of a vacuum pump (Lu et al., 2017) (Sampilvanjil et al., 2020). The CSE concentration has also been expressed as a function of tar concentration. The smoke is passed through a standard Cambridge filter and the increase in dry weight of the Cambridge filter is taken as the amount of tar not extracted into the medium. This weight is then used as a measure of the CSE concentration (Sampilvanjil et al., 2020; Higashi et al., 2016, 2014).

CSE is either used immediately after preparation or stored at -80°C. There is currently no evidence of the stability of CSE and VE and whether long-term storage affects its cytotoxicity and its ability to modulate inflammatory response. After extraction, CSE is filtered using a 0.22µm filter and adjusted to physiological pH of 7.4 (Wang et al., 2019; Lu et al., 2017; Sato et al., 1999; Metcalfe et al., 2014; Otsu et al., 2021; Fujii et al., 2012). To ensure standardisation between the different batches of CSE and VE, the optical density (OD) of the extract is measured spectroscopically. Although the absorption peak of nicotine is at 260nm, the contribution of nicotine and all other constituents in a cigarette yield a maximal absorbance of 320nm. Because of this, in studies utilizing CSE and VE, extract batches are usually standardised by measuring the UV absorbance at 320nm (Facchinetti et al., 2012) (Tatsuta et al., 2019) (Mortaz et al., 2011)

To investigate the role of DPP10 in the treated and control cells, the cells were first treated with cigarette smoke and vape without manipulation of the DPP10 gene, cytotoxicity result and gene expression data generated were termed as baseline data. The baseline studies also served as a process to determine the suitable concentration of extract for the research while also validating the extraction process. As the extraction method for cigarette smoke and especially vape takes a long period, with vape extraction taking as long as 2 days for extraction and filtration, it was also essential to determine if activity of the extracts would be affected by long term storage.

## 3.2. CIGARETTE SMOKE AND VAPE EXTRACTION

To perform in-vitro analysis on cell lines treated with vape and cigarette, the vape and cigarette smoke need to first be extracted. Historically, entire, gas phase, and side stream smoke are extracted for in vitro investigations using commercial smoking equipment. These commercial smoking machines offer enclosed systems with cigarette attachments that can light and extract different smoke types directly into flasks with cultured cells to adequately simulate the conditions of human physiological exposure, however this equipment is not only expensive, but have a large footprint and most academic laboratories cannot afford to have them if majority of their research is not smoking related. This new approach aims to lessen this by validating modest laboratory equipment that is widely available in labs and making sure that the smoke collected at various times has similar quality. To model the average smoking habit, extraction was caried out using a popularly used cigarette and vape within the UK, Benson and Hedges gold and Vuse vape pen.

### 3.2.1. APPARATUS

Vacuum pump or laboratory diaphragm pump (Charles Austen Capex 8c), autoclavable silicon tubing (Fisher scientific #15174195), Gas washing bottle (Fisher scientific #15202009) Cotton wool, forceps.

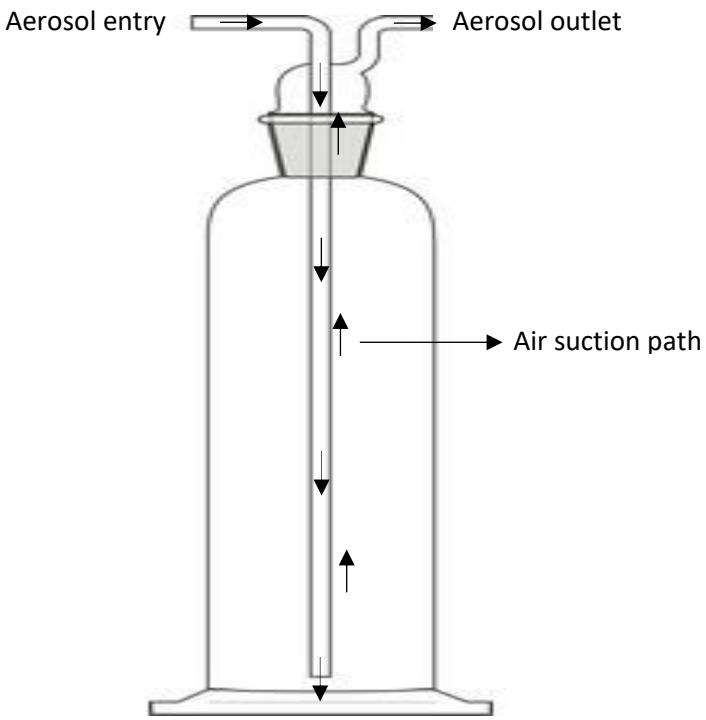


*Figure 7: Schematic of the gas washing bottle setup. The vapour entry point of the gas washing bottle is connected to the e-cigarette or cigarette using a silicone tube. The vacuum generated by the pump attached to the aerosol outlet facilitates the draw of aerosol through the system into the gas washing bottle containing cell culture medium. As the vapour bubbles through the medium, efficient mixing occurs, allowing the soluble components of the vapour to be incorporated into the culture medium for subsequent use in cell treatment experiments. The aerosol outlet of the gas washing bottle is connected to the vacuum pump using a silicone tube. When the vacuum pump is activated, negative pressure is generated within the system, drawing aerosol from the e-cigarette or cigarette through the gas washing bottle. This continuous airflow ensures efficient transfer of aerosol into the culture medium and maintains a consistent extraction process.*

### 3.2.2. METHOD

To model average smoking exposure, two commonly used UK products were employed: Benson & Hedges Gold cigarettes and the Vuse e-cigarette. The Vuse device in this study was a manual, pen-style, closed-pod system (Vuse ePen 3, British American Tobacco, UK) activated by inhalation. A non-flavoured 2 mL Vuse e-liquid pod containing 6 mg/mL nicotine, with a 50:50 ratio of propylene glycol (PG) to vegetable glycerine (VG), was vaped into cell culture medium to match the nicotine concentration extracted from twelve Benson & Hedges Gold cigarettes (0.12 mg/mL). For the nicotine-free extract, the same device was operated with a nicotine-free 2 mL pod, vaping the same volume of e-liquid as the nicotine-containing extract, ensuring that the only difference was the presence or absence of nicotine. This e-cigarette was chosen because it represents one of the most widely used vape pens among UK users, providing a realistic model for vaping exposure.

EXTRACTION FROM CIGARETTE

Autoclaving was used to sterilise all the bottles and tubing. Using forceps, two pieces of cotton wool were cut and placed into each end of a silicone tube, one inch from the tube's end, while the worker was within a ducted fume extraction cabinet The cotton wool was properly sized to prevent it from falling out too quickly and from becoming too thick to be difficult to insert or remove from the tube. The silicone tube's length was chosen such that, when attached to the vacuum pump or bottle, it wouldn't be excessively taut or trailing. As seen below, one end of the silicone tube was attached to the vacuum pump's inlet opening, while the other end was linked to the gas washing bottle's exit end.

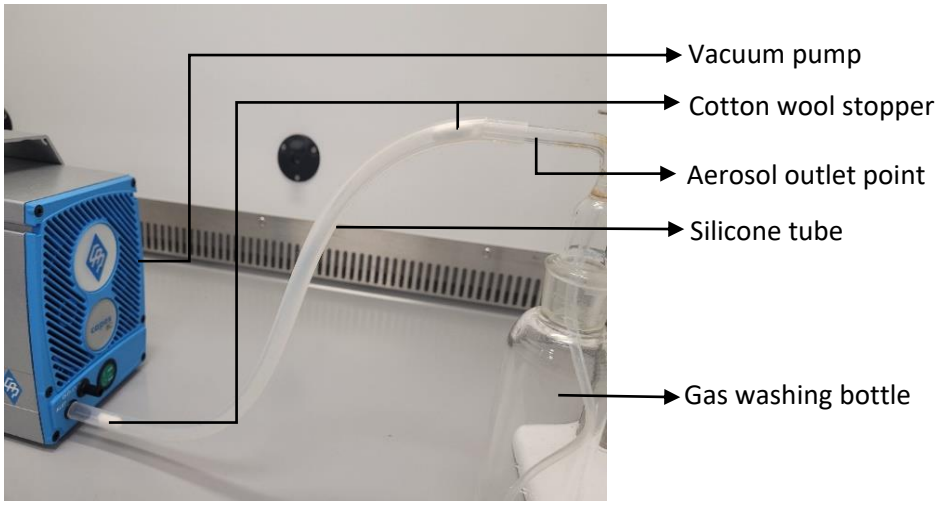


*Figure 8: Vacuum pump connection setup to the gas washing bottle. Cotton wool stoppers are inserted at the aerosol exit point and at the pump connection to prevent the entry of liquid or smoke into the pump.*

A shorter silicone tube, measuring approximately 3 inches in length, was cut and fastened to the gas washing bottle's entry end. By firmly tugging and snapping at the point where the cigarette filter originates, every filter was removed. One centimetre from the cigarette butt was marked. A cigarette extracted must burn to this point to complete one extraction. To keep the mark visible and to avoid pushing the cigarette too far into the tube, it was carefully placed through the second end of the 3-inch silicone tubing. The silicone tube and cigarette were fastened at their connecting point using a retort stand and clamp, ensuring that the clamp was not overly tight or loose but firm enough to prevent an easy pull out without depressing the tube or cigarette.

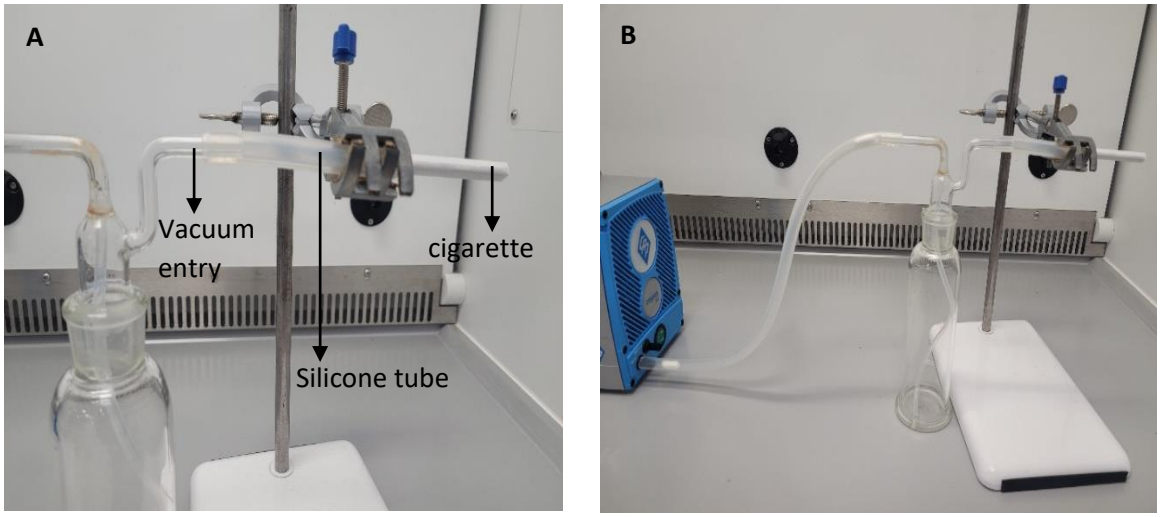


*Figure 9: Connection of the gas washing bottle to the vacuum pump and cigarette. A short silicone tube links the cigarette to the aerosol inlet of the gas washing bottle. When the vacuum pump is activated, the resulting pressure differential draws the cigarette smoke into the gas washing bottle*

To catch any ash that could be produced, an ashtray was positioned beneath the cigarette end. A measured volume of complete cell culture media was introduced to the gas cleaning container, with 1 cigarette per 10 mL of media. Using a gas lighter, the cigarette was lit, and the vacuum pump's ON button was quickly pressed to begin suction. The OFF button was clicked to stop the suction as soon as the cigarette burned to the previously designated 1 cm point. Prior to doing the subsequent extraction, the extracted smoke was given a precise 5-minute period to integrate with the media. The clamp was released, and the spent cigarette butt was taken out in order to execute the subsequent extraction. Before turning on the vacuum pump, a new, marked cigarette with its filter removed was placed into the short silicone tube and securely secured. After the extraction step was finished, a 0.2-micron syringe filter was used to filter the media that contained the extract from cigarette smoke. After that, the extracts were aliquoted and kept for further use at -20°. After storing the extract at -20°C for three months, its activity is still maintained.

EXTRACTION FROM VAPE PEN

The equipment configuration for extracting from an e-cigarette or vape pen was the same as that for extracting smoke from cigarettes. However, the mouthpiece of the vape pen was placed into the end of the 3-inch silicone tubing that was attached to the gas washing bottle's entry end, in place of the cigarette. As seen here, a clamp on a retort stand was used to secure the vape pen.

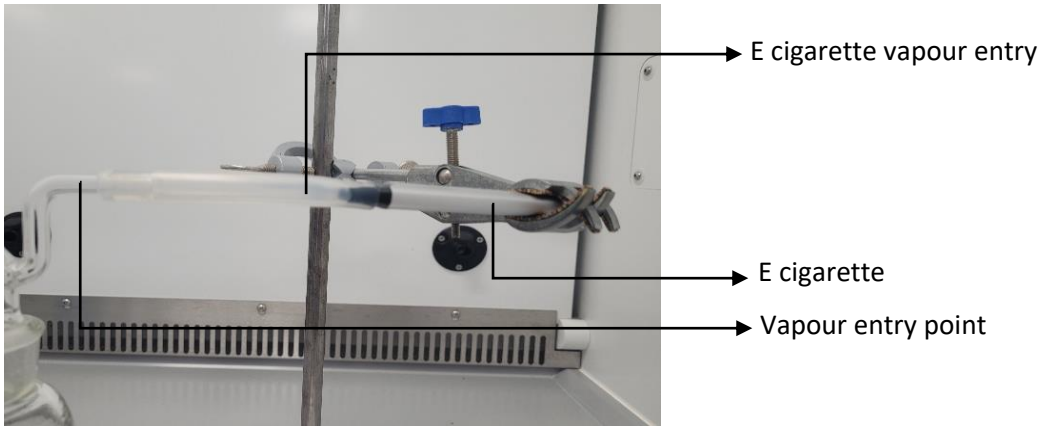


*Figure 10: Apparatus setup for e-cigarette connection. The e-cigarette pen is connected to the aerosol inlet of the gas washing bottle. The vuse e-cigarette used in this study is activated by inhalation; when the vacuum pump is switched on, it generates a negative pressure that draws the e-cigarette aerosol into the gas washing bottle.*

Three 15-second vacuum pulses were used for the extraction, separated by 45 seconds of rest (or OFF). The OFF button was pressed, and the extracted gas was allowed to mix with the media for two minutes and fifteen seconds to complete the total three minutes of rest following the last pump in the three pulses. This process was repeated until all of the liquid from the vape pen was vaporized and extracted into the culture medium. The vape smoke extract was filtered by passing through a 0.2micron syringe filter. Extracts were then aliquoted and stored at -20°C. Activity of extract is still maintained within 3 months of storage at -20°C.

This extraction approach was selected to achieve consistent, reproducible delivery of smoke or vapour using readily available laboratory equipment. The gas washing bottle setup allowed efficient mixing of the soluble smoke fraction with culture medium, simulating the exposure of airway cells to water-soluble constituents. The system is cost-effective and easy to standardise across replicates. However, it does not capture the full complexity of human airway exposure, including volatile and particulate components or direct air-cell contact. Despite these limitations, the method provides a practical and physiologically relevant model for controlled in-vitro analysis

### STANDARDISATION OF CSE, VE AND NFVE

In previous studies (Kode et al., 2006; Downs et al., 2013; Overbeek et al., 2011), the optical density (OD) of cigarette smoke extract (CSE) measured at a UV absorbance of 320 nm has been widely used to normalise extract concentration and ensure consistency between batches. Although nicotine alone has a peak absorbance at 260 nm, the presence of tar and

other combustion products in cigarette smoke shifts the maximum absorbance to around 320 nm (Figure 11), making this wavelength more representative of the overall chemical content of the extract. In contrast, e-cigarette vapour extract (VE) lacks many of the complex tar components found in cigarette smoke, and its absorbance profile therefore differs slightly, this method of standardisation is also more complicated with the addition of nicotine free vape extracts that neither have nicotine nor tar. In this current study, the 2 extracts containing nicotine were first standardised by matching their nicotine content. 10 cigarettes containing 1mg nicotine each was extracted into 100mL cell culture medium to make a 0.1mg/mL nicotine extract. For the vape extract, 2mL vuse pod containing 6mg/mL nicotine was extracted into 120mL cell culture medium to make a final concentration of 0.1mg/mL nicotine extract. To normalise the nicotine free vape extract against the nicotine containing vape extract, 2mL vuse nicotine free e-liquid with similar constituent as the nicotine containing e-liquid was extracted into 120mL cell culture as well.

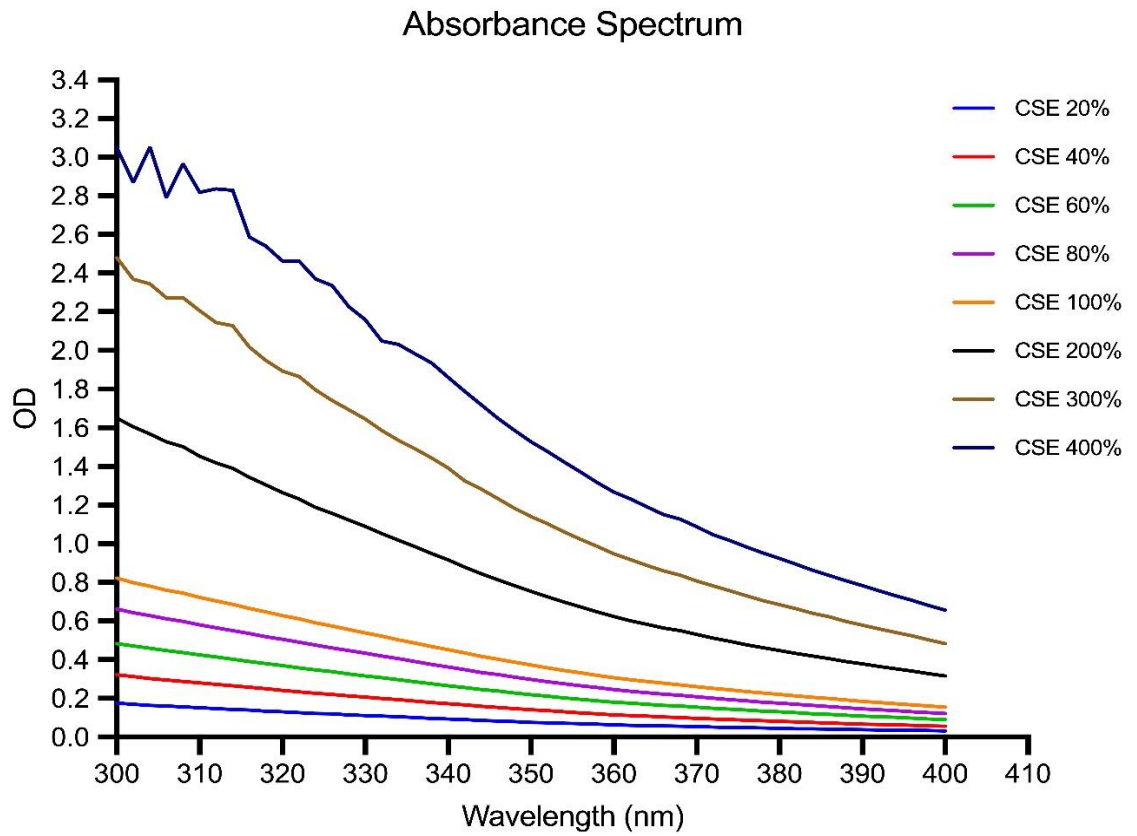


*Figure 11: The absorbance spectra of a range of dilutions of CSE was determines using a plate reader. The absorbance peak at the maximum concentration between 300-305nm.*

## 3.3. CELL VIABILITY ASSAY

### 3.3.1. ASSAY PRINCIPLE

The XTT assay is a colorimetric assay for the nonradioactive measure of cellular proliferation, cytotoxicity and viability. This assay relies on the reduction of a yellow tetrazolium salt XTT (2,3-Bis-(2-Methoxy-4-Nitro-5-Sulfophenyl)-2H-Tetrazolium-5-Carboxanilide) to an orange formazan dye in the presence of an electron coupling reagent by mitochondria dehydrogenase in metabolically active cells. The resulting formazan formed is soluble in aqueous solutions and dissolves directly into the culture medium, eliminating the need for an additional solubilization step and can be directly quantified using a multi-well spectrophotometer. The reduction process involves NADH produced in the mitochondria via trans-plasma membrane electron transport and an electron mediator (Roehm et al., 1991).

XTT assay determines changes in the number of cells based on their metabolic activity and provides insights into cell viability, cytotoxicity and cell proliferation. XTT contains a positively charged tetrazolium nucleus and two fully ionized sulfonate groups with single negative charges making a net charge of -1. Reduction of the salt to a formazan product removes the positive charge leaving a net charge of -2. The presence of this charge makes the formazan product soluble. Unlike other tetrazolium salts such as MTT where there is the absence of the sulfonate groups, reduction renders the formazan product uncharged and hence insoluble thereby requiring a solubilization step before determination on the spectrometer (Paull et al., 1988) .

### 3.3.2. METHOD

A549 and BEAS-2B cells were seeded in triplicates in 100µL/well of DMEM supplemented with 10% FBS and 1% antibiotic at a concentration range of $5 \times 10^3 – 12 \times 10^3$. In 3 wells, only complete medium was added, these wells were labelled blanks. To determine the standard curve and working range of the assay, once the cells were 70% confluent, 30µL of complete media was added to each well and incubated for 24 hours. Following 24 hours, the XTT working solution was first prepared by thawing the XTT Reagent (Component A) (Thermofisher, #X12223) in a 37°C water bath. The electron Coupling Reagent was thawed at room temperature. Both vials containing the XTT reagent and electron coupling reagent

were vortexed to ensure the reagents were fully in solution. 6 mL of XTT Reagent was measured into a 15-mL tube. 1 mL of the Electron Coupling Reagent was added to the 15 mL tube containing the XTT reagent, and the solution mixed by vortexing. This working solution was used immediately by adding 70 µL directly to each well of the 96-well plate in which the cells were seeded and also the blank wells. The plates were Incubated at 37°C for 4 hours. After incubation, the absorbance was read at 450 nm and 660 nm using a microplate reader (Clariostar). The 660 nm absorbance reading was used to eliminate the background signal contributed by cell debris or other non-specific absorbance. The specific absorbance of the sample using the formula below:

Specific Absorbance = [Abs450 nm(Test) – Abs450 nm(Blank)] – Abs660 nm(Test)

A standard curve was generated to determine the working range of the assay and determine what concentration of cells to use for the assay with treated cells. The concentration of cell used for the XTT cell viability assay was selected from the standard curve within an OD of 0.75 to 1.25nm. Tp perform the XTT assay, 7.5 X $10^3$ A549 cells and 10 x $10^3$ BEAS-2B cells were seeded into 96-well plates in triplicates, including 3 wells with only complete media for blank. After 24 hours, the cells were treated with varying concentration of CSE, NFVE and VAPE; 1%, 2%, 5%, 10%, 20% and incubated at 37°C in a $CO^2$ incubator. After 24 hours, 70 µL of XTT working solution was added to treated, untreated well (control) and blank wells and allowed to incubate for 4 hours at 37°C. The absorbance was read at 450nm and 660nm using the microplate reader. After specific absorbance of the treated wells and control wells were determined, cell viability was calculated using the formula below:

Cell viability (%) = [100 × (sample abs)/ (control abs)]

SELECTION OF CONCENTRATIONS

The concentration range of 1–20% was selected based on previously published studies investigating the cytotoxic effects of cigarette smoke and e-cigarette vapour extracts on airway epithelial cells (Rhim et al., 2021; Leigh et al., 2018; Ganapathy et al., 2017). Lower concentrations (1–5%) were used to represent sub-toxic exposure levels similar to light or short-term exposure, while higher concentrations (10–20%) modelled more intense or prolonged exposure conditions. Preliminary optimisation experiments were also conducted

to ensure that the selected concentrations produced measurable, dose-dependent effects without causing complete cell death. This allowed accurate assessment of changes in cell viability and comparison between CSE, VE and NFVE exposures.

### 3.3.3. RESULT

Cell viability was assessed in A549 and Beas-2B cells following exposure to NFVE, VE and CSE concentrations ranging from 1–20% for up to 72 hours.

In A549 cells, NFVE exposure caused only a modest decline in viability over time, with >70% viability maintained even at 20% concentration after 72 hours. VE produced a concentration- and time-dependent reduction in viability, particularly at 10–20%, where cell viability dropped to approximately 50% by 72 h. CSE had the most pronounced cytotoxic effect, with viability falling sharply and reaching ~15% at 20% after 72 hours

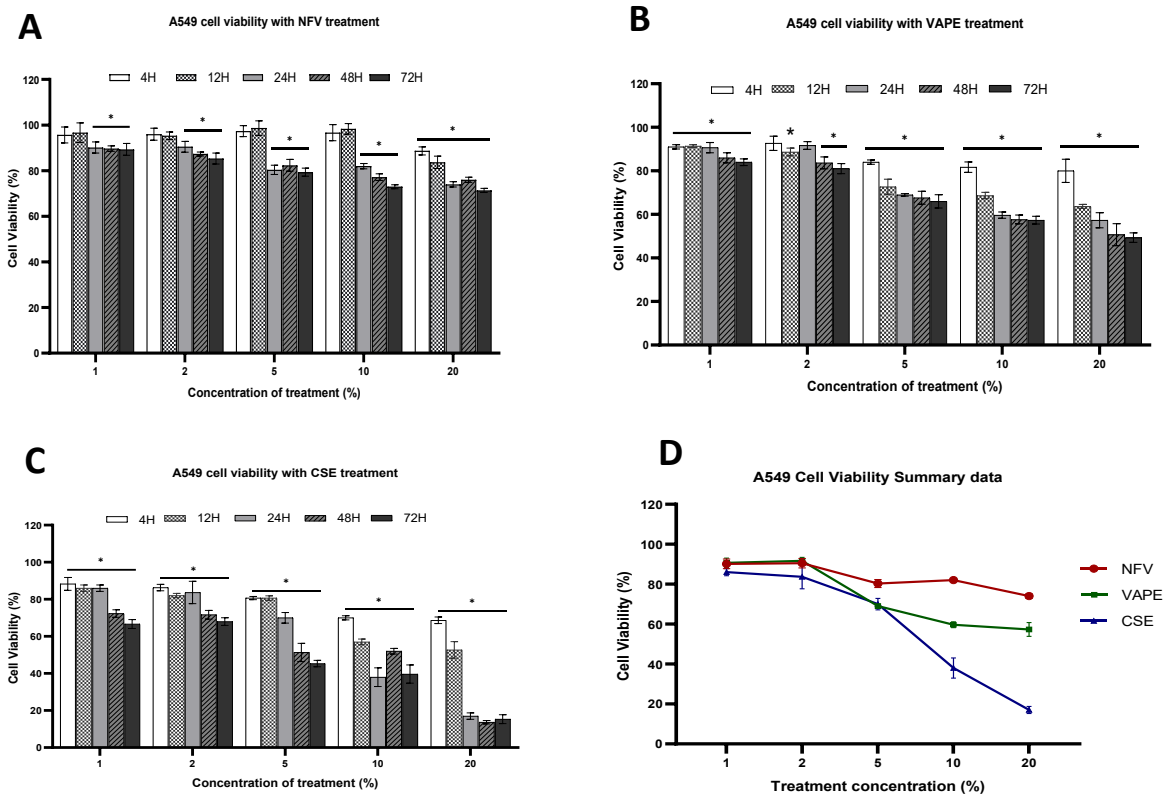


*Figure 12: XTT Assay on timed treatment of A549 cells with varying concentrations of treatment from 1% - 20% for 4, 12, 24, 48 and 72 hours where 100% CSE is 1 whole cigarette stick extracted into 10 mL complete cell culture media, and 100% NFVE is 2mL vial of nicotine free vape extracted into 60 mL complete cell culture media and 100% VE is 2mL vial of 3mg/mL vial of nicotine containing vape extracted into 60 mL complete cell culture media. A. Treatment with nicotine free vape extract (NFVE). B. Treatment with VE. C. Treatment with cigarette smoke extract (CSE). D. Cell viability at 24 hours post treatment with NFVE, VE and CSE. Data is expressed as mean±SEM of 3 biological replicates of n=3 each. *P≤0.05 vs untreated control.*

A similar pattern was observed in Beas-2B cells, though these non-cancerous bronchial epithelial cells appeared slightly less resilient at higher concentrations. NFVE again produced minimal cytotoxicity, whereas VE caused moderate, progressive decreases in viability, particularly at 10–20%. CSE exposure resulted in severe loss of viability, with <20% survival by 48–72h at concentrations ≥10%.

Overall, the results indicate a clear dose- and time-dependent cytotoxicity profile across all exposures, with toxicity following the order CSE > VE > NFVE, demonstrating that cigarette smoke remains the most damaging, while nicotine-free vapour has comparatively limited effects on epithelial cell viability.

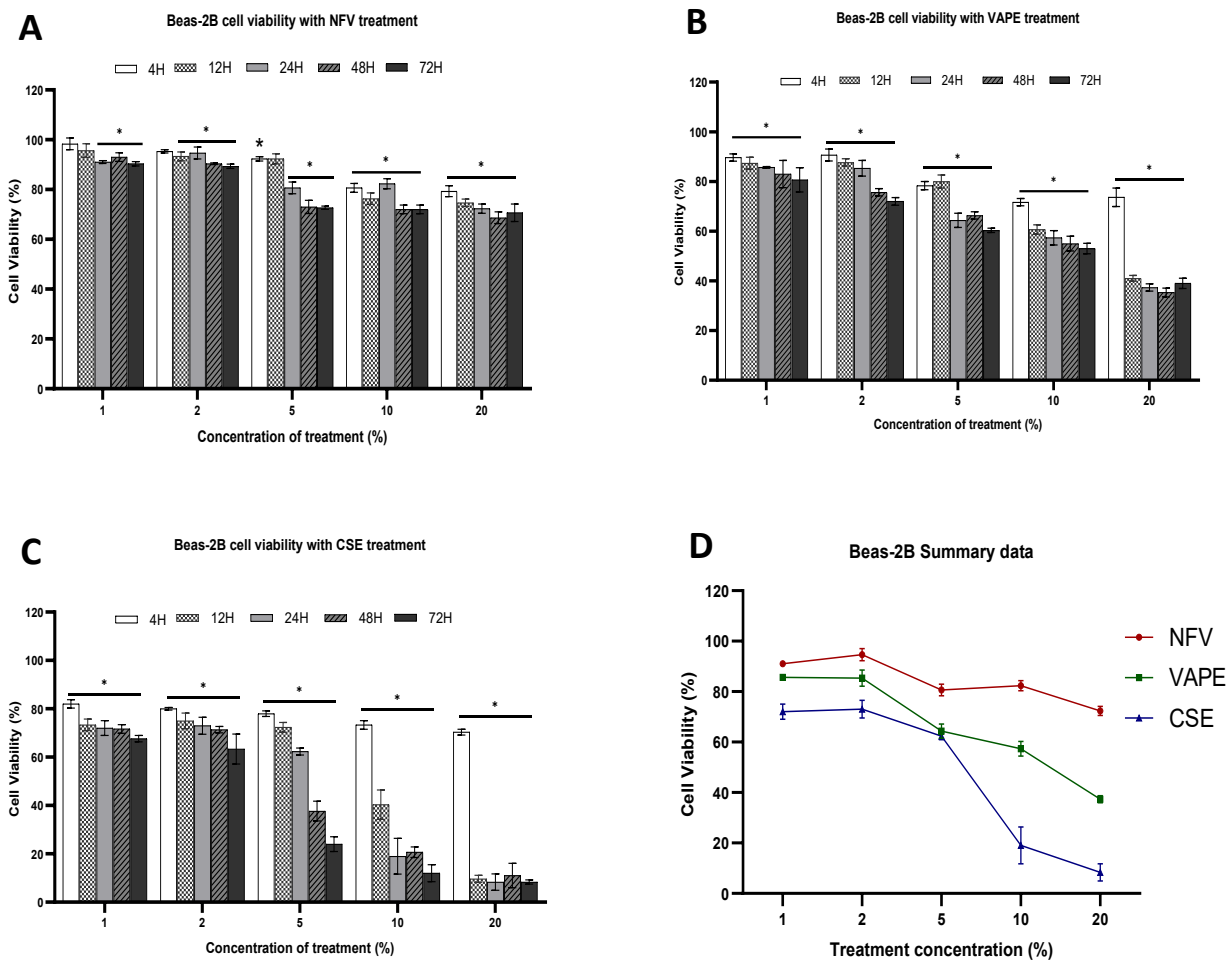


*Figure 13: XTT Assay on timed treatment of Beas-2B cells with varying concentrations of treatment from 1% - 20% for 4, 12, 24, 48 and 72 hours where 100% CSE is 1 whole cigarette stick extracted into 10 mL complete cell culture media, and 100% NFVE is 2mL vial of nicotine free vape extracted into 60 mL complete cell culture media and 100% VE is 2mL vial of 3mg/mL vial of nicotine containing vape extracted into 60 mL complete cell culture media. A. Treatment with nicotine free vape extract (NFVE). B. Treatment with VE. C. Treatment with cigarette smoke extract (CSE). D. Cell viability at 24 hours post treatment with NFVE, VE and CSE. Data is expressed as mean±SEM of 3 biological replicates of n=3 each. *P≤0.05 vs untreated control.*

### 3.3.4. DISCUSSION

Cell viability assays were conducted to identify the appropriate extract concentrations and treatment durations for subsequent experiments. The results showed CSE exerted the strongest cytotoxic effect, followed by nicotine-containing vape extract (VE) and nicotine-free vape extract (NFVE). Both A549 and Beas-2B cells exhibited dose-dependent reductions in viability, with Beas-2B cells generally being more sensitive to treatment. A concentration that reduced cell viability to approximately 70% was selected for further studies, as this range is commonly used in toxicology research to ensure cells remain viable but sensitive to treatment, allowing for measurable effects without reaching necrotic levels. This approach ensures that cells are still actively growing and not irreversibly damaged, providing a robust model for downstream analysis.

The subsequent analysis of the cytotoxic effects of NFVE, VE, and CSE demonstrated clear time- and concentration-dependent reductions in cell viability in both A549 and Beas-2B cells. CSE caused the most pronounced decrease in cell viability, with a dramatic reduction at concentrations of 5% and 10%, particularly in Beas-2B cells, which showed more susceptibility than A549 cells. The observed cytotoxicity is consistent with prior studies, which attribute the harmful effects of CSE to the complex mixture of chemicals in cigarette smoke, including nicotine, polycyclic aromatic hydrocarbons, carbon monoxide, and aldehydes, all of which induce oxidative stress and apoptosis (Weng et al., 2018; Ding et al., 2005).

VE treatment also led to significant reductions in viability, particularly at higher concentrations, with the effects being more prominent in Beas-2B cells. This aligns with previous research, such as Chaumont et al., (2019) who reported that vaping negatively impacts oxygen transport in the body, and McAlinden et al., (2021), who found that nicotine-containing vapour impairs airway epithelial cells. The toxicity of nicotine, known to induce oxidative stress and inflammation, likely contributes to the observed effects (Bahl et al., 2012). Interestingly, NFVE produced the least cytotoxicity, with cell viability remaining above 70% for all concentrations tested, even after prolonged exposure. This result supports other studies suggesting that nicotine-free vapour, composed of propylene glycol and vegetable glycerine, has a lower cytotoxic profile compared to nicotine-containing vapour (Beklen and

Uckan, 2021; Phillips et al., 2017) Overall, the results indicate that CSE exhibited the highest cytotoxicity, followed by VE, while NFVE showed the lowest cytotoxic effects. A 70% cell viability threshold was selected for subsequent experiments as it represents an appropriate balance between maintaining sufficient cell survival and ensuring detectable treatment effects. Accordingly, a 5% concentration of NFVE, VE, and CSE was chosen for further analyses, as this level produced the most suitable reduction in cell viability. (McAlinden et al., 2021).

PG and VG, though generally recognized as safe (CFR, 2022) in food and pharmaceutical applications, have been shown to contribute to cytotoxicity in inhalation studies, as observed in this experiment. Our findings indicate that PG/VG exposure, both with and without nicotine, caused a dose- and time-dependent reduction in cell viability, with more pronounced effects observed at higher concentrations (Yoo et al., 2018). The toxicity of PG/VG may be compounded by the flavouring chemicals used in e-liquids, which have been implicated in increasing the overall toxicity of vaping products (Bahl et al., 2012). Notably, Beas-2B cells were more sensitive to both VE and CSE compared to A549 cells, which is consistent with the literature suggesting that lung epithelial cells, particularly those from the airway, exhibit heightened vulnerability to inhaled toxicants (Bahl et al., 2012). This highlights the importance of selecting the appropriate cell model when studying the effects of vaping and smoking, as airway epithelial cells may be more susceptible to damage from PG/VG and other e-cigarette components than other cell types.

Overall, these results demonstrate that CSE remains the most toxic exposure, followed by nicotine-containing vapour, with nicotine-free vapour exhibiting the least cytotoxic effects. The selection of a 70% cell viability threshold for further experiments provides a suitable balance between cell survival and sensitivity to treatment, enabling meaningful downstream analyses.

# 4. BASELINE INFLAMMATORY RESPONSES OF AIRWAY EPITHELIAL CELLS TO NFVE, VE AND CSE

## 4.1. INTRODUCTION

Following the development and validation of a standardised extraction protocol for cigarette smoke extract (CSE), vape extract (VE) and nicotine-free vape extract (NFVE) described in Chapter 3, this chapter presents the baseline inflammatory response of A549 and Beas-2B airway epithelial cells following exposure to each extract. These baseline data serve two purposes: to characterise the pro-inflammatory potential of CSE, VE and NFVE under standardised and comparable conditions, and to establish a reference point against which the mechanistic investigations of DPP10 presented in Chapter 5 can be interpreted.

Airway epithelial cells play a central role in initiating inflammatory signalling following exposure to cigarette smoke and vaping aerosols, producing key pro-inflammatory cytokines including interleukin-6 (IL-6), interleukin-8 (IL-8) and tumour necrosis factor-alpha (TNFα) in response to inhaled stimuli (Scott et al., 2018; Lau et al., 2012b). These three cytokines were selected as the primary inflammatory endpoints in this study as they are abundantly produced by airway epithelial cells, are rapidly transcribed and secreted in response to epithelial injury and oxidative stress and are reliably measurable at both the mRNA and protein level using qPCR and ELISA. The molecular mechanisms underpinning their transcriptional regulation, including NF-κB activation and downstream signalling cascades, are described in detail in Chapter 5.

Although both cigarette smoke and vaping aerosols are known to induce inflammatory responses, the relative contributions of nicotine and other aerosol constituents to epithelial cytokine activation remain incompletely understood. The inclusion of NFVE alongside VE and CSE is therefore a key experimental feature of this chapter, as it enables direct separation of nicotine-dependent from nicotine-independent inflammatory effects within the same standardised exposure system. This three-way comparison addresses a gap in the existing literature where such controlled parallel designs remain limited. In addition, the use of both A549 and Beas-2B cell lines allows assessment of cell-type specific differences in cytokine responses, which is relevant to understanding which regions of the airway may be most vulnerable to smoke and vaping induced injury, as both the alveolar and bronchial epithelium are directly exposed to inhaled stimuli.

Cells were exposed to each extract at time points of 4, 12, 24, 48 and 72 hours to allow capture of both the early transcriptional response to acute exposure and the sustained cytokine secretion that develops over a longer exposure period, reflecting the progressive and cumulative nature of smoke and vaping induced epithelial injury. Changes in cytokine expression were assessed at both the transcriptional and protein levels using qPCR and ELISA, providing a comprehensive assessment of the epithelial inflammatory response to each extract.

## 4.2. LITERATURE REVIEW

Cigarette smoke has been extensively characterised as a potent inducer of airway epithelial inflammation. Numerous in vitro studies have demonstrated that exposure to CSE significantly increases the production of IL-6, IL-8 and TNFα in airway epithelial cells (Kumar et al., 2023; Zhao et al., 2023; Ma et al., 2021). These cytokine responses have been associated with the transition from acute smoke-induced epithelial injury to the chronic inflammatory state observed in conditions such as COPD and emphysema (He et al., 2009; Zhang and Bai, 2018; Aaron et al., 2001; de Moraes et al., 2014; De Diego Damiá et al., 2011). In addition to cytokine dysregulation, cells of the airway epithelium are the first line of defence against harmful chemicals inhaled from cigarettes and vapes and are affected both structurally and functionally by smoke exposure. Studies have shown exposure to cigarette smoke can cause goblet cell hypertrophy and hyperplasia with resulting mucus hypersecretion in the airways (Bodas et al., 2011; Kumar et al., 2023; Yu et al., 2019), reduction in cilia development and size (Cao et al., 2024; Aufderheide et al., 2015; Leopold et al., 2009), cytotoxicity, reduction in epithelial cell proliferation and wound repair (Kokkinidis et al., 2020; Rowell et al., 2017a; Fan Chiang et al., 2022). Sustained elevations in IL-6, TNFα and IL-8 have been associated with smoke-induced inflammation and tissue degradation in both cigarette smokers (Khan et al., 2020; Leonard et al., 2025; Elisia et al., 2020).

In comparison, the inflammatory effects of vaping aerosols remain less clearly defined. While some studies suggest that vaping induces a reduced inflammatory response relative to cigarette smoke (Tsai et al., 2019; Stokes et al., 2021), others report significant increases in cytokine production, particularly in the presence of nicotine and flavouring compounds

(Sundar et al., 2016; Muthumalage et al., 2019a; Morris et al., 2021; Roxlau et al., 2023). On exposure to ENDS with or without nicotine, epithelial cells undergo apoptosis and necrotic cell death, dysfunction of the epithelial barrier (Yu et al., 2016; Ghosh et al., 2019; Herr et al., 2020a) and reduction in epithelial cell proliferation (Rigg and Gielda, 2019) Differences between cigarette smoke and vaping also extend beyond cytokine profiles. Mice exposed to chronic cigarette smoke showed high expression of matrix metalloproteinase 12 (MMP12), airway inflammation and measurable lung tissue destruction, none of which were observed in mice exposed to vaping aerosols containing equivalent nicotine concentrations or in vehicle controls without nicotine (Madison et al., 2020). MMP8 and MMP9 appear similarly expressed in both cigarette smokers and vapers (Reidel et al., 2018b), suggesting that certain aspects of the protease-mediated airway response may be shared between the two exposure types. In contrast, epithelial cells from vapers show increased expression of MUC5AC and MUC4 compared with cigarette smokers (Ghosh et al., 2018), pointing to compositionally distinct patterns of epithelial injury between the two exposure types.

Beyond nicotine, the base constituents of e-liquids, propylene glycol (PG) and vegetable glycerine (VG), have independently been implicated in epithelial stress responses and inflammatory signalling. In vitro studies have demonstrated increased MUC5AC expression following PG/VG exposure (Song et al., 2021b; Ghosh et al., 2018; Kim et al., 2024), while animal studies have shown increased goblet cell numbers and mucin production following exposure to high concentrations of PG (Suber et al., 1989a). Bronchoalveolar lavage from PG/VG inhalation studies has additionally shown high numbers of neutrophils and lymphocytes, along with increased neutrophil granule proteins including neutrophil elastase, myeloperoxidase and proteinase 3, at levels comparable to those observed in cigarette smokers (Werley et al., 2016; Reidel et al., 2018b). This indicates that the base constituents of e-liquids are not biologically inert and can independently drive aspects of the airway inflammatory response. Flavouring additives in vaping products have also been shown to modulate inflammatory responses by increasing secretion of TNFα and IL-6, enhancing MUC5AC production and increasing oxidative stress independently of nicotine (Muthumalage et al., 2018; Moshensky et al., n.d.; Go et al., 2020)

Nicotine has been identified as an important modulator of inflammatory responses in this context, although as discussed in the next chapter, its effects appear highly context-

dependent, with evidence for both pro- and anti-inflammatory actions depending on concentration and the transcription factors involved (Bono et al., 2023; Ren et al., 2017; Wu et al., 2025). This duality highlights the importance of including a nicotine-free control condition to isolate the contribution of nicotine from that of other vape constituents. Despite growing interest in vaping-related airway inflammation, direct comparisons between CSE, nicotine-containing VE and nicotine-free NFVE under standardised and identical conditions remain limited in the published literature. Furthermore, inconsistencies in extraction and exposure methodologies across studies have made cross-study comparisons unreliable (Zhao et al., 2016; Farsalinos et al., 2013; National Academies of Sciences et al., 2018). This highlights the need for studies utilising standardised exposure systems to directly evaluate the relative inflammatory effects of these stimuli and to cleanly separate nicotine-dependent from nicotine-independent contributions to epithelial cytokine responses. By comparing CSE, VE and NFVE under controlled and identical conditions, this chapter aims to establish a clear baseline understanding of their pro-inflammatory potential in A549 and Beas-2B airway epithelial cells, directly informing the mechanistic investigations presented in Chapter 5.

## 4.3. METHODS

### 4.3.1. REAL TIME PCR ASSAY

#### ASSAY PRINCIPLE

cDNA is amplified using a mix containing DNA polymerase, nucleotides, SYBR green dye; an intercalating dye specific for dsDNA, primers complementary sequence to the target DNA and other reagents to enhance primer binding to target gene and the extension process. As the mix is heated, the dsDNA denatures and into two separate strands. As the solution cools, primers anneal to the target sequences in the single stranded DNA and the DNA polymerase then creates a new strand by extending the primers with dNTPs, thus creating a complimentary copy of the target DNA sequence. As the cycle of heating and cooling is repeated, the copy of dsDNA is amplified exponentially. As more dsDNA is created, SYBR green fluorescent continues to increase until it crosses the critical threshold of the RT-PCR equipment. Changes in gene expression can then be calculated based on how many cycling processes it takes for a sample to cross this threshold.

#### 4.3.1.1. RNA EXTRACTION

Following treatment with CSE, NFVE and VE for 4, 24, 48 and 72 hours, the growth medium was removed from the cell culture flasks. 0.4mL TRIzol reagent (Invitrogen #15596026) was added directly to the flask and cells were scraped using a cell scraper. The scraped cells in TRIzol were transferred to a 1.5mL microcentrifuge tube. Samples not requiring immediate RNA extraction were stored in TRIzol at -20°C. For immediate extraction, the cells in TRIzol reagent were allowed to incubate at room temperature for 5 minutes to allow complete dissociation of the nucleoprotein complex.

PHASE SEPARATION

0.2 mL of chloroform was added per 1 mL of TRIzol reagent used for lysis; in this case, 80µL of chloroform was added to the 0.4mL TRIzol-cell mix. The tube was capped and thoroughly mixed by shaking. The mix was left to incubated at room temperature for 3 minutes. The sample was centrifuged at 12,000 g for 15 minutes at 4°C. After centrifugation, the mixture separated into a lower red phenol-chloroform, an interphase, and a colourless upper aqueous phase. The upper aqueous phase containing the total RNA was transferred to a new tube by angling the tube at 45° before transferring.

RNA PRECIPITATION

RNA was precipitated from the aqueous phase by adding propanol at half the volume of TRIzol used for cell lysis (i.e. 200µL). The mixture was incubated for 10 minutes at 4°C, then centrifuged at 12,000g for 10 minutes at 4°C. The supernatant was removed carefully using a micro pipettor making sure not to disturb the RNA, which appears as a white gel-like pellet.

RNA WASHING

The RNA pellet was washed by resuspending in 75% ethanol of equal volume of TRIzol reagent used for cell lysis. The sample was vortexed briefly and centrifuged at 7500g for 5 minutes at 4°C. The supernatant was discarded, and the RNA pellet was dried by leaving the tube cap open and resting it at an angle for 8 minutes to allow any residual ethanol to drip out.

RNA SOLUBILIZATION AND STORAGE

the dried RNA pellet was resuspended in 20 µL of RNAse-free water and incubated in a water bath at 60°C for 10 minutes. The RNA was then placed on ice for immediate use or stored at -80°C for later experiments.

#### 4.3.1.2. RNA QUANTIFICATION AND ANALYSIS USING THE AGILENT BIOANALYSER

To use the Agilent 2100 bioanalyzer For RNA analysis, the chip priming station was first set up by unscrewing the old syringe from the lid of the chip priming station and replacing with a new one. Using a screwdriver, the base plate of the chip priming station was adjusted to the position marked for RNA (position C). The lever of the syringe clip is adjusted to the top position for RNA analysis.

A new RNA chip was placed in the chip priming station. 9µL of gel-dye mix was measured into wells marked G. The syringe plunger was positioned at 1mL, and the chip priming station closed. The plunger was pressed down until it was held by the clip. After 30 seconds the plunger was released and slowly pulled back to the 1mL mark on the syringe. The chip priming station was opened, and nine microliters of gel-dye mix was pipetted into the wells marked G. 5µL of RNA marker was pipetted into all 12 sample wells including the well for the ladder marked . 1µL each of RNA sample was pipetted into the sample wells. For each unused sample well, 1µL of RNA marker was pipetted into it. 1µL of heat denatured ladder was pipetted into the well marked . The chip was placed horizontally in the IKA vortexer and allowed to vortex for one minute at 2400 rpm.

The RNA chip was then run on the Agilent bioanalyzer 2100 within 5 minutes of vortexing. Data generated was analysed for RNA quality and quantity.

#### 4.3.1.3. REVERSE TRANSCRIPTION PCR

Total RNA extracted with TRIzol from treated were reverse transcribed to cDNA with the Tetro cDNA synthesis kit (Bioline #BIO-65042). All reagent tubes were vortexed and centrifuged briefly then mixed in volumes shown below to make a total volume of 20 µL per reaction. All reactions were carried out on ice.

The 20 µL cDNA synthesis reaction consisted of total RNA at 0.01% w/v, oligo(dT) primer 5% v/v, 10 mM dNTP mix 5% v/v, Ribosafe RNAse inhibitor 5% v/v, reverse transcriptase 5% v/v, and 5× RT buffer 20% v/v. Nuclease-free water was added to complete the reaction to 20 µL.

The reactions were mixed gently using a micropipette and incubated in the thermal cycler using the cycling parameters below

*Table 4: Thermal cycler program used for reverse transcription, detailing the temperature, duration, and purpose of each step.*

| Temperature | Time | |
|---|---|---|
| 45°C | 30 minutes | Reverse transcription |
| 85°C | 5 minutes | Reaction termination |
| 4°C | ∞ | Hold |

The reverse transcription product was stored at -20°C or used immediately for real time PCR (RT-PCR).

4.3.1.4. REAL TIME PCR

Primers were thawed at room temperature and vortexed briefly before use. Each cDNA template was diluted to a 1:10 solution using nuclease free water. 10 µL of PCR reaction mix was prepared for each treatment condition. Forward and reverse primers were prepared from 10 µM solution to make a final concentration of 0.5 µM in each reaction. Triplicates for each primer and treatment condition was measured into PCR plates in triplicates. Included was also triplicates of non-template control (NTC) reactions where cDNA was substituted for nuclease free water to check for presence of primer dimerization.

For each 10 µL qPCR reaction in a PCR plate well, 5 µL of Power UP SYBR Green master mix (50% of the total reaction volume) was combined with 0.5 µL of forward primer (5% v/v) and 0.5 µL of reverse primer (5% v/v). The reaction was completed by adding 4 µL (40% v/v) of cDNA template.

Each reaction was mixed thoroughly. The PCR plate was centrifuged at 500 g for 1 minute and loaded into the Quant studio 3. The cycling parameters was set up as shown below.

*Table 5: Thermal cycling and melt curve conditions programmed on the QuantStudio 3 real-time PCR system.*

| STEP | Temperature | Time | Cycle |
|---|---|---|---|
| UDG Activation | 50°C | 2 minutes | Hold |
| Initial denaturation | 95°C | 2 minutes | Hold |
| Denaturation | 95°C | 15 seconds | 40 |
| Annealing | 58°C | 15 seconds | |
| Extension | 72°C | 1 minute | |
| Melt curve Stage | | | |
| | Temperature | Time | Ramp rate |
| 1 | 95°C | 15 seconds | 1.6°C/second |
| 2 | 58°C | 1 minute | 1.6°C/second |
| 3 | 95°C | 15 seconds | 0.15°C/second |
| Hold Stage | | | |
| | 4°C | ∞ | Hold |

The primers used for qPCR were

IL6 - F: 5'- CCTGAACCTTCCAAAGATGGC -3', R: 5'-TTCACCAGGCAAGTCTCCTCA -3'

IL8 - F: 5'- ACTGAGAGTGATTGAGAGTGGAC -3', R: 5'- AACCCTCTGCACCCAGTTTTC -3'

DPP10 - F: 5'- CAGTATCCGTATCCTAAGGCAGG -3', R: 5'- TGTGAGTTGGTCCATACAGGTT -3'

GAPDH - F: 5'- CTGGGCTACACTGAGCACC -3', R: 5'- AAGTGGTCGTTGAGGGCAATG -3'

Kv4.2 - F: 5'- GACCGTGACCCAGACATCTTC -3', R: 5'- TGCACTCGTGGCGAGGATA -3'

TNFα - F: 5'- GAGGCCAAGCCCTGGTATG -3', R: 5'- CGGGCCGATTGATCTCAGC -3'

### 4.3.2. ELISA ANALYSIS

ELISA plates (Corning™ Costar™ 9018) were coated with 100 µL/well of capture antibody in Coating Buffer. The plate was sealed and allowed to incubate overnight at 4°C. Wells were aspirated and washed 3 times with >250 µL/well wash Buffer allowing time for soaking (~1 minute). The plate was blotted on absorbent paper to remove any residual buffer. Wells were blocked with 200 µL of ELISA/ELISPOT Diluent and incubated at room temperature for 1 hour. Standards were prepared according to reagent preparation protocol Prepare. Blocking buffer was aspirated from the wells in the ELISA plate and washed at least once with Wash Buffer. 2-fold serial dilutions of the prepared standards were done to make a standard curve for a total of 8 points. For this, 100 µL of ELISA/ELISPOT Diluent was added to wells B1/B2 to wells H1/H2 leaving wells A1/A2 empty. 200 µL/well of top standard concentration was then added to the empty wells A1/A2. 100 µL of top standard from wells A1/A2 was transferred to wells B1/B2 and mixed by repeated aspiration and ejection. From wells B1/B2, 100 µL of dilute standard was transferred to wells C1/C2 taking care not to scratch surface of the microwells. This procedure was continued 5 times till wells H1/H2. 100 µL/well of samples was added to the appropriate wells and 100 µL of ELISA/ELISPOT Diluent to the blank wells. The plate was sealed and incubated at room temperature for 2 hours. The plate was aspirated and washed for a total of 3-5 washes also allowing time for soaking (~1 minute) during each wash step to increase the effectiveness of the washes. ELISA plate was then blotted on absorbent paper to remove any residual buffer. 100 µL diluted Detection Antibody was added to all wells and the plates sealed and allowed to incubate at room temperature for 1 hour. After this time, the detection antibody was aspirated and the plates washed for a total of 3-5 washes allowing time for soaking (~1 minute) during each wash step. The plate was blotted on absorbent paper to remove any residual buffer. 100 µL of diluted Streptavidin-HRP was added to the wells and the plate sealed and allowed to incubate at room temperature for 30 minutes. The wells were aspirated and washed for a total of 5-7 washes, making sure to allow time for soaking for 1 to 2 minutes prior to aspiration. 100 µL/well of 1X TMB Solution was added to each well and incubated at room temperature for 15 minutes. 100 µL of Stop Solution was added to each well and the plate was read immediately at 450nm and 570nm.

## 4.4. RESULT

### 4.4.1. REAL TIME PCR

Quantitative PCR was used to assess the expression of IL6, IL8, and TNF in A549 and Beas-2B cells following exposure to NFVE, VE, and CSE for up to 72 hours. In A549 cells, NFVE treatment produced no notable changes in IL6, IL8, or TNF expression across all time points. In contrast, VE and CSE both induced time-dependent increases in gene expression, with CSE consistently showing the strongest effect. IL6 expression increased approximately 3.6-fold with CSE and 2.1-fold with VE at 72 hours. IL8 expression followed a similar pattern, reaching up to 4.5-fold with CSE and 3.2-fold with VE, while TNF expression rose modestly, with a maximum 2.2-fold increase observed for CSE. Overall, CSE exposure resulted in the greatest induction of pro-inflammatory genes, followed by VE, whereas NFVE had minimal impact.

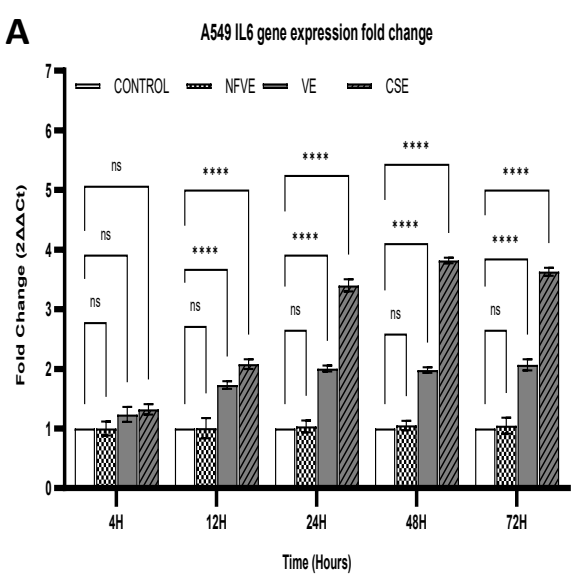


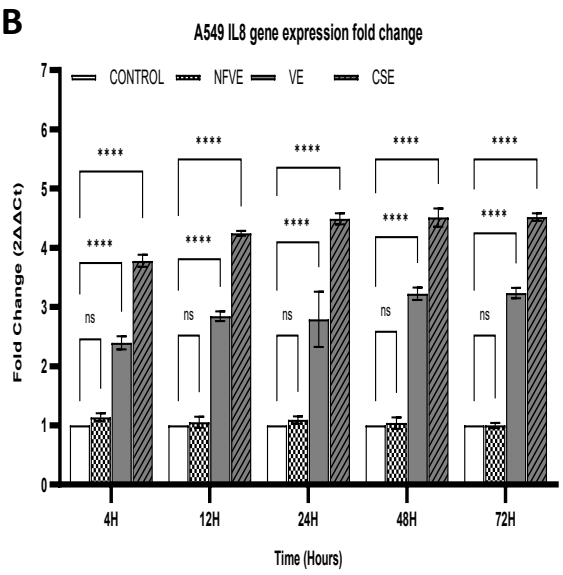

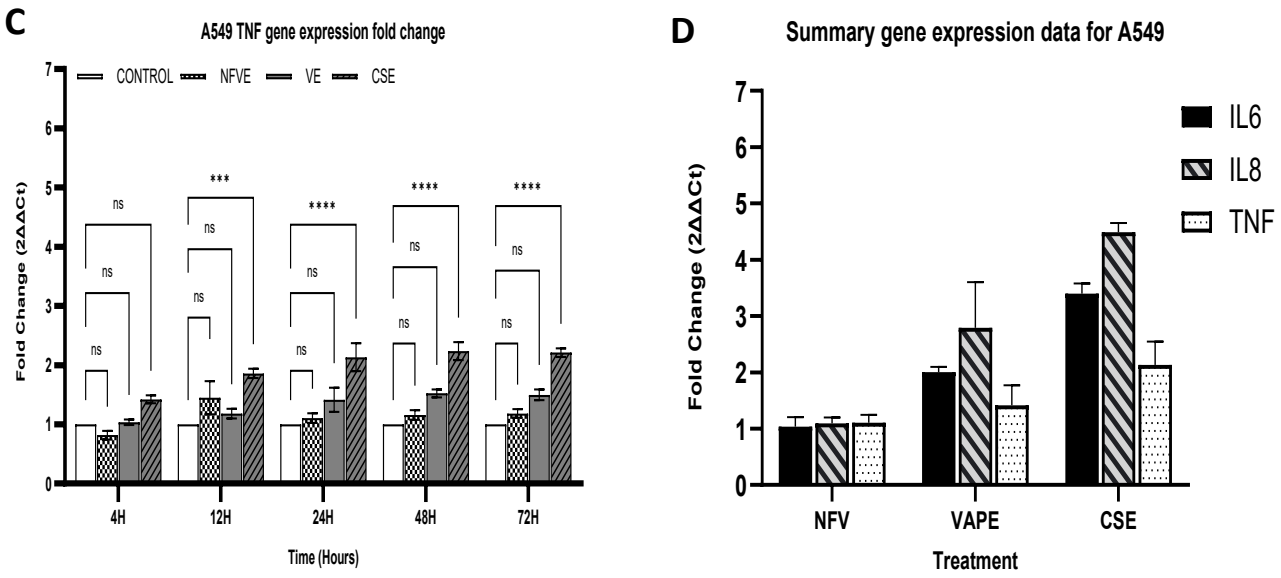


*Figure 14: Fold change in A549 cytokine gene expression following treatment with 5% NFVE, VE and CSE for 4, 12, 24, 48 and 72 hours. A. IL6 gene expression in A549 cells on treatment with 5% NFVE, VE and CSE compared with control group with no treatment. B. IL8 gene expression in A549 cells on treatment with 5% NFVE, VE and CSE compared with control group with no treatment. C. TNFα gene expression in A549 cells on treatment with 5% NFVE, VE and CSE compared with control group with no treatment. D. Summary data for cytokine gene expression 24 hours post treatment with NFVE, VE and CSE. Data is expressed as mean±SEM of 5 biological replicates, n=5 each. *P≤0.05, **P≤0.01, ***P≤0.001, ≤0.0001 vs untreated control*

In Beas-2B cells, IL6 expression remained unchanged with NFVE treatment but was significantly elevated following VE and CSE exposure, with upregulation evident from 12 hours and persisting to 72 hours. IL8 expression also showed a marked response to VE and CSE, peaking at approximately 5.7-fold and 3.3-fold increases, respectively, after 72 hours. TNF expression followed a comparable trend, showing little change with NFVE but progressive increases with VE and CSE, reaching about 3-fold after 72 hours of CSE treatment. When comparing the two cell lines, Beas-2B cells exhibited a stronger overall transcriptional response to both VE and CSE than A549 cells, particularly for IL8 and TNF, indicating greater sensitivity of the bronchial epithelial cells to these exposures.

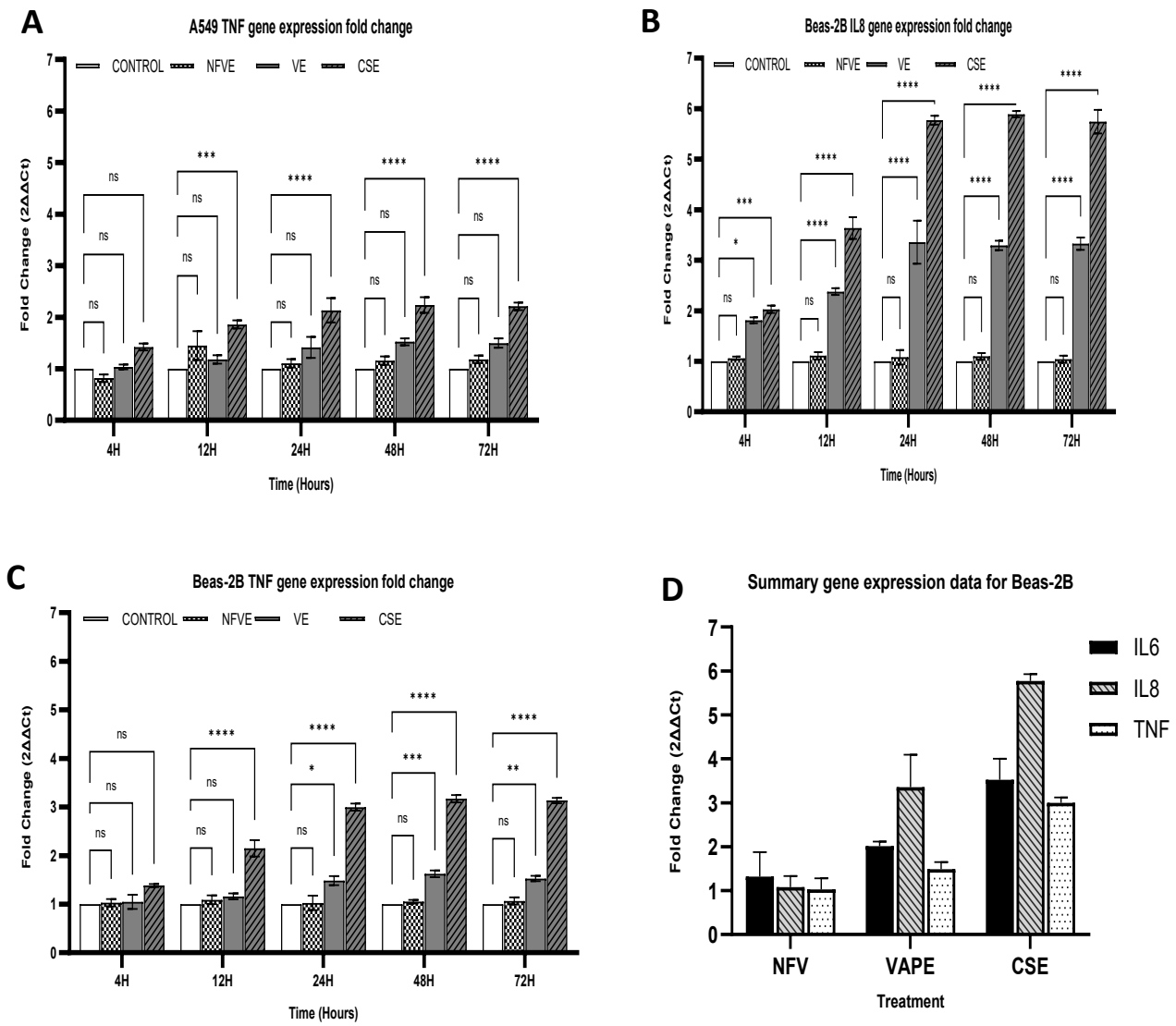


*Figure 15: Fold change in Beas-2B cytokine gene expression following treatment with 5% NFVE, VE and CSE for 4, 12, 24, 48 and 72 hours. A. IL6 gene expression in Beas-2B cells on treatment with 5% NFVE, VE and CSE compared with control group with no treatment. B. IL8 gene expression in A549 cells on treatment with 5% NFVE, VE and CSE compared with control group with no treatment. C. TNFα gene expression in Beas-2B cells on treatment with 5% NFVE, VE and CSE compared with control group with no treatment. D. Summary data for cytokine gene expression 24 hours post treatment with NFVE, VE and CSE. Data is expressed as mean±SEM of 3 biological replicates, n=3 each. *P≤0.05, **P≤0.01, ***P≤0.001, ≤0.0001 vs untreated control*

### 4.4.2. ELISA

To evaluate the inflammatory response of A549 and Beas-2B cells, secretion of IL-6, IL-8, and TNF were measured over time (4, 12, 24, 48, and 72 hours) following treatment with NFVE, VE, and CSE, compared to untreated controls.

In A549 cells, all treatment groups showed a tendency towards elevated IL-6 levels from 4 hours post-treatment. NFVE treatment did not induce a statistically significant change in IL-6 at any time point. VE treatment resulted in a statistically significant elevation in IL-6 from 12 hours post-treatment, where levels rose to 169.89 ± 13.4 pg/mL and remained consistently elevated through to 72 hours (252 ± 16.8 pg/mL). CSE induced the greatest IL-6 response, with statistically significant elevations also evident from 24 hours post-treatment, where levels peaked at 292.25 ± 16.1 pg/mL and were maintained at 288.55 ± 14.7 pg/mL at 72 hours.

IL-8 secretion in A549 control cells trended upwards as incubation time increased (89.79 ± 13.5 pg/mL at 4 hours to 129.66 ± 8.4 pg/mL at 72 hours). Neither NFVE nor VE treatments resulted in statistically significant changes in IL-8 secretion at any time point, with both showing only mild non-significant numerical increases relative to controls throughout the time course. CSE treatment was the only condition to induce a statistically significant elevation in IL-8, first detected at 12 hours post-treatment (201.27 ± 19.8 pg/mL), with levels continuing to rise steadily and reaching 351.30 ± 16.0 pg/mL by 72 hours.

TNFα secretion in A549 cells was relatively consistent across all treatment groups and time points. No statistically significant differences were detected between any of the treatment conditions and untreated controls at any time point. Although CSE treatment produced the highest recorded TNFα levels at 72 hours (232.65 ± 28.2 pg/mL), this did not reach statistical significance, suggesting that TNFα secretion is not meaningfully altered by any of the treatments tested in A549 cells.

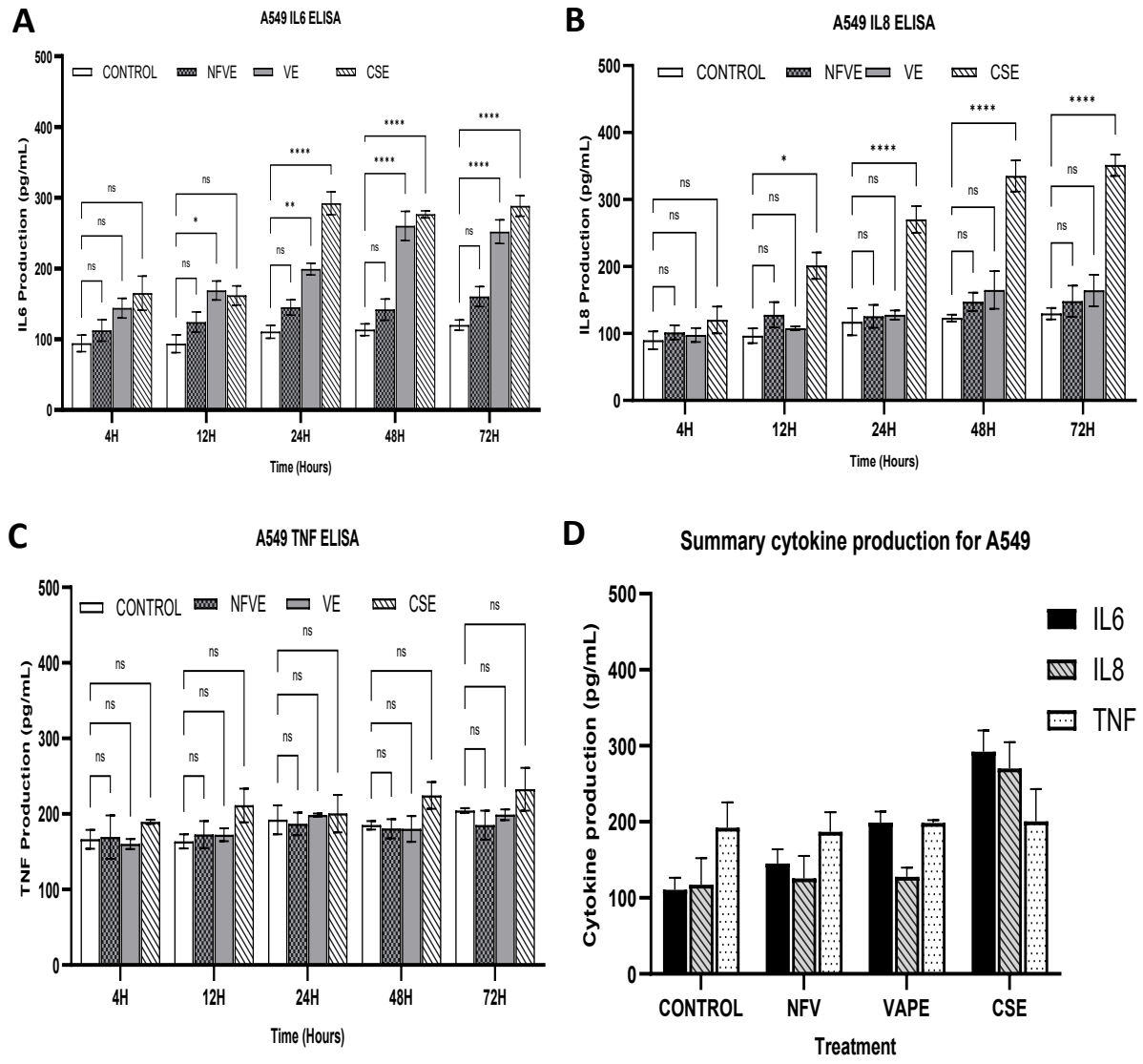


*Figure 16: Cytokine production by A549 cells following stimulation with 5% NFVE, VE and CSE for a range of duration.*

*Data is expressed as mean±SEM of 3 biological replicates, n=3 each. *P≤0.05, **P≤0.01, ***P≤0.001, ≤0.0001 vs untreated control.*

In BEAS-2B cells, IL-6 secretion was higher at baseline compared to A549 cells (106.54 ± 12.8 pg/mL vs 94.06 11.7 pg/mL). All treatment groups produced numerical increases in IL-6 compared to controls from as early as 4 hours post-treatment. CSE induced the strongest response, with statistically significant increases observed from 12 hours post-treatment, peaking at 382.4 ± 10.0 pg/mL at 24 hours and remaining elevated through to 72 hours. VE treatment also produced a statistically significant increase in IL-6, though this was not observed until 24 hours post-treatment where IL-6 levels increased to 163.19 ± 7.5 pg/mL, after which levels remained stable through to 72 hours. NFVE treatment produced only

numerical increases in IL-6 secretion across all time points that did not reach statistical significance compared to untreated control.

IL-8 levels in BEAS-2B cells showed a similar pattern with IL-6 for CSE and NFVE treatments. NFVE and VE produced only mild numerical increases in IL-8 that did not reach significance at any time point. CSE was the only treatment to induce a statistically significant increase in IL-8, which was evident from 12 hours post treatment, at which IL-8 levels had increased approximately 2.5 fold compared with baseline (114.77 ± 14.4 pg/mL), and continued to rise steadily, reaching 406.4 ± 17.4 pg/mL at 72 hours.

TNFα secretion in Beas-2B cells was comparable to A549 at baseline (182.60 ± 31.5 pg/mL vs 192.41 ± 19.1 pg/mL) and displayed no statistically significant variations across treatments and time points. CSE treatment led to slightly elevated TNF at later time points (224.8 ± 10.2 pg/mL to 233.7 ± 23 pg/mL at 48 to 72 hours), however this did not reach statistical significance, suggesting that's TNFα is not a sensitive marker of inflammatory response to treatments in this cell model.

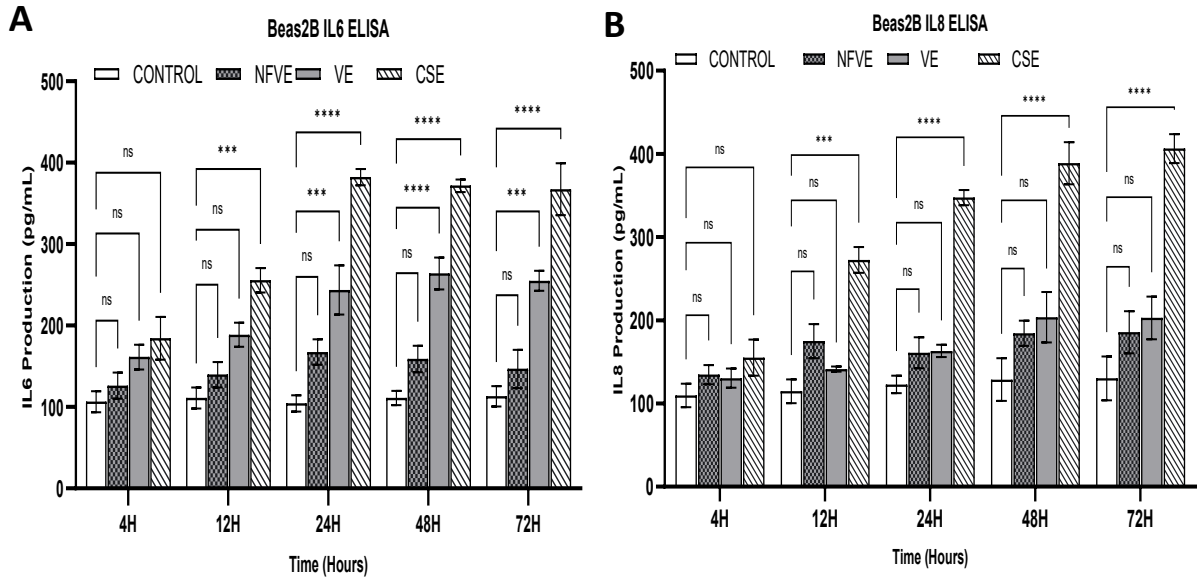

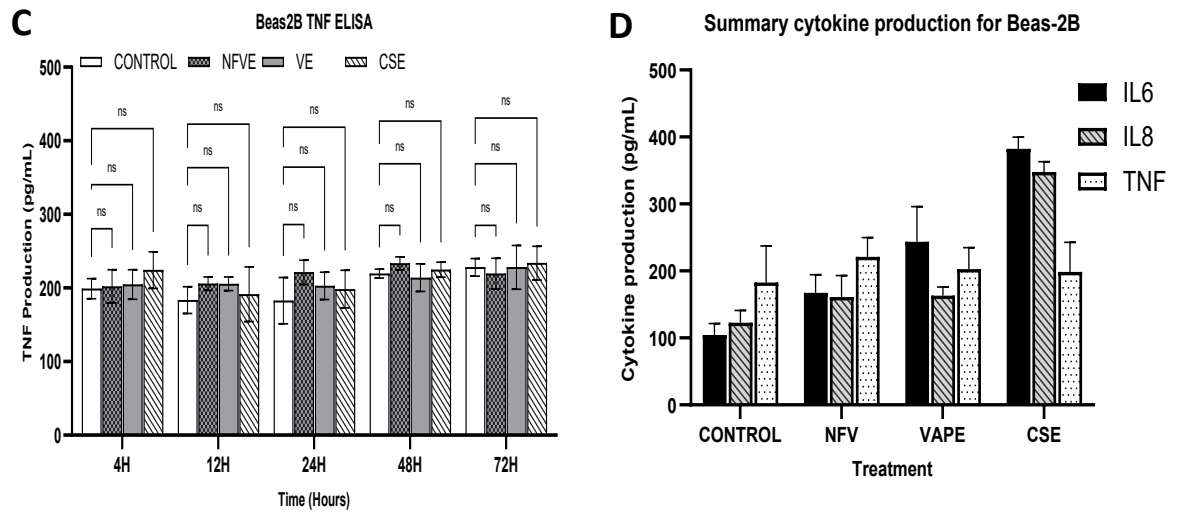


*Figure 17: Cytokine production by Beas-2B cells following stimulation with 5% NFVE, VE and CSE for a range of duration. Data is expressed as mean±SEM of 3 biological replicates, n=3 each. *P≤0.05, **P≤0.01, ***P≤0.001, ≤0.0001 vs untreated control.*

Overall, both cell lines demonstrated time- and treatment-dependent increases in IL-6 and IL-8 secretion, with CSE consistently inducing the strongest pro-inflammatory response. TNF levels were less variable, indicating that IL-6 and IL-8 are more sensitive markers of the inflammatory response in these cell models. A549 cells exhibited lower baseline cytokine levels and less pronounced TNF induction compared to BEAS-2B cells, highlighting potential cell-type-specific differences in cytokine secretion.

## 4.5. DISCUSSION

To ascertain the proinflammatory effect of NFVE, VE and CSE, IL6, IL8 and TNFα gene and protein expression changes were investigated in in-vitro smoking model in both A549 and Beas-2B cells. Although treatment with NFVE in both A549 and Beas2B cells reduces cell viability as observed in the XTT assay, pro-inflammatory cytokine release with NFVE remains unchanged even with an increased duration of treatment (up to 72 hours).

Both VE and CSE treatment significantly induced IL6, IL8 and TNFα gene expression and protein production in only IL6 and IL8 with CSE to a larger extent indicating that nicotine was the major responsible factor for inducing these pro-inflammatory cytokine release in VE treated cells. This immunomodulatory effect has been extensively investigated in various nicotine and cigarette smoking studies nicotine has been shown to be both anti-inflammatory or pro-inflammatory depending on dose and activity on the AP1 transcription factor and

NFκB nuclear translocation (Sunyer et al., 2009; Zhou et al., 2012; Rakhecha et al., 2022; Lau et al., 2006; Reidel et al., 2018a; Ung et al., 2019).

The additive effect of other chemical compounds in CSE can be observed in the larger changes found between the VE and CSE groups. Gene expression changes in IL8 was more than 2-fold after 12 hours of treatment going up to a 3-fold change after 24 hours with a more marked increase observed in Beas-2B. This sensitivity of Beas-2B compared with A549 was also observed in IL6 gene expression. In both cytokines, gene expression peaked at 24 hours after which a steady state level was maintained up to 72 hours.

Increases in gene IL6 and IL8 gene expression led to commensurate increase in protein expression. Interestingly, no significant changes in TNFα protein expression were recorded in A549 for both CSE and VE and only VE in Beas-2B even though these were significant increases in gene expression levels following treatment with VE and CSE.

The choice of IL-6, IL-8 and TNFα for this study was driven by several complementary biological and methodological considerations. First, these cytokines are abundantly produced by airway epithelial cells and represent principal epithelial mediators of lung inflammation, with IL-8 acting as a dominant neutrophil chemoattractant and IL-6 coordinating acute-phase and epithelial immune responses (Goniewicz et al., 2014; Kunkel et al., 1991)

Second, IL-6, IL-8 and TNFα are among the most extensively studied biomarkers in models of cigarette smoke– and e-cigarette–induced lung injury, which allows direct comparison of our findings with a large body of existing in vitro, in vivo and clinical literature (Mio et al., 1997; Kode et al., 2006; Mortaz et al., 2011).

Third, these cytokines are acute-phase mediators that are rapidly transcribed and secreted in response to epithelial injury or oxidative stress, making them well suited to capture early, time-dependent inflammatory responses in short exposure experiments (Nakamura et al., 1991; Harper et al., 2001).

Fourth, the biological functions of the three markers span key downstream processes relevant to smoking and vaping pathology: IL-8 drives neutrophil recruitment and degranulation that amplify tissue damage, IL-6 modulates epithelial-immune crosstalk and systemic acute-phase signalling, and TNFα regulates epithelial apoptosis, matrix

metalloproteinase expression and remodelling processes linked to emphysema and chronic airway disease (Mio et al., 1997; Churg et al., 2002; Khodayari et al., 2022).

Finally, IL-6, IL-8 and TNFα are robustly measurable at both mRNA and protein levels (qPCR and ELISA), providing complementary endpoints (transcriptional and secreted) that strengthen inference about pathway activation and allow integration with cell-based functional readouts such as cell cycle and apoptosis. This combination of biological relevance, comparability with the literature, acute responsiveness, reliable assay methods make IL-6, IL-8 and TNFα ideal markers for assessing the early epithelial inflammatory response to cigarette smoke and vaping extracts (Ju and He, 2021; Kulkarni et al., 2010)

Asides the three cytokines studies in this project, many other proteins contribute to the inflammatory effect of smoking and vaping with or without nicotine by modulating the activities of immune cells and inducing differential expression of genes that promote the severity of inflammatory diseases (Ween et al., 2020; Madison et al., 2019). High number of neutrophils and lymphocytes, along with associated neutrophil granule proteins such as neutrophil elastase (NE), proteinase 3, myeloperoxidase (MPO), and azurocidin 1 have shown significantly higher levels in BAL fluid from PG/VG inhalation and vape users compared with cigarette smokers or never smokers. High numbers of neutrophils and lymphocytes have also been observed in BAL following high dose PG/VG inhalation (Werley et al., 2016; Reidel et al., 2018a).

Epithelial cells obtained from airway biopsies of vape and cigarette smokers show differential protein expression profiles, including proteins uniquely expressed in vapers. For instance, increased expression of CYP1B1 and members of the mucin family, including MUC5AC and MUC4, has been reported. These mucins are major components of airway mucus and play a key role in epithelial protection and mucociliary clearance; however, their overexpression is also implicated in chronic bronchitis pathophysiology, contributing to sputum production and disease severity (Kesimer et al., 2017). In vitro studies using epithelial cell cultures exposed to propylene glycol (PG) and vegetable glycerin (VG) alone also demonstrate increased MUC5AC expression, in contrast to cigarette smoke exposure, which is associated with downregulation. Additionally, animal studies have shown increased goblet cell numbers and mucin production following exposure to high concentrations of PG (Suber et al., 1989b), indicating that these effects may be driven by PG/VG rather than nicotine alone.

Apart from PG/VG and nicotine, flavouring additives in vaping products can also modulate inflammatory responses by increasing secretion of pro-inflammatory cytokines such as TNF-α and IL-6 in epithelial cells, enhancing MUC5AC production, exacerbating airway hyperresponsiveness, increasing oxidative stress, and triggering inflammatory responses in animal models (Glynos et al., 2018; Ween et al., 2020).

Changes in matrix metalloproteinases appears to be one of the unique differences between Vape and Cigarette smoking. Mice exposed to chronic cigarette smoke showed high expression of matrix metalloproteinase 12 (MMP12), airway inflammation, lung tissue destruction and changes in lung volume as observed by microCT, none of these were observed in mice exposed to both vape with similar amount of nicotine nor in vape vehicle controls without nicotine (Madison et al., 2019), also, MMP8 and MMP9, appear more expressed in smokers compared with vapers. (Reidel et al., 2018a).

# 5. EFFECT OF DPP10 ON CYTOKINE EXPRESSION IN AIRWAY EPITHELIAL CELLS FOLLOWING ACUTE CIGARETTE SMOKE AND VAPING EXPOSURE

## 5.1. INTRODUCTION

After developing a model for cigarette smoking and vaping using A549 and Beas-2B cells, a baseline investigation was conducted to examine the changes in gene expression and protein production of the inflammatory cytokines IL6, TNFα, IL8 and the protein of interest DPP10. From previous research indicating differential expression of DPP10 in smokers and patients with COPD, and the protective effect of DPP10 in asthma models, the current research hypothesis is that DPP10 could also be protective in smoking and vaping. DPP10 was overexpressed and knocked out of the cell lines A549 and Beas-2B to better understand its role in smoking and vaping. The changes in the inflammatory cytokine profiles of IL-6, IL-8, and TNFα were then examined. Studies on knockouts shed light on the processes that occur after a gene is deleted, enabling an understanding of the function of specific genes in the cell. In this instance, lipid transfection was utilized in conjunction with DPP10 siRNA to silence DPP10 mRNA. Liposomal complex lipofectamine helps incorporate siRNA into the cells and is composed a 1:3 mixture of DOPE (1,2-Dioleoyl-sn-glycerophosphoethanolamine) and DOSPA (2,3-dioleoyloxy-N-[2(sperminecarboxamido)ethyl]-N,N-dimethyl-1-propaniminium trifluoroacetate). Via electrostatic interactions, the cationic lipids can form complexes with the negatively charged nucleic acid. In addition, many of the cationic lipids are formulated with a neutral helper lipid which possess positive charge in water and facilitates the interaction of the nucleic acid with the cell membrane, allowing the lipid/nucleic acid complex enter the cell through endocytosis (Chesnoy and Huang, 2000; Liu et al., 2003). RNA antisense oligonucleotides remain in the cytoplasm where one strand of the dsRNA is unwound and removed after binding to RISC, then binds to its complementary mRNA with the ultimate cleavage and degradation of the mRNA. For transfected DNA, the DNA is translocated into the nucleus for expression (Hirko et al., 2003).

To comprehend the ways in which DPP10 could contribute to pro-inflammatory cytokine expression, it is imperative to understand the molecular pathways that regulate cytokine gene expression and release. When inhaled smoke comes into close contact with the airway epithelial cells, it induces cellular stress and necrosis leading to the release of endogenous damage associated molecular patterns (DAMP) and the generation of reactive oxygen species

(ROS). This process has been well documented with studies demonstrating ROS generation and oxidative stress as major contributors to epithelial injury on exposure to traditional cigarette (Padmavathi et al., 2018; Zhao and Hopke, 2012) and e-cigarettes (Yogeswaran et al., 2021; Haddad et al., 2019).

Airway epithelial cells express Pattern recognition receptors (PRR) including Toll-like receptors (TLRs) which detect DAMP and initiate downstream signalling cascade that culminate in cytokine gene expression (Armstrong et al., 2004). Upon activation by DAMPS, TLRs recruit adaptor molecules such as MyD88 and TIRAP (Kagan and Medzhitov, 2006; Horng et al., 2002, 2001) which in turn interact with IL-1 receptor-associated kinases (IRAK1 and IRAK4) to propagate the signal.

An interaction between MyD88 and an IL-1 receptor-associated kinase IRAK4 through the death domain of the protein kinase activates another IL-1 receptor associated kinase IRAK1 (Li et al., 2000, 2002; Cao et al., 1996; Muzio et al., 1997).

Subsequently, TRAF6 a TNFα receptor associated factor is recruited and activated together with other E2 ubiquitin protein ligases, which then activates a protein complex made up of TAK1-binding protein 1 (TAB1), TAB2, TAB3 and a TGF-β-activated kinase 1(TAK1) (Chen, 2005). On activation of this complex, both NF-κB signalling pathways and MAPK is triggered (Wang et al., 2001). NF-κB is normally present in the cytosol with its nuclear translocation signal inhibited by a trio of kinases, IKK-α, IKK-β and IKK-γ known as the IKK complex. However, when NF-κB and MAPK signalling pathway is triggered, IκB-α is phosphorylated, ubiquinated, and degraded thereby allowing the nuclear translocation of NF-κB which then initiates the transcription of many pro inflammatory cytokines (Ghosh et al., 1998). The pro-inflammatory cytokines with induced gene expression because of this signalling pathway include IL6, IL8, TNFα among others.

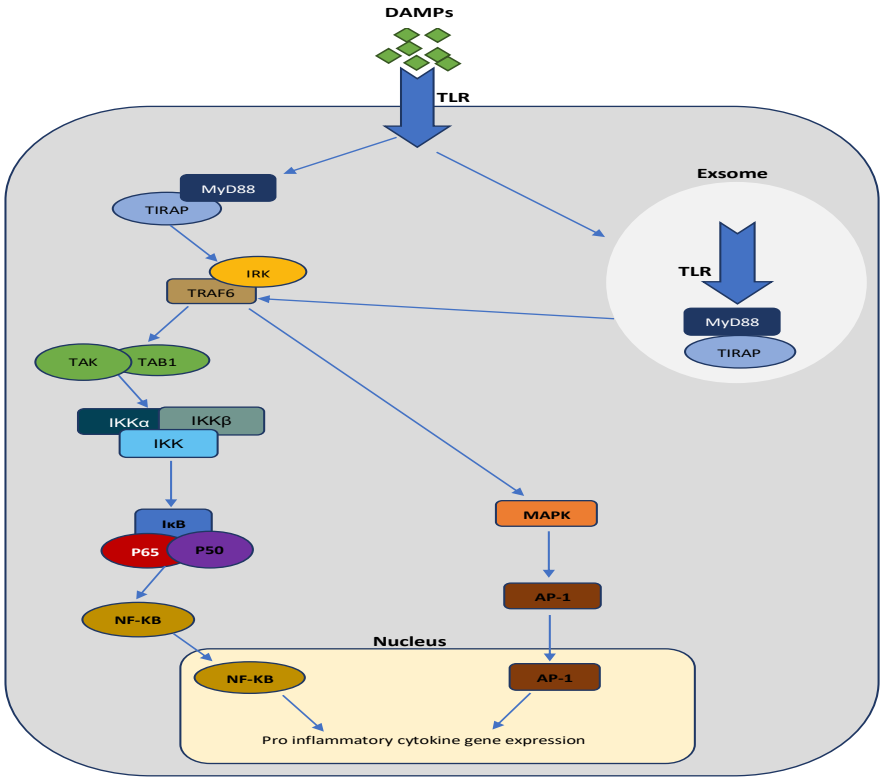


*Figure 18: Pathway for pro-inflammatory cytokine gene expression following inflammation. DAMPs generated because of smoking and vaping activate pattern recognition receptors such as TLR and recruit MyD88 and TIRP resulting into downstream NF-KB activation followed by its nuclear translocation and subsequent inducing of pro-inflammatory cytokine gene expression.*

## 5.2. LITERATURE REVIEW

Small proteins called cytokines are essential for cell signalling. Both immune and non-immune cells produce the short-lived proteins, which act locally on target cell receptors to alter gene expression and cause cell division, maturation, and proliferation. They also play a role in the start of autocrine, paracrine, and endocrine signalling. Cytokines have many functions, including embryonic development (Yockey and Iwasaki, 2018; Robertson et al., 2018; Guzeloglu-Kayisli et al., 2009), metabolism (Zoico and Roubenoff, 2002; Meex and Watt, 2017; Cao, 2014; Shi et al., 2019; Eckardt et al., 2014), angiogenesis (GEINDREAU et al., 2022; Thal and Kishore, 2013)and haematopoiesis (Alexander, 1998; Metcalf, 2008). However, they are most widely known for the role they play in immunity. In the immune system, cytokines contribute to both innate and adaptive immunity. The chief pro-inflammatory cytokines that participate in acute phase responses include IL6, TNFα and the chemokine IL8. They help immune cells respond to diseases by stimulating them to fight pathogens or kill tumor cells. They are released initially in response to DAMP and PAMP activating the inflammasome.

Once the invasive pathogen has been eliminated, the release of these pro-inflammatory cytokines typically results in a resolution of the immune response through a feedback loop, bringing the host to a homeostatic state. However, in cases of cytokine dysregulation when there is a persistent infection, autoimmune, allergy, or in cigarette smoking and vaping where there is a sustained sensitization by PAMP, cytokines can also contribute to the extension of inflammatory diseases by perpetuating the inflammatory state. (Feldmann and Saklatvala, 2000; Ramani et al., 2015). IL6, TNFα and IL8 are all produced by, and can act on epithelial cells during inflammation (Krueger et al., 1991; Eckmann et al., 1993; McRitchie et al., 2000).

IL-6 has a molecular mass ranging from 19 to 30 kDa and are serine-phosphorylated. Compared to cell culture, there is a larger level of IL6 in the peripheral circulation of patients who have been injured or infected. In contrast, TNFα is only briefly seen in the peripheral circulation and is found at very low levels. Although IL6 is unique in its systemic actions, TNFα and IL8 mostly have paracrine effects (Sehgal et al., 1989; Jayatilaka et al., 2017) Cells of the airway epithelium are the first line of defence against harmful chemicals inhaled from cigarettes and vapes and are affected both structurally and functionally. Studies have shown exposure to cigarette can cause goblet cell hypertrophy and hyperplasia with resulting mucus hypersecretion in the airways (Mullen et al., 1987; Wright et al., 1984) reduction in cilia development and size (Tamashiro et al., 2009) cytotoxicity, reduction in epithelial cell proliferation and wound repair (Luppi et al., 2005; Lan et al., 2007; Van Winkle et al., 2001) On exposure to ENDS with or without nicotine, epithelial cells undergo apoptosis and necrotic cell death, dysfunction of the epithelial barrier (Serpa et al., 2020; Muthumalage et al., 2019b; Herr et al., 2020b; Heijink et al., 2012) reduction in epithelial cell proliferation (Rowell et al., 2017b; Carpagnano et al., 2003)

Sustained elevations in IL6, TNFα, and IL8 have been associated with smoke-induced inflammation and tissue degradation in both cigarette and ENDS users. (Muthumalage et al., 2019b; Herr et al., 2020b; Gellatly et al., 2020; Churg et al., 2002; Petrescu et al., 2010)

Inflammatory disorders have complicated, multivariate pathophysiology that involves genetic, environmental, and epigenetic components (Surace and Hedrich, 2019; Marklová, 2007; David et al., 2018) (Stone et al., 2023). While asthma has been the subject of several studies on DPP10 and its function in inflammation and inflammatory diseases (Gao et al., 2010; Zhang et al., 2018; Wu et al., 2010; Adcock and Kirkham, 2010; Allen et al., 2003),

numerous genome wide and epigenome wide association studies have highlighted differential expression and differential methylation of DPP10 in smoking (Carolan et al., 2006; Harvey et al., 2007; Philibert et al., 2007; Huuskonen et al., 2008; Chhabra et al., 2014) and in chronic inflammatory diseases (Singh et al., 2011). Studies have shown that DPP10 expressed by immune cells directly induced ERK phosphorylation indicating a contribution to airway inflammatory responses via the ERK pathway. In vivo, treatment with anti DPP10 antibody reduced expression of TGF β1, CXCL1, and MMP9, inhibited immune cell infiltration, mucus formation, fibronectin expression, and epithelial thickness in the lung tissues, and inhibited the ERK pathway in a manner similar to that of dexamethasone. (Sim et al., 2022) . Further GWAS to narrow down the specific variant involved in airway hypersensitivity highlighted rs17048175 SNP as associating strongly with AERD phenotype (Kim et al., 2015; Fathollahpour et al., 2023)

As DPP10 lacks a catalytic triad and hence its enzymatic activity may only influence cytokine expression and inflammation indirectly, it cannot cleave cytokines at the penultimate proline amino acid and destroy them. Unlike DPP4, which possesses this ability. (Baggio et al., n.d.; Mulvihill and Drucker, 2014; Bezerra et al., 2015), how DPP10 might mediate its actions in inflammation is unknown.

## 5.3. METHOD

### 5.3.1. GENE SILENCING WITH siRNA TRANSFECTION

0.25 x $10^6$ A549 cells and 0.3 x $10^6$ Beas-2B cells were seeded in 6 well plates using 2mL DMEM enriched with 10% FBS and 1% Penicillin/streptomycin in each well and cultured in a 37$^o$c incubator with 5% $CO_2$ for 24 hours. 3 wells each were seeded for each siRNA to be transfected (Silencer select DPP10 siRNA Assay ID s33475 Thermofisher #4392420, Silencer select Negative control 1 Thermofisher #4390843, Silencer select GAPDH positive control siRNA Thermofisher #4390849) for the individual cell lines. After 24 hours, the siRNA was prepared for each well by adding 30 pmol of siRNA to 150 µL of Opti-MEM in a microcentrifuge tube. Lipofectamine was prepared for each well by adding 9 µL Lipofectamine RNAi Max to 150 µL Opti-MEM reagent in a microcentrifuge tube. Each tube was incubated at room temperature for 5 minutes. 250 µL of the siRNA-lipid complex was

then added to the cells in the 6 well plates and incubated for 3 days with the transfection efficiency analysed using qPCR after 24, 48 and 72 hours.

REAL TIME PCR ANALYSIS OF GENE SILENCING

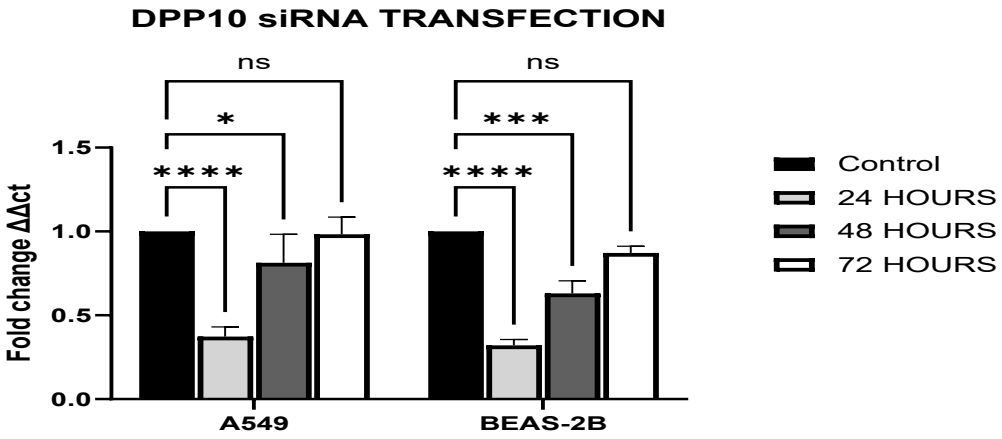


*Figure 19: siRNA transfection of A549 and Beas-2B cells with DPP10. 24 hours post transfection, DPP10 gene r=expression is more than halved. At 72 hours, gene expression returns to almost normal level.*

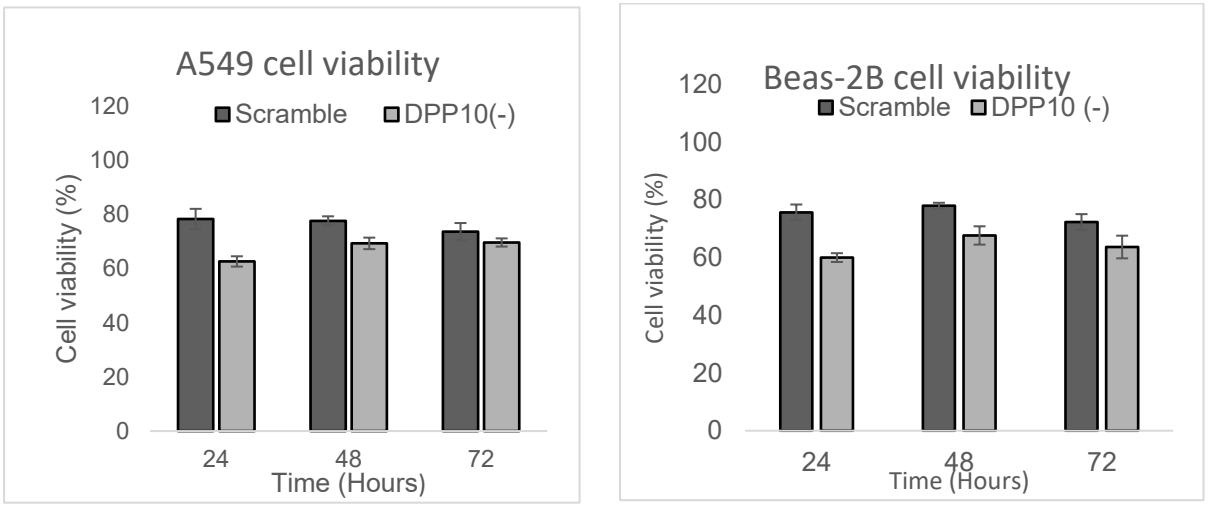


*Figure 20: Cell viability of A549 and Beas-2B cells after transfection with DPP10 siRNA using 9 µL lipofectamine RNAi Max for 24-, 48- and 72-hours vs negative control siRNA (scramble).*

5.3.2. OVEREXPRESSION OF DPP10 IN A549 AND BEAS2B CELLS

GENE CLONING

To obtain sufficient quantities for experimental use, the commercially available DPP10 ORF clone (Thermofisher #EC0113) was amplified by transformation into *E. coli* DH10B competent cells. Competent cells were transformed by first thawing on wet ice. 1.5 mL microcentrifuge

tubes were also placed on ice. The cells were gently mixed and aliquots of 50 µL were transferred to the chilled 1.5mL microcentrifuge tubes. DPP10 myc-DDK-tagged Human ORF clone (Origene #RC205435) was reconstituted by adding 100 µL of nuclease free water to the 10ng lyophylised pDNA to make a final concentration of 100ng/µL. 2 µL of reconstituted pDNA was then added directly into the tube of competent cells, mixed gently by flicking several times and allowed to incubate on ice for 30 minutes. The cells were heat shocked for 30 seconds in a 42°C water bath making sure not to shake or mix and then incubated on ice for 2 minutes. 250 µL of room-temperature S.O.C. Medium (Thermofisher #15544034) was added to the heat shocked cells and the tube placed on its side in a shaking incubator at 225 rpm for 1 hour at 37°C. 50 µL of the transformed cells were spread on LB agar plate with kanamycin (25 µg/mL). The plates were inverted and incubated overnight at 37°C. Following overnight incubation of the transformed cells, a sterile pipette tip was used to select a single colony from the plate and dropped into 5 mL LB broth with kanamycin (25 µg/mL) and swirled. The bottle of LB broth was loosely covered with its cap and the bacterial culture incubated at 37°C for 16 hours in a shaking incubator at 250 rpm.

PLASMID PREPARATION

Plasmid DNA was isolated using the GeneJet plasmid mini prep kit (Thermofisher #K0502). The bacterial culture was harvested by first transferring the broth containing the bacterial culture into a 15 mL centrifuge tube and centrifuged at 8000 rpm for 2 minutes at room temperature. The supernatant was decanted, and the cell pellets completely resuspended in 250 µL of the Resuspension Solution containing RNAse A by vortexing making sure that no clumps were remaining. The cell suspension was then transferred to a microcentrifuge tube and 250 µL of the Lysis Solution was added and mixed thoroughly by inverting the tube 5 times until the solution became viscous and slightly clear. 350 µL of the Neutralization Solution was added and mixed immediately and thoroughly by inverting the tube 5 times. The microcentrifuge tube was centrifuged for 5 min to pellet the cell debris and chromosomal DNA. The supernatant was transferred to the GeneJET spin column by pipetting making sure not to transfer the white precipitate, then centrifuged for 1 minute. The flow-through was discarded and the column placed back into the same collection tube. The GeneJET spin column was washed by adding 500 µL of Wash Solution diluted with isopropanol and centrifuged for 1 minute with the flow-through discarded after. The wash process was

repeated a second time with 500 µL of wash solution diluted with ethanol and centrifuged for 1 minute before discarding the flow through, after which the spin column was inserted back into the same collection tube. To remove all residual wash solution in the spin column, the spin column was further centrifuged for 1 minute and the flow through discarded. The GeneJET spin column was transferred into a fresh microcentrifuge tube and 50 µL of Elution Buffer added to the centre of the GeneJET spin column membrane to elute plasmid DNA. This was incubated for 2 min at room temperature and centrifuged for 2 min. Purified plasmid was collected, confirmed for the right plasmid insert (Appendix), stored at -20°C and the spin column discarded.

### DPP10 ORF CLONE TRANSFECTION

0.25 x $10^6$ A549 cells and 0.3 x $10^6$ Beas-2B cells were seeded in 6 well plates using 2mL DMEM enriched with 10% FBS and 1% Penicillin/streptomycin in each well and cultured in a 37$^o$c incubator with 5% $CO_2$ for 24 hours. 3 wells each were seeded for pDNA to be transfected and for control. After 24 hours when the cells have reached 70% confluency, two (2) microcentrifuge tubes of complexes were prepared. In tube 1, 125 mL Opti-MEM, 7.5 µL Lipofectamine 3000 (Thermofisher #L300008) was added. In a second tube, 125 µL Opti-MEM reduced serum (Thermofisher #A3635101), 2.5 µg pDNA of DPP10 clone, and 5 µL P3000 reagent was mixed. The content from tube 2 was added to tube 1 and mixed well, then allowed to incubate at room temperature for 15 minutes. 250 µL of the lipid-pDNA complex was added to each test well of cell culture, swirled and incubated at 37$^o$c incubator with 5% $CO_2$ for 24 hours. For the control wells, the same reagent for the test wells were prepared using the same quantity but without the pDNA in tube 2. 250 µL of the lipid mixed with p3000 reagent and Opti-MEM was added to each control well of cell culture, swirled and incubated at 37$^o$c incubator with 5% $CO_2$ for 24 hours. Following 24 hours, the transfection efficiency was analysed using flow cytometry.

### PREPARATION OF TRANSFECTED CELLS FOR FLOW CYTOMETERY

DPP10 ORF clone contains both a Myc and DDK tag and the DDK tag was used to analyse the uptake of the DPP10 ORF clone by A549 and Beas-2B cells using flow cytometry.
24 hours after both A549 and Beas-2B cell lines were transfected with DPP10 pDNA, cells transfected and control cells non transfected were harvested by trypanizing, assessed for cell viability, and counted. The cells were washed in PBS and resuspended to 1 x $10^7$ cells per mL

in ice cold flow cytometry (FC) buffer containing PBS containing 0.5% BSA then aliquoted into 100 µL volumes per microcentrifuge tubes and centrifuged at 400g for 5 minutes following which the supernatant removed. To fix the cells, 200 µL 4% paraformaldehyde in PBS was added to the cell pellet, resuspended, and incubated on ice for 20 minutes in the dark. The cells were then washed twice in 0.5% BSA in PBS centrifuged at 400g for 5 minutes and supernatant removed. The cell pellets were resuspended in 200 µL permeabilization buffer prepared with 0.1% saponin, 0.5% BSA in PBS, incubated at room temperature for 15 minutes, washed twice in the permeabilization buffer and centrifuged at 400g for 5 minutes. The cell pellets were resuspended in primary antibody clone OTI4C5, Anti-DDK (FLAG) mouse monoclonal antibody (Origene #TA50011) diluted 1:500 in permeabilization buffer and incubated for 1 hour with gentle shaking on ice. The cells were washed twice using permeabilization buffer, centrifuged and the supernatant removed. The cell pellets were suspended in secondary antibody Rabbit Anti-Mouse IgG H&L Alexa Fluor® 488 diluted to 1:1000 in permeabilization buffer and incubated on ice for 30 minutes after which the cells were washed twice in permeabilization buffer, centrifuged and the supernatant discarded. The cell pellets were then resuspended in FC buffer and the data read using the Guava easyCyte flow cytometer.

## 5.4. RESULT

### 5.4.1. FLOW CYTOMETRY ANALYSIS OF OVER EXPRESSION

To confirm successful transfection of the DPP10 ORF clone in A549 and Beas-2B cells, flow cytometer analysis was performed 24 hours post-transfection using an anti-DDK (FLAG) antibody to detect the DDK tag present on the DPP10 construct.

In control (non-transfected) A549 cells, all events were detected in the low fluorescence region with no measurable Alexa Flour 488 signal, confirming the absence of the background fluorescence (Figure 10 - A, B). In contrast, transfected A549 cells showed a clear shift in fluorescence intensity, with 82.2% of the gated population detected in high fluorescence region, corresponding to DPP10 DDK positive cells (Figure 10 - C, D). The remaining 17.8% of cells fell within the low fluorescence gate, representing the non-transfected or weakly expressing cells

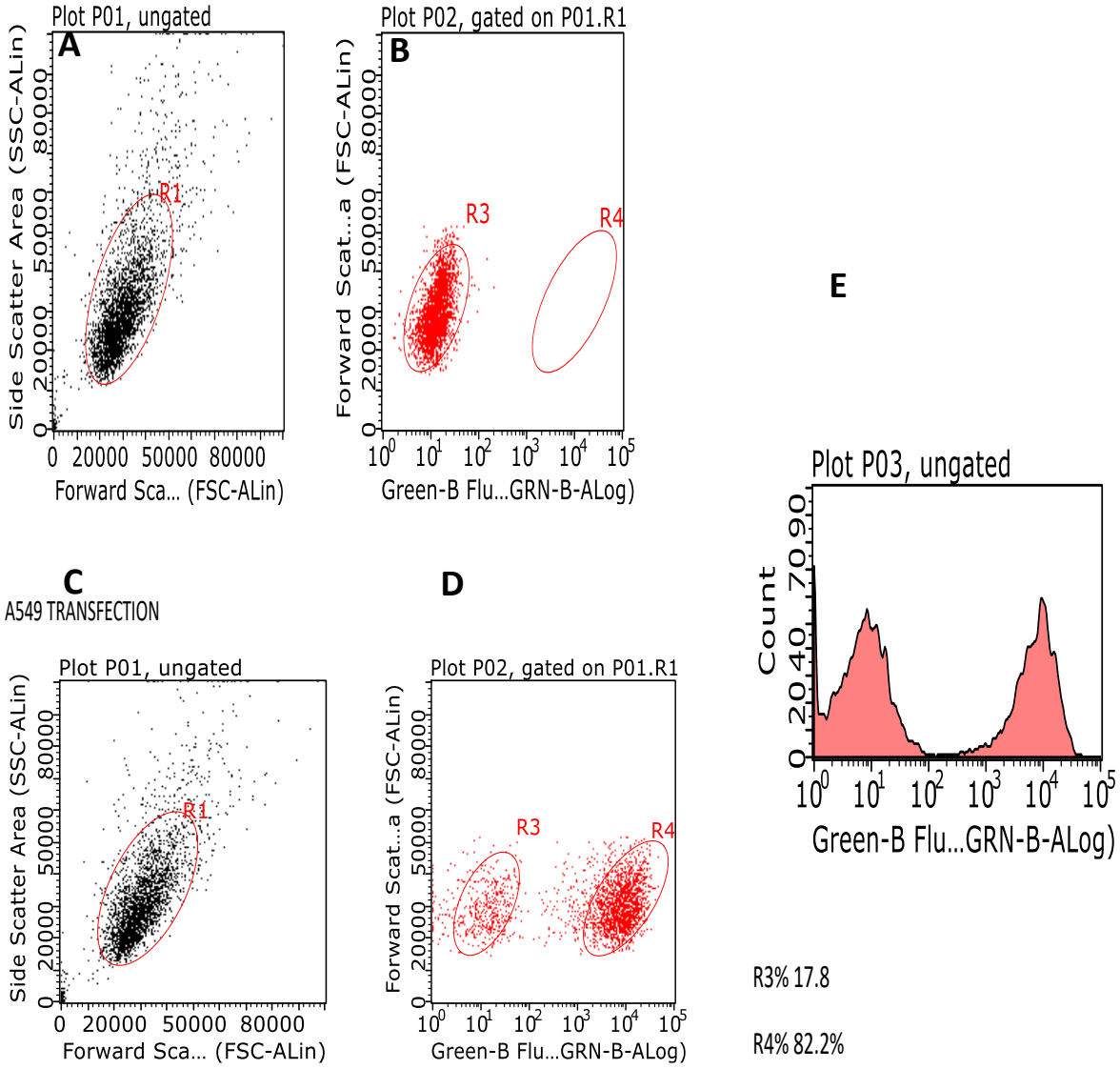


*Figure 21: Flow cytometry of DDK tag in A549 transfected with DPP10 ORF clone. A) Ungated plot of non-transfected A549 cells (control) B) Green-B fluorescence (525/30nm) gated on forward scatter of non-transfected A549 cells. R4 indicates cell population that possess DDK tag C) Ungated plot of A549 cells transfected with DPP10 ORF clone. D) Green-B fluorescence (525/30nm) gated on forward scatter of non-transfected A549 cells. R3 represents cell population without DDK tag (17.8%), R4 indicates cell population that possess DDK tag (82.2%). E) Histogram showing A549 cell population with and without the DKK tag. Presence of the DKK tag indicates that these cells have taken up the DPP10 ORF clone.*

A similar gating strategy was used for Beas-2B cells, yielding comparable results of no measurable Alexa fluor 488 signal in non-transfected cells (Figure 20 – A, B) and 85.5% gated cell population in the high fluorescence region (Figure 20 - C, D)

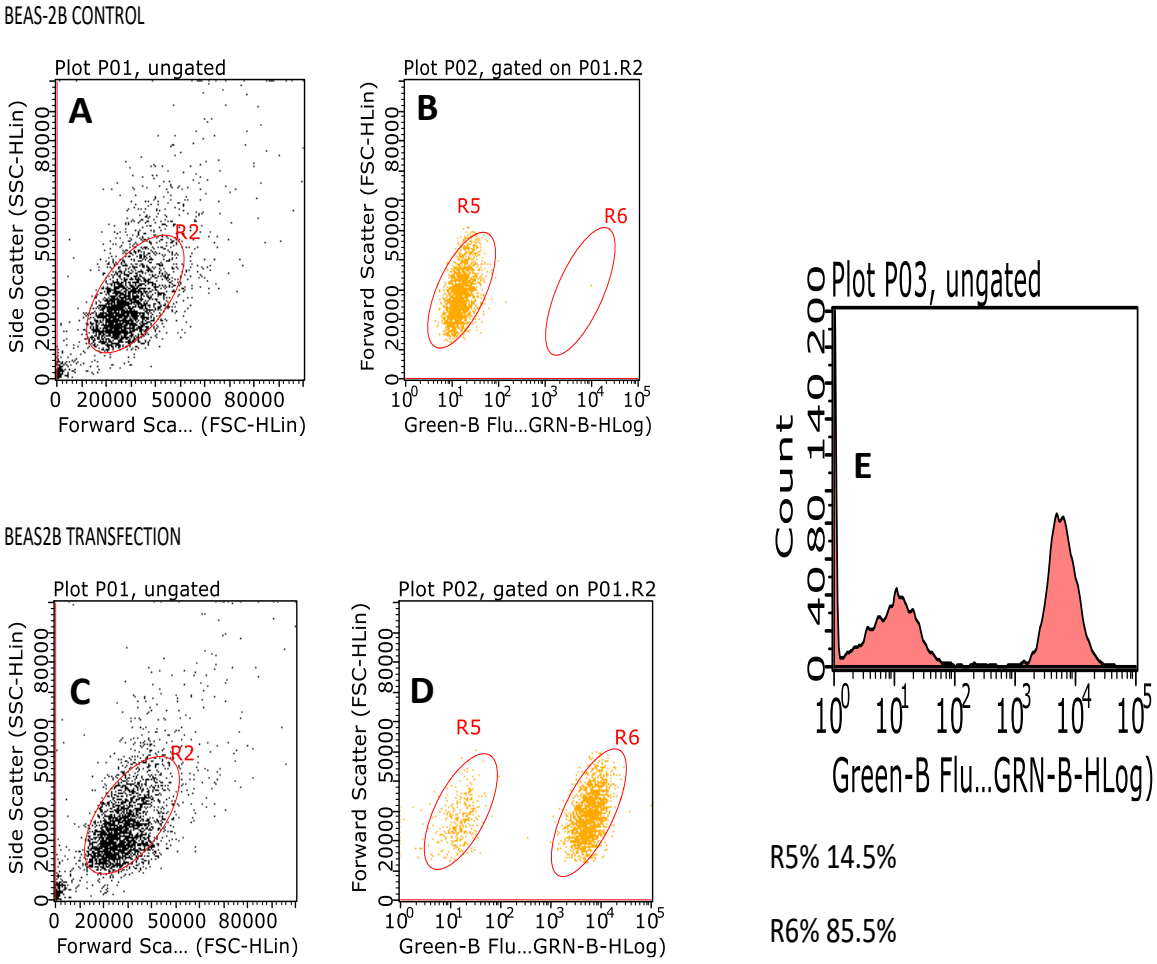


*Figure 22: Flow cytometry of DDK tag in Beas-2B cells transfected with DPP10 ORF clone. A) Ungated plot of non-transfected Beas-2B cells (control) B) Green-B fluorescence (525/30nm) gated on forward scatter of non-transfected Beas-2B cells. R4 indicates cell population that possess DDK tag C) Ungated plot of Beas-2B cells transfected with DPP10 ORF clone. D) Green-B fluorescence (525/30nm) gated on forward scatter of non-transfected Beas-2B cells. R3 represents cell population without DDK tag (17.8%), R4 indicates cell population that possess DDK tag (82.2%). E) Histogram showing Beas-2B cell population with and without the DKK tag. Presence of the DKK tag indicates that these cells have taken up the DPP10 ORF clone.*

These results confirm efficient uptake and expression of the DPP10 ORF clone in A549and Beas-2B cells with transfection efficiency of approximately 82% and 86% respectively.

### ACUTE STIMULATION OF DPP10 SILENCED AND OVEREXPRESSED A549 AND BEAS-2B CELLS

From the baseline experiments, stimulation of both A549 and Beas-2B cells for 24 hours with 5% CSE significantly increased the gene expression of IL6, IL8 and TNFα, whereas treatment with 5% VE elevated IL6 and IL8 expression but did not affect TNFα levels.

24 hours following DPP10 gene silencing or overexpression, both cell lines were treated with 5% CSE, VE or NFVE for 24 hours. After treatment, the culture supernatants were collected

for ELISA analysis to determine how much cytokine expression was translated to protein, and the cells were harvested for gene expression profiling of IL6, IL8 and TNFα.

Cells were not stimulated beyond 24 hours, as baseline studies showed cytokine production peaked at this point. Additionally, siRNA transfection efficiency was highest at 24 hours post transfection, returning to control levels by 48 hours in A549 cells. Transfection with the DPP10 ORF clone achieved efficiencies of 82% and 85.5% in A549 and Beas-2B cells respectively at 24 hours.

### 5.4.2. EFFECT OF DPP10 MODULATION ON CYTOKINE GENE EXPRESSION

Following transfection, cells were stimulated with 5% CSE, 5% VE or 5% NFVE for 24 hours. Cytokine expression was quantified by qPCR.

In control A549, CSE exposure produced the strongest upregulation in cytokine gene expression with 3.4-fold (IL6), 4.49-fold (IL8), and 2.10-fold (TNFα) increases relative to untreated controls. VE treatment also induced cytokine expression but to a lesser extent (2.01-fold for IL6 and 2.79-fold for IL8), while NFVE resulted in only minimal changes (~1.04-fold for IL6). Similar results were observed in Beas-2B cells, with CSE producing the highest induction of IL6 (3.46-fold), IL8 (2.31-fold), and TNFα (5.65-fold) (Figure 16).

When DPP10 expression was manipulated, modest directional changes in cytokine expression were observed. In A549 cells, DPP10 knockdown slightly increased IL6 (3.4 to 3.57-fold), IL8 (4.49 to 4.64-fold), and TNFα (2.10 to 2.23-fold), while DPP10 overexpression slightly reduced these values (e.g., IL6 3.4 to 3.18-fold, IL8 4.49 to 4.13-fold). Comparable trends were seen in Beas-2B cells where IL6 and TNFα were marginally elevated following knockdown and reduced with overexpression, though IL8 expression decreased slightly in DPP10-silenced cells. None of these changes reached statistical significance.

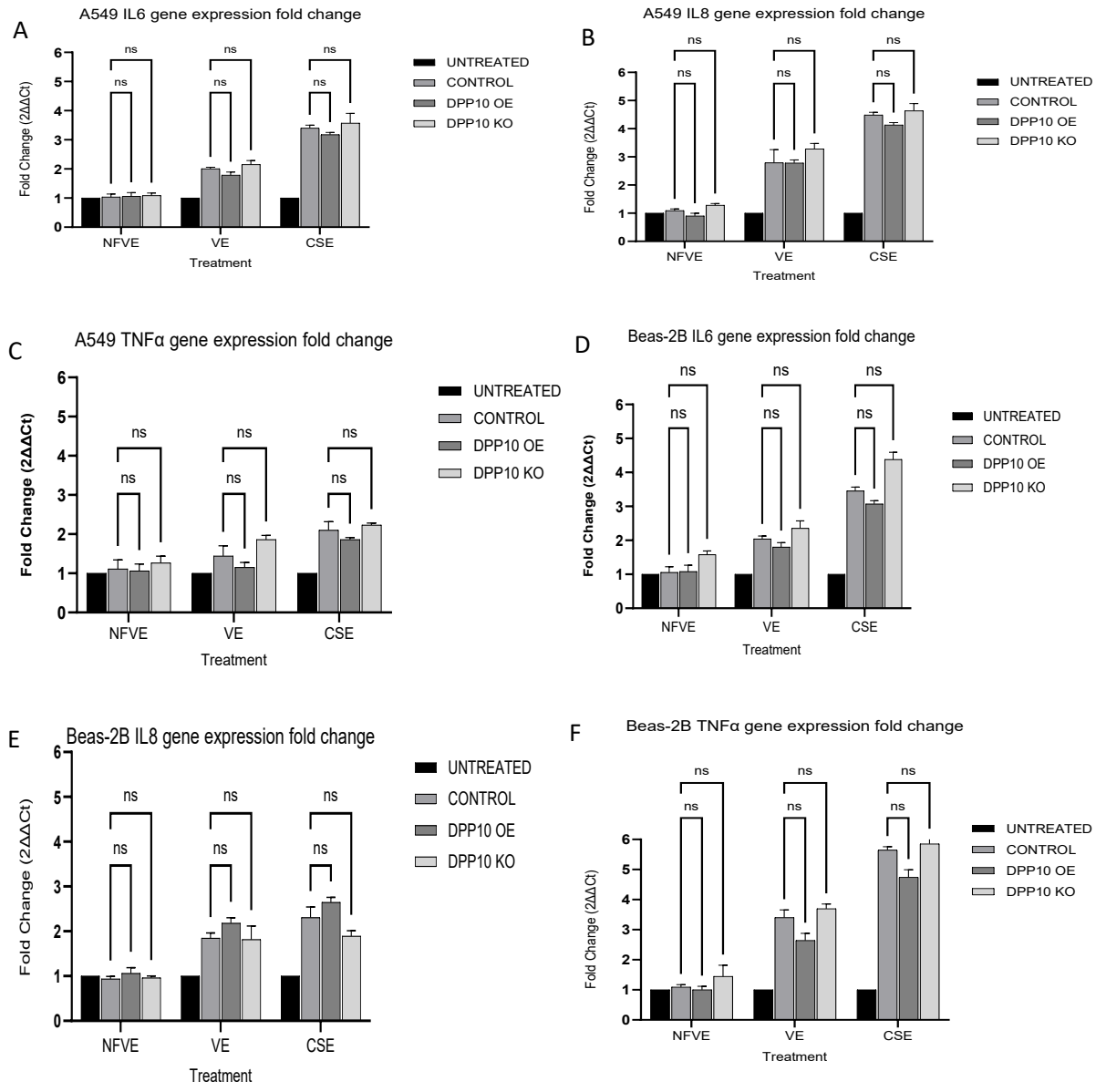


*Figure 23: Gene expression changes in lung epithelial cell lines where the DPP10 gene has been knocked down using siRNA or over expressed with an ORF clone. A. IL6 gene expression in A549 cells following lipid-based transfection with DPP10 siRNA or ORF clone. B. IL8 gene expression in A549 cells following lipid-based transfection with DPP10 siRNA or ORF clone. C. TNFα gene expression in A549 cells following lipid-based transfection with DPP10 siRNA or ORF clone. D. Changes in gene expression of IL6 in DPP10(-) and DPP10 (+) Beas-2B cells treated with NFVE, VE and CSE. E. Changes in gene expression of IL8 in DPP10(-) and DPP10 (+) Beas-2B cells treated with NFVE, VE and CSE. F. Changes in gene expression of TNFα in DPP10(-) and DPP10 (+) Beas-2B cells treated with NFVE, VE and CSE. Data is expressed as mean±SEM of 5 biological replicates, n=5 each. *P≤0.05, **P≤0.01, ***P≤0.001, ≤0.0001 vs treated control samples which are wild type cells that have been stimulated with NFVE, VE or CSE.*

### 5.4.3. EFFECT OF DPP10 ON CYTOKINE PROTEIN EXPRESSION

To investigate the potential modulatory role of DPP10 on epithelial inflammation, A549 and Beas-2B cells were treated with CSE, VE, or NFVE for 24 hours following either DPP10

knockdown, overexpression, or control transfection. Secreted IL-6, IL-8, and TNFα protein levels were measured by ELISA.

In A549 cells, exposure to CSE induced the largest increase in IL-6 levels compared with untreated cells (382.4 pg/mL in control), followed by VE (243.6 pg/mL) and NFVE (167.5 pg/mL). Knockdown of DPP10 slightly augmented IL-6 secretion across all treatments (NFVE: 167.6 pg/mL; VE: 240.5 pg/mL; CSE: 390.4 pg/mL), while DPP10 overexpression resulted in modest reductions relative to control, particularly for CSE and VE treatment (CSE: 370.3 pg/mL; VE: 236.5 pg/mL). Similar trends were observed for IL-8, with CSE again eliciting the strongest response (347.5 pg/mL control), followed by VE (163.2 pg/mL) and NFVE (161.1 pg/mL). DPP10 knockdown slightly increased IL-8 release (NFVE: 172.3 pg/mL; VE: 182.8 pg/mL; CSE: 350.2 pg/mL), whereas overexpression slightly attenuated cytokine levels (NFVE: 162.4 pg/mL; VE: 174.6 pg/mL; CSE: 337.7 pg/mL). TNFα secretion showed smaller changes across treatments, with DPP10 knockdown slightly elevating protein levels and overexpression modestly reducing them, consistent with the trends observed for IL-6 and IL-8.

Beas-2B cells displayed a comparable pattern of cytokine induction. CSE induced the highest IL-6 production (270–316 pg/mL depending on DPP10 status), followed by VE (127–212 pg/mL) and NFVE (125–146 pg/mL). DPP10 knockdown marginally increased IL-6 secretion relative to control, while overexpression generally resulted in slight reductions. TNFα responses were less pronounced, with DPP10 knockdown slightly elevating TNFα secretion and overexpression producing minor decreases. These trends were consistent across NFVE, VE, and CSE treatments, indicating that while DPP10 may subtly modulate cytokine output, the overall inflammatory response is predominantly driven by the exposure.

Across both cell lines, CSE consistently elicited the strongest inflammatory response, followed by VE, and then NFVE. DPP10 knockdown generally resulted in minor increases in cytokine secretion, whereas overexpression produced modest decreases, suggesting a potential dampening effect of DPP10 on acute epithelial cytokine responses. However, none of the observed differences reached statistical significance, indicating that DPP10 may have a subtle or modulatory role under these acute exposure conditions. The trends were broadly consistent for all three cytokines (IL-6, IL-8, TNFα) and across both A549 and Beas-2B cells, supporting the reliability of these findings.

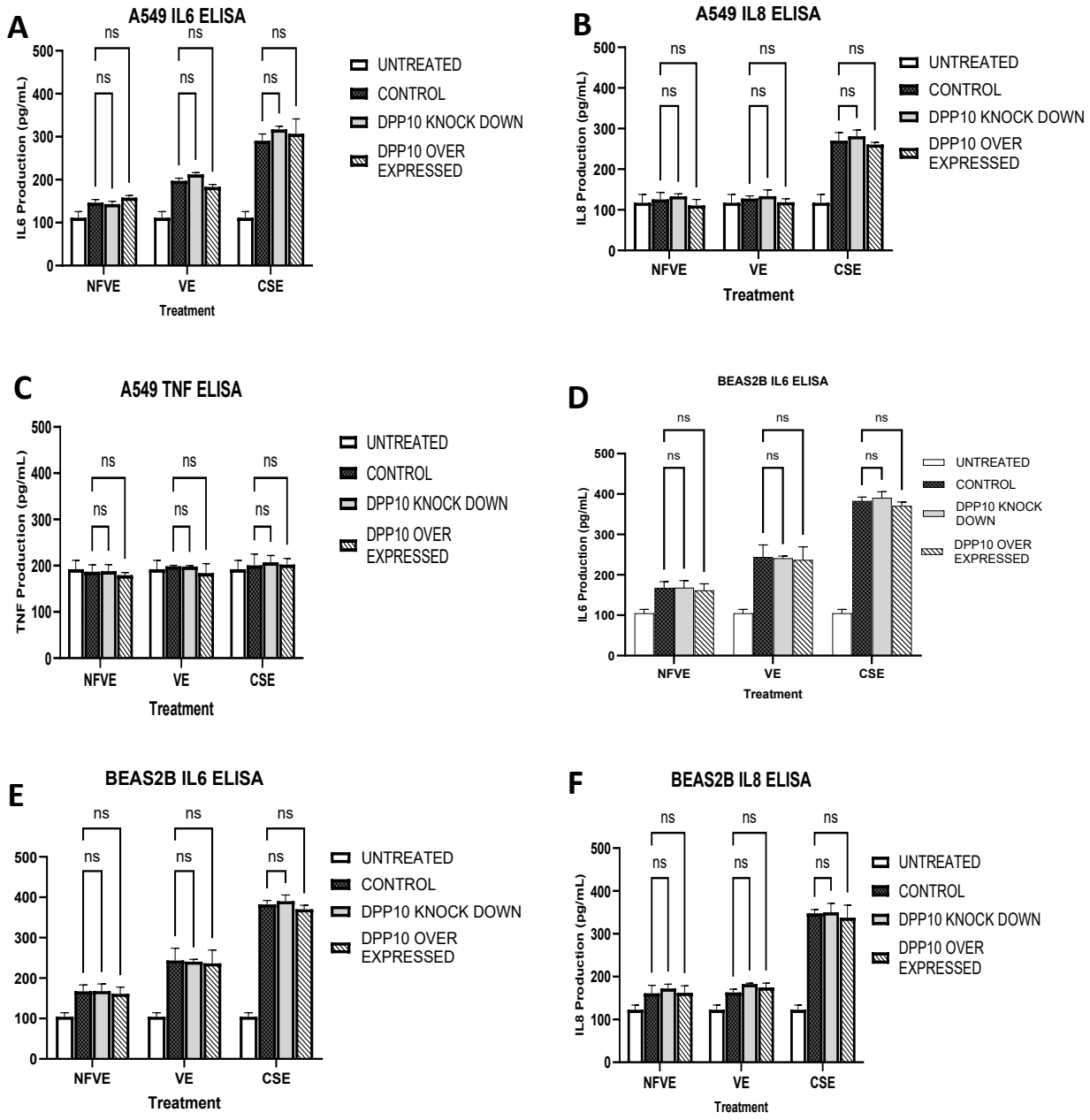


*Figure 24: Cytokine production changes in lung epithelial cell lines where the DPP10 gene has been knocked down using siRNA or over expressed with an ORF clone. A. IL6 protein expression in A549 cells following lipid-based transfection with DPP10 siRNA or ORF clone. B. IL8 protein production in A549 cells following lipid-based transfection with DPP10 siRNA or ORF clone. C. TNFα level in A549 cells following lipid-based transfection with DPP10 siRNA or ORF clone. D. Changes in protein level of IL6 in DPP10(-) and DPP10 (+) Beas-2B cells treated with NFVE, VE and CSE. Changes in IL8 protein production in DPP10(-) and DPP10 (+) Beas-2B cells treated with NFVE, VE and CSE. F. Changes in protein level of TNFα in DPP10(-) and DPP10 (+) Beas-2B cells treated with NFVE, VE and CSE. Data is expressed as mean±SEM of 5 biological replicates, n=5 each. *P≤0.05, **P≤0.01, ***P≤0.001, ≤0.0001 vs treated control samples which are wild type cells that have been stimulated with NFVE, VE or CSE.*

## 5.5. DISCUSSION

This study aimed to elucidate whether DPP10 contributes to regulating the inflammatory response of human airway epithelial cells during exposure to cigarette smoke and vaping extracts. By employing both gene silencing and overexpression approaches, this investigation explored the impact of DPP10 modulation on IL6, IL8, and TNFα expression at the transcriptional and translational levels.

When DPP10 expression was manipulated, no statistically significant changes in cytokine gene expression or protein release were observed under any of the experimental conditions. The magnitude of cytokine induction changed modestly. In A549 cells, DPP10 knockdown resulted in a small but consistent increase in IL6 (3.4 to 3.57-fold), IL8 (4.49 to 4.64-fold) and TNFα (2.10 to 2.23-fold) gene expression after CSE stimulation, while overexpression slightly reduced these responses. Similar modest trends were observed in Beas-2B cells for IL6 (3.46 to 4.38-fold) and TNFα (5.65 to 5.85-fold), whereas IL8 expression was slightly reduced after DPP10 knockdown (2.31 to 1.89-fold). These findings suggest that while DPP10 may influence inflammatory signalling, its effect under the present experimental conditions is limited.

In the initial experiments, stimulation with CSE and VE significantly upregulated IL6 and IL8 gene expression in both epithelial cell lines, consistent with baseline experiment. The strongest response was observed with CSE treatment 3.4- and 4.5-fold increases respectively followed by VE treatment 2-fold and 2.79-fold for IL6 and IL8 respectively. In contrast, NFVE induced minimal changes in cytokine expression (1.04-fold increase) suggesting that nicotine and other combustion related chemicals contribute substantially to observed pro-inflammatory response.

Although only minimal changes are observed in cytokine expression after DPP10 gene manipulation, subtle changes in gene expression trends hint at a potential modulatory or protective role. The slightly higher cytokine levels observed in DPP10 knockdown cells and marginal reductions in overexpressed cells suggest that DPP10 could dampen the pro-inflammatory response to CSE and VE exposure.

Cytokine protein expression mirrored gene expression changes and only very modest increases in cytokine were observed in DPP10 knockdown conditions, none of these changes reached significance.

Importantly, this study represents the first attempt to examine DPP10's role in a smoking and vaping model. Previous studies (Horng et al., 2001, 2002; Fitzgerald et al., 2001; Kagan and Medzhitov, 2006; Yamamoto et al., 2003) have investigated IL8 and IL6 protein levels in DPP10 knock down and over expressed NHBE (Normal human bronchial epithelial cell lines) stimulated with IL1β, a potent activator of pro-inflammatory cytokines. Building on this knowledge, the present study is the first to investigate whether DPP10 modulates thus pathway in a smoking and vaping model using A549 and Beas-2B cells. The modest cytokine trends observed here may indicate that DPP10 plays a stabilising role rather than a primary regulatory role during epithelial inflammatory response.

Furthermore, the reduced cell survival seen in DPP10 knockdown populations compared with scrambled siRNA controls suggests a potential role of DPP10 in cell viability and stress tolerance. Although liposome-based siRNA transfection can itself cause cell toxicity (Goodwin and Huang, 2014; Filion and Phillips, 1997), the consistent reduction in viable cells following both DPP10 silencing siRNA transfection and control with scramble siRNA implies that loss of DPP10 may increase susceptibility to CSE or VE cell death.

# 6. EFFECT OF DPP10 ON CELL CYCLE AND APOPTOSIS

## 6.1. INTRODUCTION

Cell cycle is a complex process that is required for cell growth, proliferation, and DNA repair. Morphologically, a complete cell cycle is made of 2 parts; an interphase and a mitotic phase (M phase). The interphase is comprised of the S phase and 2 gap phases G1, G2 which are landmarks between DNA synthesis (S phase) and mitosis. Cells in the G1 phase grow in size, synthesize proteins and RNA required for DNA synthesis, and more importantly produce the centromere; a microtubule structure which holds the 2 sister chromatids of a chromosome. Cells then move into the S phase where all copies of DNA are made. At the end of S phase, each cell has 2 copies of genetic material. In G2 phase, the cells start to condense their genetic material in preparation for cell division in the M phase. Within the different stages of cell cycle are regulatory protein complexes made of cyclin dependent kinase (cdk) and cyclins. Cdks depend on cyclins for their function and only possess protein kinase activity when tightly bound to cyclins. Unlike cdk levels which are constant through the cell cycle, cyclins undergo a cycle of synthesis and degradation in each cell cycle. Three (3) classes of cyclins bind to cdk depending on the cell cycle phase. G1/S cyclins bind at the end of the G1 phase thus commit5ting the cell to DNA replication, S cyclins bind during the s phase and is critical for initiating DNA replication. M cyclins bind in the M phase to promote mitosis.

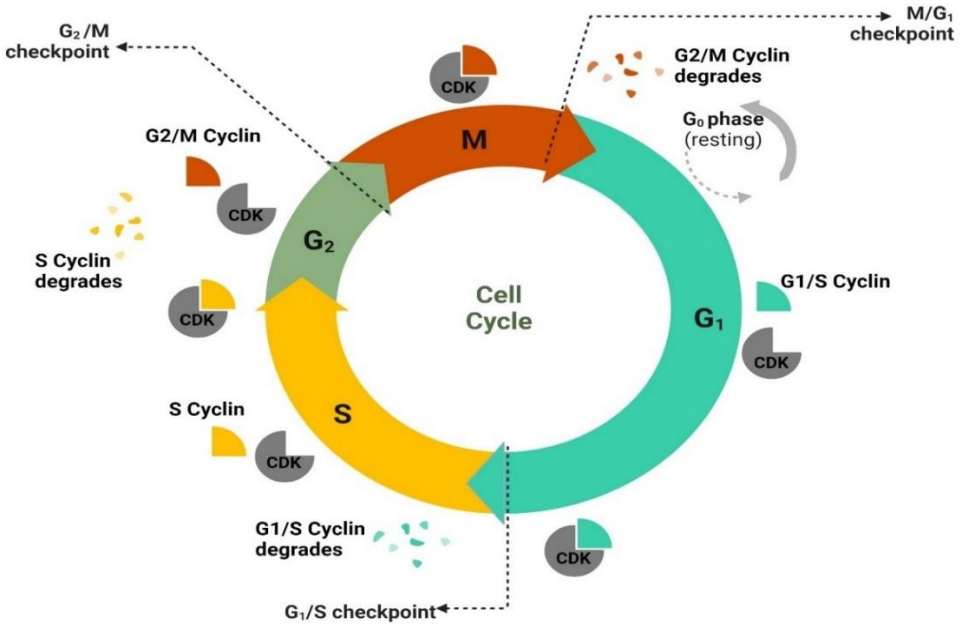


*Figure 25: Cell cycle showing the checkpoint regions and cyclin recycling stages*

Within the cells, apoptosis serves as a distinct means of arresting cell growth, and thus an inability of the cells to progress to the S phase. During apoptosis, cells undergo programmed cell death, a process used as a homeostatic mechanism to maintain cell population or as a protective mechanism following cell damage by disease or harmful agents, for instance when cells encounter harmful agents such as DAMPs (Norbury and Hickson, 2001). Typically, cells that die due to acute injury swell, burst and release their endogenous content into the cell surrounding thereby initiating inflammatory responses. This process is known as cell necrosis and contrasts with apoptosis where the nuclear membrane's integrity is maintained till cell death. Here, the cells shrink, condense, with an associated break up in DNA fragment and rapid phagocytosis before any release of its intracellular content (Kerr, 1969, 1971; Kerr et al., 1972; Taatjes et al., 2008). Although a wide variety of stimuli can trigger apoptosis, not all cells respond similarly to the same stimulus. For instance, oestrogen has been shown to have anti apoptotic and cell proliferating functions in epithelial cells but is also capable of inducing apoptosis in some breast cancer cells (Gompel et al., 2000; Marino and Ascenzi, 2008; Jordan et al., 2005; Lewis et al., 2004, 2005; Song et al., 2001; Wolf and Jordan, 1993).
Two distinct (2) pathways lead to apoptosis; an extrinsic pathway (extracellularly induced) and an intrinsic pathway also known as the mitochondrial apoptosis, due to its dependence on factors released by the mitochondria and its activation in response to intracellular stress signals, including reactive oxygen species, viral infection and DNA damage (Krammer, 2000; Lossi, 2022).

In the extrinsic pathway, extracellular signals such as Fas ligand or TNFα released by other cells bind to death receptors on the cell surfaces. Death receptors (DR) are a subgroup of the TNF receptor superfamily characterised by repeats of cysteine rich extracellular domain which are crucial for ligand specificity (Ashkenazi and Dixit, 1998). These DRs have an 80 amino acid cytosolic sequence also known as the death domain and are highly conserved in this sub-group (La et al., 1993). The extrinsic pathway follows either the TNF or Fas pathway depending on the binding ligand. The Fas pathway is characterised by the binding of the Fas Ligand, a type 2 membrane protein expressed by cytotoxic T lymphocytes or natural killer (NK) cells L to the FAS receptor, which initiates the recruitment of Fas adapter proteins such as Fas associated death domain protein (FADD). FADD protein is made up of a death domain which dimerizes with the DD of the FAS receptor located in the cell cytosol, leaving its DED

available to form a complex with the DED of initiator pro caspases such as caspase 8 and 10. The initiator procaspase is cleaved to its active form and these activated initiator caspases then go on to cleave executor procaspase turning them into their active form and initiating the apoptotic pathway (Suda et al., 1993; Chinnaiyan et al., 1995; Bang et al., 2000; Boldin et al., 1995; Stanger et al., 1995; Svandova et al., 2017).

Similarly, the TNF pathway is initiated by the binding of TNF to TNF receptor (TNFR). In its inactive state, TNFR is bound to SODD which keeps the DD silence and prevents apoptosis. When TNF binds to the TNFR, DD undergoes conformational changes with the subsequent release of SODD and activation of its DD, this leads to the recruitment of the adaptor proteins TNFR1-associated death domain protein (TRADD), receptor interacting protein (RIP1) and Tumour necrosis factor (TNF) receptor associated factor-2 (TRAF2). This complex made up of TRADD, RIP1 and TRAF2 ligates and binds to FADD to form the death inducing signalling complex (DISC). The DISC is cleaved off from the DD of TNFR1 and binds to FADD followed by a cleavage of the initiator procaspase 8 or 10 to its active form caspase 8 and activation of the effector caspases with subsequent apoptosis (Chinnaiyan et al., 1995; Hsu et al., 1996a, 1996b; Bang et al., 2000).

Following the release of intracellular signalling damage molecules, ATM kinase, a protein involved in S checkpoint regulation is activated. The kinase phosphorylates p53, which in turn phosphorylates and activates BCl2. In its inactive form, BCl2 is bound to BAX/BAK and act as inhibitory molecules to these proteins. Once BCl2 is activated, BAX/BAK present on the mitochondrial membrane is liberated and induces the formation of channels on the mitochondrial membrane causing the outflow of cytochrome C. Outside of the mitochondria, a complex made of cytochrome C, Apaf1, and procaspase 9 is formed, this complex is known as the apoptosome and functions by cleaving executor procaspases into their active form (T et al., 2002; I et al., 1998; Green and Kroemer, 2004; Cain et al., 2000; Cory and Adams, 2002; Kluck et al., 1997).

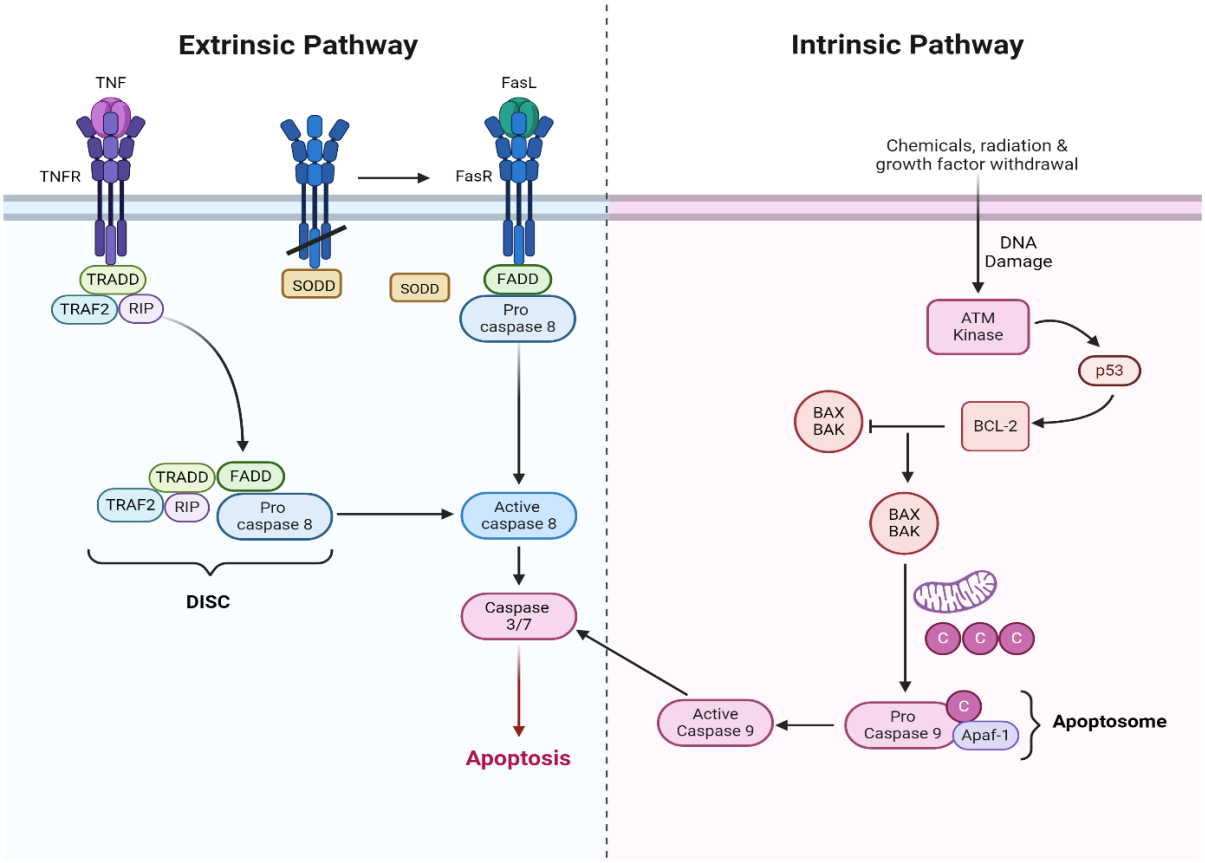


*Figure 26: Extrinsic and Intrinsic Apoptotic pathway*

Both the intrinsic and extrinsic pathways activate caspases, a family of cysteine endoproteases that facilitate the cleavage of several structural proteins leading to an irreversible commitment to cell death (Widmann et al., 1998). Some of the important caspase substrate include flippase and scramblase, two important proteins involved in the formation and dissolution of the membrane asymmetry observed in apoptosis (Daleke, 2003; Graham, 2004). Non apoptotic cells are characterised by an asymmetric phospholipid bilayer in its plasma membrane structure Sphingolipids and phosphatidylcholine (PC) in the external leaflet while the internal leaflet is made chiefly of phosphatidyl serine. The sequestering of PS to the cytosolic leaflet is maintained by flippase. When cells become apoptotic, this membrane asymmetry is lost, and PS moves bidirectionally to the cell surface in a process catalysed by phospholipid scramblase. On the external leaflet of the cells, PS act as “eat me signals” for phagocytic cells to clear the apoptotic cells. Caspases reduce the activity of flippase and activate scramblase through cleavage reactions thereby promoting apoptosis (Segawa et al., 2014; Sakuragi et al., 2019; Fadok et al., 1992; Suzuki et al., 2013, 2014).

## 6.2. LITERATURE REVIEW

Cigarette smoke contains many chemicals which are known carcinogens and have been proven to impact the apoptotic pathway. Studies have shown that caspases are activated on exposure of lung cells to cigarette smoke extract through the mitochondrial pathway (Lee et al., 2016). In addition, exposure to cigarette smoke has also been associated with higher levels of oxidative stress which contributes to intrinsic apoptosis by disrupting DNA integrity and mitochondrial function (Solanki et al., 2018; Tang et al., 2022; Chen et al., 2015b). A loss in the aryl hydrocarbon receptor expression on exposure to cigarette smoke has also been shown to lead to the classic occurrence observed in intrinsic apoptosis such as chromatin condensation, release of cytochrome c, and cleavage of the procaspase-3 (Rogers et al., 2017).

The effect of cigarette smoke on cell apoptosis affects more than just the cells of the airways and appear to be a contributing factor to many of the chronic diseases observed with long term smokers such as cancers, and cardiovascular diseases. For instance, immune cells, endothelial cells and epithelial cells outside of the lungs which are exposed to cigarette smoke show many signs of apoptotic dysregulation (Bellamri et al., 2022; Chen et al., 2012; Song et al., 2021a)

Like apoptosis, cell cycle dysregulation has also been observed in exposure to cigarette smoke contributing to the development and progression of many types of cancers and chronic lung disease where aberrant cell turnover is implicated. Many key regulators of the cell cycle such as cyclins, CDKs and tumour suppressor proteins are affected by cigarette smoke. Perhaps the most studied effect of cigarette smoke on cell cycle is the G1 to S phase transition with many conflicting outcomes.

CSE enhances phospholipid transfer protein (PLTP) a common regulatory protein in apoptosis and cell cycle, knockdown of which can partly abrogate caspase 3 cleavage (Chen et al., 2015a) and the expression of TGF beta 1, a potent anti-mitogen capable of blocking late G1 activation and preventing S phase entry of cells. CS exposure also causes cyclin D1 and its partner kinase CDK4 to be suppressed thereby arresting cell at G1 phase (Chai et al., 2016; Hocevar and Howe, 1998). The long non coding RNA, linc00152 which regulates G1/S phase checkpoint is also increased in serum of smokers with an associated decrease on S phase cells when observed invitro in lung cell lines exposed to CSE (Liu et al., 2019). Interestingly, there

have also been studies showing that CDK4 and cyclin D1 is induced on exposure to cigarette smoke. Expression of nuclear factor-κB (NF-κB) and it's signalling product cyclin D1 was induced persistently for 24 hours in lung adenocarcinoma cell line exposed to cigarette smoke condensate (Shishodia and Aggarwal, 2004) CSE was also observed to induce the downregulation of P16, a tumour suppressor and CDK4/6 inhibitor preventing G1/S phase transition (Guo et al., 2017) and blocking senescent signals thereby promoting progression of malignancies associated with cancer (Witkiewicz et al., 2011). D'Anna et al., (2015) showed that by exposing lung fibroblasts to cigarette smoke extract, both P38 and ERK1/2, a mitogen activated protein which is necessary for the G1/S phase transition is highly expressed accompanied by a decrease in the percentage of cells in S phase and an increase in G1/G2 cells. Indicating that there may be many other signalling pathways that cause this G1/S phase arrest outside of ERK1/2 or that the activity of ERK1/2 is not sustained till the end of the G1 phase (Xamamoto, T et al., 2006; Meloche, S, 1995). These differences in G1/S phase transition in response to cigarette smoke exposure may also be due to differences in cigarette smoke doses across different laboratories. For instance, Wang et al., (2020b) observed changes in both mRNA and protein expression levels of cyclin D1 in cells exposed to CSE in a dose dependent manner with lower concentration of CSE associated with significant increases compared with control, while at higher concentrations, this expression is decreased significantly. Both CDK4/6 and cyclin D1 are required for G1/S phase transition (Montalto and De Amicis, 2020; Fassl et al., 2022)

Although e-cigarettes have gained popularity as a perceived safer alternative to traditional cigarettes, many emerging evidence suggest that the combustion product of liquids used in the e-cigarette contain numerous potentially harmful chemicals (Goniewicz et al., 2014; Kosmider et al., 2014; Uchiyama et al., 2020). These constituents can impact cellular processes such as apoptosis and cell cycle thereby contributing to adverse health outcomes. E cigarette vapour induced apoptosis via caspase 3 pathway in human gingival epithelial cells (Rouabhia et al., 2017). Using acridine orange (AO) and Hoechst33258 staining, E cigarette aerosol condensate induced apoptosis was observed by Su et al (2023)
in human gingival epithelial cells although less marked when compared with traditional cigarette extract. The effect of E cigarette on DNA damage and mitochondrial depolarisation,

marks of intrinsic apoptosis were also observed by Wang et al (2022) although this was not associated with cytochrome c release even at high doses.

The effect of nicotine, a constituent of electronic cigarette on apoptosis has also been well documented (Zanetti et al., 2014; Villablanca, 1998; Galitovsky et al., 2004; Jang et al., 2002; Kim et al., 2005), however many nicotine free e cigarette exposure have also been shown to induce apoptosis (Sancilio et al., 2016; Holliday et al., 2016) . Flavour choice of e cigarette liquid can also have an effect on apoptosis with an increase in flavour profile complexity associated with increased apoptosis (Ween et al., 2020) and ROS production (Lerner et al., 2015). Comparisons between other components of E cigarette liquid propylene glycol (PG) and glycerol which form the bulk of the E-liquid indicate a higher propensity of PG to cause cellular damage compared with glycerol. In a study by Komura et al (2022) small airway epithelial cells were positive for the phosphorylated histone H2AX a DNA damage marker with an increase in cells with activated caspase 3 and 7. These effects were also observed but markedly less in cells stimulated with just glycerol. PG also increases the number of activated caspase 3 cells in the brain of rats injected with PG in a dose dependent manner (Lau et al., 2012a)

Although not many studies have been done regarding how e-cigarette exposure can affect the cell cycle, nicotine has been implicated in modulating cell cycle progression through increase in cyclin D1 expression and activity (Chu et al., 2005), suppression of cyclin B1 (Hajiasgharzadeh et al., 2020) and G0/G1 cell cycle arrest (Lee et al., 2005a).

## 6.3. EFFECT OF DPP10 ON CELL CYCLE

### 6.3.1. ASSAY PRINCIPLE

Cell cycle regulation is critical to cell survival because it controls repair of DNA damage and prevents uncontrolled cell division. Defects in the cell cycle regulation are often characteristic of exposure to mutagens and are very common on cancer or tumour cells. occur. The Muse™ Cell Cycle Kit uses fluorescent intensity of the nuclear DNA intercalating stain propidium iodide (PI) and RNAse A (which increases the DNA staining specificity) to quantify cell cycle phases. Resting cells in G0/G1 contain two copies of each chromosome. As the cells begin to divide, chromosomal DNA is synthesized (S phase). The fluorescence intensity from PI

continues to increase till all chromosomal DNA have doubled which is the G2/M. At this stage, the fluorescent intensity is twice as observed in the G0/G1 phase with twice the intensity of the G0/G1 population. Cells in G2/M cells eventually divide into two daughter cells. PI is stoichiometric and binds in proportion to the amount of DNA present and is thus able to differentiate cells into these 3 cell cycle phases based on fluorescent intensity.

### 6.3.2. METHOD

A549 and Beas2B cells were treated with siRNA or pDNA to induce knockdown or over expression of the DPP10 gene. After 24 hours, the cells were treated with CSE, VE and NFVE and incubated for a further 24 hours. A single cell suspension was generated by transferring 1 x $10^6$ cells to a 1.5 mL microcentrifuge tube. The tube was centrifuged at 300g for 5minutes. Supernatant was removed and discarded without removing cell pellets. 1mL of PBS per 1 x $10^6$ cells was added to each tube and mixed by gentle vortexing. The cells were centrifuged at 300g for 5 minutes and supernatant was removed and discarded without disturbing the cell pellets leaving approximately 50µL of PBS per 1 x $10^6$ cells. The cell pellet was resuspended in the residual PBS by gentle vortexing. To fix the cell sample, resuspended cells were added drop-wise into a micro centrifuge tube containing 1 mL of ice cold 70% ethanol while vortexing at medium speed.

200 µL of ethanol fixed cells was added to a 1.5ml polystyrene tube. The tube was centrifuged at 300g for 5mins at room temperature. Supernatant was removed and discarded with a micro pipettor, and the cell pellets resuspended in 0.5ml PBS per 1 x $10^6$ cells. Cells were centrifuged at 300g for 5mins at room temperature and the supernatant was removed and discarded. The cell pellets were resuspended in 200µL of muse cell cycle reagent and incubated for 30mins at room temperature protected from light. Cell suspension sample was transferred to a 1.5ml screw cap micro centrifuge tube and analysed on the muse cell analyser. Instrument settings were adjusted by loading and running a stained negative control sample before running the treated samples.

### 6.3.3. RESULT

To investigate the effects of NFVE, VE, and CSE on cell proliferation, we analyzed cell cycle distribution in A549 and BEAS-2B cells. Cells were categorized into G0/G1, S, and G2/M

phases, and comparisons were made across DPP10 genotypes: wild-type (WT), knockout (KO), and overexpression (OE).

Across all treatment groups and in both cell lines, DPP10 knockdown or overexpression did not significantly alter cell cycle distribution. In untreated A549 cells, most cells were in S phase (54 ± 1.3), and G2/M phase (42.8 ± 0.66), with only a small proportion in G0/G1 (0.22 ± 0.07). This distribution was consistent across WT, KO, and OE lines.

NFVE treatment induced a marked shift in cell cycle distribution, characterized by an increase in the G0/G1 population (29.2 ± 1.16) and a corresponding decrease in S phase (30.8 ± 1.46), indicating G0/G1 arrest. The G2/M population was modestly reduced (33.4 ± 1.08). These effects were consistent across all genotypes, suggesting that NFVE-induced cell cycle arrest occurs independently of DPP10 status.

VE exposure increased the proportion of cells in G0/G1 phase (44.2 ± 1.28) with a concurrent reduction in S phase (19.6 ± 0.93) and G2/M phase (23.4 ± 1.63) across all genotypes, indicating that vape components may slow S phase entry and contribute to reduced proliferation.

CSE treatment produced the most pronounced effect, with the highest proportion of cells accumulating in G0/G1 (53 ± 1.14) and a marked reduction in S phase (13.8 ± 0.97). Compared to VE-treated cells, the G2/M fraction remained relatively stable (24.6 ± 1.17). Overall, these findings indicate a strong G0/G1 arrest following CSE exposure.

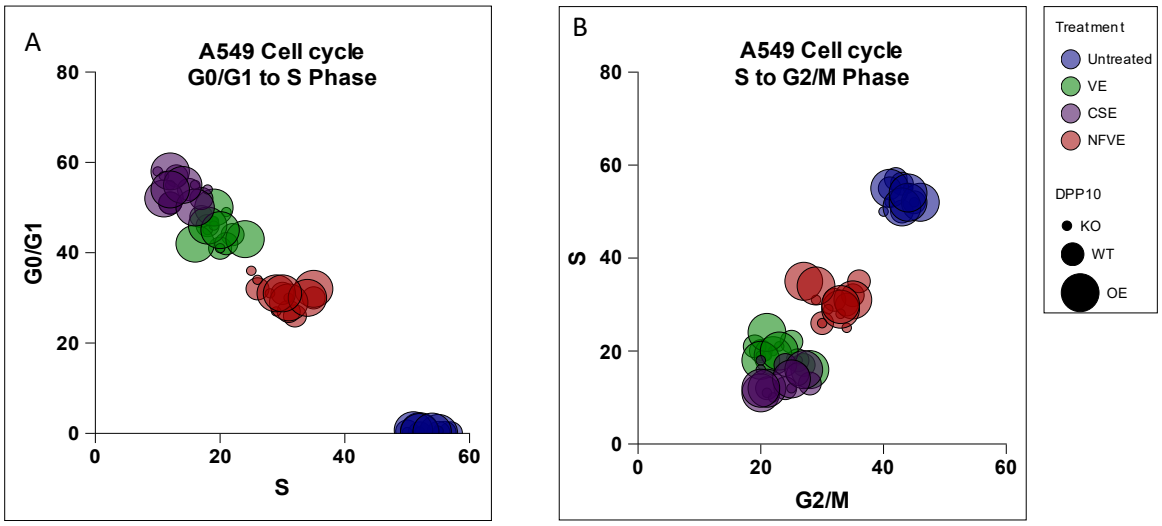

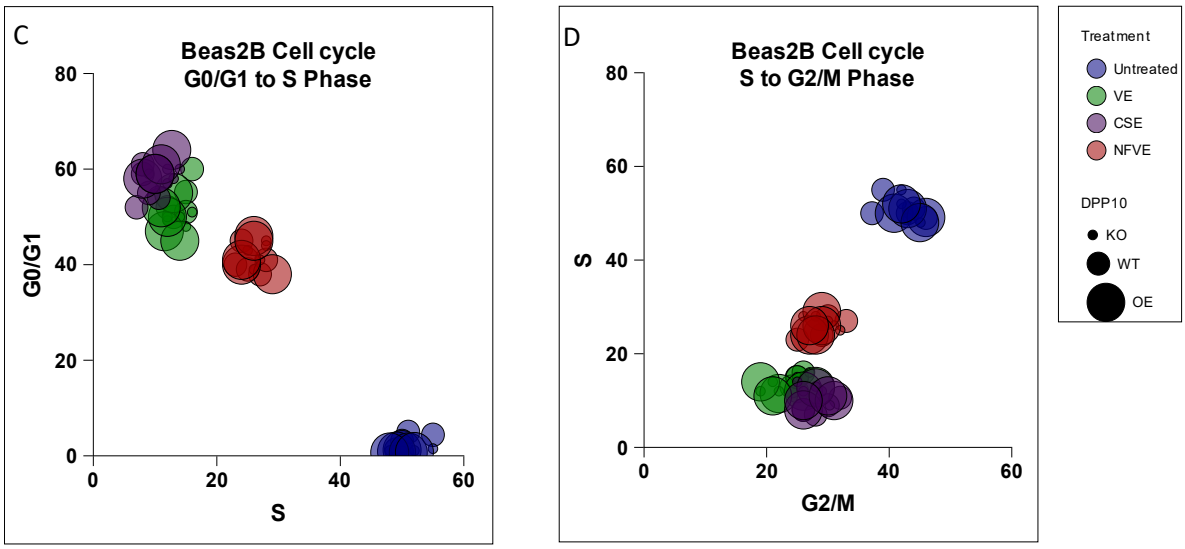


*Figure 27: Cell Cycle changes in lung epithelial cell lines A549 (A,B) and Beas-2B (C,D) where the DPP10 gene has been knocked down using siRNA or over expressed with an ORF clone. DPP10(-) and DPP10 (+) cells treated with NFVE, VE and CSE. Data is expressed as mean±SEM of 5 biological replicates, n=5 each. *P≤0.05, **P≤0.01, ***P≤0.001, ≤0.0001 vs treated - control samples which are wild type cells that have been stimulated with NFVE, VE or CSE. NFVE: Nicotine free vape extract, VE: Vape extract, CSE: Cigarette smoke extract, KO: Knock out, WT: Wild type, OE: Over expressed.*

Similar trends were observed in Beas-2B cells. Untreated cells exhibited a cell cycle distribution profile with 2.9 ± 0.83 in G0/G1, 51 ± 1.05 in S phase, and 41.84 ± 1.6% in G2/M. NFVE treatment caused a clear shift toward G0/G1 (40 ± 1.21) with a reduction in S phase (25.4 ± 0.93%, mirroring the effects in A549 cells. These changes were consistent across WT, KO, and OE lines, indicating that DPP10 manipulation did not significantly alter the response.

VE exposure increased the G0/G1 population (53.64 ± 1.81) and reduced S phase (14.2 ± 0.73), whereas G2/M remained largely unchanged (24.98 ± 0.32). CSE induced the most pronounced accumulation in G0/G1 (56.2 ± 1.66) with a significant reduction in S phase (8.52 ± 0.61), consistent with a strong cell cycle arrest effect.

Overall, NFVE, VE, and CSE treatments led to cell cycle redistribution characterized by accumulation of cells in G0/G1 and a reduction in S phase, with CSE producing the most pronounced effect. This indicates that both vaping and cigarette smoke components inhibit cell cycle progression, potentially contributing to impaired proliferation. These effects were observed across all DPP10 genotypes, suggesting that DPP10 expression does not significantly alter the cell cycle response under these treatment conditions. The stronger G0/G1 arrest

induced by CSE compared with VE highlights the additive effects of additional toxicants present in cigarette smoke.

## 6.4. EFFECT OF DPP10 ON APOPTOSIS

### 6.4.1. CASPASE ASSAY PRINCIPLE

Caspases are cysteine proteases that perform a central role in propagating apoptosis (programmed cell death). Many caspases act in various parts of the apoptosis network, some act upstream mainly to initiate intracellular event cascade, others like Caspase-3 and Caspase-7 act further downstream and modulate cellular breakdown through the cleavage of structural proteins. The Muse® Caspase-3/7 Kit determines early and late apoptosis together with cell death by combining a DNA binding dye conjugated to a DEVD peptide which is a substrate for caspase 3 and 7 and a dead cell marker 7-AAD which is excluded form live cells with intact membrane but can permeate dead cells or cells in late apoptotic state with increased fluorescence. The presence of caspase 3/7 causes cleavage of the DNA dye/DEVD peptide and the DNA dye is then able to translocate to the nucleus and bind to DNA and give off high fluorescence detected by the flow cytometer. When bound to DEVD, the dye is unable to bind DNA.

### 6.4.2. METHOD

A549 and Beas2B cells were treated with siRNA or pDNA to induce knockdown or over expression of the DPP10 gene. After 24 hours, the cells were treated with CSE or VE or NFVE and incubated for a further 24 hours. Growth medium was removed from the cell culture flasks used to grow A549 cells BEAS-2B cells. The flasks were rinsed twice with prewarmed PBS. Adherent cells were detached using trypsin/EDTA and resuspended in complete growth medium, centrifuged at 150g for 2 minutes and supernatant removed. Cells were resuspended in 1x assay buffer BA to a final concentration of between $1 \times 10^5$ to $1 \times 10^6$ per ml 50µL of cell suspension in 1x assay buffer BA was added to a 1.5mL screw cap micro centrifuge tube. 5µL of muse caspase 3/7 reagent working solution was added to each tube of cell suspension and vortexed at medium speed for 3-5 seconds. The tubes were loosely capped and incubated for 30 minutes in a 37°C incubator with 5% $CO_2$. After incubation, 150µL of muse caspase 7-AAD working solution was added to each tube and vortexed at medium speed for 3-5 seconds. The

tubes were incubated at room temperature for 30 minutes protected from light. Following 30 minutes, system settings were first adjusted by running untreated samples in the muse cell analyser. After adjusting the gating parameters, the treated samples were run to determine percentage of live cells, cells in early apoptosis, late apoptosis and dead cells.

### 6.4.3. RESULTS

To assess whether NFVE, CSE or VE influence cell death pathways, apoptosis and necrosis were quantified in A549 and BEAS-2B cells using Annexin V/PI staining and Caspase 3/7 activation assays. The distribution of live, early apoptotic, late apoptotic, and necrotic cells was analyzed across wild-type (WT), DPP10 knockout (KO), and overexpression (OE) lines.

In untreated A549 cells, most cells remained viable (73–81%), with low basal apoptosis (14–20%) and minimal necrosis (<1%). This indicates healthy baseline cell survival across all DPP10 genotypes.

NFVE treatment modestly increased the total apoptotic fraction to approximately 25–32% in all genotypes, largely driven by an increase in early apoptotic cells, while necrosis remained negligible (<1%). This suggests NFVE induces mild apoptotic activation without causing overt necrotic damage. The KO and OE variants showed no significant differences compared to WT, implying that DPP10 expression does not substantially modulate NFVE mediated apoptosis.

VE exposure caused a pronounced apoptotic response in A549 cells, with total apoptosis rising to ~55–61% across all genotypes. Most apoptotic cells were in the early phase, indicating activation of apoptotic signalling rather than complete cell disintegration. Correspondingly, live cell percentages dropped to ~40%, and necrosis remained minimal (<1%). DPP10 status did not significantly alter this response, although KO cells exhibited a slightly higher proportion of late apoptotic cells, suggesting potential increased susceptibility to vape-induced apoptotic progression.

CSE treatment resulted in the most severe cytotoxic response. In WT cells, total apoptosis reached 81–85%, characterized by a marked increase in early apoptotic cells (~70–75%) and a smaller late apoptotic fraction (8–12%). KO and OE cells displayed similar overall apoptosis levels (76–85%), though KO cells tended to exhibit higher late apoptotic populations,

suggesting delayed or sustained apoptotic progression. Viability dropped sharply to ~15–17%, confirming that CSE induces extensive apoptotic cell death with minimal necrosis.

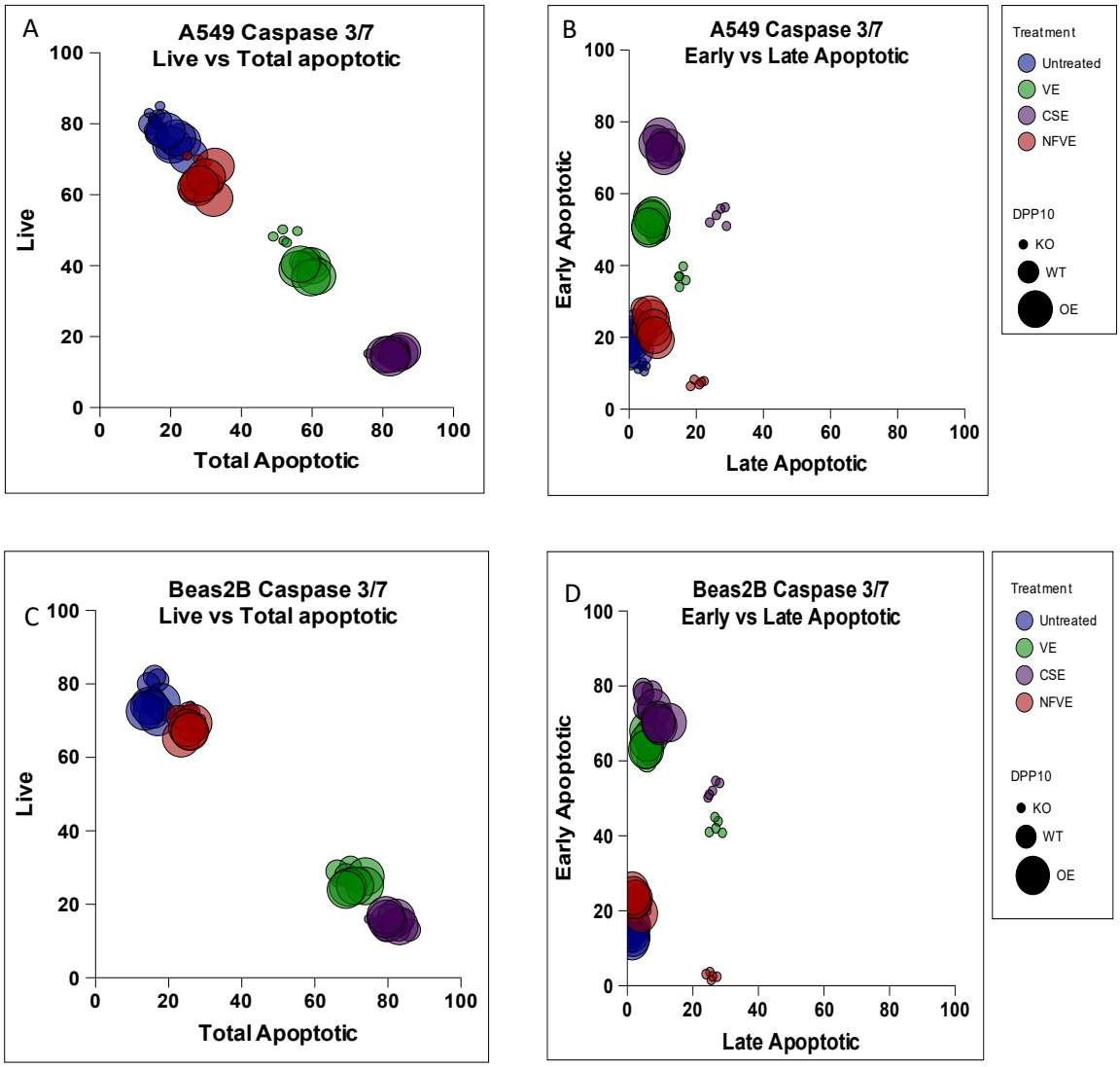


*Figure 28: Annexin PI assay to determine apoptosis. A549 (A,B) and Beas-2B cell lines (C,D) where the DPP10 gene has been knocked down using siRNA or over expressed with an ORF clone. DPP10(-) and DPP10 (+) were treated with NFVE, VE and CSE for 24 hours. Cells in early apoptosis have an intact membrane that prevents the entry of propidium iodide (PI) a nuclear stain. Cells in late apoptosis have reduced membrane integrity and allows both the entry of PI and the binding of Annexin V to the membrane lipid phosphatidyl serine. Data is expressed as mean±SEM of 5 biological replicates, n=5 each. *P≤0.05, **P≤0.01, ***P≤0.001, ≤0.0001 vs treated -control samples which are wild type cells that have been stimulated with NFVE, VE or CSE. NFVE: Nicotine free vape, VE: Vape extract, CSE: Cigarette smoke extract, KO: Knock out, WT: Wild type, OE: Over expressed.*

BEAS-2B cells showed a broadly similar pattern to A549 cells but were generally more sensitive to treatment-induced apoptosis. Untreated cells maintained high viability (71–82%) and low total apoptosis (~14–18%), consistent across DPP10 genotypes.

NFVE treatment produced a moderate rise in apoptosis (~22–27%), primarily in the early phase, with necrosis below 1%. KO cells again showed slightly higher late apoptotic fractions, but overall trends were consistent among genotypes.

VE exposure led to a dramatic increase in apoptosis, with total apoptotic populations ranging from 66–74% across genotypes. In WT and OE cells, apoptosis was predominantly early-phase (~60–68%), whereas KO cells exhibited higher late apoptosis (25–29%), reflecting possible enhanced apoptotic progression in the absence of DPP10. Cell viability correspondingly decreased to ~25–30%, confirming significant apoptotic induction.

CSE treatment caused the most extensive cell death in BEAS-2B cells, with total apoptosis between 79–86% across all DPP10 genotypes. Similar to A549, early apoptosis dominated (~70–78%), while late apoptosis accounted for 6–12%. KO cells showed the highest late apoptotic levels (24–28%), suggesting that DPP10 deficiency may increase vulnerability to sustained apoptotic signalling. Necrosis remained negligible (<1%), indicating that the observed cytotoxicity was predominantly apoptotic rather than necrotic.

Overall, both Annexin V/PI and Caspase 3/7 assays demonstrated a treatment-dependent induction of apoptosis in A549 and BEAS-2B cells, with the order of severity being CSE > VE > NFVE. The increase in Caspase 3/7 activity correlated strongly with Annexin V data, confirming that treatments primarily triggered caspase-dependent apoptosis. DPP10 genotype exerted a minimal effect on basal apoptosis but showed a consistent trend towards increased late apoptosis in KO cells, particularly under VE and CSE exposure, although these differences did not reach statistical significance and should therefore be interpreted with caution. The stronger apoptotic response observed in BEAS-2B compared to A549 cells suggests a potentially higher sensitivity of normal bronchial epithelial cells to smoke and vape exposure.

## 6.5. Bcl-2 ASSAY SIGNALLING

### 6.5.1. Bcl-2 ASSAY PRINCIPLE

Bcl-2 is an anti-apoptotic member of the Bcl-2 family of proteins that regulates intrinsic apoptosis by regulating the proteins that control mitochondrial membrane permeability. Under normal conditions, Bcl-2 is found sequestered with Bax. Once apoptotic signal is received, the activation of Bcl-2 causes it to release Bax, which then forms a complex with mitochondrial membrane that releases cytochrome C into the cytosol leading to caspase cleavage and activation. Using 2 directly conjugated antibodies; phospho-specific anti-phospho-Bcl-2 (Ser70)-Alexa Fluor®555 and an anti-Bcl-2-PECy5 conjugated-antibody, total levels of BCl-2 expression can be determined. Activation of BCl-2 is induced by its phosphorylation and levels of BCl-2 relative to its total expression can be quantified.

### 6.5.2. METHOD

A549 and Beas2B cells were treated with siRNA or pDNA to induce knockdown or over expression of the DPP10 gene. After 24 hours, the cells were treated with CSE, NFVE or VE and incubated for a further 24 hours. CSE, NFVE or VE treatment were deactivated by exchanging out the growth media with fresh growth media. After cellular deactivation, both treated and untreated were spun at 300 x g for 5 minutes and the media discarded. Cells were resuspended by adding 500 µL of 1X Assay Buffer per one million and an equal part Fixation Buffer to cell suspension (1:1) added. The sample was mixed by gently pipetting up and down and incubated for 5 minutes on ice. Cells were spun down at 300 x g for 5 minutes in a centrifuge and supernatant discarded. After completing the fixation process, the cells were permeabilize by adding 1 mL ice-cold Permeabilization Buffer per one million cells and incubating on ice for 5 minutes and spun down at 300 x g for 5 minutes in a centrifuge after which the supernatant was discarded. Cells were resuspended in 450 µL 1X Assay Buffer per one million cells and aliquoted at 90 µL per microcentrifuge tube. Cells were stained by adding 10 µL the antibody working cocktail solution made up of 5 µL of antiphospho-Bcl-2 (Ser70), Alexa Fluor® 555 and 5 µL of anti-Bcl-2, PECy5 conjugated antibodies. The tubes containing the stained cells were incubated for 30 minutes in the dark at room temperature. Following the incubation step, 100 µL of 1x Assay Buffer was added to each microcentrifuge of stained cells and centrifuged at 300 x g for 5 minutes. The supernatant was discarded, and

the cells resuspend cells in each microcentrifuge tube with 200 µL of 1x Assay Buffer. Samples were acquired on the Muse™ Cell Analyzer using the onscreen instructions.

### 6.5.3. RESULT

In untreated A549 wild-type (WT) cells, approximately 34% of the total population expressed Bcl-2, with 6% showing activated (phosphorylated) Bcl-2. This baseline pattern remained similar in both DPP10 knockout (KO) and overexpressing (OE) cells, indicating that under normal conditions, DPP10 does not significantly influence basal Bcl-2 activation or expression.

Following exposure to 5% NFVE, VE, or CSE for 24 hours, a distinct increase in the proportion of Bcl-2–expressing cells was observed across all treatments (Figure 18). NFVE treated WT cells showed 32.8% expression, with a 9.6% activation level, representing a ~60% increase in Bcl-2 activation relative to untreated controls. VE treated WT cells displayed a more pronounced effect, with 46.2% of cells expressing Bcl-2 and 16.7% showing activated Bcl-2. CSE treatment produced the most substantial increase, with nearly the entire cell population (99.1%) expressing Bcl-2, and 91.7% showing activation, confirming the strong stress-induced apoptotic and anti-apoptotic signaling associated with CSE exposure.

When DPP10 was knocked out, total Bcl-2 expression remained comparable to WT, but the fraction of activated Bcl-2 significantly decreased across all treatments. Specifically, Bcl-2 activation dropped from 9.6% to 0.7% in NFVE treated KO cells, 16.7% to 0.2% in VE-treated KO cells, and 91.7% to 71.9% in CSE-treated KO cells. These results indicate that while DPP10 does not directly alter Bcl-2 expression, it appears essential for effective Bcl-2 activation following cellular stress induced by smoke or vape exposure.

In contrast, DPP10 overexpression did not lead to further enhancement in Bcl-2 activation compared to WT in untreated cells. Bcl-2 activation levels in NFVE-, VE-, and CSE-treated OE cells (9.4%, 15.6%, and 91.4%, respectively) were statistically similar to WT ($p > 0.05$), suggesting that normal levels of DPP10 are sufficient for maximal Bcl-2 activation in these conditions.

Similar trends were observed in Beas-2B cells. In untreated WT cells, 33.2% of the population expressed Bcl-2, with 7.1% in the activated state. Under these basal, untreated conditions,

DPP10 KO and OE lines showed no significant changes in Bcl-2 expression or activation, consistent with observations in A549 cells. However, following treatment with NFVE, VE, or CSE, DPP10 status significantly influenced Bcl-2 activation, as described further below.

Exposure to NFVE, VE, and CSE induced significant upregulation and activation of Bcl-2 (Figure 29). NFVE treatment resulted in ~51.0% Bcl-2 expression and 41.0% activation in WT cells. VE and CSE elicited markedly higher activation, with 98.4% and 97.8% of cells showing active Bcl-2, respectively. The sharp increase in activation in both VE and CSE treated WT and OE cells indicates a strong stress-induced mitochondrial signalling response.

Following treatment, DPP10 deficiency significantly reduced Bcl-2 activation in Beas-2B cells despite comparable total Bcl-2 expression levels. NFVE-treated KO cells showed a decline in activation from ~41% to 27.8%, VE-treated KO cells decreased from ~98% to 64.9%, and CSE-treated KO cells showed a reduction from ~97.8% to 61.4%. Conversely, DPP10 overexpression did not produce a significant increase in Bcl-2 activation above WT levels, with activation rates remaining comparable to those observed in wild-type cells under all treatment conditions.

Overall, both A549 and Beas-2B cell lines demonstrated that NFVE, VE, and CSE exposure strongly induce Bcl-2 expression and activation, with CSE eliciting the most robust response. However, DPP10 knockout consistently reduced Bcl-2 activation, supporting a role for DPP10 in facilitating anti-apoptotic signalling through Bcl-2 phosphorylation and activation rather than in regulating its expression.

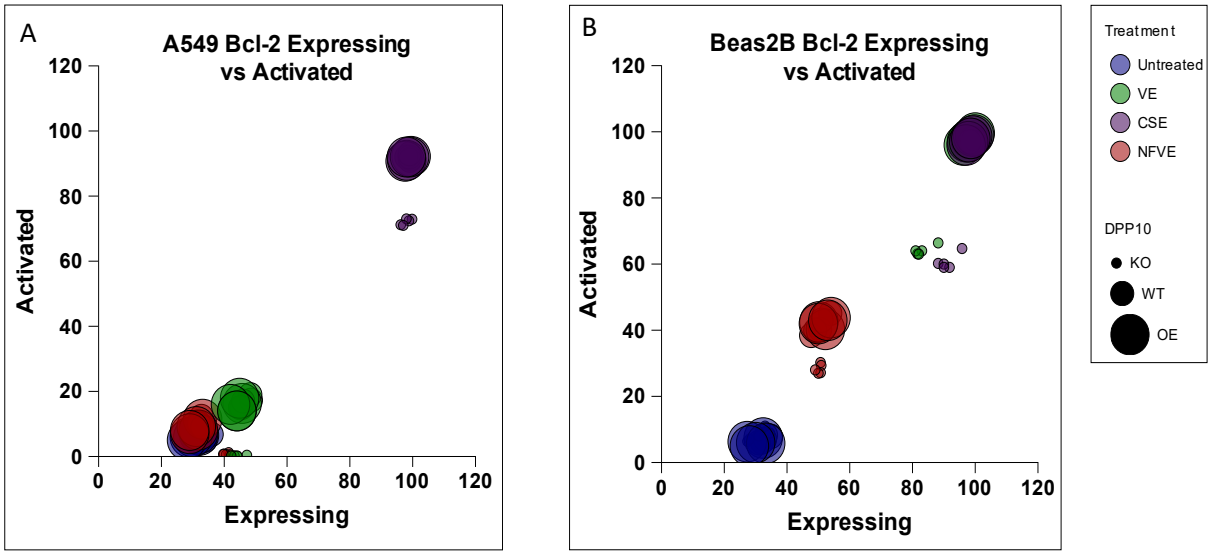


*Figure 29: Bcl-2 Assay to further investigate the role of Bcl-2 in DPP10 knock out and over expressed lung epithelial cells.. A549 (A,B) and Beas-2B cell lines (C,D) where the DPP10 gene has been knocked down using siRNA or over expressed with an ORF clone. DPP10(-) and DPP10 (+) were treated with NFVE, VE and CSE for 24 hours. Data is expressed as mean±SEM of 5 biological replicates, n=5 each. *P≤0.05, **P≤0.01, ***P≤0.001, ≤0.0001 vs treated -control samples which are wild type cells that have been stimulated with NFVE, VE or CSE. NFVE: Nicotine free vape, VE: Vape extract, CSE: Cigarette smoke extract, KO: Knock out, WT: Wild type, OE: Over expressed.*

## 6.6. DISCUSSION

### 6.6.1. CSE, NFVE AND VE PROMOTE G1/S PHASE CELL CYCLE ARREST INDEPENDENT OF DPP10 EXPRESSION

The regulation of the eukaryotic cell cycle is a tightly coordinated process involving the sequential transition of cells through the G1, S, G2 and M phases, governed by cyclin–CDK complexes and checkpoint control proteins (Alberts et al., 2002). Perturbations to these checkpoints, particularly the G1/S transition, are among the earliest cellular responses to chemical or oxidative stress, allowing cells to repair damaged DNA before replication proceeds.

In the present study, treatment of A549 and Beas-2B cells with CSE, NFVE and VE for 24 hours induced a pronounced G1/S phase arrest. The reduction in S-phase population from ~53% in untreated A549 cells to 31%, 19.7%, and 14% for NFVE, VE and CSE respectively, coupled with an increase in G0/G1 phase cells, indicates inhibition of DNA synthesis and entry into S phase. Comparable findings were observed in Beas-2B cells, confirming the effect across both alveolar and bronchial epithelial cell types. These data suggest that the arrest is a general response to these exposures rather than cell-line specific.

The G1/S arrest observed is consistent with previous studies demonstrating that short-term exposure (≤24 h) to cigarette smoke or e-cigarette condensates can activate DNA damage response pathways that inhibit G1/S transition (Ueda et al., 2023; Tang et al., 2023; Lee et al., 2018; Huang et al., 2021). Mechanistically, such arrest is typically mediated by suppression of the Cdc25A phosphatase and inhibition of CDK4/Cyclin D and CDK2/Cyclin E complexes (Falck et al., 2001; Hoffmann et al., 1994; Molinari et al., 2000; Jinno et al., 1994)(Zhang et al., 2018; Sim et al., 2022). The observed reduction in S-phase cells and corresponding accumulation in the G0/G1 phase in this study are consistent with this well-characterized checkpoint response to genotoxic stress.

Among the three treatments, CSE caused the strongest G1/S arrest, followed by VE and then NFVE, suggesting a cumulative effect of nicotine and other chemical constituents. This pattern supports earlier observations by Nyunoya et al., (2006) that whole smoke extract exerts greater oxidative and genotoxic stress than nicotine or vapor components alone.

It is worth noting that while short-term exposures typically result in transient G1/S arrest, prolonged exposure or recovery in complete medium can trigger compensatory proliferation once DNA repair mechanisms are restored (Liu et al., 2005). Therefore, the 24-hour exposure window used here captures an early checkpoint response, and further time-course studies could determine whether the arrest is reversible or leads to senescence. A key strength of this study lies in the comparison across both CSE and VE standardized for nicotine concentration, which allowed the dissection of nicotine-independent toxic mechanisms. However, the use of pooled extracts rather than individual chemical constituents may limit mechanistic specificity.

Overall, the data demonstrate that CSE, VE, and NFVE induce a G1/S phase arrest in both A549 and Beas-2B cells, indicative of DNA damage–induced checkpoint activation, and that DPP10 does not influence this arrest, suggesting its role may lie downstream of cell cycle regulation.

### 6.6.2. DPP10 MODULATES CELL SURVIVAL DURING CSE AND VE EXPOSURE THROUGH REGULATION OF BCL-2 ACTIVATION

Apoptosis is a critical mechanism by which epithelial cells eliminate damaged or stressed cells to maintain tissue homeostasis. In this study, exposure to NFVE, VE, and CSE induced marked

apoptotic responses in both A549 and Beas-2B cells, with the most pronounced effects observed following CSE treatment. Cell viability decreased to 15–40% in CSE- and VE-treated groups, consistent with previous findings that both cigarette and e-cigarette aerosol induce oxidative stress, mitochondrial dysfunction, and apoptosis in airway epithelial cells (Su et al., 2022; Marinucci et al., 2022; Taylor et al., 2016). The comparable toxicity of VE and CSE observed in some studies may reflect shared aldehydes and reactive carbonyl species in both aerosols (Ogunwale et al., 2017; Conklin et al., 2018; Wu et al., 2012). However, in this nicotine-normalized system, CSE remained significantly more cytotoxic than VE, suggesting additional harmful constituents in conventional cigarette smoke that exacerbate cell death.

Interestingly, DPP10 modulation significantly affected the apoptotic response. Knockout of DPP10 increased late-stage apoptosis across all treatments, whereas DPP10 overexpression had no significant effect on the proportion of apoptotic cells compared to wild-type controls. This pattern suggests that DPP10 exerts a protective role during chemically induced stress, possibly by stabilizing anti-apoptotic signalling pathways. Similar pro-survival roles for DPP10 have been indirectly inferred from studies linking DPP10 polymorphisms with asthma severity and airway remodelling (Zhang et al., 2018; Sim et al., 2022), although no prior studies have directly assessed DPP10 in the context of apoptosis.

To explore the mechanism underlying this effect, Bcl-2 expression and activation were evaluated. Bcl-2, a key regulator of the intrinsic mitochondrial apoptotic pathway, inhibits apoptosis by binding to Bax/Bak and preventing cytochrome c release (Riedl and Salvesen, 2007; Qian et al., 2008; Green and Kroemer, 2004). In this study, CSE, VE, and NFVE treatments all increased total Bcl-2 expression, consistent with a cellular attempt to counterbalance pro-apoptotic signalling. However, activation of Bcl-2 (measured as phosphorylation at serine 70) was markedly reduced in DPP10 knockout cells. This reduction was most pronounced following CSE and VE treatment, with decreases of up to 20%. These findings suggest that DPP10 facilitates the activation (rather than expression) of Bcl-2, potentially through modulation of upstream kinases such as JNK or ERK, which have previously been shown to regulate Bcl-2 phosphorylation and activity (Qian et al., 2008).

Taken together, these findings position DPP10 as a novel modulator of the intrinsic apoptotic pathway, contributing to epithelial cell survival under oxidative stress. While the precise molecular mechanism remains to be elucidated, it is plausible that DPP10 interacts with

signalling cascades that converge on Bcl-2 activation. This is consistent with recent reports suggesting that DPP10 participates in ion channel regulation and inflammatory signalling pathways relevant to epithelial remodelling (Sim et al., 2022).

A key strength of this work lies in the comparison of cigarette smoke and vaping extracts at matched nicotine concentrations which allowed the isolation of nicotine-independent cytotoxicity. However, the study's in vitro design limits extrapolation to in vivo airway responses, where immune cell interactions and repair mechanisms play significant roles. Additionally, only one exposure duration and concentration were tested; future studies using time- and dose-response analyses, or transcriptomic profiling, would help elucidate the signalling pathways linking DPP10 to Bcl-2 activation.

In summary, these results demonstrate that DPP10 plays a contributory role in epithelial cell survival following exposure to CSE and VE. Its influence appears to act through the modulation of Bcl-2 activation rather than expression, highlighting a potential protective function of DPP10 during chemically induced stress. This novel finding expands the understanding of DPP10's biological role beyond its established associations with asthma and airway remodelling and may have implications for therapeutic strategies targeting epithelial injury and repair in smoking-related diseases.

# 7. DISCUSSION AND FUTURE CONSIDERATIONS

This study set out to investigate whether the gene DPP10, previously identified as a susceptibility locus for asthma, plays a modulatory role in regulating airway epithelial inflammatory responses to cigarette smoke and vaping extracts. The overarching aim was to determine whether changes in DPP10 expression influence the cellular responses commonly observed in smoking-related airway injury, including inflammation, cell cycle disruption, and apoptosis. By integrating bioinformatic analysis of DPP10 expression in smokers with functional in vitro experiments using cigarette smoke extract (CSE), vaping extract (VE), and nicotine-free vaping extract (NFVE), this project provides new mechanistic insight into how airway epithelial cells respond to inhaled toxicants and how DPP10 may contribute to epithelial resilience.

Preliminary bioinformatics analysis demonstrated that DPP10 and its antisense transcripts were upregulated in smokers compared to non-smokers across multiple tissue types. This finding together with previous reports suggest that DPP10 expression is induced under stress conditions and may exert a protective effect in airway disease (Zhang et al., 2018; Sim et al., 2022). While the biological function of the antisense transcripts remains unclear, the known positive regulatory relationship between DPP10-AS1 and DPP10 expression (Tian et al., 2021; Liu et al., 2021) supports the hypothesis that DPP10 upregulation represents a compensatory response to environmental insult. This observation formed the basis for investigating DPP10's role in modulating epithelial stress responses under controlled exposure conditions.

To model exposure to cigarette smoke and e-cigarette vapour, a reproducible in vitro system was developed and validated. This model enabled direct comparison of combustion and nicotine dependent effects, with extracts standardised by nicotine concentration and confirmed to be stable when stored at –20°C. Cell viability assays revealed a consistent toxicity hierarchy of CSE > VE > NFVE, confirming that combustion products contribute most significantly to cytotoxicity. Nevertheless, VE exposure still reduced cell viability even at equivalent nicotine levels, demonstrating that e-cigarette aerosols are not biologically inert. These findings are consistent with prior studies showing that reactive aldehydes and free radicals generated during e-liquid heating can induce oxidative stress, mitochondrial dysfunction, and apoptosis (McAlinden et al., 2021; Chaumont et al., 2019). Beas-2B bronchial epithelial cells were more sensitive than A549 alveolar epithelial cells, reflecting

their anatomical position as the first tissue exposed to inhaled toxicants. From a public health standpoint, these results reinforce the emerging consensus that while vaping may present reduced toxicity relative to smoking, it cannot be considered risk-free, and chronic exposure could contribute cumulatively to epithelial injury and inflammation.

Inflammatory cytokine profiling further highlighted the proinflammatory nature of both CSE and VE exposures. Real time PCR and ELISA data collectively demonstrated that CSE produced the strongest induction of IL6, IL8, and TNFα, followed by VE, with NFVE eliciting minimal effects. The close correspondence between transcriptional and protein-level responses suggests that acute cytokine release is primarily driven by transcriptional activation, with limited post-transcriptional regulation under the tested conditions. These findings align with previous reports of smoke and nicotine induced cytokine expression in airway epithelial models (Reidel et al., 2018a; Kode et al., 2006; Mio et al., 1997) The magnitude of cytokine upregulation observed here (up to 4.5-fold) confirms that even short-term exposure to e-cigarette vapour can activate canonical inflammatory pathways, likely through nicotine mediated stimulation of nicotinic acetylcholine receptors and downstream MAPK/NF-κB signalling (Ung et al., 2019; Chen et al., 2020; Lian et al., 2022). This pattern reinforces the view that e-cigarette vapour, particularly when containing nicotine, has immunomodulatory potential that may predispose users to airway inflammation and increased susceptibility to infection or chronic respiratory conditions (Wu et al., 2014; Miyashita et al., 2018).

Modulation of DPP10 expression produced consistent but subtle shifts in inflammatory output. DPP10 knockdown slightly enhanced cytokine mRNA and protein expression across all exposures, whereas overexpression dampened these responses. Although none of these changes reached statistical significance, their reproducibility across both cell lines and exposure types is consistent with the possibility that DPP10 acts as a negative regulator of epithelial inflammation. These results mirror earlier findings that DPP10 silencing increased IL8 secretion in IL1β-stimulated bronchial epithelial cells (Zhang et al., 2018) and suggest that DPP10 may influence the amplitude of inflammatory responses rather than serving as a primary determinant. Mechanistically, DPP10 could act by modulating MAPK or NF-κB activity, thereby fine-tuning cytokine transcription and preventing excessive or prolonged activation. Such a modulatory role would be consistent with DPP10's proposed function as an accessory protein influencing signalling and membrane stability. Importantly, the alignment

between mRNA and protein data is consistent with a biological effect and provides modest support for DPP10's potential contribution to epithelial homeostasis under stress conditions.

Beyond inflammation, this study explored how smoke and vape exposures affect cell cycle progression and apoptosis, two fundamental processes underpinning epithelial integrity. All extracts induced G1/S phase arrest, with CSE showing the most pronounced effect. This is consistent with activation of DNA damage checkpoints mediated by ATM/ATR kinases and p53 signalling (Xu et al., 2016; Tanaka et al., 2007). DPP10 modulation did not alter this arrest, suggesting that it acts downstream or in parallel to early DNA damage responses. However, DPP10 knockdown significantly increased late-stage apoptosis, while overexpression provided minor protection. This pattern implies that DPP10 may contribute to cell survival under oxidative or toxic stress. Supporting this, reduced phosphorylation of the anti-apoptotic protein Bcl-2 at serine 70 was observed in DPP10 deficient cells, suggesting impaired activation of pro-survival pathways. Since phosphorylation at this residue enhances Bcl-2 stability, it is possible that DPP10 may facilitate Bcl-2 activation, potentially through regulation of ERK or JNK kinases. These findings suggest a previously unrecognised role for DPP10 in modulating apoptotic signalling in the context of environmental stress, linking it to both inflammatory control and epithelial survival.

Integrating these findings, a conceptual model emerges in which cigarette smoke and e-cigarette vapour initiate oxidative stress that activates proinflammatory and stress response pathways in airway epithelial cells. DPP10 may function as a modulatory buffer, dampening cytokine transcription and promoting cell survival through Bcl-2 stabilisation. Loss or reduction of DPP10 function appears to result in heightened apoptosis and slightly increased cytokine release, leading to greater epithelial injury. This model aligns with epidemiological data linking DPP10 polymorphisms to asthma severity and airway hyperreactivity (Zhang et al., 2018; Sim et al., 2022) and extends this understanding to environmental exposures relevant to smoking and vaping. The findings suggest that DPP10 contributes not only to disease susceptibility but also to the epithelial capacity to withstand repeated toxicant exposure, a feature highly relevant in chronic airway conditions.

Taken together, this work provides a cohesive response to the original research question by demonstrating that DPP10 acts as a subtle yet consistent modulator of airway epithelial responses to smoking and vaping exposures. While DPP10 does not appear to prevent

inflammatory activation, it may limit its magnitude and potentially contribute to epithelial survival, supporting a protective role in maintaining airway integrity. These effects, though modest in acute in vitro conditions, may have greater physiological significance in vivo, where chronic low-level exposure and genetic variability can magnify small differences in inflammatory tone or survival capacity. The identification of DPP10 as a potential protective factor contributes to a growing body of evidence that individual genetic differences influence susceptibility to smoking and vaping related disease.

In the context of the wider literature, these results add nuance to our understanding of vaping safety and airway biology. They highlight that even in the absence of combustion, vaping aerosols provoke cellular stress responses comparable in nature, if not in magnitude, to those induced by cigarette smoke. Furthermore, they suggest that genes like DPP10 may partially determine how effectively epithelial cells adapt to such insults. This finding has potential translational relevance. DPP10 or its regulatory network could represent a biomarker of epithelial resilience or a target for therapeutic intervention aimed at reducing inflammation and preventing epithelial damage in smokers and vapers alike.

Future research should build on this foundation through longer term, repeated exposure studies that better reflect real-world vaping and smoking behaviours. Expanding analysis to include transcriptomic and proteomic profiling would clarify the broader pathways under DPP10 regulation and identify co-regulated genes involved in stress adaptation. Mechanistic assays examining DPP10's interaction with kinases, ion channels, and components of the NF-κB pathway could elucidate its molecular mode of action. Clinically, assessing DPP10 expression or polymorphism patterns in cohorts of smokers, vapers, and individuals with chronic respiratory disease could establish its value as a biomarker for airway susceptibility or recovery potential.

In conclusion, this study provides new evidence that cigarette smoke and e-cigarette vapour elicit distinct but overlapping inflammatory and cytotoxic responses in airway epithelial cells and that DPP10 plays a modulatory role in shaping these outcomes. It suggests that DPP10 may dampen inflammatory signalling and supports epithelial survival, thereby contributing to epithelial resilience. These findings suggest DPP10 as a potential biologically relevant link between genetic susceptibility, environmental exposure, and airway health. In doing so, this work extends current understanding of smoke and vape induced epithelial injury and opens

new avenues for future research into the genetic and molecular determinants of respiratory vulnerability.

# REFERENCES


Aaron, S.D., Angel, J.B., Lunau, M., et al. (2001) Granulocyte inflammatory markers and airway infection during acute exacerbation of chronic obstructive pulmonary disease. *American journal of respiratory and critical care medicine*, 163 (2): 349–355. doi:10.1164/ajrccm.163.2.2003122.

Abbott, C.A., Baker, E., Sutherland, G.R., et al. (1994) Genomic organization, exact localization, and tissue expression of the human CD26 (dipeptidyl peptidase IV) gene. *Immunogenetics*, 40 (5): 331–338. doi:10.1007/BF01246674.

Abo, K.M., de Aja, J.S., Lindstrom-Vautrin, J., et al. (2022) Air-liquid interface culture promotes maturation and allows environmental exposure of pluripotent stem cell–derived alveolar epithelium. *JCI Insight*, 7 (6). doi:10.1172/JCI.INSIGHT.155589.

Action on Smoking and Health (2022) *Smoking costs society £17bn – £5bn more than previously estimated*. Action on Smoking and Health. Available at: https://ash.org.uk/media-centre/news/press-releases/smoking-costs-society-17bn-5bn-more-than-previously-estimated (Accessed: 25 February 2025).

Action on Smoking and Health (2023a) *Use of E-cigarettes among Adults in Great Britain*. Available at: https://ash.org.uk/resources/view/use-of-e-cigarettes-among-adults-in-great-britain-2021.

Action on Smoking and Health (2023b) *Use of e-cigarettes among young people in Great Britain*. Available at: https://ash.org.uk/resources/view/use-of-e-cigarettes-among-young-people-in-great-britain.

Action on Smoking and Health (2024) *Smoking statistics*. Available at: https://ash.org.uk/resources/view/smoking-statistics.

Adam, M., Bain, M., Ashraf, T., et al. (2025) Exploring the influence of vaping on the pharmacokinetic fate of inhaled therapeutics. *Archives of Toxicology*, 99 (8): 3133–3145. doi:10.1007/s00204-025-04060-w.

Adcock, I.M. and Kirkham, P.A. (2010) PHF11 and DPP10: a tale of two genes in asthma. *Respiration; International Review of Thoracic Diseases*, 79 (1): 14–16. doi:10.1159/000235972.

Agraval, H., Sharma, J.R. and Yadav, U.C.S. (2022) Method of Preparation of Cigarette Smoke Extract to Assess Lung Cancer-Associated Changes in Airway Epithelial Cells. *Methods in Molecular Biology (Clifton, N.J.)*, 2413: 121–132. doi:10.1007/978-1-0716-1896-7_13.

Alberts, B., Johnson, A., Lewis, J., et al. (2002) *Molecular Biology of the Cell. An overview of the cell cycle.* 4th edn. New York, NY: Garland Science. Available at: https://www.ncbi.nlm.nih.gov/books/NBK26869/.

Alexander, W.S. (1998) Cytokines in hematopoiesis. *International Reviews of Immunology*, 16 (5–6): 651–682. doi:10.3109/08830189809043013.

Allen, J.G., Flanigan, S.S., LeBlanc, M., et al. (2016) Flavoring Chemicals in E-Cigarettes: Diacetyl, 2,3-Pentanedione, and Acetoin in a Sample of 51 Products, Including Fruit-, Candy-, and Cocktail-Flavored E-Cigarettes. *Environmental Health Perspectives*, 124 (6): 733–739. doi:10.1289/ehp.1510185.

Allen, M., Heinzmann, A., Noguchi, E., et al. (2003) Positional cloning of a novel gene influencing asthma from chromosome 2q14. *Nature genetics*, 35 (3): 258–263. doi:10.1038/ng1256.

Ancel, J., Belgacemi, R., Diabasana, Z., et al. (2021) Impaired Ciliary Beat Frequency and Ciliogenesis Alteration during Airway Epithelial Cell Differentiation in COPD. *Diagnostics (Basel, Switzerland)*, 11 (9): 1579. doi:10.3390/diagnostics11091579.

Apperson, G.L. (1914) *The social history of smoking*. M. Secker.

Armstrong, L., Medford, A.R.L., Uppington, K.M., et al. (2004) Expression of functional toll-like receptor-2 and -4 on alveolar epithelial cells. *American Journal of Respiratory Cell and Molecular Biology*, 31 (2): 241–245. doi:10.1165/rcmb.2004-0078OC.

Ashkenazi, A. and Dixit, V.M. (1998) Death Receptors: Signaling and Modulation. *Science*, 281 (5381): 1305–1308. doi:10.1126/science.281.5381.1305.

Aslaner, D.M., Alghothani, O., Saldana, T.A., et al. (2022) E-cigarette vapor exposure in utero causes long-term pulmonary effects in offspring. *American Journal of Physiology - Lung Cellular and Molecular Physiology*, 323 (6): L676–L682. doi:10.1152/ajplung.00233.2022.

Aufderheide, M., Scheffler, S., Ito, S., et al. (2015) Ciliatoxicity in human primary bronchiolar epithelial cells after repeated exposure at the air–liquid interface with native mainstream smoke of K3R4F cigarettes with and without charcoal filter. *Experimental and Toxicologic Pathology*, 67 (7): 407–411. doi:10.1016/j.etp.2015.04.006.

Avis and Hutton (1993) Acute benzene poisoning: a report of three fatalities. *Journal of forensic sciences*, 38 (3). Available at: https://pubmed.ncbi.nlm.nih.gov/8515211/ (Accessed: 7 May 2024).

Baassiri, M., Talih, S., Salman, R., et al. (2017) Clouds and "throat hit": Effects of liquid composition on nicotine emissions and physical characteristics of electronic cigarette aerosols. *Aerosol science and technology : the journal of the American Association for Aerosol Research*, 51 (11): 1231–1239. doi:10.1080/02786826.2017.1341040.

Baggio, L.L., Varin, E.M., Koehler, J.A., et al. (n.d.) *Plasma levels of DPP4 activity and sDPP4 are dissociated from inflammation in mice and humans*. doi:10.1038/s41467-020-17556-z.

Bahl, V., Lin, S., Xu, N., et al. (2012) Comparison of electronic cigarette refill fluid cytotoxicity using embryonic and adult models. *Reproductive Toxicology*, 34 (4): 529–537. doi:https://doi.org/10.1016/j.reprotox.2012.08.001.

Bang, S., Jeong, E.J., Kim, I.K., et al. (2000) Fas- and tumor necrosis factor-mediated apoptosis uses the same binding surface of FADD to trigger signal transduction. A typical model for convergent signal transduction. *The Journal of Biological Chemistry*, 275 (46): 36217–36222. doi:10.1074/jbc.M006620200.

Barnes, P.J., Shapiro, S.D. and Pauwels, R.A. (2003) Chronic obstructive pulmonary disease: Molecular and cellular mechanisms. *European Respiratory Journal*. doi:10.1183/09031936.03.00040703.

Beard, J.M., Collom, C., Liu, J.Y., et al. (2024) *In vitro* toxicity and chemical analysis of e-cigarette aerosol produced amid dry hitting. *Toxicology*, 506: 153865. doi:10.1016/j.tox.2024.153865.

Beaver, L.M., Stemmy, E.J., Schwartz, A.M., et al. (2009) Lung Inflammation, Injury, and Proliferative Response after Repetitive Particulate Hexavalent Chromium Exposure. *Environmental Health Perspectives*, 117 (12): 1896–1902. doi:10.1289/ehp.0900715.

Behar, R.Z., Luo, W., Lin, S.C., et al. (2016) Distribution, quantification and toxicity of cinnamaldehyde in electronic cigarette refill fluids and aerosols. *Tobacco Control*, 25 (Suppl 2): ii94–ii102. doi:10.1136/tobaccocontrol-2016-053224.

Behar, R.Z., Luo, W., McWhirter, K.J., et al. (2018) Analytical and toxicological evaluation of flavor chemicals in electronic cigarette refill fluids. *Scientific Reports*, 8: 8288. doi:10.1038/s41598-018-25575-6.

Bekki, K., Uchiyama, S., Ohta, K., et al. (2014) Carbonyl Compounds Generated from Electronic Cigarettes. *International Journal of Environmental Research and Public Health*, 11 (11): 11192–11200. doi:10.3390/ijerph111111192.

Beklen, A. and Uckan, D. (2021) Electronic cigarette liquid substances propylene glycol and vegetable glycerin induce an inflammatory response in gingival epithelial cells. *Human & Experimental Toxicology*, 40: 096032712094393. doi:10.1177/0960327120943934.

Bellamri, M., Walmsley, S.J., Brown, C., et al. (2022) DNA Damage and Oxidative Stress of Tobacco Smoke Condensate in Human Bladder Epithelial Cells. *Chemical Research in Toxicology*, 35 (10): 1863–1880. doi:10.1021/acs.chemrestox.2c00153.

Berridge, M.S., Apana, S.M., Nagano, K.K., et al. (2010) Smoking produces rapid rise of [11C]nicotine in human brain. *Psychopharmacology*, 209 (4): 383–394. doi:10.1007/s00213-010-1809-8.

Bezerra, G.A., Dobrovetsky, E., Seitova, A., et al. (2015) Structure of human dipeptidyl peptidase 10 (DPPY): a modulator of neuronal Kv4 channels. *Scientific reports*, 5: 8769. doi:10.1038/srep08769.

Bhatta, D.N. and Glantz, S.A. (2020) Association of E-Cigarette Use With Respiratory Disease Among Adults: A Longitudinal Analysis. *American journal of preventive medicine*, 58 (2): 182–190. doi:10.1016/j.amepre.2019.07.028.

Bird, K. and Memon, J. (2025) "Bronchiectasis." In *StatPearls*. Treasure Island (FL): StatPearls Publishing. Available at: http://www.ncbi.nlm.nih.gov/books/NBK430810/ (Downloaded: 27 March 2025).

Birnbaum, S.G., Varga, A.W., Yuan, L.-L., et al. (2004) Structure and Function of Kv4-Family Transient Potassium Channels. *Physiological Reviews*, 84 (3): 803–833. doi:10.1152/physrev.00039.2003.

Blakey, J.D., Sayers, I., Ring, S.M., et al. (2009) Positionally cloned asthma susceptibility gene polymorphisms and disease risk in the British 1958 Birth Cohort. *Thorax*, 64 (5): 381–387. doi:10.1136/thx.2008.102053.

Blount, B.C., Karwowski, M.P., Shields, P.G., et al. (2020) Vitamin E Acetate in Bronchoalveolar-Lavage Fluid Associated with EVALI. *The New England journal of medicine*, 382 (8): 697–705. doi:10.1056/NEJMoa1916433.

Bodas, M., Min, T. and Vij, N. (2011) Critical role of CFTR-dependent lipid rafts in cigarette smoke-induced lung epithelial injury. *American Journal of Physiology-Lung Cellular and Molecular Physiology*, 300 (6): L811–L820. doi:10.1152/ajplung.00408.2010.

Boldin, M.P., Varfolomeev, E.E., Pancer, Z., et al. (1995) A novel protein that interacts with the death domain of Fas/APO1 contains a sequence motif related to the death domain. *The Journal of Biological Chemistry*, 270 (14): 7795–7798. doi:10.1074/jbc.270.14.7795.

Boniotto, M., Jordan, W.J., Eskdale, J., et al. (2006) Human β-Defensin 2 Induces a Vigorous Cytokine Response in Peripheral Blood Mononuclear Cells. *Antimicrobial Agents and Chemotherapy*, 50 (4): 1433. doi:10.1128/AAC.50.4.1433-1441.2006.

Bono, F., Fiorentini, C., Mutti, V., et al. (2023) Central nervous system interaction and crosstalk between nAChRs and other ionotropic and metabotropic neurotransmitter receptors. *Pharmacological Research*, 190: 106711. doi:10.1016/j.phrs.2023.106711.

Brekman, A., Walters, M.S., Tilley, A.E., et al. (2014) FOXJ1 prevents cilia growth inhibition by cigarette smoke in human airway epithelium in vitro. *American Journal of Respiratory Cell and Molecular Biology*, 51 (5): 688–700. doi:10.1165/rcmb.2013-0363OC.

Brown, J., Beard, E., Kotz, D., et al. (2014) Real-world effectiveness of e-cigarettes when used to aid smoking cessation: a cross-sectional population study. *Addiction (Abingdon, England)*, 109 (9): 1531–1540. doi:10.1111/add.12623.

Buist, A.S., Vollmer, W.M. and McBurnie, M.A. (2008) Worldwide burden of COPD in high- and low-income countries. Part I. The burden of obstructive lung disease (BOLD) initiative. *The international journal of tuberculosis and lung disease : the official journal of the International Union against Tuberculosis and Lung Disease*, 12 (7): 703–708.

Cain, K., Bratton, S.B., Langlais, C., et al. (2000) Apaf-1 oligomerizes into biologically active approximately 700-kDa and inactive approximately 1.4-MDa apoptosome complexes. *The Journal of Biological Chemistry*, 275 (9): 6067–6070. doi:10.1074/jbc.275.9.6067.

Cao, H. (2014) Adipocytokines in obesity and metabolic disease. *The Journal of Endocrinology*, 220 (2): T47-59. doi:10.1530/JOE-13-0339.

Cao, W., Li, J., Che, L., et al. (2024) Single-cell transcriptomics reveals e-cigarette vapor-induced airway epithelial remodeling and injury. *Respiratory Research*, 25: 353. doi:10.1186/s12931-024-02962-4.

Cao, Z., Xiong, J., Takeuchi, M., et al. (1996) TRAF6 is a signal transducer for interleukin-1. *Nature*, 383 (6599): 443–446. doi:10.1038/383443a0.

Caplin, M. (1941) AMMONIA-GAS POISONING FORTY-SEVEN CASES IN A LONDON SHELTER. *The Lancet*, 238 (6152): 95–96. doi:10.1016/S0140-6736(00)72016-2.

Caponnetto, P., Campagna, D., Cibella, F., et al. (2013) EffiCiency and Safety of an eLectronic cigAreTte (ECLAT) as tobacco cigarettes substitute: a prospective 12-month randomized control design study. *PloS One*, 8 (6): e66317. doi:10.1371/journal.pone.0066317.

Carlier, F.M., de Fays, C. and Pilette, C. (2021) Epithelial Barrier Dysfunction in Chronic Respiratory Diseases. *Frontiers in Physiology*, 12. doi:10.3389/fphys.2021.691227.

Carolan, B.J., Heguy, A., Harvey, B.-G., et al. (2006) Up-regulation of expression of the ubiquitin carboxyl-terminal hydrolase L1 gene in human airway epithelium of cigarette smokers. *Cancer Research*, 66 (22): 10729–10740. doi:10.1158/0008-5472.CAN-06-2224.

Carpagnano, G.E., Kharitonov, S.A., Foschino-Barbaro, M.P., et al. (2003) Increased inflammatory markers in the exhaled breath condensate of cigarette smokers. *European Respiratory Journal*, 21 (4): 589–593. doi:10.1183/09031936.03.00022203.

CDC (2010) *How Tobacco Smoke Causes Disease: The Biology and Behavioral Basis for Smoking-Attributable Disease: A Report of the Surgeon General. Atlanta (GA)*. Available at: https://www.ncbi.nlm.nih.gov/books/NBK53010/.

CDC (2020) *Outbreak of Lung Injury Associated with the Use of E-Cigarette, or Vaping, Products*. Available at: https://www.cdc.gov/tobacco/basic_information/e-cigarettes/severe-lung-disease.html.

CFR (2022) *TITLE 21--FOOD AND DRUGS CHAPTER I--FOOD AND DRUG ADMINISTRATION DEPARTMENT OF HEALTH AND HUMAN SERVICES SUBCHAPTER B - FOOD FOR HUMAN CONSUMPTION*. Available at: https://www.accessdata.fda.gov/scripts/cdrh/cfdocs/cfcfr/cfrsearch.cfm?fr=184.1666.

Chai, X.-M., Li, Y.-L., Chen, H., et al. (2016) Cigarette smoke extract alters the cell cycle via the phospholipid transfer protein/transforming growth factor-β1/CyclinD1/CDK4 pathway. *European Journal of Pharmacology*, 786: 85–93. doi:10.1016/j.ejphar.2016.05.037.

Chaumont, M., van de Borne, P., Bernard, A., et al. (2019) Fourth generation e-cigarette vaping induces transient lung inflammation and gas exchange disturbances: results from two randomized clinical trials. *American journal of physiology. Lung cellular and molecular physiology*, 316 (5): L705–L719. doi:10.1152/ajplung.00492.2018.

Chen, H., Liao, K., Cui-Zhao, L., et al. (2015a) Cigarette smoke extract induces apoptosis of rat alveolar Type II cells *via* the PLTP/TGF-β1/Smad2 pathway. *International Immunopharmacology*, 28 (1): 707–714. doi:10.1016/j.intimp.2015.07.029.

Chen, I.-L., Todd, I., Tighe, P.J., et al. (2020) Electronic cigarette vapour moderately stimulates pro-inflammatory signalling pathways and interleukin-6 production by human monocyte-derived dendritic cells. *Archives of Toxicology*, 94 (6): 2097–2112. doi:10.1007/s00204-020-02757-8.

Chen, T., Ajami, K., McCaughan, G.W., et al. (2006) Molecular characterization of a novel dipeptidyl peptidase like 2-short form (DPL2-s) that is highly expressed in the brain and lacks dipeptidyl peptidase activity. *Biochimica et Biophysica Acta (BBA) - Proteins and Proteomics*, 1764 (1): 33–43. doi:https://doi.org/10.1016/j.bbapap.2005.09.013.

Chen, T., Gai, W.-P. and Abbott, C.A. (2014) Dipeptidyl peptidase 10 (DPP10(789)): a voltage gated potassium channel associated protein is abnormally expressed in Alzheimer's and other neurodegenerative diseases. *BioMed research international*, 2014: 209398. doi:10.1155/2014/209398.

Chen, W., Wang, P., Ito, K., et al. (2018) Measurement of heating coil temperature for e-cigarettes with a "top-coil" clearomizer. *PLoS ONE*, 13 (4): e0195925. doi:10.1371/journal.pone.0195925.

Chen, Y., Luo, H., Kang, N., et al. (2012) Beraprost sodium attenuates cigarette smoke extract-induced apoptosis in vascular endothelial cells. *Molecular Biology Reports*, 39 (12): 10447–10457. doi:10.1007/s11033-012-1924-1.

Chen, Z., Wang, D., Liu, X., et al. (2015b) Oxidative DNA damage is involved in cigarette smoke-induced lung injury in rats. *Environmental Health and Preventive Medicine*, 20 (5): 318–324. doi:10.1007/s12199-015-0469-z.

Chen, Z.J. (2005) Ubiquitin signalling in the NF-kappaB pathway. *Nature Cell Biology*, 7 (8): 758–765. doi:10.1038/ncb0805-758.

Chesnoy, S. and Huang, L. (2000) Structure and function of lipid-DNA complexes for gene delivery. *Annual review of biophysics and biomolecular structure*, 29: 27–47. doi:10.1146/annurev.biophys.29.1.27.

Chhabra, D., Sharma, S., Kho, A.T., et al. (2014) Fetal lung and placental methylation is associated with in utero nicotine exposure. *Epigenetics*, 9 (11): 1473–1484. doi:10.4161/15592294.2014.971593.

Chinnaiyan, A.M., O'Rourke, K., Tewari, M., et al. (1995) FADD, a novel death domain-containing protein, interacts with the death domain of Fas and initiates apoptosis. *Cell*, 81 (4): 505–512. doi:10.1016/0092-8674(95)90071-3.

Chu, M., Guo, J. and Chen, C.-Y. (2005) Long-term exposure to nicotine, via ras pathway, induces cyclin D1 to stimulate G1 cell cycle transition. *The Journal of Biological Chemistry*, 280 (8): 6369–6379. doi:10.1074/jbc.M408947200.

Chung, S., Baumlin, N., Dennis, J.S., et al. (2019) Electronic Cigarette Vapor with Nicotine Causes Airway Mucociliary Dysfunction Preferentially via TRPA1 Receptors. *American Journal of Respiratory and Critical Care Medicine*, 200 (9): 1134–1145. doi:10.1164/rccm.201811-2087OC.

Churg, A., Dai, J., Tai, H., et al. (2002) Tumor necrosis factor-α is central to acute cigarette smoke-induced inflammation and connective tissue breakdown. *American Journal of Respiratory and Critical Care Medicine*. doi:10.1164/rccm.200202-097OC.

Cirillo, S., Urena, J.F., Lambert, J.D., et al. (2019) Impact of electronic cigarette heating coil resistance on the production of reactive carbonyls, reactive oxygen species and induction of cytotoxicity in human lung cancer cells *in vitro*. *Regulatory Toxicology and Pharmacology*, 109: 104500. doi:10.1016/j.yrtph.2019.104500.

Clapp, P.W., Lavrich, K.S., van Heusden, C.A., et al. (2019) Cinnamaldehyde in flavored e-cigarette liquids temporarily suppresses bronchial epithelial cell ciliary motility by dysregulation of mitochondrial function. *American Journal of Physiology - Lung Cellular and Molecular Physiology*, 316 (3): L470–L486. doi:10.1152/ajplung.00304.2018.

Clapp, P.W., Pawlak, E.A., Lackey, J.T., et al. (2017) Flavored e-cigarette liquids and cinnamaldehyde impair respiratory innate immune cell function. *American Journal of Physiology - Lung Cellular and Molecular Physiology*, 313 (2): L278–L292. doi:10.1152/ajplung.00452.2016.

Conklin, D.J., Ogunwale, M.A., Chen, Y., et al. (2018) Electronic cigarette-generated aldehydes: The contribution of e-liquid components to their formation and the use of urinary aldehyde metabolites as biomarkers of exposure. *Aerosol Science and Technology*, 52 (11): 1219–1232. doi:10.1080/02786826.2018.1500013.

Cory, S. and Adams, J.M. (2002) The Bcl2 family: regulators of the cellular life-or-death switch. *Nature Reviews. Cancer*, 2 (9): 647–656. doi:10.1038/nrc883.

Cory-Slechta, D.A. (1996) Legacy of lead exposure: consequences for the central nervous system. *Otolaryngology--Head and Neck Surgery: Official Journal of American Academy of Otolaryngology-Head and Neck Surgery*, 114 (2): 224–226. doi:10.1016/S0194-59989670171-7.

Covarrubias, M., Bhattacharji, A., De Santiago-Castillo, J.A., et al. (2008) The Neuronal Kv4 Channel Complex. *Neurochemical research*, 33 (8): 1558. doi:10.1007/S11064-008-9650-8.

Cozens, A.L., Yezzi, M.J., Kunzelmann, K., et al. (1994) CFTR expression and chloride secretion in polarized immortal human bronchial epithelial cells. *American journal of respiratory cell and molecular biology*, 10 (1): 38–47. doi:10.1165/AJRCMB.10.1.7507342.

Crotty Alexander, L.E., Vyas, A., Schraufnagel, D.E., et al. (2015) Electronic cigarettes: the new face of nicotine delivery and addiction. *Journal of Thoracic Disease*, 7 (8): E248–E251. doi:10.3978/j.issn.2072-1439.2015.07.37.

Daleke, D.L. (2003) Regulation of transbilayer plasma membrane phospholipid asymmetry. *Journal of Lipid Research*, 44 (2): 233–242. doi:10.1194/jlr.R200019-JLR200.

D'Anna, C., Cigna, D., Costanzo, G., et al. (2015) Cigarette smoke alters cell cycle and induces inflammation in lung fibroblasts. *Life Sciences*, 126: 10–18. doi:10.1016/j.lfs.2015.01.017.

David, T., Ling, S.F. and Barton, A. (2018) Genetics of immune-mediated inflammatory diseases. *Clinical and Experimental Immunology*, 193 (1): 3–12. doi:10.1111/cei.13101.

De Diego Damiá, A., Cortijo Gimeno, J., Selma Ferrer, M.J., et al. (2011) A Study of the Effect of Proinflammatory Cytokines on the Epithelial Cells of Smokers, With or Without COPD. *Archivos de Bronconeumología*, 47 (9): 447–453. doi:10.1016/j.arbr.2011.04.007.

Dearman, R.J., Cumberbatch, M., Maxwell, G., et al. (2009) Toll-like receptor ligand activation of murine bone marrow-derived dendritic cells. *Immunology*, 126 (4): 475. doi:10.1111/J.1365-2567.2008.02922.X.

Decramer, M., Rennard, S., Troosters, T., et al. (2008) COPD as a lung disease with systemic consequences--clinical impact, mechanisms, and potential for early intervention. *COPD*, 5 (4): 235–256. doi:10.1080/15412550802237531.

Delgado-Ortega, M., Olivier, M., Sizaret, P.Y., et al. (2014) Newborn pig trachea cell line cultured in air-liquid interface conditions allows a partial in vitro representation of the porcine upper airway tissue. *BMC cell biology*, 15 (1). doi:10.1186/1471-2121-15-14.

Ding, Y.S., Trommel, J.S., Yan, X.J., et al. (2005) Determination of 14 polycyclic aromatic hydrocarbons in mainstream smoke from domestic cigarettes. *Environmental Science & Technology*, 39 (2): 471–478. doi:10.1021/es048690k.

Diver, W.R., Jacobs, E.J. and Gapstur, S.M. (2018) Secondhand Smoke Exposure in Childhood and Adulthood in Relation to Adult Mortality Among Never Smokers. *American journal of preventive medicine*, 55 (3): 345–352. doi:10.1016/J.AMEPRE.2018.05.005.

Djurovic, S., Gustafsson, O., Mattingsdal, M., et al. (2010) A genome-wide association study of bipolar disorder in Norwegian individuals, followed by replication in Icelandic sample. *Journal of Affective Disorders*, 126 (1): 312–316. doi:https://doi.org/10.1016/j.jad.2010.04.007.

Doll, R. and Hill, A.B. (1954) The Mortality of Doctors in Relation to Their Smoking Habits. *British Medical Journal*, 1 (4877): 1451–1455.

Downs, C.A., Kreiner, L.H., Trac, D.Q., et al. (2013) Acute Effects of Cigarette Smoke Extract on Alveolar Epithelial Sodium Channel Activity and Lung Fluid Clearance. *American Journal of Respiratory Cell and Molecular Biology*, 49 (2): 251–259. doi:10.1165/rcmb.2012-0234OC.

Duell, A.K., Pankow, J.F., Gillette, S.M., et al. (2018) Boiling points of the propylene glycol + glycerol system at 1 atmosphere pressure: 188.6-292 °C without and with added water or nicotine. *Chemical Engineering Communications*, 205 (12): 1691–1700. doi:10.1080/00986445.2018.1468758.

Dutta, J., Singh, S., Greeshma, M.V., et al. (2024) Diagnostic Challenges and Pathogenetic Differences in Biomass-Smoke-Induced versus Tobacco-Smoke-Induced COPD: A Comparative Review. *Diagnostics*, 14 (19): 2154. doi:10.3390/diagnostics14192154.

Ebersole, J., Samburova, V., Son, Y., et al. (2020) Harmful chemicals emitted from electronic cigarettes and potential deleterious effects in the oral cavity. *Tobacco Induced Diseases*, 18: 41. doi:10.18332/tid/116988.

Eckardt, K., Görgens, S.W., Raschke, S., et al. (2014) Myokines in insulin resistance and type 2 diabetes. *Diabetologia*, 57 (6): 1087–1099. doi:10.1007/s00125-014-3224-x.

Eckmann, L., Kagnoff, M.F. and Fierer, J. (1993) Epithelial cells secrete the chemokine interleukin-8 in response to bacterial entry. *Infection and Immunity*, 61 (11): 4569–4574.

Edwards, R. (2004) The problem of tobacco smoking. *BMJ (Clinical research ed.)*, 328 (7433): 217–219. doi:10.1136/bmj.328.7433.217.

Elisia, I., Lam, V., Cho, B., et al. (2020) The effect of smoking on chronic inflammation, immune function and blood cell composition. *Scientific Reports*, 10: 19480. doi:10.1038/s41598-020-76556-7.

Erythropel, H.C., Jabba, S.V., DeWinter, T.M., et al. (2018) Formation of flavorant–propylene Glycol Adducts With Novel Toxicological Properties in Chemically Unstable E-Cigarette Liquids. *Nicotine & Tobacco Research*, 21 (9): 1248–1258. doi:10.1093/ntr/nty192.

Evans, R.E., Herbert, S., Owen, W., et al. (2021) Case of e-cigarette or vaping product use-associated lung injury (EVALI) in London, UK. *BMJ Case Reports CP*, 14 (4): e240700. doi:10.1136/bcr-2020-240700.

Facchinetti, F., Amadei, F., Geppetti, P., et al. (2012) α,β-Unsaturated Aldehydes in Cigarette Smoke Release Inflammatory Mediators from Human Macrophages. *https://doi.org/10.1165/rcmb.2007-0130OC*, 37 (5): 617–623. doi:10.1165/RCMB.2007-0130OC.

Fadok, V.A., Voelker, D.R., Campbell, P.A., et al. (1992) Exposure of phosphatidylserine on the surface of apoptotic lymphocytes triggers specific recognition and removal by macrophages. *Journal of Immunology (Baltimore, Md.: 1950)*, 148 (7): 2207–2216.

Falck, J., Mailand, N., Syljuåsen, R.G., et al. (2001) The ATM-Chk2-Cdc25A checkpoint pathway guards against radioresistant DNA synthesis. *Nature*, 410 (6830): 842–847. doi:10.1038/35071124.

Fan Chiang, Y., Lee, Y., Lam, F., et al. (2022) Smoking increases the risk of postoperative wound complications: A propensity score-matched cohort study. *International Wound Journal*, 20 (2): 391–402. doi:10.1111/iwj.13887.

Farsalinos, K.E., Romagna, G., Tsiapras, D., et al. (2013) Evaluation of electronic cigarette use (vaping) topography and estimation of liquid consumption: implications for research protocol standards definition and for public health authorities' regulation. *International Journal of Environmental Research and Public Health*, 10 (6): 2500–2514. doi:10.3390/ijerph10062500.

Fassl, A., Geng, Y. and Sicinski, P. (2022) CDK4 and CDK6 kinases: from basic science to cancer therapy. *Science (New York, N.Y.)*, 375 (6577): eabc1495. doi:10.1126/science.abc1495.

Fathollahpour, A., Abyaneh, F.A., Darabi, B., et al. (2023) Aspirin-Exacerbated Respiratory Disease Polymorphisms; a review study. *Gene*, 870: 147326. doi:https://doi.org/10.1016/j.gene.2023.147326.

Feldmann, M. and Saklatvala, J. (2000) *Proinflammatory cytokines*., 1.

Filion, M.C. and Phillips, N.C. (1997) Toxicity and immunomodulatory activity of liposomal vectors formulated with cationic lipids toward immune effector cells. *Biochimica et Biophysica Acta (BBA) - Biomembranes*, 1329 (2): 345–356. doi:10.1016/S0005-2736(97)00126-0.

Fischer, M.H. (1905) THE TOXIC EFFECTS OF FORMALDEHYDE AND FORMALIN. *The Journal of Experimental Medicine*, 6 (4–6): 487–518.

Fitzgerald, K.A., Palsson-McDermott, E.M., Bowie, A.G., et al. (2001) Mal (MyD88-adapter-like) is required for Toll-like receptor-4 signal transduction. *Nature*, 413 (6851): 78–83. doi:10.1038/35092578.

Flower, M., Nandakumar, L., Singh, M., et al. (2017) Respiratory bronchiolitis-associated interstitial lung disease secondary to electronic nicotine delivery system use confirmed with open lung biopsy. *Respirology Case Reports*, 5 (3): e00230. doi:10.1002/rcr2.230.

Foeger, N.C., Norris, A.J., Wren, L.M., et al. (2012) Augmentation of Kv4.2-encoded currents by accessory dipeptidyl peptidase 6 and 10  subunits reflects selective cell surface Kv4.2 protein stabilization. *The Journal of biological chemistry*, 287 (12): 9640–9650. doi:10.1074/jbc.M111.324574.

Fois, A.G., Paliogiannis, P., Sotgia, S., et al. (2018) Evaluation of oxidative stress biomarkers in idiopathic pulmonary fibrosis and therapeutic applications: a systematic review. *Respiratory Research*, 19 (1): 51. doi:10.1186/s12931-018-0754-7.

Forey, B.A., Thornton, A.J. and Lee, P.N. (2011) Systematic review with meta-analysis of the epidemiological evidence relating smoking to COPD, chronic bronchitis and emphysema. *BMC Pulmonary Medicine*, 11 (1): 1–61. doi:10.1186/1471-2466-11-36/TABLES/17.

Fraile, J.M., Ordóñez, G.R., Quirós, P.M., et al. (2013) Identification of novel tumor suppressor proteases by degradome profiling of colorectal carcinomas. *Oncotarget*, 4 (11): 1919–1932.

Fujii, S., Hara, H., Araya, J., et al. (2012) Insufficient autophagy promotes bronchial epithelial cell senescence in chronic obstructive pulmonary disease. *Oncoimmunology*, 1 (5): 630. doi:10.4161/ONCI.20297.

Fusco, A., Savio, V., Cammarota, M., et al. (2017) Beta-Defensin-2 and Beta-Defensin-3 Reduce Intestinal Damage Caused by *Salmonella typhimurium* Modulating the Expression of Cytokines and Enhancing the Probiotic Activity of *Enterococcus faecium* Dwivedi, M. (ed.). *Journal of Immunology Research*, 2017: 6976935. doi:10.1155/2017/6976935.

Galitovsky, V., Chowdhury, P. and Zharov, V.P. (2004) Photothermal detection of nicotine-induced apoptotic effects in pancreatic cancer cells. *Life Sciences*, 75 (22): 2677–2687. doi:10.1016/j.lfs.2004.05.022.

Gao, J., Li, W., Willis-Owen, S.A., et al. (2010) Polymorphisms of *PHF11* and *DPP10* Are Associated with Asthma and Related Traits in a Chinese Population. *Respiration*, 79 (1): 17–24. doi:10.1159/000235545.

Garcia-Arcos, I., Geraghty, P., Baumlin, N., et al. (2016) Chronic electronic cigarette exposure in mice induces features of COPD in a nicotine-dependent manner. *Thorax*, 71 (12): 1119–1129. doi:10.1136/THORAXJNL-2015-208039.

GBD 2015 Chronic Respiratory Disease Collaborators (2017) Global, regional, and national deaths, prevalence, disability-adjusted life years, and years lived with disability for chronic obstructive pulmonary disease and asthma, 1990-2015: a systematic analysis for the Global Burden of Disease Study 2015. *The Lancet. Respiratory medicine*, 5 (9): 691–706. doi:10.1016/S2213-2600(17)30293-X.

GEINDREAU, M., BRUCHARD, M. and VEGRAN, F. (2022) Role of Cytokines and Chemokines in Angiogenesis in a Tumor Context. *Cancers*, 14 (10): 2446. doi:10.3390/cancers14102446.

Gellatly, S., Pavelka, N., Crue, T., et al. (2020) Nicotine-Free e-Cigarette Vapor Exposure Stimulates IL6 and Mucin Production in Human Primary Small Airway Epithelial Cells. *Journal of Inflammation Research*, 13: 175–185. doi:10.2147/JIR.S244434.

Ghosh, A., Coakley, R.C., Mascenik, T., et al. (2018) Chronic E-Cigarette Exposure Alters the Human Bronchial Epithelial Proteome. *American Journal of Respiratory and Critical Care Medicine*, 198 (1): 67–76. doi:10.1164/rccm.201710-2033OC.

Ghosh, B., Nishida, K., Chandrala, L., et al. (2019) Effect of Vaping on Airway Barrier Function: A Pilot Study. *European Respiratory Journal*, 54 (suppl 63). doi:10.1183/13993003.congress-2019.PA2395.

Ghosh, B., Park, B., Bhowmik, D., et al. (2020) Strong correlation between air-liquid interface cultures and in vivo transcriptomics of nasal brush biopsy. *American journal of physiology. Lung cellular and molecular physiology*, 318 (5): L1056–L1062. doi:10.1152/AJPLUNG.00050.2020.

Ghosh, S., May, M.J. and Kopp, E.B. (1998) NF-kappa B and Rel proteins: evolutionarily conserved mediators of immune responses. *Annual Review of Immunology*, 16: 225–260. doi:10.1146/annurev.immunol.16.1.225.

Girirajan, S., Dennis, M.Y., Baker, C., et al. (2013) Refinement and discovery of new hotspots of copy-number variation associated with autism spectrum disorder. *American journal of human genetics*, 92 (2): 221–237. doi:10.1016/j.ajhg.2012.12.016.

Glynos, C., Bibli, S.-I., Katsaounou, P., et al. (2018) Comparison of the effects of e-cigarette vapor with cigarette smoke on lung function and inflammation in mice. *American journal of physiology. Lung cellular and molecular physiology*, 315 (5): L662–L672. doi:10.1152/ajplung.00389.2017.

Go, Y.Y., Mun, J.Y., Chae, S.-W., et al. (2020) Comparison between in vitro toxicities of tobacco- and menthol-flavored electronic cigarette liquids on human middle ear epithelial cells. *Scientific Reports*, 10 (1): 2544. doi:10.1038/s41598-020-59290-y.

GOLD (2025) *Global strategy for the diagnosis, management and prevention of chronic obstructive pulmonary disease (2025 Report)*. Available at: https://goldcopd.org/2025-gold-report/.

Gompel, A., Somaï, S., Chaouat, M., et al. (2000) Hormonal regulation of apoptosis in breast cells and tissues. *Steroids*, 65 (10–11): 593–598. doi:10.1016/s0039-128x(00)00172-0.

Goniewicz, M.L., Knysak, J., Gawron, M., et al. (2014) Levels of selected carcinogens and toxicants in vapour from electronic cigarettes. *Tobacco Control*, 23 (2): 133–139. doi:10.1136/tobaccocontrol-2012-050859.

Goodwin, T. and Huang, L. (2014) "Chapter One - Nonviral Vectors: We Have Come a Long Way." In Huang, L., Liu, D. and Wagner, E. (eds) *Advances in Genetics*. Nonviral Vectors for Gene Therapy. Academic Press. pp. 1–12. doi:10.1016/B978-0-12-800148-6.00001-8.

Gorguner, M. and Akgun, M. (2010) Acute Inhalation Injury. *The Eurasian Journal of Medicine*, 42 (1): 28–35. doi:10.5152/eajm.2010.09.

Gorrell, M.D., Wickson, J. and McCaughan, G.W. (1991) Expression of the rat CD26 antigen (dipeptidyl peptidase IV) on subpopulations of rat lymphocytes. *Cellular immunology*, 134 (1): 205–215. doi:10.1016/0008-8749(91)90343-a.

Gozubuyuk, A.A., Dag, H., Kacar, A., et al. (2017) Epidemiology, pathophysiology, clinical evaluation, and treatment of carbon monoxide poisoning in child, infant, and fetus. *Northern Clinics of Istanbul*, 4 (1): 100–107. doi:10.14744/nci.2017.49368.

Graham, T.R. (2004) Flippases and vesicle-mediated protein transport. *Trends in Cell Biology*, 14 (12): 670–677. doi:10.1016/j.tcb.2004.10.008.

Grainger, C.I., Greenwell, L.L., Lockley, D.J., et al. (2006) Culture of Calu-3 cells at the air interface provides a representative model of the airway epithelial barrier. *Pharmaceutical Research*, 23 (7): 1482–1490. doi:10.1007/S11095-006-0255-0/FIGURES/3.

Gras, D., Martinez-Anton, A., Bourdin, A., et al. (2017) Human bronchial epithelium orchestrates dendritic cell activation in severe asthma. *European Respiratory Journal*, 49 (3). doi:10.1183/13993003.02399-2016.

Green, D.R. and Kroemer, G. (2004) The Pathophysiology of Mitochondrial Cell Death. *Science*, 305 (5684): 626–629. doi:10.1126/science.1099320.

Grider, M.H., Jessu, R. and Kabir, R. (2022) *Physiology, Action Potential.* In Treasure Island (FL).

Guo, T., Chai, X., Liu, Q., et al. (2017) Downregulation of P16 promotes cigarette smoke extract-induced vascular smooth muscle cell proliferation via preventing G1/S phase transition. *Experimental and Therapeutic Medicine*, 14 (1): 214–220. doi:10.3892/etm.2017.4468.

Guzeloglu-Kayisli, O., Kayisli, U.A. and Taylor, H.S. (2009) The Role of Growth Factors and Cytokines during Implantation: Endocrine and Paracrine Interactions. *Seminars in reproductive medicine*, 27 (1): 62–79. doi:10.1055/s-0028-1108011.

Haddad, C., Salman, R., El-Hellani, A., et al. (2019) Reactive Oxygen Species Emissions from Supra- and Sub-Ohm Electronic Cigarettes. *Journal of Analytical Toxicology*, 43 (1): 45–50. doi:10.1093/jat/bky065.

Hajek, P., Phillips-Waller, A., Przulj, D., et al. (2019) A Randomized Trial of E-Cigarettes versus Nicotine-Replacement Therapy. *New England Journal of Medicine*, 380 (7): 629–637. doi:10.1056/NEJMoa1808779.

Hajiasgharzadeh, K., Somi, M.H., Mansoori, B., et al. (2020) Alpha7 Nicotinic Acetylcholine Receptor Mediates Nicotine-induced Apoptosis and Cell Cycle Arrest of Hepatocellular Carcinoma HepG2 Cells. *Advanced Pharmaceutical Bulletin*, 10 (1): 65–71. doi:10.15171/apb.2020.008.

Hammond, E.C. and Horn, D. (1954) The relationship between human smoking habits and death rates: a follow-up study of 187,766 men. *Journal of the American Medical Association*, 155 (15): 1316–1328. doi:10.1001/jama.1954.03690330020006.

Harper, R., Wu, K., Chang, M.M., et al. (2001) Activation of nuclear factor-kappa b transcriptional activity in airway epithelial cells by thioredoxin but not by N-acetyl-cysteine and glutathione. *American Journal of Respiratory Cell and Molecular Biology*, 25 (2): 178–185. doi:10.1165/ajrcmb.25.2.4471.

Harvey, B.-G., Heguy, A., Leopold, P.L., et al. (2007) Modification of gene expression of the small airway epithelium in response to cigarette smoking. *Journal of Molecular Medicine (Berlin, Germany)*, 85 (1): 39–53. doi:10.1007/s00109-006-0103-z.

Haws, C., Krouse, M.E., Xia, Y., et al. (1992) CFTR channels in immortalized human airway cells. *The American journal of physiology*, 263 (6 Pt 1). doi:10.1152/AJPLUNG.1992.263.6.L692.

He, J.-Q., Foreman, M.G., Shumansky, K., et al. (2009) Associations of IL6 polymorphisms with lung function decline and COPD. *Thorax*, 64 (8): 698–704. doi:10.1136/thx.2008.111278.

He, T., Wang, K., Zhao, P., et al. (2022) Integrative computational approach identifies immune-relevant biomarkers in ulcerative colitis. *FEBS open bio*, 12 (2): 500–515. doi:10.1002/2211-5463.13357.

Heguy, A., Harvey, B.-G., Leopold, P.L., et al. (2007) Responses of the human airway epithelium transcriptome to in vivo injury. *Physiological Genomics*, 29 (2): 139–148. doi:10.1152/physiolgenomics.00167.2006.

Heijink, I.H., Brandenburg, S.M., Postma, D.S., et al. (2012) Cigarette smoke impairs airway epithelial barrier function and cell–cell contact recovery. *European Respiratory Journal*, 39 (2): 419–428. doi:10.1183/09031936.00193810.

Heinrich, H., Grunitz, J., Stonawski, V., et al. (2017) Attention, cognitive control and motivation in ADHD: Linking event-related brain potentials and DNA methylation patterns in boys at early school age. *Scientific reports*, 7 (1): 3823. doi:10.1038/s41598-017-03326-3.

Herr, C., Tsitouras, K., Niederstraßer, J., et al. (2020a) Cigarette smoke and electronic cigarettes differentially activate bronchial epithelial cells. *Respiratory Research*, 21 (1): 67. doi:10.1186/s12931-020-1317-2.

Herr, C., Tsitouras, K., Niederstraßer, J., et al. (2020b) Cigarette smoke and electronic cigarettes differentially activate bronchial epithelial cells. *Respiratory Research*, 21 (1): 67. doi:10.1186/s12931-020-1317-2.

Higashi, T., Mai, Y., Mazaki, Y., et al. (2016) A Standardized Method for the Preparation of a Gas Phase Extract of Cigarette Smoke. *Biological & pharmaceutical bulletin*, 39 (6): 898–902. doi:10.1248/BPB.B16-00062.

Higashi, T., Mai, Y., Noya, Y., et al. (2014) A simple and rapid method for standard preparation of gas phase extract of cigarette smoke. *PloS one*, 9 (9). doi:10.1371/JOURNAL.PONE.0107856.

Higham, A., Dungwa, J., Jackson, N., et al. (2022) Relationships between Airway Remodeling and Clinical Characteristics in COPD Patients. *Biomedicines*, 10 (8): 1992. doi:10.3390/biomedicines10081992.

Hirko, A., Tang, F. and Hughes, J.A. (2003) Cationic lipid vectors for plasmid DNA delivery. *Current medicinal chemistry*, 10 (14): 1185–1193. doi:10.2174/0929867033457412.

Hocevar, B.A. and Howe, P.H. (1998) Mechanisms of TGF-beta-induced cell cycle arrest. *Mineral and Electrolyte Metabolism*, 24 (2–3): 131–135. doi:10.1159/000057360.

Hoffmann, I., Draetta, G. and Karsenti, E. (1994) Activation of the phosphatase activity of human cdc25A by a cdk2-cyclin E dependent phosphorylation at the G1/S transition. *The EMBO journal*, 13 (18): 4302–4310. doi:10.1002/j.1460-2075.1994.tb06750.x.

Horng, T., Barton, G.M., Flavell, R.A., et al. (2002) The adaptor molecule TIRAP provides signalling specificity for Toll-like receptors. *Nature*, 420 (6913): 329–333. doi:10.1038/nature01180.

Horng, T., Barton, G.M. and Medzhitov, R. (2001) TIRAP: an adapter molecule in the Toll signaling pathway. *Nature Immunology*, 2 (9): 835–841. doi:10.1038/ni0901-835.

Howard Reed (2020) *The impact of smoking history on employment prospects, earnings and productivity: an analysis using UK panel data*. Landman Economics. Available at: https://ash.org.uk/uploads/LandmanEconomics-smoking-employment-earnings-technical-report.pdf (Accessed: 25 February 2025).

HSS and Services, U.S.D. of H. and H. (2006) *The health consequences of involuntary exposure to tobacco smoke: a report of the Surgeon General*.

HSS and Services, U.S.D. of H. and H. (2010) A report of the surgeon general: how tobacco smoke causes disease: what it means to you. *http://www. cdc. gov/tobacco/data_statistics/sgr/2010/consumer_booklet/pdfs/consumer. pdf*.

HSS and Services, U.S.D. of H. and H. (2014) Let's make the next generation tobacco-free: your guide to the 50th anniversary Surgeon General's report on smoking and health. Atlanta: US Department of Health and Human Services, Centers for Disease Control and Prevention. *National Center for Chronic Disease Prevention and Health Promotion, Office on Smoking and Health*.

Hsu, H., Huang, J., Shu, H.B., et al. (1996a) TNF-dependent recruitment of the protein kinase RIP to the TNF receptor-1 signaling complex. *Immunity*, 4 (4): 387–396. doi:10.1016/s1074-7613(00)80252-6.

Hsu, H., Shu, H.-B., Pan, M.-G., et al. (1996b) TRADD–TRAF2 and TRADD–FADD Interactions Define Two Distinct TNF Receptor 1 Signal Transduction Pathways. *Cell*, 84 (2): 299–308. doi:10.1016/S0092-8674(00)80984-8.

Hu, Y., Huang, Y., Zong, L., et al. (2024) Emerging roles of ferroptosis in pulmonary fibrosis: current perspectives, opportunities and challenges. *Cell Death Discovery*, 10 (1): 301. doi:10.1038/s41420-024-02078-0.

Huang, C.-C., Lai, C.-Y., Tsai, C.-H., et al. (2021) Combined effects of cigarette smoking, DNA methyltransferase 3B genetic polymorphism, and DNA damage on lung cancer. *BMC Cancer*, 21: 1066. doi:10.1186/s12885-021-08800-w.

Hutzler, C., Paschke, M., Kruschinski, S., et al. (2014) Chemical hazards present in liquids and vapors of electronic cigarettes. *Archives of Toxicology*, 88 (7): 1295–1308. doi:10.1007/s00204-014-1294-7.

Huuskonen, P., Storvik, M., Reinisalo, M., et al. (2008) Microarray analysis of the global alterations in the gene expression in the placentas from cigarette-smoking mothers. *Clinical Pharmacology and Therapeutics*, 83 (4): 542–550. doi:10.1038/sj.clpt.6100376.

I, M., C, B., N, Z., et al. (1998) Bax and adenine nucleotide translocator cooperate in the mitochondrial control of apoptosis. *Science (New York, N.Y.)*, 281 (5385). doi:10.1126/science.281.5385.2027.

Invernizzi, G., Ruprecht, A., De Marco, C., et al. (2009) Inhaled steroid/tobacco smoke particle interactions: a new light on steroid resistance. *Respiratory Research*, 10 (1): 48. doi:10.1186/1465-9921-10-48.

Jabba, S.V., Diaz, A.N., Erythropel, H.C., et al. (2020) Chemical Adducts of Reactive Flavor Aldehydes Formed in E-Cigarette Liquids Are Cytotoxic and Inhibit Mitochondrial Function in Respiratory Epithelial Cells. *Nicotine & Tobacco Research*, 22 (Suppl 1): S25–S34. doi:10.1093/ntr/ntaa185.

Jaegers, N.R., Hu, W., Weber, T.J., et al. (2021) Low-temperature (< 200 °C) degradation of electronic nicotine delivery system liquids generates toxic aldehydes. *Scientific Reports*, 11 (1): 7800. doi:10.1038/s41598-021-87044-x.

Jang, M.-H., Shin, M.-C., Jung, S.-B., et al. (2002) Alcohol and nicotine reduce cell proliferation and enhance apoptosis in dentate gyrus. *Neuroreport*, 13 (12): 1509–1513. doi:10.1097/00001756-200208270-00004.

Jansen, D.F., Schouten, J.P., Vonk, J.M., et al. (1999) Smoking and Airway Hyperresponsiveness Especially in the Presence of Blood Eosinophilia Increase the Risk to Develop Respiratory Symptoms. *American Journal of Respiratory and Critical Care Medicine*, 160 (1): 259–264. doi:10.1164/ajrccm.160.1.9811015.

Jayatilaka, H., Tyle, P., Chen, J.J., et al. (2017) Synergistic IL-6 and IL-8 paracrine signalling pathway infers a strategy to inhibit tumour cell migration. *Nature Communications*, 8: 15584. doi:10.1038/ncomms15584.

Jerng, H.H. and Pfaffinger, P.J. (2014) Modulatory mechanisms and multiple functions of somatodendritic A-type K+ channel auxiliary subunits. *Frontiers in Cellular Neuroscience*, 8 (MAR). doi:10.3389/FNCEL.2014.00082.

Jerng, H.H., Qian, Y. and Pfaffinger, P.J. (2004) Modulation of Kv4.2 channel expression and gating by dipeptidyl peptidase 10 (DPP10). *Biophysical journal*, 87 (4): 2380–2396. doi:10.1529/biophysj.104.042358.

Jindal, S.K., Aggarwal, A.N., Chaudhry, K., et al. (2006) A multicentric study on epidemiology of chronic obstructive pulmonary disease and its relationship with tobacco smoking and environmental tobacco smoke exposure. *The Indian journal of chest diseases & allied sciences*, 48 (1): 23–29.

Jinno, S., Suto, K., Nagata, A., et al. (1994) Cdc25A is a novel phosphatase functioning early in the cell cycle. *The EMBO Journal*, 13 (7): 1549–1556.

Jo, B., Zh, G., A, K., et al. (2010) Effects of cigarette smoke on the human oral mucosal transcriptome. *Cancer prevention research (Philadelphia, Pa.)*, 3 (3). doi:10.1158/1940-6207.CAPR-09-0192.

Jordan, V.C., Lewis, J.S., Osipo, C., et al. (2005) The apoptotic action of estrogen following exhaustive antihormonal therapy: a new clinical treatment strategy. *Breast (Edinburgh, Scotland)*, 14 (6). doi:10.1016/j.breast.2005.08.022.

Joseph, P. (2009) Mechanisms of cadmium carcinogenesis. *Toxicology and Applied Pharmacology*, 238 (3): 272–279. doi:10.1016/j.taap.2009.01.011.

Ju, J. and He, Y. (2021) PRMT5 promotes inflammation of cigarette smoke extract-induced bronchial epithelial cells by up-regulation of CXCL10. *Allergologia Et Immunopathologia*, 49 (5): 131–136. doi:10.15586/aei.v49i5.482.

Kagan, J.C. and Medzhitov, R. (2006) Phosphoinositide-mediated adaptor recruitment controls Toll-like receptor signaling. *Cell*, 125 (5): 943–955. doi:10.1016/j.cell.2006.03.047.

Kei, O., Tadanori, Y., Masahiko, U., et al. (2004) CD26 up-regulates expression of CD86 on antigen-presenting cells by means of caveolin-1. *Proceedings of the National Academy of Sciences*, 101 (39): 14186–14191. doi:10.1073/pnas.0405266101.

Kerr, J.F. (1971) Shrinkage necrosis: a distinct mode of cellular death. *The Journal of pathology*, 105 (1): 13–20. doi:10.1002/path.1711050103.

Kerr, J.F., Wyllie, A.H. and Currie, A.R. (1972) Apoptosis: a basic biological phenomenon with wide-ranging implications in tissue kinetics. *British journal of cancer*, 26 (4): 239–257. doi:10.1038/bjc.1972.33.

Kerr, J.F.R. (1969) An electron-microscope study of liver cell necrosis due to heliotrine. *The Journal of Pathology*, 97 (3): 557–562. doi:10.1002/path.1710970314.

Kesimer, M., Ford, A.A., Ceppe, A., et al. (2017) Airway Mucin Concentration as a Marker of Chronic Bronchitis. *The New England journal of medicine*, 377 (10): 911–922. doi:10.1056/NEJMoa1701632.

Khan, N.A., Lawyer, G., McDonough, S., et al. (2020) Systemic biomarkers of inflammation, oxidative stress and tissue injury and repair among waterpipe, cigarette and dual tobacco smokers. *Tobacco Control*, 29 (Suppl 2): s102–s109. doi:10.1136/tobaccocontrol-2019-054958.

Khodayari, N., Oshins, R., Mehrad, B., et al. (2022) Cigarette smoke exposed airway epithelial cell-derived EVs promote pro-inflammatory macrophage activation in alpha-1 antitrypsin deficiency. *Respiratory Research*, 23 (1): 232. doi:10.1186/s12931-022-02161-z.

Kim, A.S., Ko, H.J., Kwon, J.H., et al. (2018) Exposure to Secondhand Smoke and Risk of Cancer in Never Smokers: A Meta-Analysis of Epidemiologic Studies. *International journal of environmental research and public health*, 15 (9). doi:10.3390/IJERPH15091981.

Kim, K.-H., Joo, K.-J., Park, H.-J., et al. (2005) Nicotine induces apoptosis in TM3 mouse Leydig cells. *Fertility and Sterility*, 83 Suppl 1: 1093–1099. doi:10.1016/j.fertnstert.2004.12.013.

Kim, M.D., Chung, S., Baumlin, N., et al. (2024) The combination of propylene glycol and vegetable glycerin e-cigarette aerosols induces airway inflammation and mucus hyperconcentration. *Scientific Reports*, 14: 1942. doi:10.1038/s41598-024-52317-8.

Kim, M.D., Chung, S., Dennis, J.S., et al. (2022) Vegetable glycerin e-cigarette aerosols cause airway inflammation and ion channel dysfunction. *Frontiers in Pharmacology*, 13: 1012723. doi:10.3389/fphar.2022.1012723.

Kim, S.H., Choi, H., Yoon, M.G., et al. (2015) Dipeptidyl-peptidase 10 as a genetic biomarker for the aspirin-exacerbated respiratory disease phenotype. *Annals of Allergy, Asthma and Immunology*, 114 (3): 208–213. doi:10.1016/j.anai.2014.12.003.

Kluck, R.M., Bossy-Wetzel, E., Green, D.R., et al. (1997) The release of cytochrome c from mitochondria: a primary site for Bcl-2 regulation of apoptosis. *Science (New York, N.Y.)*, 275 (5303): 1132–1136. doi:10.1126/science.275.5303.1132.

Ko, F.W.S., Hui, D.S.C. and Lai, C.K.W. (2008) Worldwide burden of COPD in high- and low-income countries. Part III. Asia-Pacific studies. *The international journal of tuberculosis and lung disease : the official journal of the International Union against Tuberculosis and Lung Disease*, 12 (7): 713–717.

Kode, A., Yang, S.-R. and Rahman, I. (2006) Differential effects of cigarette smoke on oxidative stress and proinflammatory cytokine release in primary human airway epithelial cells and in a variety of transformed alveolar epithelial cells. *Respiratory Research*, 7 (1): 132. doi:10.1186/1465-9921-7-132.

Kokkinidis, D.G., Giannopoulos, S., Haider, M., et al. (2020) Active smoking is associated with higher rates of incomplete wound healing after endovascular treatment of critical limb ischemia. *Vascular medicine (London, England)*, 25 (5): 427–435. doi:10.1177/1358863X20916526.

Komura, M., Sato, T., Yoshikawa, H., et al. (2022) Propylene glycol, a component of electronic cigarette liquid, damages epithelial cells in human small airways. *Respiratory research*, 23 (1): 216. doi:10.1186/s12931-022-02142-2.

Korsbæk, N., Landt, E.M. and Dahl, M. (2021) Second-Hand Smoke Exposure Associated with Risk of Respiratory Symptoms, Asthma, and COPD in 20,421 Adults from the General Population. *Journal of asthma and allergy*, 14: 1277–1284. doi:10.2147/JAA.S328748.

Kosmider, L., Sobczak, A., Fik, M., et al. (2014) Carbonyl Compounds in Electronic Cigarette Vapors: Effects of Nicotine Solvent and Battery Output Voltage. *Nicotine & Tobacco Research*, 16 (10): 1319–1326. doi:10.1093/ntr/ntu078.

Kotoulas, S.-C., Katsaounou, P., Riha, R., et al. (2021) Electronic Cigarettes and Asthma: What Do We Know So Far? *Journal of Personalized Medicine*, 11 (8): 723. doi:10.3390/jpm11080723.

Krammer, P.H. (2000) CD95's deadly mission in the immune system. *Nature*, 407 (6805): 789–795. doi:10.1038/35037728.

Krawczyk, C.M., Holowka, T., Sun, J., et al. (2010) Toll-like receptor–induced changes in glycolytic metabolism regulate dendritic cell activation. *Blood*, 115 (23): 4742. doi:10.1182/BLOOD-2009-10-249540.

Kreiss, K. (2014) Work-Related Spirometric Restriction in Flavoring Manufacturing Workers. *American journal of industrial medicine*, 57 (2): 129–137. doi:10.1002/ajim.22282.

Krueger, J., Ray, A., Tamm, I., et al. (1991) Expression and function of interleukin-6 in epithelial cells. *Journal of Cellular Biochemistry*, 45 (4): 327–334. doi:10.1002/jcb.240450404.

Kulkarni, R., Rampersaud, R., Aguilar, J.L., et al. (2010) Cigarette Smoke Inhibits Airway Epithelial Cell Innate Immune Responses to Bacteria. *Infection and Immunity*, 78 (5): 2146–2152. doi:10.1128/IAI.01410-09.

Kumar, S., Parveen, S., Swaroop, S., et al. (2023) TNF-α and MMPs mediated mucus hypersecretion induced by cigarette smoke: An in vitro study. *Toxicology in vitro : an international journal published in association with BIBRA*, 92: 105654. doi:10.1016/j.tiv.2023.105654.

Kunkel, S.L., Standiford, T., Kasahara, K., et al. (1991) Interleukin-8 (IL-8): the major neutrophil chemotactic factor in the lung. *Experimental Lung Research*, 17 (1): 17–23. doi:10.3109/01902149109063278.

Kuo, Y.-L., Cheng, J.-K., Hou, W.-H., et al. (2017) K(+) Channel Modulatory Subunits KChIP and DPP Participate in Kv4-Mediated Mechanical Pain Control. *The Journal of neuroscience : the official journal of the Society for Neuroscience*, 37 (16): 4391–4404. doi:10.1523/JNEUROSCI.1619-16.2017.

La, T., Tm, A., Gh, W., et al. (1993) A novel domain within the 55 kd TNF receptor signals cell death. *Cell*, 74 (5). doi:10.1016/0092-8674(93)90464-2.

Lambeir, A.M., Proost, P., Durinx, C., et al. (2001) Kinetic Investigation of Chemokine Truncation by CD26/Dipeptidyl Peptidase IV Reveals a Striking Selectivity within the Chemokine Family. *Journal of Biological Chemistry*, 276 (32): 29839–29845. doi:10.1074/JBC.M103106200.

Lan, M.-Y., Ho, C., Lee, T.-C., et al. (2007) Cigarette smoke extract induces cytotoxicity on human nasal epithelial cells. *American Journal of Rhinology*, 21 (2): 218–223. doi:10.2500/ajr.2007.21.2966.

Lau, K., Swiney, B.S., Reeves, N., et al. (2012a) Propylene glycol produces excessive apoptosis in the developing mouse brain, alone and in combination with phenobarbital. *Pediatric Research*, 71 (1): 54–62. doi:10.1038/pr.2011.12.

Lau, P.P., Li, L., Merched, A.J., et al. (2006) Nicotine Induces Proinflammatory Responses in Macrophages and the Aorta Leading to Acceleration of Atherosclerosis in Low-Density Lipoprotein Receptor−/− Mice. *Arteriosclerosis, Thrombosis, and Vascular Biology*, 26 (1): 143–149. doi:10.1161/01.ATV.0000193510.19000.10.

Lau, W.K.-W., Mak, J.C.-W., Chan, K.-H., et al. (2012b) Cigarette smoke-induced cerebral cortical interleukin-6 elevation is not mediated through oxidative stress. *Neurotoxicity research*, 22 (2): 170–176. doi:10.1007/s12640-011-9301-8.

Layden, J.E., Ghinai, I., Pray, I., et al. (2020) Pulmonary Illness Related to E-Cigarette Use in Illinois and Wisconsin - Final Report. *The New England Journal of Medicine*, 382 (10): 903–916. doi:10.1056/NEJMoa1911614.

Lee, H., Park, J.-R., Kim, E.-J., et al. (2016) Cigarette smoke-mediated oxidative stress induces apoptosis via the MAPKs/STAT1 pathway in mouse lung fibroblasts. *Toxicology Letters*, 240 (1): 140–148. doi:10.1016/j.toxlet.2015.10.030.

Lee, H.-J., Guo, H.-Y., Lee, S.-K., et al. (2005a) Effects of nicotine on proliferation, cell cycle, and differentiation in immortalized and malignant oral keratinocytes. *Journal of Oral Pathology & Medicine: Official Publication of the International Association of Oral Pathologists and the American Academy of Oral Pathology*, 34 (7): 436–443. doi:10.1111/j.1600-0714.2005.00342.x.

Lee, H.-W., Park, S.-H., Weng, M., et al. (2018) E-cigarette smoke damages DNA and reduces repair activity in mouse lung, heart, and bladder as well as in human lung and bladder cells. *Proceedings of the National Academy of Sciences*, 115 (7): E1560–E1569. doi:10.1073/pnas.1718185115.

Lee, M.K., Yoo, J.W., Lin, H., et al. (2005b) Air-liquid interface culture of serially passaged human nasal epithelial cell monolayer for in vitro drug transport studies. *Drug delivery*, 12 (5): 305–311. doi:10.1080/10717540500177009.

Lee, P.N. (2018) Tar level of cigarettes smoked and risk of smoking-related diseases. *Inhalation Toxicology*, 30 (1): 5–18. doi:10.1080/08958378.2018.1443174.

Lee, S.A., Kim, Y.R., Yang, E.J., et al. (2013) CD26/DPP4 Levels in Peripheral Blood and T Cells in Patients With Type 2 Diabetes Mellitus. *The Journal of Clinical Endocrinology & Metabolism*, 98 (6): 2553–2561. doi:10.1210/jc.2012-4288.

Leonard, S.E., Ghanbari, M., Lahousse, L., et al. (2025) Immune Signatures of Smoking: Cytokine and Immunoglobulin Dysregulation and Partial Reversibility in a Population-Based Study. *Journal of Clinical Immunology*, 46 (1): 9. doi:10.1007/s10875-025-01975-y.

Leopold, P.L., O'Mahony, M.J., Lian, X.J., et al. (2009) Smoking Is Associated with Shortened Airway Cilia. *PLoS ONE*, 4 (12): e8157. doi:10.1371/journal.pone.0008157.

Lerner, C.A., Sundar, I.K., Yao, H., et al. (2015) Vapors produced by electronic cigarettes and e-juices with flavorings induce toxicity, oxidative stress, and inflammatory response in lung epithelial cells and in mouse lung. *PloS One*, 10 (2): e0116732. doi:10.1371/journal.pone.0116732.

Lewis, J.S., Cheng, D. and Jordan, V.C. (2004) Targeting oestrogen to kill the cancer but not the patient. *British journal of cancer*, 90 (5). doi:10.1038/sj.bjc.6601627.

Lewis, J.S., Meeke, K., Osipo, C., et al. (2005) Intrinsic mechanism of estradiol-induced apoptosis in breast cancer cells resistant to estrogen deprivation. *Journal of the National Cancer Institute*, 97 (23). doi:10.1093/jnci/dji400.

Li, L., Cousart, S., Hu, J., et al. (2000) Characterization of interleukin-1 receptor-associated kinase in normal and endotoxin-tolerant cells. *The Journal of Biological Chemistry*, 275 (30): 23340–23345. doi:10.1074/jbc.M001950200.

Li, S., Strelow, A., Fontana, E.J., et al. (2002) IRAK-4: a novel member of the IRAK family with the properties of an IRAK-kinase. *Proceedings of the National Academy of Sciences of the United States of America*, 99 (8): 5567–5572. doi:10.1073/pnas.082100399.

Lian, S., Li, S., Zhu, J., et al. (2022) Nicotine stimulates IL-8 expression via ROS/NF-κB and ROS/MAPK/AP-1 axis in human gastric cancer cells. *Toxicology*, 466: 153062. doi:10.1016/j.tox.2021.153062.

Lin, L., Long, L.K., Hatch, M.M., et al. (2014) DPP6 Domains Responsible for Its Localization and Function *. *Journal of Biological Chemistry*, 289 (46): 32153–32165. doi:10.1074/jbc.M114.578070.

Lin, L., Murphy, J.G., Karlsson, R.-M., et al. (2018) *DPP6 Loss Impacts Hippocampal Synaptic Development and Induces Behavioral Impairments in Recognition, Learning and Memory*. Available at: https://www.frontiersin.org/article/10.3389/fncel.2018.00084.

Lin, L., Sun, W., Throesch, B., et al. (2013) DPP6 regulation of dendritic morphogenesis impacts hippocampal synaptic development. *Nature Communications*, 4 (1): 2270. doi:10.1038/ncomms3270.

Liu, D., Ren, T. and Gao, X. (2003) Cationic transfection lipids. *Current medicinal chemistry*, 10 (14): 1307–1315. doi:10.2174/0929867033457386.

Liu, G., Zhao, H., Song, Q., et al. (2021) Long non-coding RNA DPP10-AS1 exerts anti-tumor effects on colon cancer via the upregulation of ADCY1 by regulating microRNA-127-3p. *Aging*, 13 (7): 9748–9765. doi:10.18632/aging.202729.

Liu, X., Conner, H., Kobayashi, T., et al. (2005) Cigarette Smoke Extract Induces DNA Damage but Not Apoptosis in Human Bronchial Epithelial Cells. *American Journal of Respiratory Cell and Molecular Biology*, 33 (2): 121–129. doi:10.1165/rcmb.2003-0341OC.

Liu, Z., Liu, A., Nan, A., et al. (2019) The linc00152 Controls Cell Cycle Progression by Regulating CCND1 in 16HBE Cells Malignantly Transformed by Cigarette Smoke Extract. *Toxicological Sciences: An Official Journal of the Society of Toxicology*, 167 (2): 496–508. doi:10.1093/toxsci/kfy254.

Løkke, A., Lange, P., Scharling, H., et al. (2006) Developing COPD: A 25 year follow up study of the general population. *Thorax*, 61 (11). doi:10.1136/thx.2006.062802.

Lossi, L. (2022) The concept of intrinsic versus extrinsic apoptosis. *Biochemical Journal*, 479 (3): 357–384. doi:10.1042/BCJ20210854.

Lu, J., Xie, L., Liu, C., et al. (2017) PTEN/PI3k/AKT Regulates Macrophage Polarization in Emphysematous mice. *Scandinavian Journal of Immunology*, 85 (6): 395–405. doi:10.1111/SJI.12545.

Lundbäck, B., Lindberg, A., Lindström, M., et al. (2003) Not 15 But 50% of smokers develop COPD? - Report from the Obstructive Lung Disease in Northern Sweden studies. *Respiratory Medicine*, 97 (2). doi:10.1053/rmed.2003.1446.

Luppi, F., Aarbiou, J., van Wetering, S., et al. (2005) Effects of cigarette smoke condensate on proliferation and wound closure of bronchial epithelial cells in vitro: role of glutathione. *Respiratory Research*, 6 (1): 140. doi:10.1186/1465-9921-6-140.

Ma, Y., Luo, L., Liu, X., et al. (2021) Pirfenidone mediates cigarette smoke extract induced inflammation and oxidative stress in vitro and in vivo. *International immunopharmacology*, 96: 107593. doi:10.1016/j.intimp.2021.107593.

Madison, M.C., Landers, C.T., Gu, B.-H., et al. (2019) Electronic cigarettes disrupt lung lipid homeostasis and innate immunity independent of nicotine. *The Journal of clinical investigation*, 129 (10): 4290–4304. doi:10.1172/JCI128531.

Madison, M.C., Landers, C.T., Gu, B.-H., et al. (2020) Electronic cigarettes disrupt lung lipid homeostasis and innate immunity independent of nicotine. *The Journal of Clinical Investigation*, 129 (10): 4290–4304. doi:10.1172/JCI128531.

Maffie, J. and Rudy, B. (2008) Weighing the evidence for a ternary protein complex mediating A-type K+ currents in neurons. *The Journal of Physiology*, 586 (Pt 23): 5609. doi:10.1113/JPHYSIOL.2008.161620.

Makena, P., Kikalova, T., Prasad, G.L., et al. (2023) Oxidative Stress and Lung Fibrosis: Towards an Adverse Outcome Pathway. *International Journal of Molecular Sciences*, 24 (15): 12490. doi:10.3390/ijms241512490.

Marino, M. and Ascenzi, P. (2008) Membrane association of estrogen receptor alpha and beta influences 17beta-estradiol-mediated cancer cell proliferation. *Steroids*, 73 (9–10): 853–858. doi:10.1016/j.steroids.2007.12.003.

Marinucci, L., Coniglio, M., Valenti, C., et al. (2022) In Vitro effects of alternative smoking devices on oral cells: Electronic cigarette and heated tobacco product versus tobacco smoke. *Archives of Oral Biology*, 144: 105550. doi:10.1016/j.archoralbio.2022.105550.

Marklová, E. (2007) Inflammation and genes. *Acta Medica (Hradec Kralove)*, 50 (1): 17–21.

Marrocco, A., Singh, D., Christiani, D.C., et al. (2022) E-cigarette vaping associated acute lung injury (EVALI): state of science and future research needs. *Critical Reviews in Toxicology*, 52 (3): 188–220. doi:10.1080/10408444.2022.2082918.

Mathias, R.A., Grant, A.V., Rafaels, N., et al. (2010) A genome-wide association study on African-ancestry populations for asthma. *The Journal of Allergy and Clinical Immunology*, 125 (2): 336-346.e4. doi:10.1016/j.jaci.2009.08.031.

Mattern, T., Scholz, W., Feller, A.C., et al. (1991) Expression of CD26 (dipeptidyl peptidase IV) on resting and activated human T-lymphocytes. *Scandinavian journal of immunology*, 33 (6): 737–748. doi:10.1111/j.1365-3083.1991.tb02548.x.

McAlinden, K.D., Lu, W., Ferdowsi, P.V., et al. (2021) Electronic Cigarette Aerosol Is Cytotoxic and Increases ACE2 Expression on Human Airway Epithelial Cells: Implications for SARS-CoV-2 (COVID-19). *Journal of clinical medicine*, 10 (5). doi:10.3390/jcm10051028.

McRitchie, D.I., Isowa, N., Edelson, J.D., et al. (2000) Production of tumour necrosis factor alpha by primary cultured rat alveolar epithelial cells. *Cytokine*, 12 (6): 644–654. doi:10.1006/cyto.1999.0656.

Meex, R.C.R. and Watt, M.J. (2017) Hepatokines: linking nonalcoholic fatty liver disease and insulin resistance. *Nature Reviews. Endocrinology*, 13 (9): 509–520. doi:10.1038/nrendo.2017.56.

Meloche, S (1995) Cell cycle reentry of mammalian fibroblasts is accompanied by the sustained activation of p44mapk and p42mapk isoforms in the G1 phase and their inactivation at the G1/S transition. *Journal of cellular physiology*, 163 (3). doi:10.1002/jcp.1041630319.

Mendel, J.R., Baig, S.A., Hall, M.G., et al. (2018) Brand switching and toxic chemicals in cigarette smoke: A national study. *PloS one*, 13 (1): e0189928–e0189928. doi:10.1371/journal.pone.0189928.

Metcalf, D. (2008) Hematopoietic cytokines. *Blood*, 111 (2): 485–491. doi:10.1182/blood-2007-03-079681.

Metcalfe, H.J., Lea, S., Hughes, D., et al. (2014) Effects of cigarette smoke on Toll-like receptor (TLR) activation of chronic obstructive pulmonary disease (COPD) macrophages. *Clinical and Experimental Immunology*, 176 (3): 461. doi:10.1111/CEI.12289.

Metzemaekers, M., Van Damme, J., Mortier, A., et al. (2016) *Regulation of Chemokine Activity – A Focus on the Role of Dipeptidyl Peptidase IV/CD26*.

Mio, T., Romberger, D.J., Thompson, A.B., et al. (1997) Cigarette smoke induces interleukin-8 release from human bronchial epithelial cells. *American Journal of Respiratory and Critical Care Medicine*, 155 (5): 1770–1776. doi:10.1164/ajrccm.155.5.9154890.

Mitran, E., Callender, T., Orha, B., et al. (1997) Neurotoxicity associated with occupational exposure to acetone, methyl ethyl ketone, and cyclohexanone. *Environmental Research*, 73 (1–2): 181–188. doi:10.1006/enrs.1997.3703.

Miyashita, L., Suri, R., Dearing, E., et al. (2018) E-cigarette vapour enhances pneumococcal adherence to airway epithelial cells. *The European Respiratory Journal*, 51 (2): 1701592. doi:10.1183/13993003.01592-2017.

Molinari, M., Mercurio, C., Dominguez, J., et al. (2000) Human Cdc25 A inactivation in response to S phase inhibition and its role in preventing premature mitosis. *EMBO Reports*, 1 (1): 71–79. doi:10.1093/embo-reports/kvd018.

Montalto, F.I. and De Amicis, F. (2020) Cyclin D1 in Cancer: A Molecular Connection for Cell Cycle Control, Adhesion and Invasion in Tumor and Stroma. *Cells*, 9 (12): 2648. doi:10.3390/cells9122648.

de Moraes, M.R., da Costa, A.C., Corrêa, K. de S., et al. (2014) Interleukin-6 and interleukin-8 blood levels' poor association with the severity and clinical profile of ex-smokers with COPD. *International Journal of Chronic Obstructive Pulmonary Disease*, 9: 735–743. doi:10.2147/COPD.S64135.

Morris, A.M., Leonard, S.S., Fowles, J.R., et al. (2021) Effects of E-Cigarette Flavoring Chemicals on Human Macrophages and Bronchial Epithelial Cells. *International Journal of Environmental Research and Public Health*, 18 (21): 11107. doi:10.3390/ijerph182111107.

Mortaz, E., Henricks, P.A.J., Kraneveld, A.D., et al. (2011) Cigarette smoke induces the release of CXCL-8 from human bronchial epithelial cells via TLRs and induction of the inflammasome. *Biochimica et Biophysica Acta (BBA) - Molecular Basis of Disease*, 1812 (9): 1104–1110. doi:10.1016/J.BBADIS.2011.06.002.

Moshensky, A., Brand, C.S., Alhaddad, H., et al. (n.d.) Effects of mango and mint pod-based e-cigarette aerosol inhalation on inflammatory states of the brain, lung, heart, and colon in mice. *eLife*, 11: e67621. doi:10.7554/eLife.67621.

Mullen, J.B., Wright, J.L., Wiggs, B.R., et al. (1987) Structure of central airways in current smokers and ex-smokers with and without mucus hypersecretion: relationship to lung function. *Thorax*, 42 (11): 843–848. doi:10.1136/thx.42.11.843.

Müller, F.H. (1940) Tabakmißbrauch und Lungencarcinom. *Zeitschrift für Krebsforschung*, 49 (1): 57–85. doi:10.1007/BF01633114.

Mulvihill, E.E. and Drucker, D.J. (2014) *Pharmacology, Physiology, and Mechanisms of Action of Dipeptidyl Peptidase-4 Inhibitors*. doi:10.1210/er.2014-1035.

Muthumalage, T., Lamb, T., Friedman, M.R., et al. (2019a) E-cigarette flavored pods induce inflammation, epithelial barrier dysfunction, and DNA damage in lung epithelial cells and monocytes. *Scientific Reports*, 9 (1): 19035. doi:10.1038/s41598-019-51643-6.

Muthumalage, T., Lamb, T., Friedman, M.R., et al. (2019b) E-cigarette flavored pods induce inflammation, epithelial barrier dysfunction, and DNA damage in lung epithelial cells and monocytes. *Scientific Reports*, 9 (1): 19035. doi:10.1038/s41598-019-51643-6.

Muthumalage, T., Prinz, M., Ansah, K.O., et al. (2018) Inflammatory and Oxidative Responses Induced by Exposure to Commonly Used e-Cigarette Flavoring Chemicals and Flavored e-Liquids without Nicotine. *Frontiers in Physiology*, 8: 1130. doi:10.3389/fphys.2017.01130.

Muzio, M., Ni, J., Feng, P., et al. (1997) IRAK (Pelle) family member IRAK-2 and MyD88 as proximal mediators of IL-1 signaling. *Science (New York, N.Y.)*, 278 (5343): 1612–1615. doi:10.1126/science.278.5343.1612.

Nadal, M.S., Ozaita, A., Amarillo, Y., et al. (2003) The CD26-Related Dipeptidyl Aminopeptidase-like Protein DPPX Is a Critical Component of Neuronal A-Type $K^+$ Channels. *Neuron*, 37 (3): 449–461. doi:10.1016/S0896-6273(02)01185-6.

Nakamura, H., Yoshimura, K., Jaffe, H.A., et al. (1991) Interleukin-8 gene expression in human bronchial epithelial cells. *The Journal of Biological Chemistry*, 266 (29): 19611–19617.

National Academies of Sciences, E., Division, H. and M., Practice, B. on P.H. and P.H., et al. (2018) "E-Cigarette Devices, Uses, and Exposures." In *Public Health Consequences of E-Cigarettes*. National Academies Press (US). Available at: https://www.ncbi.nlm.nih.gov/books/NBK507187/ (Downloaded: 19 May 2026).

National Army Museum (n.d.) *Pack of Camel cigarettes, 1944 (c)*. Available at: https://collection.nam.ac.uk/detail.php?acc=1989-04-116-838-5.

Nawrot, T., Geusens, P., Nulens, T.S., et al. (2010) Occupational cadmium exposure and calcium excretion, bone density, and osteoporosis in men. *Journal of Bone and Mineral Research: The Official Journal of the American Society for Bone and Mineral Research*, 25 (6): 1441–1445. doi:10.1002/jbmr.22.

NHS Digital (2020) *Statistics on Smoking, England 2020*. Available at: https://digital.nhs.uk/data-and-information/publications/statistical/statistics-on-smoking/statistics-on-smoking-england-2020 (Accessed: 14 April 2026).

Nishi, K., Ito, N., Mizumoto, J., et al. (1985) Death associated with butane inhalation: report of a case. *Nihon Hoigaku Zasshi = The Japanese Journal of Legal Medicine*, 39 (3): 214–216.

Norbury, C.J. and Hickson, I.D. (2001) Cellular responses to DNA damage. *Annual Review of Pharmacology and Toxicology*, 41: 367–401. doi:10.1146/annurev.pharmtox.41.1.367.

Nyunoya, T., Monick, M.M., Klingelhutz, A., et al. (2006) Cigarette Smoke Induces Cellular Senescence. *American Journal of Respiratory Cell and Molecular Biology*, 35 (6): 681–688. doi:10.1165/rcmb.2006-0169OC.

O'Boyle, N., Sutherland, E., Berry, C.C., et al. (2017) Temporal dynamics of ovine airway epithelial cell differentiation at an air-liquid interface. *PLOS ONE*, 12 (7): e0181583. doi:10.1371/JOURNAL.PONE.0181583.

O'Byrne, P.M. and Inman, M.D. (2003) Airway Hyperresponsiveness. *Chest*, 123 (3, Supplement): 411S-416S. doi:10.1378/chest.123.3_suppl.411S.

Oelsner, E.C., Balte, P.P., Bhatt, S.P., et al. (2020) Lung function decline in former smokers and low-intensity current smokers: the NHLBI Pooled Cohorts Study. *The Lancet. Respiratory medicine*, 8 (1): 34–44. doi:10.1016/S2213-2600(19)30276-0.

Ogunwale, M.A., Li, M., Ramakrishnam Raju, M.V., et al. (2017) Aldehyde Detection in Electronic Cigarette Aerosols. *ACS omega*, 2 (3): 1207–1214. doi:10.1021/acsomega.6b00489.

Ohkawa, T., Fukata, Y., Yamasaki, M., et al. (2013) Autoantibodies to epilepsy-related LGI1 in limbic encephalitis neutralize LGI1-ADAM22 interaction and reduce synaptic AMPA receptors. *The Journal of neuroscience : the official journal of the Society for Neuroscience*, 33 (46): 18161–18174. doi:10.1523/JNEUROSCI.3506-13.2013.

Ohnuma, K., Munakata, Y., Ishii, T., et al. (2001) Soluble CD26/Dipeptidyl Peptidase IV Induces T Cell Proliferation Through CD86 Up-Regulation on APCs. *The Journal of Immunology*, 167 (12): 6745 LP – 6755. doi:10.4049/jimmunol.167.12.6745.

Ohnuma, K., Uchiyama, M., Yamochi, T., et al. (2007) Caveolin-1 Triggers T-cell Activation via CD26 in Association with CARMA1 *. *Journal of Biological Chemistry*, 282 (13): 10117–10131. doi:10.1074/jbc.M609157200.

Ohnuma, K., Yamochi, T., Uchiyama, M., et al. (2005) CD26 mediates dissociation of Tollip and IRAK-1 from caveolin-1 and induces upregulation of CD86 on antigen-presenting cells. *Molecular and cellular biology*, 25 (17): 7743–7757. doi:10.1128/MCB.25.17.7743-7757.2005.

Oliynyk, I., Varelogianni, G., Roomans, G.M., et al. (2010) Effect of duramycin on chloride transport and intracellular calcium concentration in cystic fibrosis and non-cystic fibrosis epithelia. *APMIS : acta pathologica, microbiologica, et immunologica Scandinavica*, 118 (12): 982–990. doi:10.1111/J.1600-0463.2010.02680.X.

Omaiye, E.E., McWhirter, K.J., Luo, W., et al. (2019) High concentrations of flavor chemicals are present in electronic cigarette refill fluids. *Scientific Reports*, 9 (1): 2468. doi:10.1038/s41598-019-39550-2.

ONS (2024) *Adult smoking habits in the UK: 2023*. Available at: https://www.ons.gov.uk/peoplepopulationandcommunity/healthandsocialcare/healthandlifeexpectancies/bulletins/adultsmokinghabitsingreatbritain/2023 (Accessed: 6 June 2025).

Oransky, I. (2004) Ancel Keys. *The Lancet*, 364 (9452): 2174. doi:10.1016/S0140-6736(04)17578-8.

Otsu, W., Ishida, K., Chinen, N., et al. (2021) Cigarette smoke extract and heated tobacco products promote ferritin cleavage and iron accumulation in human corneal epithelial cells. *Scientific Reports*, 11 (1): 18555. doi:10.1038/S41598-021-97956-3.

Overbeek, S.A., Braber, S., Henricks, P.A.J., et al. (2011) Cigarette smoke induces β2-integrin-dependent neutrophil migration across human endothelium. *Respiratory Research*, 12 (1): 75. doi:10.1186/1465-9921-12-75.

Pacheco, R., M., M.-N.J., M., L., et al. (2005) CD26, adenosine deaminase, and adenosine receptors mediate costimulatory signals in the immunological synapse. *Proceedings of the National Academy of Sciences*, 102 (27): 9583–9588. doi:10.1073/pnas.0501050102.

Padmavathi, P., Raghu, P.S., Reddy, V.D., et al. (2018) Chronic cigarette smoking-induced oxidative/nitrosative stress in human erythrocytes and platelets. *Molecular & Cellular Toxicology*, 14 (1): 27–34. doi:10.1007/s13273-018-0004-6.

Pakulska, D. and Czerczak, S. (2006) Hazardous effects of arsine: a short review. *International Journal of Occupational Medicine and Environmental Health*, 19 (1): 36–44. doi:10.2478/v10001-006-0003-z.

Parascandola, M. and Xiao, L. (2019) Tobacco and the lung cancer epidemic in China. *Translational lung cancer research*, 8 (Suppl 1): S21–S30. doi:10.21037/tlcr.2019.03.12.

Park, H.S., Yeo, H.Y., Chang, H.J., et al. (2013) Dipeptidyl peptidase 10, a novel prognostic marker in colorectal cancer. *Yonsei medical journal*, 54 (6): 1362–1369. doi:10.3349/ymj.2013.54.6.1362.

Park, J.-A., Alexander, L.E.C. and Christiani, D.C. (2022) Vaping and Lung Inflammation and Injury. *Annual review of physiology*, 84: 611–629. doi:10.1146/annurev-physiol-061121-040014.

Paull, K.D., Shoemaker, R.H., Boyd, M.R., et al. (1988) The synthesis of XTT: A new tetrazolium reagent that is bioreducible to a water-soluble formazan. *Journal of Heterocyclic Chemistry*, 25 (3): 911–914. doi:https://doi.org/10.1002/jhet.5570250340.

Perng, D.-W. and Chen, P.-K. (2017) The Relationship between Airway Inflammation and Exacerbation in Chronic Obstructive Pulmonary Disease. *Tuberculosis and Respiratory Diseases*, 80 (4): 325–335. doi:10.4046/trd.2017.0085.

Petrescu, F., Voican, S.C. and Silosi, I. (2010) Tumor necrosis factor-α serum levels in healthy smokers and nonsmokers. *International Journal of Chronic Obstructive Pulmonary Disease*, 5: 217–222.

Philibert, R.A., Ryu, G.-Y., Yoon, J.-G., et al. (2007) Transcriptional profiling of subjects from the Iowa adoption studies. *American Journal of Medical Genetics. Part B, Neuropsychiatric Genetics: The Official Publication of the International Society of Psychiatric Genetics*, 144B (5): 683–690. doi:10.1002/ajmg.b.30512.

Phillips, B., Titz, B., Kogel, U., et al. (2017) Toxicity of the main electronic cigarette components, propylene glycol, glycerin, and nicotine, in Sprague-Dawley rats in a 90-day OECD inhalation study complemented by molecular endpoints. *Food and Chemical Toxicology: An International Journal Published for the British Industrial Biological Research Association*, 109 (Pt 1): 315–332. doi:10.1016/j.fct.2017.09.001.

Piatkowski, A., Gröger, A., Bozkurt, A., et al. (2007) Acetone associated inhalation injury and rhabdomyolysis. *Burns: Journal of the International Society for Burn Injuries*, 33 (7): 932–934. doi:10.1016/j.burns.2006.08.033.

Polosa, R., Morjaria, J.B., Prosperini, U., et al. (2020) COPD smokers who switched to e-cigarettes: health outcomes at 5-year follow up. *Therapeutic advances in chronic disease*, 11: 2040622320961617. doi:10.1177/2040622320961617.

Pongs, O. and Schwarz, J.R. (2010) Ancillary subunits associated with voltage-dependent K+ channels. *Physiological reviews*, 90 (2): 755–796. doi:10.1152/physrev.00020.2009.

Poon, A.H., Houseman, E.A., Ryan, L., et al. (2014) Variants of asthma and chronic obstructive pulmonary disease genes and lung function decline in aging. *The journals of gerontology. Series A, Biological sciences and medical sciences*, 69 (7): 907–913. doi:10.1093/gerona/glt179.

Proctor, R.N. (2012) The history of the discovery of the cigarette–lung cancer link: evidentiary traditions, corporate denial, global toll. *Tobacco Control*, 21 (2): 87–91. doi:10.1136/tobaccocontrol-2011-050338.

Proost, P., Struyf, S., Schols, D., et al. (1999) Truncation of Macrophage-derived Chemokine by CD26/ Dipeptidyl-Peptidase IV beyond Its Predicted Cleavage Site Affects Chemotactic Activity and CC Chemokine Receptor 4 Interaction. *Journal of Biological Chemistry*, 274 (7): 3988–3993. doi:10.1074/JBC.274.7.3988.

Qian, S., Wang, W., Yang, L., et al. (2008) Structure of transmembrane pore induced by Bax-derived peptide: evidence for lipidic pores. *Proceedings of the National Academy of Sciences of the United States of America*, 105 (45): 17379–17383. doi:10.1073/pnas.0807764105.

Rakhecha, B., Agnihotri, P., Dakal, T.C., et al. (2022) Anti-inflammatory activity of nicotine isolated from Brassica oleracea in rheumatoid arthritis. *Bioscience Reports*, 42 (4): BSR20211392. doi:10.1042/BSR20211392.

Ramani, T., Auletta, C.S., Weinstock, D., et al. (2015) Cytokines: The Good, the Bad, and the Deadly. *International Journal of Toxicology*, 34 (4): 355–365. doi:10.1177/1091581815584918.

Rasmussen, H.B., Branner, S., Wiberg, F.C., et al. (2003) Crystal structure of human dipeptidyl peptidase IV/CD26 in complex with a substrate analog. *Nature structural biology*, 10 (1): 19–25. doi:10.1038/nsb882.

Reidel, B., Radicioni, G., Clapp, P.W., et al. (2018a) E-Cigarette Use Causes a Unique Innate Immune Response in the Lung, Involving Increased Neutrophilic Activation and Altered Mucin Secretion. *American journal of respiratory and critical care medicine*, 197 (4): 492–501. doi:10.1164/rccm.201708-1590OC.

Reidel, B., Radicioni, G., Clapp, P.W., et al. (2018b) E-Cigarette Use Causes a Unique Innate Immune Response in the Lung, Involving Increased Neutrophilic Activation and Altered Mucin Secretion. *American Journal of Respiratory and Critical Care Medicine*, 197 (4): 492–501. doi:10.1164/rccm.201708-1590OC.

Ren, C., Tong, Y., Li, J., et al. (2017) The Protective Effect of Alpha 7 Nicotinic Acetylcholine Receptor Activation on Critical Illness and Its Mechanism. *International Journal of Biological Sciences*, 13 (1): 46–56. doi:10.7150/ijbs.16404.

Rieder-Scharinger, J., Peer, R., Rabl, W., et al. (2000) [Multiple organ failure following inhalation of butane gas: a case report]. *Wiener Klinische Wochenschrift*, 112 (24): 1049–1052.

Riedl, S.J. and Salvesen, G.S. (2007) The apoptosome: signalling platform of cell death. *Nature Reviews. Molecular Cell Biology*, 8 (5): 405–413. doi:10.1038/nrm2153.

Rigg, S. and Gielda, L.M. (2019) E-Cigarette Vapor Decreases Cellular Proliferation through Nicotine-Dependent Mechanisms. *Journal of Biosciences and Medicines*, 7 (7): 121–134. doi:10.4236/jbm.2019.77010.

Robertson, S.A., Chin, P.-Y., Femia, J.G., et al. (2018) Embryotoxic cytokines-Potential roles in embryo loss and fetal programming. *Journal of Reproductive Immunology*, 125: 80–88. doi:10.1016/j.jri.2017.12.003.

Rodgman, A., Smith, C.J. and Perfetti, T.A. (2000) The composition of cigarette smoke: a retrospective, with emphasis on polycyclic components. *Human & experimental toxicology*, 19 (10): 573–595. doi:10.1191/096032700701546514.

Roehm, N.W., Rodgers, G.H., Hatfield, S.M., et al. (1991) An improved colorimetric assay for cell proliferation and viability utilizing the tetrazolium salt XTT. *Journal of Immunological Methods*, 142 (2): 257–265. doi:10.1016/0022-1759(91)90114-U.

Rogers, S., de Souza, A.R., Zago, M., et al. (2017) Aryl hydrocarbon receptor (AhR)-dependent regulation of pulmonary miRNA by chronic cigarette smoke exposure. *Scientific Reports*, 7. doi:10.1038/srep40539.

van Rooy, F.G.B.G.J., Rooyackers, J.M., Prokop, M., et al. (2007) Bronchiolitis obliterans syndrome in chemical workers producing diacetyl for food flavorings. *American Journal of Respiratory and Critical Care Medicine*, 176 (5): 498–504. doi:10.1164/rccm.200611-1620OC.

Rose, J.E., Mukhin, A.G., Lokitz, S.J., et al. (2010) Kinetics of brain nicotine accumulation in dependent and nondependent smokers assessed with PET and cigarettes containing 11C-nicotine. *Proceedings of the National Academy of Sciences of the United States of America*, 107 (11): 5190–5195. doi:10.1073/pnas.0909184107.

Rouabhia, M., Park, H.J., Semlali, A., et al. (2017) E-Cigarette Vapor Induces an Apoptotic Response in Human Gingival Epithelial Cells Through the Caspase-3 Pathway. *Journal of Cellular Physiology*, 232 (6): 1539–1547. doi:10.1002/jcp.25677.

Rowell, T.R., Reeber, S.L., Lee, S.L., et al. (2017a) Flavored e-cigarette liquids reduce proliferation and viability in the CALU3 airway epithelial cell line. *American Journal of Physiology. Lung Cellular and Molecular Physiology*, 313 (1): L52–L66. doi:10.1152/ajplung.00392.2016.

Rowell, T.R., Reeber, S.L., Lee, S.L., et al. (2017b) Flavored e-cigarette liquids reduce proliferation and viability in the CALU3 airway epithelial cell line. *American Journal of Physiology. Lung Cellular and Molecular Physiology*, 313 (1): L52–L66. doi:10.1152/ajplung.00392.2016.

Roxlau, E.T., Pak, O., Hadzic, S., et al. (2023) Nicotine promotes e-cigarette vapour-induced lung inflammation and structural alterations. *The European Respiratory Journal*, 61 (6): 2200951. doi:10.1183/13993003.00951-2022.

Ruth, T., Daniel, J., König, A., et al. (2023) Inhalation toxicity of thermal transformation products formed from e-cigarette vehicle liquid using an *in vitro* lung model exposed at the Air–Liquid Interface. *Food and Chemical Toxicology*, 182: 114157. doi:10.1016/j.fct.2023.114157.

Sadeghi, M., Shabib, G., Masoumi, G., et al. (2021) A Systematic Review and Meta-analysis on the Prevalence of Smoking Cessation in Cardiovascular Patients After Participating in Cardiac Rehabilitation. *Current problems in cardiology*, 46 (3): 100719. doi:10.1016/j.cpcardiol.2020.100719.

Sajjan, U., Wang, Q., Zhao, Y., et al. (2008) Rhinovirus disrupts the barrier function of polarized airway epithelial cells. *American journal of respiratory and critical care medicine*, 178 (12): 1271–1281. doi:10.1164/RCCM.200801-136OC.

Sakuragi, T., Kosako, H. and Nagata, S. (2019) Phosphorylation-mediated activation of mouse Xkr8 scramblase for phosphatidylserine exposure. *Proceedings of the National Academy of Sciences of the United States of America*, 116 (8): 2907–2912. doi:10.1073/pnas.1820499116.

Sampilvanjil, A., Karasawa, T., Yamada, N., et al. (2020) Cigarette smoke extract induces ferroptosis in vascular smooth muscle cells. *American journal of physiology. Heart and circulatory physiology*, 318 (3): H508–H518. doi:10.1152/AJPHEART.00559.2019/ASSET/IMAGES/LARGE/ZH40022030220006.JPEG.

Sato, E., Koyama, S., Takamizawa, A., et al. (1999) Smoke extract stimulates lung fibroblasts to release neutrophil and monocyte chemotactic activities. *American Journal of Physiology - Lung*

*Cellular and Molecular Physiology*, 277 (6 21-6). doi:10.1152/AJPLUNG.1999.277.6.L1149/ASSET/IMAGES/LARGE/ALUN61202010W.JPEG.

Schairer, E. and Schöniger, E. (1944) Lungenkrebs und Tabakverbrauch. *Zeitschrift für Krebsforschung*, 54 (4): 261–269. doi:10.1007/BF01628727.

Scheffels, J. (2008) A difference that makes a difference: Young adult smokers' accounts of cigarette brands and package design. *Tobacco Control: An International Journal*, 17 (2): 118–122. doi:10.1136/tc.2007.021592.

Scott, A., Lugg, S.T., Aldridge, K., et al. (2018) Pro-inflammatory effects of e-cigarette vapour condensate on human alveolar macrophages. *Thorax*, 73 (12): 1161–1169. doi:10.1136/thoraxjnl-2018-211663.

Segawa, K., Kurata, S., Yanagihashi, Y., et al. (2014) Caspase-mediated cleavage of phospholipid flippase for apoptotic phosphatidylserine exposure. *Science*, 344 (6188): 1164–1168. doi:10.1126/science.1252809.

Sehgal, P.B., Grieninger, G. and Tosato, G. (1989) *Regulation of the acute phase and immune responses*. New York, NY (USA); The New York Academy of Sciences.

Selman, M. (2003) The Spectrum of Smoking-Related Interstitial Lung Disorders: The Never-Ending Story of Smoke and Disease. *CHEST*, 124 (4): 1185–1187. doi:10.1378/chest.124.4.1185.

Semple, F. and Dorin, J.R. (2012) β-Defensins: Multifunctional Modulators of Infection, Inflammation and More? *Journal of Innate Immunity*, 4 (4): 337–348. doi:10.1159/000336619.

Serapinas, D., Narbekovas, A., Juskevicius, J., et al. (2011) Systemic inflammation in COPD in relation to smoking status. *Multidisciplinary Respiratory Medicine*, 6 (4): 214–219. doi:10.1186/2049-6958-6-4-214.

Serpa, G.L., Renton, N.D., Lee, N., et al. (2020) Electronic Nicotine Delivery System Aerosol-induced Cell Death and Dysfunction in Macrophages and Lung Epithelial Cells. *American Journal of Respiratory Cell and Molecular Biology*, 63 (3): 306–316. doi:10.1165/rcmb.2019-0200OC.

Shi, J., Dai, W., Chavez, J., et al. (2022) One Acute Exposure to E-Cigarette Smoke Using Various Heating Elements and Power Levels Induces Pulmonary Inflammation. *Cardiology Research*, 13 (6): 323–332. doi:10.14740/cr1425.

Shi, J., Fan, J., Su, Q., et al. (2019) Cytokines and Abnormal Glucose and Lipid Metabolism. *Frontiers in Endocrinology*, 10: 703. doi:10.3389/fendo.2019.00703.

Shishani, K. (2018) Waterpipe Tobacco Cessation. *Journal of Global Oncology*, 4 (Supplement 2): 29s–29s. doi:10.1200/jgo.18.45800.

Shishodia, S. and Aggarwal, B.B. (2004) Cyclooxygenase (COX)-2 inhibitor celecoxib abrogates activation of cigarette smoke-induced nuclear factor (NF)-kappaB by suppressing activation of IkappaBalpha kinase in human non-small cell lung carcinoma: correlation with suppression of cyclin D1, COX-2, and matrix metalloproteinase-9. *Cancer Research*, 64 (14): 5004–5012. doi:10.1158/0008-5472.CAN-04-0206.

Sieminska, A. and Kuziemski, K. (2014) Respiratory bronchiolitis-interstitial lung disease. *Orphanet Journal of Rare Diseases*, 9: 106. doi:10.1186/s13023-014-0106-8.

Sim, S., Choi, Y., Lee, D.H., et al. (2022) Contribution of dipeptidyl peptidase 10 to airway dysfunction in patients with NSAID-exacerbated respiratory disease. *Clinical and experimental allergy : journal of the British Society for Allergy and Clinical Immunology*, 52 (1): 115–126. doi:10.1111/CEA.14003.

Simet, S.M., Sisson, J.H., Pavlik, J.A., et al. (2010) Long-Term Cigarette Smoke Exposure in a Mouse Model of Ciliated Epithelial Cell Function. *American Journal of Respiratory Cell and Molecular Biology*, 43 (6): 635–640. doi:10.1165/rcmb.2009-0297OC.

Singh, D., Fox, S.M., Tal-Singer, R., et al. (2011) Induced sputum genes associated with spirometric and radiological disease severity in COPD ex-smokers. *Thorax*, 66 (6): 489–495. doi:10.1136/thx.2010.153767.

Snoeck-Stroband, J.B., Postma, D.S., Lapperre, T.S., et al. (2006) Airway inflammation contributes to health status in COPD: a cross-sectional study. *Respiratory Research*, 7 (1): 140. doi:10.1186/1465-9921-7-140.

Sobonya, R. (1977) Fatal anhydrous ammonia inhalation. *Human Pathology*, 8 (3): 293–299. doi:10.1016/s0046-8177(77)80026-9.

Solanki, H.S., Babu, N., Jain, A.P., et al. (2018) Cigarette smoke induces mitochondrial metabolic reprogramming in lung cells. *Mitochondrion*, 40: 58–70. doi:10.1016/j.mito.2017.10.002.

Sompa, S.I., Ji, J., Rahman, M., et al. (2025) Local and systemic effects in e-cigarette users compared to cigarette smokers, dual users, and non-smokers. *Respiratory Research*, 26 (1): 207. doi:10.1186/s12931-025-03289-4.

Son, Y., Mainelis, G., Delnevo, C., et al. (2020a) Investigating E-Cigarette Particle Emissions and Human Airway Depositions under Various E-Cigarette-Use Conditions. *Chemical research in toxicology*, 33 (2): 343–352. doi:10.1021/acs.chemrestox.9b00243.

Son, Y., Mishin, V., Laskin, J.D., et al. (2019) Hydroxyl Radicals in E-Cigarette Vapor and E-Vapor Oxidative Potentials under Different Vaping Patterns. *Chemical research in toxicology*, 32 (6): 1087–1095. doi:10.1021/acs.chemrestox.8b00400.

Son, Y., Wackowski, O., Weisel, C., et al. (2018) Evaluation of E-Vapor Nicotine and Nicotyrine Concentrations under Various E-Liquid Compositions, Device Settings, and Vaping Topographies. *Chemical research in toxicology*, 31 (9): 861–868. doi:10.1021/acs.chemrestox.8b00063.

Son, Y., Weisel, C., Wackowski, O., et al. (2020b) The Impact of Device Settings, Use Patterns, and Flavorings on Carbonyl Emissions from Electronic Cigarettes. *International Journal of Environmental Research and Public Health*, 17 (16): 5650. doi:10.3390/ijerph17165650.

Song, Q., Chen, P. and Liu, X.-M. (2021a) The role of cigarette smoke-induced pulmonary vascular endothelial cell apoptosis in COPD. *Respiratory Research*, 22 (1): 39. doi:10.1186/s12931-021-01630-1.

Song, R.X., Mor, G., Naftolin, F., et al. (2001) Effect of long-term estrogen deprivation on apoptotic responses of breast cancer cells to 17beta-estradiol. *Journal of the National Cancer Institute*, 93 (22). doi:10.1093/jnci/93.22.1714.

Song, S.-Y., Na, H.G., Kwak, S.Y., et al. (2021b) Changes in Mucin Production in Human Airway Epithelial Cells After Exposure to Electronic Cigarette Vapor With or Without Nicotine. *Clinical and Experimental Otorhinolaryngology*, 14 (3): 303–311. doi:10.21053/ceo.2020.01907.

Spears, M., McSharry, C., Chaudhuri, R., et al. (2013) Smoking in Asthma Is Associated with Elevated Levels of Corticosteroid Resistant Sputum Cytokines—An Exploratory Study. *PLoS ONE*, 8 (8): e71460. doi:10.1371/journal.pone.0071460.

Spindle, T.R., Talih, S., Hiler, M.M., et al. (2018) Effects of electronic cigarette liquid solvents propylene glycol and vegetable glycerin on user nicotine delivery, heart rate, subjective effects, and puff topography. *Drug and alcohol dependence*, 188: 193–199. doi:10.1016/j.drugalcdep.2018.03.042.

Srinivasan, B., Kolli, A.R., Esch, M.B., et al. (2015) TEER measurement techniques for in vitro barrier model systems. *Journal of laboratory automation*, 20 (2): 107. doi:10.1177/2211068214561025.

Staessen, J.A., Roels, H.A., Emelianov, D., et al. (1999) Environmental exposure to cadmium, forearm bone density, and risk of fractures: prospective population study. Public Health and Environmental Exposure to Cadmium (PheeCad) Study Group. *Lancet (London, England)*, 353 (9159): 1140–1144. doi:10.1016/s0140-6736(98)09356-8.

Stanger, B.Z., Leder, P., Lee, T.H., et al. (1995) RIP: a novel protein containing a death domain that interacts with Fas/APO-1 (CD95) in yeast and causes cell death. *Cell*, 81 (4): 513–523. doi:10.1016/0092-8674(95)90072-1.

Stokes, A.C., Xie, W., Wilson, A.E., et al. (2021) Association of Cigarette and Electronic Cigarette Use Patterns with Levels of Inflammatory and Oxidative Stress Biomarkers among US Adults, Population Assessment of Tobacco and Health Study. *Circulation*, 143 (8): 869–871. doi:10.1161/CIRCULATIONAHA.120.051551.

Stone, W.L., Basit, H. and Burns, B. (2023) “Pathology, Inflammation.” In *StatPearls*. Treasure Island (FL): StatPearls Publishing. Available at: http://www.ncbi.nlm.nih.gov/books/NBK534820/ (Downloaded: 10 August 2023).

Su, L., Liu, J., Yue, Q., et al. (2023) Evaluation of the effects of e-cigarette aerosol extracts and tobacco cigarette smoke extracts on human gingival epithelial cells. *Toxicology in vitro: an international journal published in association with BIBRA*, p. 105605. doi:10.1016/j.tiv.2023.105605.

Su, L., Zhao, M., Ma, F., et al. (2022) A comparative assessment of e-cigarette aerosol extracts and tobacco cigarette smoke extracts on in vitro endothelial cell inflammation response. *Human & Experimental Toxicology*, 41: 09603271221088996. doi:10.1177/09603271221088996.

Suber, R.L., Deskin, R., Nikiforov, I., et al. (1989a) Subchronic nose-only inhalation study of propylene glycol in Sprague-Dawley rats. *Food and Chemical Toxicology: An International Journal Published for the British Industrial Biological Research Association*, 27 (9): 573–583. doi:10.1016/0278-6915(89)90016-1.

Suber, R.L., Deskin, R., Nikiforov, I., et al. (1989b) Subchronic nose-only inhalation study of propylene glycol in Sprague-Dawley rats. *Food and chemical toxicology : an international journal published for the British Industrial Biological Research Association*, 27 (9): 573–583. doi:10.1016/0278-6915(89)90016-1.

Subramaniyan, M. and Dani, J.A. (2015) Dopaminergic and cholinergic learning mechanisms in nicotine addiction. *Annals of the New York Academy of Sciences*, 1349 (1): 46–63. doi:10.1111/nyas.12871.

Suda, T., Takahashi, T., Golstein, P., et al. (1993) Molecular cloning and expression of the Fas ligand, a novel member of the tumor necrosis factor family. *Cell*, 75 (6): 1169–1178. doi:10.1016/0092-8674(93)90326-l.

Sundar, I.K., Javed, F., Romanos, G.E., et al. (2016) E-cigarettes and flavorings induce inflammatory and pro-senescence responses in oral epithelial cells and periodontal fibroblasts. *Oncotarget*, 7 (47): 77196–77204. doi:10.18632/oncotarget.12857.

Sunyer, J., Forastiere, F., Pekkanen, J., et al. (2009) Interaction between smoking and the interleukin-6 gene affects systemic levels of inflammatory biomarkers. *Nicotine & Tobacco Research*, 11 (11): 1347–1353. doi:10.1093/ntr/ntp144.

Surace, A.E.A. and Hedrich, C.M. (2019) The Role of Epigenetics in Autoimmune/Inflammatory Disease. *Frontiers in Immunology*, 10: 1525. doi:10.3389/fimmu.2019.01525.

Sutherland, E.R. and Martin, R.J. (2003) Airway inflammation in chronic obstructive pulmonary disease: Comparisons with asthma. *Journal of Allergy and Clinical Immunology*, 112 (5): 819–827. doi:10.1016/S0091-6749(03)02011-6.

Suzuki, J., Denning, D.P., Imanishi, E., et al. (2013) Xk-Related Protein 8 and CED-8 Promote Phosphatidylserine Exposure in Apoptotic Cells. *Science*, 341 (6144): 403–406. doi:10.1126/science.1236758.

Suzuki, J., Imanishi, E. and Nagata, S. (2014) Exposure of Phosphatidylserine by Xk-related Protein Family Members during Apoptosis *. *Journal of Biological Chemistry*, 289 (44): 30257–30267. doi:10.1074/jbc.M114.583419.

Svandova, E.B., Vesela, B., Lesot, H., et al. (2017) Expression of Fas, FasL, caspase-8 and other factors of the extrinsic apoptotic pathway during the onset of interdigital tissue elimination. *Histochemistry and Cell Biology*, 147 (4): 497–510. doi:10.1007/s00418-016-1508-6.

T, K., Mr, M., G, P., et al. (2002) Bid, Bax, and lipids cooperate to form supramolecular openings in the outer mitochondrial membrane. *Cell*, 111 (3). doi:10.1016/s0092-8674(02)01036-x.

Taatjes, D.J., Sobel, B.E. and Budd, R.C. (2008) Morphological and cytochemical determination of cell death by apoptosis. *Histochemistry and cell biology*, 129 (1): 33–43. doi:10.1007/s00418-007-0356-9.

Taha, H., Al-Sawalha, N., Alzoubi, K., et al. (2020) Effect of E-Cigarette aerosol exposure on airway inflammation in a murine model of asthma. *Inhalation Toxicology*, 32: 503–511. doi:10.1080/08958378.2020.1856238.

Takahashi, H., Fujimura, Y., Hayashi, M., et al. (2008) Enhanced dopamine release by nicotine in cigarette smokers: a double-blind, randomized, placebo-controlled pilot study. *International Journal of Neuropsychopharmacology*, 11 (3): 413–417. doi:10.1017/S1461145707008103.

Takeda, N., Maghni, K., Daigle, S., et al. (2009) Long-term pathologic consequences of acute irritant-induced asthma. *Journal of Allergy and Clinical Immunology*, 124 (5): 975-981.e1. doi:10.1016/j.jaci.2009.08.008.

Talih, S., Salman, R., El-Hage, R., et al. (2020) Effect of free-base and protonated nicotine on nicotine yield from electronic cigarettes with varying power and liquid vehicle. *Scientific Reports*, 10 (1): 16263. doi:10.1038/s41598-020-73385-6.

Tamashiro, E., Xiong, G., Anselmo-Lima, W.T., et al. (2009) Cigarette smoke exposure impairs respiratory epithelial ciliogenesis. *American Journal of Rhinology & Allergy*, 23 (2): 117–122. doi:10.2500/ajra.2009.23.3280.

Tanaka, T., Duke-Cohan, J.S., Kameoka, J., et al. (1994) Enhancement of antigen-induced T-cell proliferation by soluble CD26/dipeptidyl peptidase IV. *Proceedings of the National Academy of Sciences*, 91 (8): 3082–3086. doi:10.1073/pnas.91.8.3082.

Tanaka, T., Huang, X., Jorgensen, E., et al. (2007) ATM activation accompanies histone H2AX phosphorylation in A549 cells upon exposure to tobacco smoke. *Bmc Cell Biology*, 8. doi:10.1186/1471-2121-8-26.

Tang, H., Zhang, Y., Wang, Q., et al. (2023) Astaxanthin attenuated cigarette smoke extract-induced apoptosis via decreasing oxidative DNA damage in airway epithelium. *Biomedicine & Pharmacotherapy*, 167: 115471. doi:10.1016/j.biopha.2023.115471.

Tang, M.-S., Lee, H.-W., Weng, M.-W., et al. (2022) DNA damage, DNA repair and carcinogenicity: Tobacco smoke versus electronic cigarette aerosol. *Mutation Research. Reviews in Mutation Research*, 789: 108409. doi:10.1016/j.mrrev.2021.108409.

Tatsuta, M., Kan-O, K., Ishii, Y., et al. (2019) Effects of cigarette smoke on barrier function and tight junction proteins in the bronchial epithelium: protective role of cathelicidin LL-37. *Respiratory Research*, 20 (1). doi:10.1186/S12931-019-1226-4.

Taylor, M., Carr, T., Oke, O., et al. (2016) E-cigarette aerosols induce lower oxidative stress in vitro when compared to tobacco smoke. *Toxicology Mechanisms and Methods*, 26 (6): 465–476. doi:10.1080/15376516.2016.1222473.

Tayyarah, R. and Long, G.A. (2014) Comparison of select analytes in aerosol from e-cigarettes with smoke from conventional cigarettes and with ambient air. *Regulatory Toxicology and Pharmacology*, 70 (3): 704–710. doi:10.1016/j.yrtph.2014.10.010.

Thal, M.A. and Kishore, R. (2013) “Role of Cytokines in Angiogenesis: Turning It On and Off.” In Mehta, J.L. and Dhalla, N.S. (eds) *Biochemical Basis and Therapeutic Implications of Angiogenesis*. Advances in Biochemistry in Health and Disease. New York, NY: Springer. pp. 47–61. doi:10.1007/978-1-4614-5857-9_3.

*The Tobacco and Related Products Regulations, 2016*. .

Thoma, R., Löffler, B., Stihle, M., et al. (2003) Structural Basis of Proline-Specific Exopeptidase Activity as Observed in Human Dipeptidyl Peptidase-IV. *Structure*, 11 (8): 947–959. doi:https://doi.org/10.1016/S0969-2126(03)00160-6.

Tian, H., Pan, J., Fang, S., et al. (2021) LncRNA DPP10-AS1 promotes malignant processes through epigenetically activating its cognate gene DPP10 and predicts poor prognosis in lung cancer patients. *Cancer biology & medicine*, 18 (3): 675–692. doi:10.20892/j.issn.2095-3941.2020.0136.

Tinkler, P. (2001) “Red tips for hot lips”: advertising cigarettes for young women in Britain, 1920-70. *Women’s History Review*, 10 (2): 249–272. doi:10.1080/09612020100200289.

*Tobacco and Vapes Bill, 2024*. (220). Available at: https://bills.parliament.uk/bills/3703 (Accessed: 27 May 2024).

*Tobacco Product Directive, 2014*. (No 4, Title III, Article 20). Available at: https://www.legislation.gov.uk/eudr/2014/40/article/20 (Accessed: 27 May 2024).

Tripathi, P.M., Kant, S., Yadav, R.S., et al. (2017) Effect of chronic obstructive pulmonary disease on interleukin-8 level in sputum and peripheral blood neutrophils: A case control study. *Journal of Clinical and Diagnostic Research*, 11 (11): OC13–OC17. doi:10.7860/JCDR/2017/28279.10849.

Tsai, M., Song, M.-A., McAndrew, C., et al. (2019) Electronic versus Combustible Cigarette Effects on Inflammasome Component Release into Human Lung. *American Journal of Respiratory and Critical Care Medicine*, 199 (7): 922–925. doi:10.1164/rccm.201808-1467LE.

Tuck, S.A., Ramos-Barbón, D., Campbell, H., et al. (2008) Time course of airway remodelling after an acute chlorine gas exposure in mice. *Respiratory Research*, 9 (1): 61. doi:10.1186/1465-9921-9-61.

Tweed, J.O., Hsia, S.H., Lutfy, K., et al. (2012) The endocrine effects of nicotine and cigarette smoke. *Trends in endocrinology and metabolism: TEM*, 23 (7): 334–342. doi:10.1016/j.tem.2012.03.006.

Uchiyama, S., Noguchi, M., Sato, A., et al. (2020) Determination of Thermal Decomposition Products Generated from E-Cigarettes. *Chemical Research in Toxicology*, 33 (2): 576–583. doi:10.1021/acs.chemrestox.9b00410.

Ueda, K., Sakai, C., Ishida, T., et al. (2023) Cigarette smoke induces mitochondrial DNA damage and activates cGAS-STING pathway: application to a biomarker for atherosclerosis. *Clinical Science (London, England : 1979)*, 137 (2): 163–180. doi:10.1042/CS20220525.

*UK Statutory Instrument, 2015*. *895*.

Ung, T.T., Nguyen, T.T., Lian, S., et al. (2019) Nicotine stimulates IL-6 expression by activating the AP-1 and STAT-3 pathways in human endothelial EA.hy926 cells. *Journal of Cellular Biochemistry*, 120 (4): 5531–5541. doi:10.1002/jcb.27837.

Van Tongeren, J., Reinartz, S.M., Fokkens, W.J., et al. (2008) Interactions between epithelial cells and dendritic cells in airway immune responses: lessons from allergic airway disease. *Allergy*, 63 (9): 1124–1135. doi:10.1111/J.1398-9995.2008.01791.X.

Van Winkle, L.S., Evans, M.J., Brown, C.D., et al. (2001) Prior exposure to aged and diluted sidestream cigarette smoke impairs bronchiolar injury and repair. *Toxicological Sciences: An Official Journal of the Society of Toxicology*, 60 (1): 152–164. doi:10.1093/toxsci/60.1.152.

Villablanca, A.C. (1998) Nicotine stimulates DNA synthesis and proliferation in vascular endothelial cells in vitro. *Journal of Applied Physiology (Bethesda, Md.: 1985)*, 84 (6): 2089–2098. doi:10.1152/jappl.1998.84.6.2089.

Votavova, H., Dostalova Merkerova, M., Fejglova, K., et al. (2011) Transcriptome alterations in maternal and fetal cells induced by tobacco smoke. *Placenta*, 32 (10): 763–770. doi:10.1016/j.placenta.2011.06.022.

Wald, N. and Nicolaides-Bouman, A. (eds) (1991) *UK Smoking Statistics*. Oxford University Press. doi:10.1093/oso/9780192616807.001.0001.

Walton, M. (1973) Industrial ammonia gassing. *British Journal of Industrial Medicine*, 30 (1): 78–86.

Wang, C., Deng, L., Hong, M., et al. (2001) TAK1 is a ubiquitin-dependent kinase of MKK and IKK. *Nature*, 412 (6844): 346–351. doi:10.1038/35085597.

Wang, H., Chen, H., Fu, Y., et al. (2022a) Effects of Smoking on Inflammatory-Related Cytokine Levels in Human Serum. *Molecules*, 27 (12): 3715. doi:10.3390/molecules27123715.

Wang, H., Han, S., Chen, H., et al. (2022b) In Vitro Toxicological Investigation and Risk Assessment of E-Cigarette Aerosols Based on a Novel Solvent-Free Extraction Method. *ACS omega*, 7 (51): 48403–48415. doi:10.1021/acsomega.2c06663.

Wang, M., Zhang, Y., Xu, M., et al. (2019) Roles of TRPA1 and TRPV1 in cigarette smoke -induced airway epithelial cell injury model. *Free Radical Biology and Medicine*, 134: 229–238. doi:10.1016/J.FREERADBIOMED.2019.01.004.

Wang, P., Chen, W., Liao, J., et al. (2017) A Device-Independent Evaluation of Carbonyl Emissions from Heated Electronic Cigarette Solvents. *PLoS ONE*, 12 (1): e0169811. doi:10.1371/journal.pone.0169811.

Wang, W.C., Cheng, C.F. and Tsaur, M.L. (2015) Immunohistochemical localization of DPP10 in rat brain supports the existence of a Kv4/KChIP/DPPL ternary complex in neurons. *The Journal of comparative neurology*, 523 (4): 608–628. doi:10.1002/CNE.23698.

Wang, X., Su, Y.-R., Petersen, P.S., et al. (2020a) Exploratory Genome-Wide Interaction Analysis of Nonsteroidal Anti-inflammatory Drugs and Predicted Gene Expression on Colorectal Cancer Risk. *Cancer epidemiology, biomarkers & prevention : a publication of the American Association for Cancer Research, cosponsored by the American Society of Preventive Oncology*, 29 (9): 1800–1808. doi:10.1158/1055-9965.EPI-19-1018.

Wang, X., Wang, W., Liu, C., et al. (2020b) Involvement of TRPC1 and Cyclin D1 in Human Pulmonary Artery Smooth Muscle Cells Proliferation Induced by Cigarette Smoke Extract. *Current Medical Science*, 40 (6): 1085–1091. doi:10.1007/s11596-020-2290-1.

Watson, A.Y., Bates, R.R. and Kennedy, D. (1988) "Biological Disposition of Airborne Particles: Basic Principles and Application to Vehicular Emissions." In *Air Pollution, the Automobile, and Public Health*. National Academies Press (US). Available at: https://www.ncbi.nlm.nih.gov/books/NBK218161/ (Downloaded: 29 March 2025).

Wavreil, F.D.M. and Heggland, S.J. (2019) Cinnamon-flavored electronic cigarette liquids and aerosols induce oxidative stress in human osteoblast-like MG-63 cells. *Toxicology Reports*, 7: 23–29. doi:10.1016/j.toxrep.2019.11.019.

Ween, M.P., Hamon, R., Macowan, M.G., et al. (2020) Effects of E-cigarette E-liquid components on bronchial epithelial cells: Demonstration of dysfunctional efferocytosis. *Respirology*, 25 (6): 620–628. doi:https://doi.org/10.1111/resp.13696.

Weng, M.-W., Lee, H.-W., Park, S.-H., et al. (2018) Aldehydes are the predominant forces inducing DNA damage and inhibiting DNA repair in tobacco smoke carcinogenesis. *Proceedings of the National Academy of Sciences of the United States of America*, 115 (27): E6152–E6161. doi:10.1073/pnas.1804869115.

Werley, M.S., Kirkpatrick, D.J., Oldham, M.J., et al. (2016) Toxicological assessment of a prototype e-cigaret device and three flavor formulations: a 90-day inhalation study in rats. *Inhalation toxicology*, 28 (1): 22–38. doi:10.3109/08958378.2015.1130758.

Werner, A.K., Koumans, E.H., Chatham-Stephens, K., et al. (2020) Hospitalizations and Deaths Associated with EVALI. *The New England Journal of Medicine*, 382 (17): 1589–1598. doi:10.1056/NEJMoa1915314.

WHO (2021) *WHO global report on trends in prevalence of tobacco use 2000-2025, fourth edition*. Available at: https://www.who.int/publications/i/item/9789240039322 (Accessed: 18 April 2024).

WHO (n.d.) *Burden of COPD*. Available at: http://www.who.int/respiratory/copd/burden/en/.

Widmann, C., Gibson, S. and Johnson, G.L. (1998) Caspase-dependent cleavage of signaling proteins during apoptosis. A turn-off mechanism for anti-apoptotic signals. *The Journal of Biological Chemistry*, 273 (12): 7141–7147. doi:10.1074/jbc.273.12.7141.

Willemse, B.W.M., Postma, D.S., Timens, W., et al. (2004) The impact of smoking cessation on respiratory symptoms, lung function, airway hyperresponsiveness and inflammation. *The European Respiratory Journal*, 23 (3): 464–476. doi:10.1183/09031936.04.00012704.

Winek Cl and Collom Wd (1971) Benzene and toluene fatalities. *Journal of occupational medicine. : official publication of the Industrial Medical Association*, 13 (5). Available at: https://pubmed.ncbi.nlm.nih.gov/5103143/ (Accessed: 7 May 2024).

Winek Cl, Collom Wd, and Wecht Ch (1967) Fatal benzene exposure by glue-sniffing. *Lancet (London, England)*, 1 (7491). doi:10.1016/s0140-6736(67)92578-0.

Wing, V.C., Payer, D.E., Houle, S., et al. (2015) Measuring Cigarette Smoking-Induced Cortical Dopamine Release: A [11C]FLB-457 PET Study. *Neuropsychopharmacology*, 40 (6): 1417–1427. doi:10.1038/npp.2014.327.

Winnicka, L. and Shenoy, M.A. (2020) EVALI and the Pulmonary Toxicity of Electronic Cigarettes: A Review. *Journal of General Internal Medicine*, 35 (7): 2130–2135. doi:10.1007/s11606-020-05813-2.

Witkiewicz, A.K., Knudsen, K.E., Dicker, A.P., et al. (2011) The meaning of p16(ink4a) expression in tumors: functional significance, clinical associations and future developments. *Cell Cycle (Georgetown, Tex.)*, 10 (15): 2497–2503. doi:10.4161/cc.10.15.16776.

Wolf, D.M. and Jordan, V.C. (1993) A laboratory model to explain the survival advantage observed in patients taking adjuvant tamoxifen therapy. *Recent results in cancer research. Fortschritte der Krebsforschung. Progres dans les recherches sur le cancer*, 127. doi:10.1007/978-3-642-84745-5_4.

Woodruff, P.G., Koth, L.L., Yang, Y.H., et al. (2005) A distinctive alveolar macrophage activation state induced by cigarette smoking. *American Journal of Respiratory and Critical Care Medicine*, 172 (11): 1383–1392. doi:10.1164/rccm.200505-686OC.

Wright, J.L., Lawson, L.M., Paré, P.D., et al. (1984) The detection of small airways disease. *The American Review of Respiratory Disease*, 129 (6): 989–994. doi:10.1164/arrd.1984.129.6.989.

Wu, H., Romieu, I., Shi, M., et al. (2010) Evaluation of candidate genes in a genome-wide association study of childhood asthma in Mexicans. *The Journal of allergy and clinical immunology*, 125 (2): 321-327.e13. doi:10.1016/j.jaci.2009.09.007.

Wu, J., Rickert, W.S. and Masters, A. (2012) An improved high performance liquid chromatography-fluorescence detection method for the analysis of major phenolic compounds in cigarette smoke and

smokeless tobacco products. *Journal of Chromatography A*, 1264: 40–47. doi:10.1016/j.chroma.2012.09.060.

Wu, Q., Jiang, D., Minor, M., et al. (2014) Electronic cigarette liquid increases inflammation and virus infection in primary human airway epithelial cells. *PloS One*, 9 (9): e108342. doi:10.1371/journal.pone.0108342.

Wu, X., Tian, Y., Wang, H., et al. (2025) Dual Regulation of Nicotine on NLRP3 Inflammasome in Macrophages with the Involvement of Lysosomal Destabilization, ROS and α7nAChR. *Inflammation*, 48 (1): 61–74. doi:10.1007/s10753-024-02036-z.

Xu, J., Gaddis, N.C., Bartz, T.M., et al. (2019) Omega-3 Fatty Acids and Genome-Wide Interaction Analyses Reveal DPP10-Pulmonary Function Association. *American journal of respiratory and critical care medicine*, 199 (5): 631–642. doi:10.1164/rccm.201802-0304OC.

Xu, X., Wang, H., Liu, S., et al. (2016) TP53-dependent autophagy links the ATR-CHEK1 axis activation to proinflammatory VEGFA production in human bronchial epithelial cells exposed to fine particulate matter (PM2.5). *Autophagy*, 12 (10): 1832–1848. doi:10.1080/15548627.2016.1204496.

Xue, D., Ma, Y., Li, M., et al. (2015) Mycoplasma ovipneumoniae induces inflammatory response in sheep airway epithelial cells via a MyD88-dependent TLR signaling pathway. *Veterinary immunology and immunopathology*, 163 (1–2): 57–66. doi:10.1016/J.VETIMM.2014.11.008.

Yamamoto, M., Sato, S., Hemmi, H., et al. (2003) TRAM is specifically involved in the Toll-like receptor 4-mediated MyD88-independent signaling pathway. *Nature Immunology*, 4 (11): 1144–1150. doi:10.1038/ni986.

Yamamoto, T, Ebisuya, M, Ashida, F, et al. (2006) Continuous ERK activation downregulates antiproliferative genes throughout G1 phase to allow cell-cycle progression. *Current biology : CB*, 16 (12). doi:10.1016/j.cub.2006.04.044.

Yang, X., Che, W., Zhang, L., et al. (2025) Chronic airway inflammatory diseases and e-cigarette use: a review of health risks and mechanisms. *European Journal of Medical Research*, 30 (1): 223. doi:10.1186/s40001-025-02492-9.

Yockey, L.J. and Iwasaki, A. (2018) Role of Interferons and Cytokines in Pregnancy and Fetal Development. *Immunity*, 49 (3): 397–412. doi:10.1016/j.immuni.2018.07.017.

Yogeswaran, S., Muthumalage, T. and Rahman, I. (2021) Comparative Reactive Oxygen Species (ROS) Content among Various Flavored Disposable Vape Bars, including Cool (Iced) Flavored Bars. *Toxics*, 9 (10): 235. doi:10.3390/toxics9100235.

Yokotani, N., Doi, K., J.Wenthold, R., et al. (1993) Non-conservation of a catalytic residue in a dipeptidyl aminopeptidase IV-related protein encoded by a gene on human chromosome 7. *Human Molecular Genetics*, 2 (7): 1037–1039. doi:10.1093/hmg/2.7.1037.

Yoo, J., Lim, Y.-M., Kim, H., et al. (2018) Potentiation of Sodium Metabisulfite Toxicity by Propylene Glycol in Both in Vitro and in Vivo Systems. *Frontiers in pharmacology*, 9: 161. doi:10.3389/fphar.2018.00161.

Yu, Q., Yang, D., Chen, X., et al. (2019) CD147 increases mucus secretion induced by cigarette smoke in COPD. *BMC pulmonary medicine*, 19 (1): 29. doi:10.1186/s12890-019-0791-0.

Yu, V., Rahimy, M., Korrapati, A., et al. (2016) Electronic cigarettes induce DNA strand breaks and cell death independently of nicotine in cell lines. *Oral Oncology*, 52: 58–65. doi:10.1016/j.oraloncology.2015.10.018.

Zagha, E., Ozaita, A., Chang, S.Y., et al. (2005) DPP10 modulates Kv4-mediated A-type potassium channels. *The Journal of biological chemistry*, 280 (19): 18853–18861. doi:10.1074/jbc.M410613200.

Zanetti, F., Giacomello, M., Donati, Y., et al. (2014) Nicotine mediates oxidative stress and apoptosis through cross talk between NOX1 and Bcl-2 in lung epithelial cells. *Free Radical Biology & Medicine*, 76: 173–184. doi:10.1016/j.freeradbiomed.2014.08.002.

Zanini, A., Cherubino, F., Zampogna, E., et al. (2015) Bronchial hyperresponsiveness, airway inflammation, and reversibility in patients with chronic obstructive pulmonary disease. *International Journal of Chronic Obstructive Pulmonary Disease*, 10: 1155–1161. doi:10.2147/COPD.S80992.

Zhang, J. and Bai, C. (2018) The Significance of Serum Interleukin-8 in Acute Exacerbations of Chronic Obstructive Pulmonary Disease. *Tanaffos*, 17 (1): 13–21.

Zhang, Y., Poobalasingam, T., Yates, L.L., et al. (2018) Manipulation of dipeptidylpeptidase 10 in mouse and human in vivo and in vitro models indicates a protective role in asthma. *Disease models & mechanisms*, 11 (1): dmm031369. doi:10.1242/dmm.031369.

Zhang, Y., Zou, H.-Y., Shi, P., et al. (2016) Determination of benzo[a]pyrene in cigarette mainstream smoke by using mid-infrared spectroscopy associated with a novel chemometric algorithm. *Analytica Chimica Acta*, 902: 43–49. doi:10.1016/j.aca.2015.10.029.

Zhang, Z.-W., Xu, Y.-B., Wang, C.-H., et al. (2011) Direct determination of hydrogen cyanide in cigarette mainstream smoke by ion chromatography with pulsed amperometric detection. *Journal of Chromatography. A*, 1218 (7): 1016–1019. doi:10.1016/j.chroma.2010.12.100.

Zhao, C., Xie, Y., Zhou, X., et al. (2020) The effect of different tobacco tar levels on DNA damage in cigarette smoking subjects. *Toxicology Research*, 9 (3): 302–307. doi:10.1093/toxres/tfaa031.

Zhao, G., Wang, S., Fu, Y., et al. (2014) Analysis of the Heterocyclic Aromatic Amines in Cigarette Smoke by Liquid Chromatography–Tandem Mass Spectrometry. *Chromatographia*, 77 (11): 813–820. doi:10.1007/s10337-014-2687-8.

Zhao, H., Wu, L., Yan, G., et al. (2021) Inflammation and tumor progression: signaling pathways and targeted intervention. *Signal Transduction and Targeted Therapy*, 6 (1): 263. doi:10.1038/s41392-021-00658-5.

Zhao, J. and Hopke, P.K. (2012) Concentration of Reactive Oxygen Species (ROS) in Mainstream and Sidestream Cigarette Smoke. *Aerosol Science and Technology*, 46 (2): 191–197. doi:10.1080/02786826.2011.617795.

Zhao, J., Pyrgiotakis, G. and Demokritou, P. (2016) Development and characterization of electronic-cigarette exposure generation system (Ecig-EGS) for the physico-chemical and toxicological assessment of electronic cigarette emissions. *Inhalation toxicology*, 28 (14): 658–669. doi:10.1080/08958378.2016.1246628.

Zhao, Z., Xu, Z., Chang, J., et al. (2023) Sodium pyruvate exerts protective effects against cigarette smoke extract-induced ferroptosis in alveolar and bronchial epithelial cells through the GPX4/Nrf2 axis. *Journal of inflammation (London, England)*, 20 (1): 28. doi:10.1186/s12950-023-00347-w.

Zhou, H., Hong, X., Jiang, S., et al. (2009) Analyses of associations between three positionally cloned asthma candidate genes and asthma or asthma-related phenotypes in a Chinese population. *BMC medical genetics*, 10: 123. doi:10.1186/1471-2350-10-123.

Zhou, Y., Zuo, X., Li, Y., et al. (2012) Nicotine inhibits tumor necrosis factor-α induced IL-6 and IL-8 secretion in fibroblast-like synoviocytes from patients with rheumatoid arthritis. *Rheumatology International*, 32 (1): 97–104. doi:10.1007/s00296-010-1549-4.

Zoico, E. and Roubenoff, R. (2002) The role of cytokines in regulating protein metabolism and muscle function. *Nutrition Reviews*, 60 (2): 39–51. doi:10.1301/00296640260085949.

# APPENDIX

## Supplementary figures

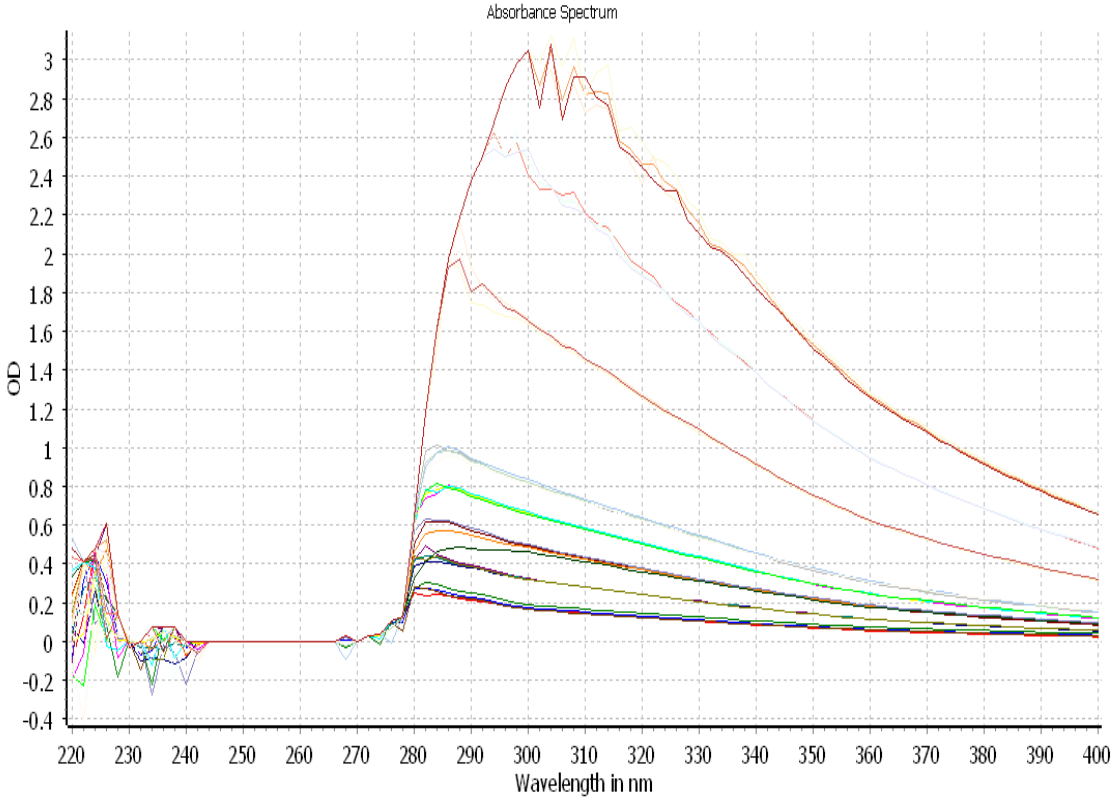


*A 1: Absorbance spectra of CSE dilutions (5-400%) measured on the Clariostar plate reader. Measurement were taken at 220-400 nm wavelength.*

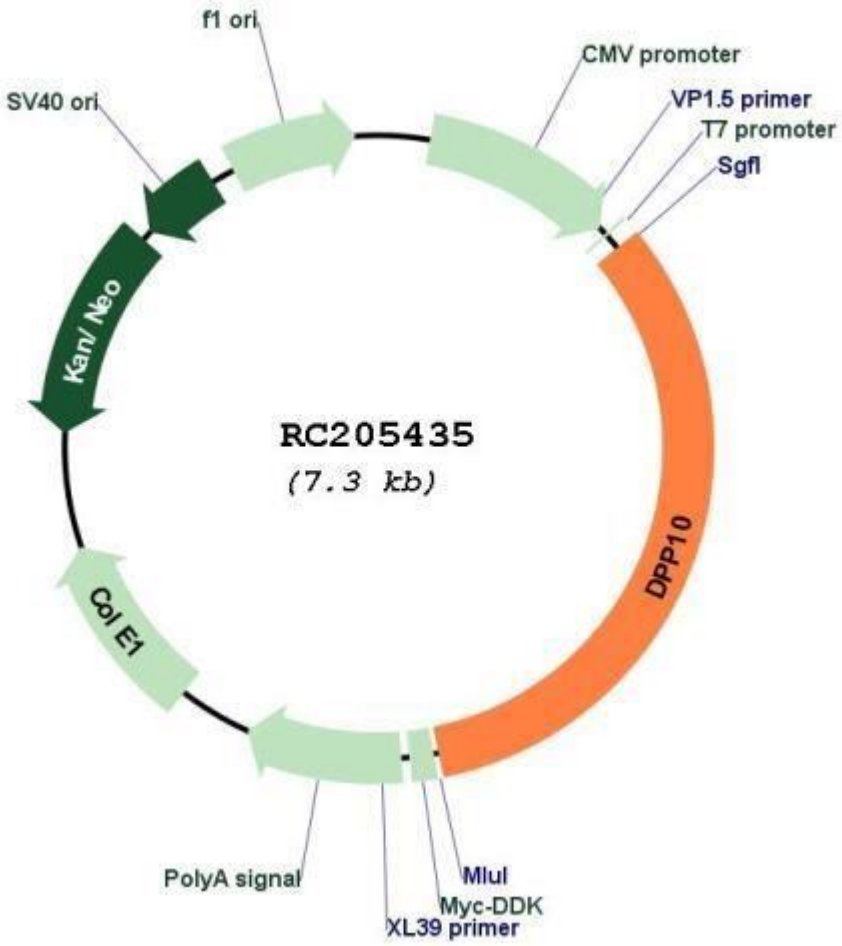


*A 2: DPP10 ORF clone used in the transfection of A549 and Beas-2B cells for over expression*

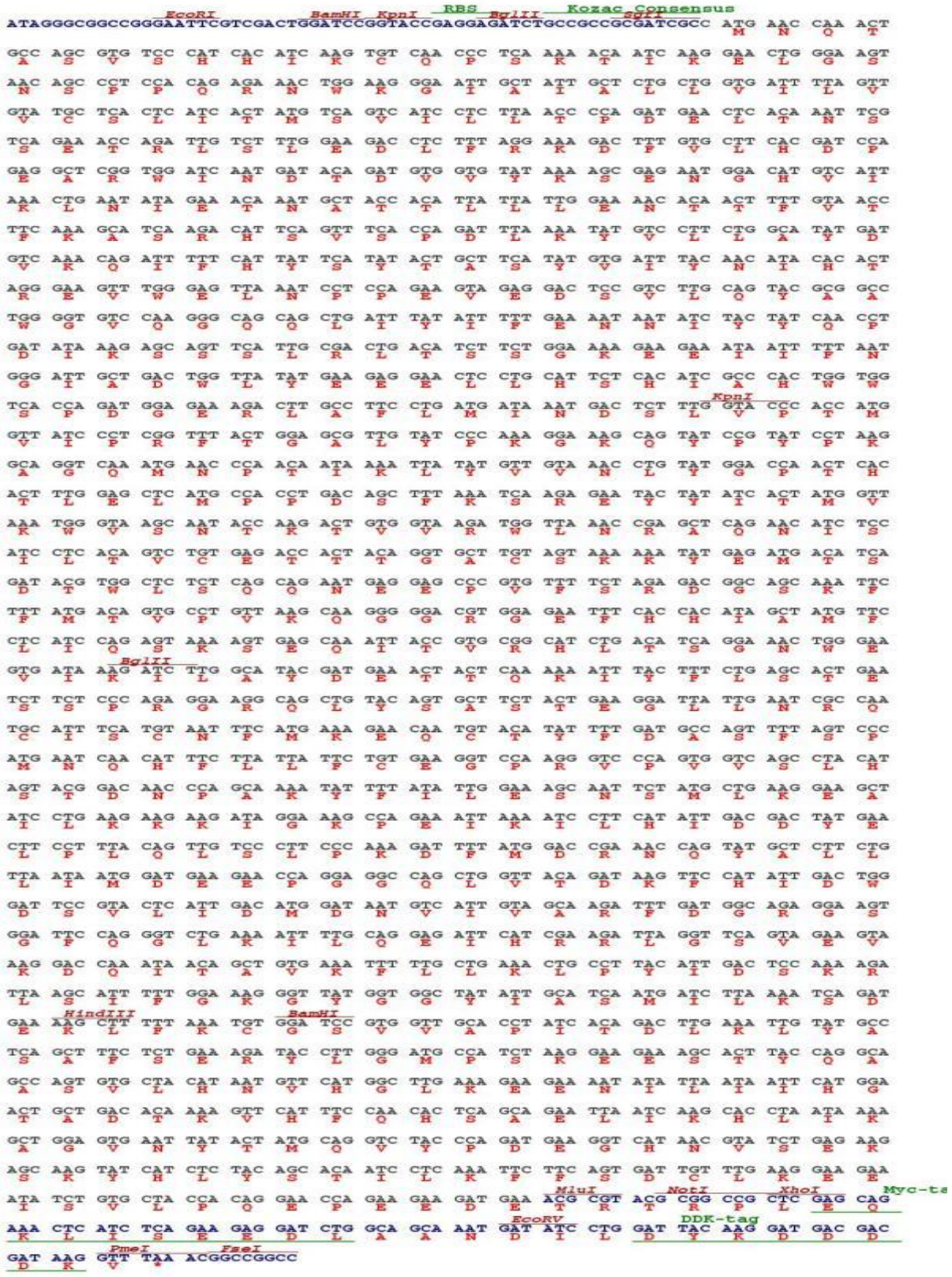


*A 3: Nucleotide sequence of DPP10 ORF clone used in the transfection of A549 and Beas-2B cells for over expression*

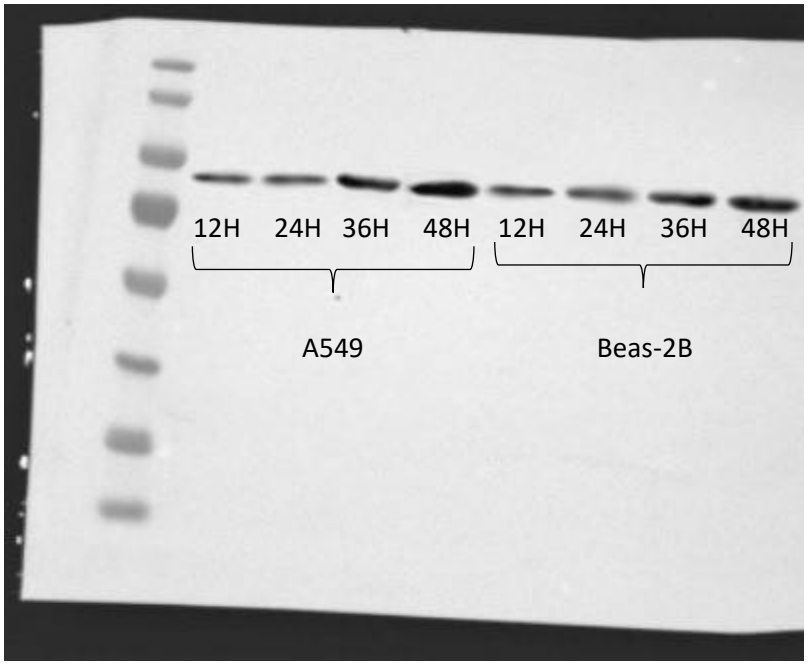


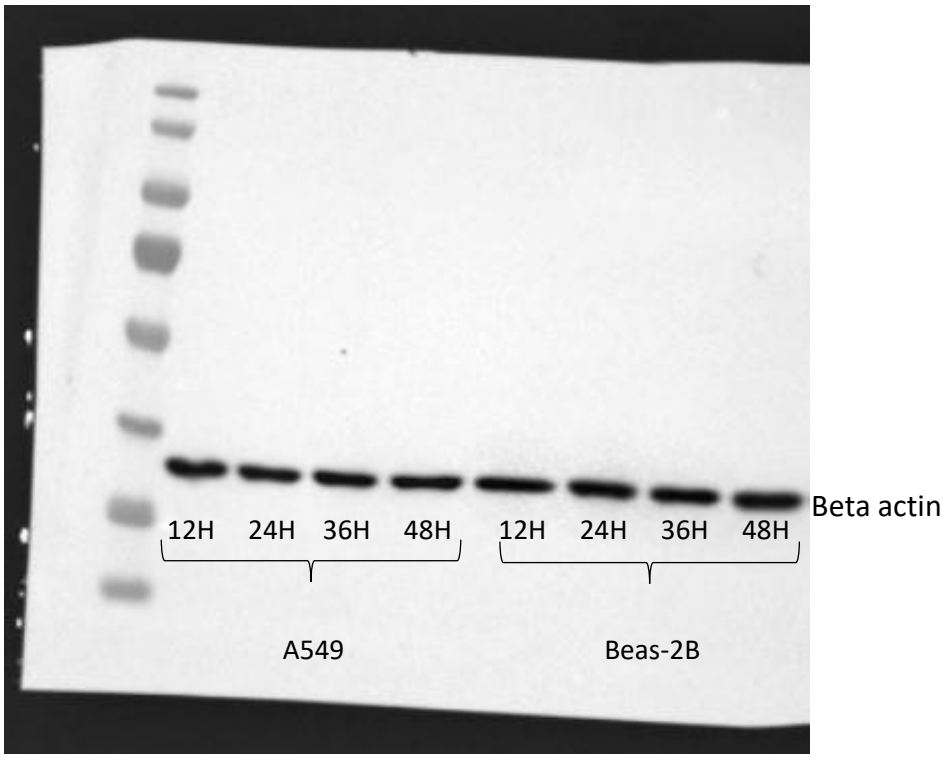


*A 4: Western blot of protein extract from A549 and Beas-2B cells following siRNA transfection of DPP10.*